Development of a human 3D tissue-engineered blood vessel model for the study of haemostasis

Faiza Musa

School of Postgraduate

Medicine Institute for Science and Technology in Medicine (ISTM)

Keele University

Thesis submitted to Keele University for the degree of Doctor of Philosophy in Cell and Tissue Engineering

June 2018

Abstract

In this project, we have designed, constructed, and validated a human tissue-engineered blood vessel construct (TEBV) to assess whether it could be used as a new model system in which to study thrombus formation under physiologically relevant conditions.

A layer-by-layer fabrication technique was adopted to fabricate the TEBV. This allowed for the biological properties of both the medial and intimal layers of the construct to be assessed individually, as well as in combination as the full TEBV. The TEBV model was shown to mimic the anatomical structure and cellular phenotype of the native human artery. In addition, a novel technique for quantitatively assessing the pro- and anti-aggregatory properties of these constructs was developed, utilising real-time measurements of cytosolic Ca^{2+} signalling to assess real-time human platelet activation when exposed to the tissue-engineered blood vessels constructs. The real-time measurement of cytosolic Ca^{2+} signalling of human platelets when exposed to the TEBV models was shown to be a sensitive technique to assess the haemostatic properties of the 3-dimensional (3D) TEBV to validate the physiological relevance of the construct. Experiments conducted with this novel methodology, alongside other traditional platelet function assays, demonstrated that our TEBV had an anti-aggregatory intimal layer and a pro-aggregatory medial layer, consistent with the haemostatic functions of this blood vessel layers *in vivo.*

We have also established an *ex vivo* ferric chloride ($FeCl_3$) arterial injury model to be used as an alternative to intravital microscopy study of *in vivo* thrombus formation in mice models. Treatment of the TEBV with $FeCl_3$ elicited a significant increase in platelet aggregation upon the surface of the construct when these cells were perfused over the construct at arterial shear stresses. By using this perfusion system, experiments also provided initial evidence that the use of the general anaesthetic ketamine, in intravital microscopy experiments may interfere with thrombus formation, and therefore could affect the validity of results seen in previous *in vivo* studies. In conclusion, we have

successfully created a TEBV that is able to replicate the functional properties of the native vessel and which may be useful as a novel model to study human thrombus formation.

Table of Contents

List of Figures

Chapter 1

Chapter 2

Chapter 3

Chapter 4

Chapter 5

Chapter 6

List of Tables

Abbreviations

αMEM	Minimum essential medium-α
$[Ca^{2+}]_{cyt}$	Cytosolic calcium concentration
2D	2-dimensional
3D	3-dimensional
AC	Adenylate cyclase
ACD	Acid citrate dextrose
ADP	Adenosine di-phosphate
AM	Acetoxymethyl
ASA	Aspirin
ATP	Adenosine triphosphate
BSA	Bovine serum albumin
Ca^{2+}	Calcium
$CaCl_2$	Calcium chloride
cAMP	Cyclic adenosine monophosphate
CFDA	5(6)-CFDA, SECFSE (5-(and-6)-Carboxyfluorescein Diacetate, Succinimidyl Ester), mixed isomers
CMAC	7-amino-4-chloromethylcoumarin
CO_2	Carbon dioxide
COX	Cyclooxygenase
CVDs	Cardiovascular diseases
dH_2O	Distilled water
$DiOC_6$	3,3'-dihexyloxacarbocyanine iodide
ECM	Extracellular matrix
ECs	Endothelial cells
ELISA	Enzyme-linked immunosorbent assay
eNOS	Endothelial NOS
EPCs	Endothelial precursor cells
$FeCl_3$	Ferric chloride
FITC	Fluorescein isothiocyanate

GBD	Global Burden of Disease
GPVI	Glycoprotein VI
HAECs	Human aortic endothelial cells
HBS	HEPES –Buffered Saline
HCASMCs	Human coronary artery smooth muscle cells
HUVECs	Human umbilical vein endothelial cells
ICAM-1	Intercellular adhesion molecule-1
IEL	Internal elastic lamina
iNOS	Inducible NOS
IP_3	Inositol 1,4,5-trisphosphate
IP	Prostacyclin receptor
LSGS	low serum growth supplement
LTA	Light transmission aggregometry
L-NAME	L-N^G-Nitroarginine methyl ester
L-NIO	N^5-(1-Iminoethyl)-L-ornithine dihydrochloride
L-NMMA	NG-Monomethyl-**L**-arginine, monoacetate salt
L-NOARG	NG-nitro-L-arginine
MSCs	Mesenchymal stem cells
NETs	Neutrophil extracellular traps
NaOH	Sodium hydroxide
NO	Nitric oxide
NOS	Nitric oxide synthase
P-VASP	Phosphorylated- vasodilator-stimulated phosphoprotein
PAF	Platelet-activating factor
PARs	Protease-activated receptors
PECAM-1	Platelet endothelial cell adhesion molecule- 1
PDMS	Polydimethylsiloxane
PGI_2	Prostacyclin
PLA	Poly-L,D-lactic acid
PLC	Phospholipase C
PLGA	Polylactic-co-glycolic acid

PCL	Polycaprolactone
PRP	Platelet-rich plasma
PS	Phosphatidylserine
PTFE	Polytetrafluoroethylene
SERCA	Sarco/endoplasmic reticulum Ca^{2+}-ATPasa
SMCs	Smooth muscle cells
SMGS	Smooth muscle growth supplement
SOCE	Store-operated Ca^{2+} entry
TAFI	Thrombin-activatable fibrinolysis inhibitor
TEBV	Tissue-engineered blood vessel
TEIL	Tissue-engineered intimal layer
TEML	Tissue-engineered medial layer
TF	Tissue factor
TNF-α	Tumour necrosis factor-α
tPA	Tissue-type plasminogen activator
TRITC	Tetramethylrhodamine
TXA_2	Thromboxane A_2
uPA	Urokinase-type plasminogen activator
VASP	Vasodilator-stimulated phosphoprotein
vWF	Von Willebrand factor
VCAM-1	Vascular cell adhesion molecule-1
VEGF	Vascular endothelial growth factor

Associated publications in peer reviewed journals

Musa FI, Harper AGS, Yang Y (2016) A Real-Time Monitoring System to Assess the Platelet Aggregatory Capacity of Components of a Tissue-Engineered Blood Vessel Wall. Tissue Eng Part C Methods. 2016 Jul 1; 22(7): 691–699

Other peer reviewed journals publications

Law JX, **Musa F**, Ruszymah BH, El Haj AJ, Yang Y (2016) A comparative study of skin cell activities in collagen and fibrin constructs. Med Eng Phys. 2016 Sep;38(9):854-61

T Walford, **F I Musa**, A G S Harper (2016) Nicergoline inhibits human platelet Ca2+ signalling through triggering a microtubule-dependent reorganization of the platelet ultrastructure. Br J Pharmacol. 2016 Jan; 173(1): 234–247

Acknowledgement

Thanks to Allah SWT for I am what I am because of you. You have blessed me with too much and I am grateful.

First and foremost, I would like to express my deep gratitude towards both of my supervisors, Prof. Ying Yang and Dr. Alan Harper without whom this thesis would not have been possible. I feel very lucky to have Ying and Alan as my supervisors as both have supported me enormously throughout my experiments and to finish my thesis. Ying has continually provided me with immense knowledge, motivation experience and guidance. Likewise Alan, with his great knowledge and expertise, he continuously supported me in my project, motivated me and provided me with not only with supporting me in my project but also in developing my personal skills and career. I would like to say thank you both although thank you may not be enough.

I would also like to thank my greatest parents and siblings in the world. This thesis is dedicated to my family and I will never forget the sacrifices and the support that you have provided me with. You were patient with me, especially my mum Khadra and both my twin sisters Hamda and Hanan. Thank you for all the babysitting you did for my son Ibrahim. Thanks to my family in law for all the support you have given me in understanding my busy life.

Thank you to all my blood donors and my friends who used to advise me with my PhD journey. Thank you to Sandhya, Anthony, Yanny, Hati, Hamza, Lanxin and Ipek. Each one of these great friends has helped me directly or indirectly with my project.

Last but not least, I would like to thank my husband for being so patient with me and the enormous encouragement I have received from him from the start to finish of my PhD. Words cannot describe how grateful I am to have you in my life. I would also like to deeply thank my son Ibrahim for all the time I sacrificed in spending on the thesis.

Chapter 1

Literature review

1. Introduction

1.1. Haemostasis

Haemostasis is the physiological response to reduce the extent of haemorrhage at sites of vascular injury, while maintaining normal blood flow elsewhere in the circulation (Gale, 2011). This process is tightly regulated as it must be rapidly activated within seconds of an injury to the blood vessel, but the response must also remain localized here to ensure unwanted blood clotting does not occur elsewhere in the undamaged circulation. Haemostasis comprise of two main phases - primary and secondary haemostasis. These two phases of haemostasis are mechanistically intertwined and happen simultaneously (Gale, 2011). Primary haemostasis involves platelet aggregation upon the subendothelial lining exposed by vascular damage to produce a plug which patches up the damaged blood vessel wall, whereas secondary haemostasis involves the activation of the blood coagulation system and deposition of insoluble fibrin to help scaffold together and strengthen the developing blood clot (Palta et al., 2014). Blood vessel damage or endothelial cells (ECs) exposure to particular proinflammatory cytokines causes the balance to shift towards procoagulant or pro-thrombotic phenotype (Van Kruchten et al., 2012). The next section will discuss the multi-stage process that underlies the formation and regulation of thrombus formation.

1.2. The multi-stage process of thrombus formation

1.2.1. Endothelium inhibition of platelets

In a healthy blood vessel exposed to normal blood flow conditions, platelets circulate in an inactive state and do not adhere to the vessel wall or other platelets. ECs normally provide an anti-thrombotic and anti-coagulant surface by secreting several inhibitors of platelet function, as well as inhibitors of the coagulation cascade. Prostacyclin (PGI_2) and nitric oxide (NO) are the main anti-platelet agents secreted by ECs (Bunting et al., 1983). Both molecules trigger a signalling cascade leading to an increase in cytosolic cAMP in platelets, that works to block their aggregation (Mitchell et al., 2008). PGI_2 and NO are continuously released from ECs but their production increases in

response to certain molecules involved in coagulation processes such as bradykinin and thrombin. Aggregating platelets also release adenosine triphosphate (ATP) which increases PGI_2 and NO production from surviving ECs around the edge of the site of puncture, limiting thrombus formation to the site of vascular damage. These give-and-take responses between ECs and platelets are key to regulating the localised activation of the haemostasis system.

PGI_2 is produced by vascular endothelium and acts as a vasodilator and an inhibitor of platelet aggregation (Bunting et al., 1983). PGI_2 is a product of arachidonic acid metabolism by cyclooxygenase (COX) followed by metabolism of the COX product, prostaglandin H_2, by prostacyclin synthase. The importance of endogenous PGI_2 in preventing arterial thrombosis has been convincingly demonstrated by use of the prostacyclin receptor knockout mice (Murata et al., 1997). After endothelial damage to the carotid arteries, prostacyclin receptor $(IP)^{-/-}$ mice had extensive carotid thrombi that were occlusive and led to death in a proportion of the mice, whereas wild-type mice had smaller, non-occlusive thrombi and there were no deaths (Murata et al., 1997). It follows that the regulation of vascular PGI_2 production is an important process for normal regulation of haemostasis.

NO is a soluble gas with a half-life of 6 – 30 s, continuously synthesized from the amino acid L-arginine in endothelial cells by the constitutive calcium calmodulin-dependent enzyme nitric oxide synthase (NOS; Palmer et al., 1988). There are two forms of NOS expressed in the endothelium: endothelial NOS (eNOS; type III) and inducible NOS (iNOS, type II). In the intact blood vessel wall, most of the NO is presumed to arise from the activity of endothelial eNOS (Förstermann et al., 1991). There is a continuous, basal release of NO dependent upon eNOS activity which represents a sizeable portion of the total nitric oxide-releasing capacity of native endothelial cells. Once the endothelium has been damaged, exposure of smooth muscle cells (SMCs) to cytokines and other stimulators of NOS induction may have important physiological consequences for the blood vessel. eNOS has been shown to play a minor role in inhibiting arterial thrombus formation using

eNOS knockout mice (Ozüyaman et al., 2005). A minimal effect on platelet aggregation was observed and this was found not to be linked with accelerated arterial thrombosis *in vivo*. This was tested using aggregometry studies of platelets from WT and eNOS$^{-/-}$ mice which showed no significant difference between the two. Also, no marked increase in cGMP formation and vasodilator-stimulated phosphoprotein (VASP) phosphorylation was observed. In addition, thrombin-induced *P*-selectin surface expression remained unchanged in eNOS$^{-/-}$ platelets. Another study has shown eNOS$^{-/-}$ knockout mice had significantly decreased bleeding times even after endothelial NO production was controlled (Freedman et al., 1999). This suggests that platelet-derived NO appears to play an important counterregulatory role after platelet activation by inhibiting the recruitment of platelets to the growing thrombus (Freedman et al., 1997). Others have shown that eNOS deficiency is associated with increased platelet recruitment and enhanced fibrinolysis due to the lack of NO-dependent inhibition of Weibel-Palade body release (Iafrati et al., 2005). These anti-aggregatory mechanisms are crucial for maintaining a physiological laminar blood flow without disruption to the closed vascular system. It is only when these barriers are overcome that platelets can become activated. That can happen after local injury or in response to the rupture of an atherosclerotic plaque.

1.2.2. Platelet adhesion to subendothelial matrix

Upon vascular injury, the endothelial lining is damaged removing its inhibitory effect and the flowing blood becomes exposed to the subendothelial matrix. This allows platelets to become activated by binding to adhesive ligands in the subendothelial matrix such as collagen, laminin, fibronectin and thrombospondin (Watson et al., 2010). Type I and III collagens, are the most potent activators of platelets providing much of the thrombogenic potential of the subendothelial matrix (Clemetson and Clemetson, 2001). In addition these collagens can also bind to von Willebrand Factor (vWF) with high affinity (Lecut et al., 2004). VWF also binds to exposed collagen to further increase the adhesive potential of the subendothelial matrix. At high shear rate, vWF acts by slowing down the platelets to allow adhesion and binding to other components of the

subendothelial matrix. This occurs by reversibly joining its A1 domain with GPIbα found on platelets. This rolling and tethering stage facilitate the formation of subsequent interactions between platelet receptors (integrin α2β1 and glycoprotein VI; GPVI) to collagen, leading to firm adhesion and platelet arrest. Synergistic actions between the platelet receptors cause platelets to adhere optimally. For instance, binding of integrin α2β1 and to collagen strengthen each other's action (Auger et al., 2005). These interactions are further strengthened by activation of GPVI (Lecut et al., 2004; Pugh et al., 2010; Siljander et al., 2004). In addition to these adhesive ligands, platelets are also activated by thrombin produced by tissue factor (TF) released from the vessel wall. Thrombin cleaves and activates the Protease-activated receptors (PARs), PAR1 and PAR4, and may also bind to GPIb activating distinct signalling pathways through each of these receptors that lead to different degrees of platelet activation (Nieman, 2016).

Upon activation, platelets undergo a number of changes mediated by an agonist-evoked rise in cytosolic Ca^{2+} concentration ($[Ca^{2+}]_{cyt}$). This is elicited by platelet cell-surface receptors binding to both the adhesive and soluble ligands listed above to their respective receptors. The activation of these receptors generally leads to either phospholipase C (PLC) β or γ activation, which catalyses the production of Inositol 1,4,5-trisphosphate (IP_3). IP_3 in turn triggers Ca^{2+} release from the dense tubular system (the platelet equivalent of the endoplasmic reticulum) through its ability to activate IP_3 receptors. An increase in $[Ca^{2+}]_{cyt}$ plays a vital role in platelet activation where all stages of platelet plug formation requires a rise in the cytosolic Ca^{2+} concentration as well as, shape change and alternation of αIIbβ3 integrins to high affinity ligand binding (Tadokoro et al., 2011). The earliest observable events in response to these Ca^{2+} rises are changes of platelet shape from quiescent discoid shaped platelet and starting to spread over the subendothelial matrix extended thin filopodia to create spiny spheres.

1.2.3. Secretion and Thromboxane formation

After the initial adhesion and activation of platelets to the subendothelial matrix, platelets start to produce thromboxane A_2 from arachidonic acid, as well as release stored autocrine activators of

platelets from their dense granules to try to recruit more circulating platelets to the surface of the thrombus. Dense granules release adenosine di-phosphate (ADP), ATP and serotonin which facilitates the second wave of platelet aggregation following integrin activation (Johnston-Cox et al., 2011). ADP binds to the P_{2Y1} and P_{2Y12} receptor on platelets which acts to enhance and extend platelet activation allowing the platelet by both enhancing cytosolic Ca^{2+} rises as well as mediating G_i-mediated activation of integrin $\alpha_{IIb}\beta_3$ (Stefanini and Bergmeier, 2010).

1.2.4. Platelet aggregation and plug stabilisation

In quiescent platelet, the fibrinogen receptor, integrin $\alpha_{IIb}\beta_3$ a is normally kept in a resting or low-affinity state in circulating platelets, but transforms into a high-affinity "activated" state after platelet activation. Upon platelet activation, activated integrin $\alpha_{IIb}\beta_3$ a, binds to its ligands (fibrinogen) mediating a stable platelet aggregation, and thrombus formation. The integrin–proximal intracellular signalling mechanism that induces changes in the extracellular ligand binding domain of integrins from a "low-affinity" state to the activated state is referred to as "inside-out" signalling (Figure 1.1; Li et al., 2010). This process activates the ligand binding function of integrins via the binding of talin and kindlin proteins to the cytoplasmic domains of integrin $\alpha_{IIb}\beta_3$ (Shen et al., 2012).

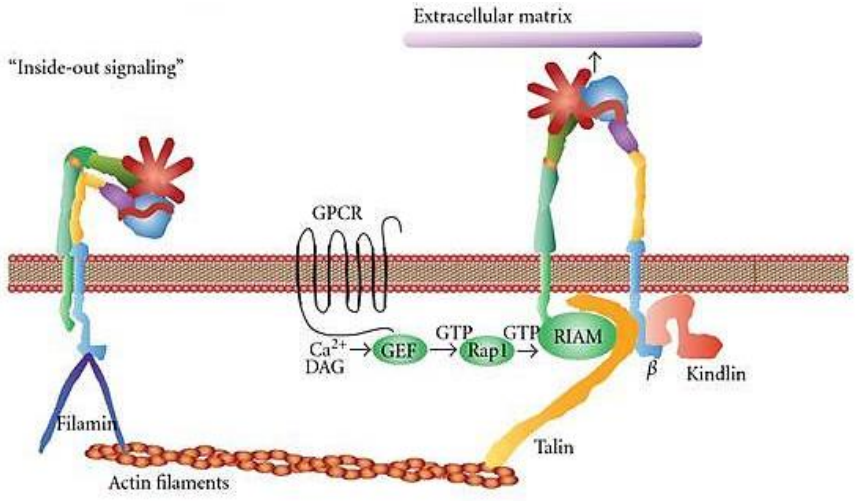

Figure 1.1 – "Inside-out" signalling. The "Inside-out" signalling strengthens adhesive contacts and the appropriate force necessary for integrin-mediated cell migration, invasion, ECM remodelling, and matrix assembly (Shen et al., 2012).

1.2.5. Secondary haemostasis - Activation and regulation of the blood coagulation cascade

The blood coagulation system is a cascade of events involving proteolytic activation of plasma-based zymogenic forms of clotting factors to generate thrombin and fibrin to support haemostasis. Briefly, this cascade is composed of intrinsic and extrinsic pathways which are triggered by either negatively-charged surfaces such as inorganic polyphosphates secreted from the platelet dense granules, as well as TF in the subendothelium which becomes exposed to plasma in response to vessel damage (Adams and Bird, 2009). Both pathways converge on a final common pathway to activate factor X, causing the conversion of prothrombin (factor II) to thrombin and finishing with the conversion of fibrinogen to fibrin. This section will cover a brief discussion about the link between platelet activation and localised regulation of the coagulation system at the site of vessel damage as part of fibrin clot formation as well as its resolution through the fibrinolysis pathway.

The coagulation cascade can be categorised into three phases: (a) initiation phase, (b) amplification phase and (c) propagation phase. The initiation phase simply involves TF exposure to coagulation factors by forming a catalytic complex with factor VIIa (TF:FVIIa). This forms what is known as the 'extrinsic factor tenase complex' thus activating the extrinsic pathway leading to small amount of thrombin generation (Adams and Bird, 2009; Bates and Weitz, 2005). The next phase follows (amplification phase) involves the thrombin triggering the activation of factor VIII to factor VIIIa, as well as the formation of factor IXa by the extrinsic tenase complex to form the 'intrinsic factor tenase' complex (FIXa:FVIIIa) on platelets' surfaces but also on microparticles (Figure 1.2). This pathway is significant as it results in an increased thrombin production and also 50 - 100-fold increase in factor Xa production (Adams and Bird, 2009).

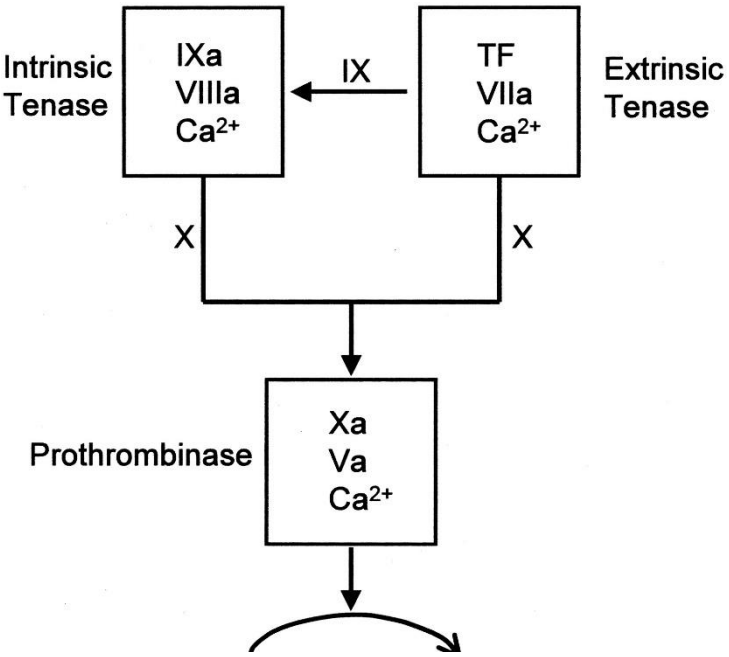

Figure 1.2 – Factor VIIa binds to tissue factor to form the extrinsic tenase, initiating the coagulation cascade. This in turns activates factors IX and X into factors IXa and Xa, respectively. Factor IXa binds to negatively charged phospholipid surfaces where it interacts with factor VIIIa to form intrinsic tenase. This complex activates factor X into factor Xa. Factor Xa then binds to factor Va to form prothrombinase, thereby increasing the rate of factor Xa–mediated conversion of prothrombin to thrombin. Thrombin then converts fibrinogen to fibrin (Bates and Weitz, 2005).

This phase involves platelet recruitment at the site of injury as well as the activation of the clotting cascade on their surface. This stage is dependent upon the number of platelets involved and results in a 'thrombin burst' causing fibrin formation from fibrinogen to generate a stabilised clot. The binding of these clotting factor to the platelet surface is dependent on the availability of extracellular Ca^{2+} to act as a cofactor, alongside surface expression of negatively charged phospholipids such as phosphatidylserine (PS) on the platelet surface. The expression of PS on the platelet surface is dependent on strong platelet activation, leading to large, prolonged Ca^{2+} signals triggering the activation of the platelet phospholipid scramblase, anoctamin 6 to move phosphatidylserine from the inner to the outer leaflet of the platelet membrane (Heemskerk et al., 2013). This requirement for the platelets to provide a catalytic surface coagulation, helps localise the amplification stage of coagulation in the vicinity of the thrombus. The action of locally-formed thrombin on PAR1 and PAR4 platelet receptors ultimately helps in this process by reinforcing

platelet activation triggering the prolonged platelet activation required for PS exposure. Thrombin also helps trigger other locally circulating platelets lead to the activation of integrin αIIbβ3 – therefore providing a basis for the concomitant development of the thrombus as well as the fibrin deposition that will structurally support it (Mehrbod et al., 2013).

Fibrin monomers join together to form polymers and the action of factor XIIIa (activated by thrombin) leads to cross-linkage of fibrin strands. This forms a stable fibrin interaction. Thrombin-activatable fibrinolysis inhibitor (TAFI) is also activated by thrombin which acts to protect the clot from plasma-mediated fibrinolysis (Adams and Bird, 2009). Hence, we summarise that the coagulation cascade is essential for homeostasis, acting to seal localised vascular injuries and that platelet activation and coagulation are complementary processes.

The fibrinolysis pathway also plays an important role in haemostasis (Kolev and Longstaff, 2016). Fibrinolysis typically results in clot dissolution and is initiated endogenously as plasminogen is converted to plasmin by either of two primary serine proteases, proteases tissue-type plasminogen activator (tPA) and urokinase-type plasminogen activator (uPA; Chapin and Hajjar, 2015). The formed plasmin cleaves and breaks down fibrin leading to clot breakdown and dissociation. Dysregulation of this pathway may lead to vascular occlusion due to thrombosis, and so these serine proteases are down-regulated by plasma-localised protease inhibitors, such as antithrombin and tissue factor pathways inhibitor, or the activity of protein C on the surface of endothelial cells (Gale, 2011; Palta et al., 2014). These regulatory systems help localise the activity of the blood coagulation system and prevent aberrant activation of this cascade in undamaged areas of the vasculature. Therefore, haemostasis should be maintained by simultaneously avoiding thrombosis via maintaining a balance between pro-thrombotic and anti-thrombotic systems. However, if the primary or secondary haemostatic system is impaired or activated unnecessarily this can lead to a number of haemostatic pathologies.

1.3. Diseases linked to haemostasis

There are a number of congenital disorders that affect the normal activation of primary and secondary haemostasis that cause excessive bleeding in patients. These include haemophilia types A and B which are both caused by a recessive expression of the defective gene by the X chromosome. Hemophilia A is due to deficiency of the coagulation factor VIII, and hemophilia B is due to deficiency of factor IX. Other bleeding disorders include von Willebrand disease which is a congenital deficiency in vWF. This disease causes defects in platelet aggregation but also causes a deficiency of factor VIII (Ruggeri, 2007). In addition, defects in other coagulation factors exists such as factors XI, factor VII and prothrombin, however these are low in frequency. Moreover, bleeding disorders can arise from deficiencies in α2 antiplasmin, a plasminogen inhibitor, or plasminogen activator inhibitor-1. The former resulting in an increased fibrinolysis and the latter resulting in a lack of control of fibrinolysis by not breaking the activity of plasminogen activation factor (Carpenter and Mathew, 2008). There are also bleeding disorders caused by platelet function defects which include storage pool disorders. This heterogeneous group of congenital disorders have a common deficiency in granules or their constituents such as defects in ADP release from activated platelets. In addition to storage pool disorders, Glanzmann thrombasthenia and Bernard–Soulier Syndrome are other defects that are known to cause excessive bleeding in patients affected by these diseases. Glanzmann thrombasthenia is a genetic disorder that leads to qualitative or quantitative disturbance in the platelet membrane GPIIb-IIIa complex. Bernard–Soulier Syndrome also caused by a lack or qualitative defect in the platelet membrane receptor GPIb-IX-V complex, leading to inability of platelets to bind to vWF during the initial steps of platelet adhesion (Simon et al., 2008).

In contrast to bleeding disorders, thrombosis is caused by overactivity of the primary or secondary haemostasis system and leads to the formation of unwanted blood clots within the intact circulatory system. These can be classified into three different forms, (i) arterial, (ii) venous

thrombosis and (iii) mixed microvascular form. Venous and arterial thrombi are formed in their respective parts of the circulatory tree, where they are triggered by distinct pathological processes. Arterial thrombi are generally formed principally from platelets usually triggered by the rupture of an atherosclerotic plaque leading to abnormal release of collagen and tissue factor into the bloodstream. These form white clots which are distinct from the red clots found in venous thrombosis (Franchini and Mannucci, 2008). Virchow established the risk factors for venous thrombosis back in the 19th Century where he identified roles for venous stasis, injury to the vessel wall and a hypercoagulable state as key risk factors in the development of venous thrombosis. Nonetheless, it is only recently that the cellular mechanisms underlying venous thrombosis have been identified. However, Wagner *et al* (2012)., have shown that neutrophils become activated under conditions associated with changes associated with each part of Virchow's triad (Wagner and Frenette, 2008). These activated leukocytes release their nuclei as neutrophil extracellular traps (NETs). The negatively charged histones provide a surface that appears to be able to activate both platelets and the intrinsic coagulation cascade, leading to the onset of thrombosis formation. These thrombi can do significant damage through their ability to occlude blood vessels blood vessels either directly or by breaking off from the initial clot (embolisation) and lodging in another distant circulation (Heit et al., 2016).

Blocking blood supply to the downstream tissue can trigger a number of potentially life-threatening disorders such as heart attacks, strokes and pulmonary embolisms. These acute cardiovascular events are amongst the deadliest of range of cardiovascular diseases (CVDs) which including diseases of the cardiac muscle and of the vascular system supplying the heart, brain, and other vital organs. CVDs remain the most common cause of death worldwide, with the 2013 Global Burden of Disease (GBD) study estimating that CVDs caused 17.3 million deaths globally (Townsend et al., 2016). CVDs accounts for more than 4 million deaths each year across Europe, accounting for 45% of all deaths (Townsend et al., 2016).

1.4. Haemostasis models

1.4.1. In vitro models

Due to ethical issues involved in undertaking *in vivo* testing in humans, many studies of human platelet function and thrombus formation are conducted *in vitro*. A variety of methods are available to assess platelet function such as measuring platelet aggregation using light transmission aggregometry (LTA), expression of activation markers such as P-selectin or phosphatidylserine exposure using flow cytometry, or measurement of soluble markers of granule secretion such as ATP or 5-HT. Others include, solid-phase binding assays using coverslips, an enzyme-linked immunosorbent assay (ELISA)-based binding assay using specific antibodies or Immunodetection via colorimetry is an alternative for using radioactive iodine as the detector (Ledford-Kraemer, 2010; Lopez and Zheng, 2013). These assays however fail to capture much of the physical flow conditions inside the human body.

1.4.1.1. Parallel plate flow chambers (2-dimensional models)

A more realistic *in vitro* model is the perfusion of platelets or whole blood through a parallel plate flow chamber in which physiological shear rates of blood flow can be generated (Chung et al., 2003; Dong et al., 2002; Sakariassen et al., 2001; Van Kruchten et al., 2012). These chambers are used to study platelet adhesion and aggregation upon a coverslide coated with an adhesive platelet ligand. In addition, blood coagulation can also be simultaneously studied when whole blood is used. Unlike most other platelet function tests, experiments with flow chambers take into account the physical parameter of blood flow and therefore the influence of haemodynamics on the participating cells and biomolecules. Therefore, these are useful tools to use in determining the signalling events underlying blood clotting at a molecular level.

Currently used parallel plate flow chambers include custom-made and commercial flow devices, that are widely used in studying thrombus formation (Van Kruchten et al., 2012). Parallel plate flow chambers usually involve perfusion of platelets over a platelet-activating surface at physiological

shear rates. Hence the device can provide a novel insight into the haemostatic function of platelet activation, particularly in combination with fluorescence microscopy. Microscopes are continuously being improved by the use of high-resolution cameras to improve the quality of digital images. Currently used flow chambers include parallel-plate flow chambers, newly developed biochips with microfluidic channels and rectangular microcapillaries, all of which have been used to study the thrombus-forming processes (Roest et al., 2011). This facilitates real-time monitoring of platelets aggregation under shear stress. However, these chambers are mainly used to assess platelets behaviour upon exposure to immobilised agonists in the absence of the cells of the blood vessel wall and cannot be used to study 3-dimensional vascular models. A previous study compared the effect of currently used *in vitro* devices with regards to pre-coating the devices for flow experiments (Roest et al., 2011). Most studies used collagen coating (92%) for their assays, with less popular coatings including fibrinogen, vWF, synthetic peptides or the use of an endothelial cell monolayer (Roest et al., 2011; Shi et al., 2016; Van Kruchten et al., 2012). The study concluded that care should be taken to maintain laminar flow and recommended the use of Horm type I collagen for testing platelet aggregation. The use of collagen-coated surfaces are the closest resemblance to physiological conditions *in vivo* and are thus preferred for flow assays (Heemskerk et al., 2011).

There are at least 20 different subtypes of collagen (Manon-Jensen et al., 2016). The presence of these differing collagen isoforms in the vasculature is dependent on the structure and function of the vessel in question. In an uninjured arterial wall, type I and III collagen are the predominant collagen isoforms found in the Tunica media and adventitia. Platelet assays mainly use fibrillar and monomeric forms of these arterial collagen isoforms d to study platelet aggregation to attempt to replicate *in vivo* conditions. *In vitro* assays mainly use fibrillar forms of type I collagen from equine tendons, calf skin, and human placenta, although types III, and IV have also been used (Li et al., 2013; Wu et al., 2000). Monomeric collagen forms can also be used to allow the monitoring of platelet aggregation under physiological flow conditions *in vitro*. To do this they are typically solubilised in acetic acid and further coated onto perfusion chambers prior to perfusion with

platelet suspensions, plasma or whole blood (Li et al., 2013; Wu et al., 2000). These types of collagens differ from Horm collagen, a native form of type I and III collagens. These include differences in the (i) mix of collagen isoforms being used and (ii) their tertiary and quaternary structures of the collagen formed during re-construction. The commercially available Horm collagen is described as a solution of type I (95%) and type III (5%) fibrils isolated from equine tendon (Bianchini et al., 2015). Hence this suggests that the presence of both these types of collagen is essential and how they present themselves in the matrix to the platelets.

Shi et al., (2016) perfused whole blood over collagen-coated microfluidic channels using different shear rates. This study showed that platelet thrombus formation varied under different shear rates (Shi et al., 2016). The thickness of the formed thrombi was shown to be proportional to shear rate used. Using a high shear rate (2500-5000 s^{-1}) causes thick thrombus formation with tendency to embolise, which was regulated by an attachment-detachment balance. These data therefore highlight the importance of recreating the physical environment in which thrombus formation occurs.

Lopez & Zheng designed a model consisting of *in vitro* tissue engineered synthetic capillary model using endothelial cell-coated microchannels, to study biological events occurring in microcirculation such as remodelling, angiogenesis and ECs function (Lopez and Zheng, 2013). This study aimed to overcome the limitation of previous challenges faced by microfluidic chambers that include: (i) difficulty with fabricating a chamber in which the vessel has cylindrical morphology and (ii) non-distensible. Polydimethylsiloxane (PDMS) and collagen were used to create channels in which ECs were seeded. However, this system is only representative of capillaries and lacks other key cells found in larger veins and arteries. This simplified model involving a single layer of ECs is missing the more complex biological and chemical environment of arteries required to study vascular diseases such as atherosclerosis. Though much progress has been made in the fabrication of microfluidic chambers, they still have limitations in their ability to mimic the geometry of actual blood vessels.

One disadvantage is that conventional microfluidic chambers have square or rectangular cross sections resulting from the limitations of the fabrication procedures. These features result in inhomogeneous and unphysiological shear conditions on the vessel wall, as the shear stresses are very different at corners than at the centre of the walls (Zheng et al., 2014). This inhomogeneity creates artfactually-high shear stresses that hinder interpretation of studies of shear-dependent platelet-vessel wall interactions. Extensive studies have been studied to establish the foundations of adhesion, activation, aggregation and granule secretion concepts in platelets *in vitro* (Zheng et al., 2014).

Though these *in vitro* studies are reasonable starting point for studying the basic mechanisms of thrombus formation, these studies lack the precise control of the properties of the blood vessel surface that plays a central role in regulating the formation of platelet thrombi. Thus, *in vivo* studies in animal models provides a system which can more faithfully recreate the physical and chemical environment found in native human blood vessels (Falati et al., 2002; Furie and Furie, 2008, 2007, 2005).

1.4.2. In vivo models

In vitro studies fail to replicate the haemodynamic factors and/or the complexity of *in vivo* system with regards to direct and indirect platelet activation with other cells such as endothelium and leukocytes. To address these weaknesses and limitations, research has turned into animal models to study haemostasis (Bellido-Martín et al., 2011a; Falati et al., 2002; Furie and Furie, 2008), emphasising techniques such as intravital microscopy, a tool that allows imaging of several biological processes in live animals (Masedunskas et al., 2012). In these experiments thrombus formation is induced by using a variety of methods to artificially damage the endothelial lining during the course of experiment. The effects of this formation on blood flow through the injured vessel can be measured using doppler or temperature sensing probes. In addition, intravital

microscopy can be used to allow direct visualisation of thrombus formation using fluorescently labelled platelets.

Several *in vivo* blood vessel injuries can be introduced in mice and these include: (i) mechanical disruption, (ii) photo-oxidation of ECs using Rose Bengal dye, (iii) vessel ligation, (iv) oxidation with $FeCl_3$ and finally (v) the commonly used laser-induced vessel wall injury. Laser induced vessel wall injury is the second mostly used technique after $FeCl_3$, due to its high level of resolution (Denis et al., 2011), nevertheless the rest of the techniques employed can create reliable clotting responses. Though there are known differences in the molecular mechanism underlying the formation of thrombi in these different models. Due to these differences, the next section will review each of these methods.

1.4.2.1. Ferric chloride model

The use of $FeCl_3$ as a thrombogenic agent has become a common method for investigating the mechanisms of thrombosis in transgenic mice (Bonnard and Hagemeyer, 2015; W. Li et al., 2013). This agent is typically applied to the outer aspect of arteries inducing oxidative damage to vascular cells. However, it can also be applied on the luminal side of the vessel wall, since Tseng et al., (2006) have shown that ferric ion permeates the endothelial basal lamina before entering the arterial lumen via an endocytic-exocytic pathway, damaging not only endothelial cells but also SMCs (Tseng et al., 2006). A similar study was recently done in rats using ZsGreen1 green fluorescent protein-labelled platelets where $FeCl_3$ caused time-dependent increase in fluorescent thrombi (Mizuno et al., 2016). Studies of genetically-altered mouse models have showed two independent pathways involved in platelet activation (Dubois et al., 2006a; Furie and Furie, 2008). The ferric chloride model, which causes denudation of the endothelium and exposure of the subendothelial matrix, has shown to be dependent on collagen pathway. Using this method, a range of times measured between 5 and 30 minutes has been reported from injury to complete vessel occlusion (Bonnard and Hagemeyer, 2015), which suggests that $FeCl_3$ concentrations, types of anaesthesia, surgical techniques, mouse age and genomic background, method of measuring blood flow, and other

environmental variables have substantial effects in this model. This wide variability may be acceptable for a single study, but it makes it very difficult to compare studies from different groups and may make detection of subtle differences difficult.

1.4.2.2. Laser and mechanical injury models

The laser-induced injury model uses a laser to create a defined area of damage to the blood vessel of interest to trigger a clotting response. Platelets aggregation in this model has been found to be dependent on tissue factor and thrombin production, since this type of injury causes an insignificant amount of collagen exposure. This therefore represents a difference of the $FeCl_3$ model as the clotting observed in the laser injury model is independent of the collagen receptor GPVI and vWF (Dubois et al., 2006a). Together, both $FeCl_3$ and laser induced injury models trigger two independent pathways of platelet activation suggesting that both of these pathways may mediate the response in the human circulation (Bellido-Martín et al., 2011a). Despite the difference in the initiating trigger for the onset of thrombus formation, the consequences of platelet activation are the same in these two types of injury models. However, it is still unclear how platelets are recruited to adhere to the laser injured vessel wall in the absence of collagen exposure, this may be caused by activation of surrounding endothelial cells caused by the laser, leading to the expression of adhesive molecules that are able to bind platelets to the damaged vessel wall.

Tang et al., (2016) have standardised an *in vivo* mouse model to study thrombus formation induced by mechanical injury (Tang et al., 2016). The study defined two degrees of injury induced by pinching the abdominal aorta with haemostatic forceps. This technique is able to induce two different grades of vessel wall damage (moderate and severe). Thrombus formation was monitored in real-time using a fluorescent microscope coupled to a CCD camera. A moderate type of injury has shown a thrombus formation that peaks are 1 minute post injury and resolves within 3 minutes whereas a larger thrombus was observed in the severe type injury (Tang et al., 2016).

1.4.2.3. Benefits and limitations of mouse models

In the past, *in vivo* animal studies of thrombus formation have benefited significantly from using genetically modified mice. These allow targeted manipulations of the expression of a range proteins involved in the signal transduction pathways underlying platelet activation to help us understand their role in thrombus formation and allowing us to study haemostasis at a molecular level under physiological conditions (Sachs and Nieswandt, 2007). Mice models are attractive for use in platelet research owing to their small size, high fertility and exceptional reproductive capacity as well as low costs involved in maintaining them. In addition, 99% of mice genes are equivalent to humans, making them an ideal mode for i*n vivo* study of human diseases (Guénet, 2005).

Besides all these advantages there are also limitations in studying haemostasis and clotting disorders in mouse models. Extrapolation of data from mouse to human platelets should be performed cautiously as there are known variations between the two species that may influence the interpretation of data. These differences include: (i) platelet count and volume; (ii) differences in expression of some platelet receptors such as PARs and FcγRIIa; (iii) variations in haemodynamic shear rates in mice and human and (iv) the use of general anaesthetics in mice for *in vivo* studies, which may interfere with normal thrombus formation (Atkinson et al., 1985; Rowley et al., 2011; Sachs and Nieswandt, 2007; Weinberg and Ross Ethier, 2007). Together, these limitations therefore suggest that a humanised model system in which to recreate the *in vivo* environment found with the human circulatory system may provide additional insight into human thrombus formation.

1.5. Tissue engineering of blood vessel models

1.5.1. Principles of tissue-engineering

Tissue engineering is a multidisciplinary field that combines the principles of engineering and life sciences to develop biological replicas of native tissues for the replacement of damaged organs in human patients. This employs the notion of using the body's natural healing responses in combination with engineering principles to grow a new tissue (Langer and Vacanti, 1993). Tissue

engineering approaches have been intensively used to develop a human blood vessel constructs to recreate the physiological features found in the human body to study the processes of haemostasis and the pathological processes of thrombosis or be used in grafting to replace damaged blood vessel tissues. An ideal tissue engineered blood vessel construct should closely replicate the structure and function of the native vascular tissue. It is pre-requisite to fully understand the anatomy and physiology of blood vessel layers to enable the fabrication of functional TEBVs.

1.5.2. Anatomical structure and function of native blood vessel wall

The native arterial and venous wall is composed of three layers - the *tunica intima*, *tunica media* and *tunica adventitia*, (Figure 1.3; Patel et al., 2006).

1.5.2.1. Intimal layer

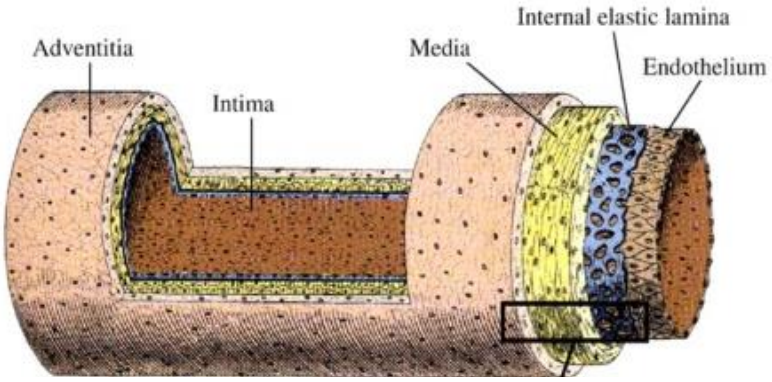

Figure 1.3 Shows layers of the blood vessel wall (Patel et al., 2006)

The tunica intima forms the innermost layer composing of a continuous layer of ECs. This layer is separated from the subsequent (medial) layer by a dense elastic layer known as the *internal elastic lamina (IEL)*. The IEL represents a flexible barrier between the endothelium and inner SMCs layer and may have a role in atherogenesis via its modulation of diffusion across the artery wall (Sandow et al., 2009). Fenestrations in the IEL are implicated in myoendothelial signalling, enabling the passage of endothelial and SMCs projections and subsequent contact between these cell layers in some vessels (de Wit et al., 2006). The endothelial cell layer is crucial in negatively regulating the activation of the haemostasis system by both creating a physical barrier between the blood and the subendothelial matrix, as well as through its ability to secrete inhibitors of platelet function.

The endothelial cell layer's impermeability is created by the formation of tight junctions between the endothelial cells. Three types of EC junction have been identified and these are: (i) tight

junctions; (ii) adherens junctions and (iii) gap junctions (Figure 1.4; Wallez and Huber, 2008). The main constituent of tight junctions is a transmembrane protein known as 'occludins'. This transmembrane is associated with other cytosolic proteins to seal the EC layer. Tight junctions connecting the ECs, limit the diffusion of even smaller molecules (< 1 kD) to go through the vessel (Yuan and Rigor, 2010). These junctions cause the ECs to appear to some extent fused together. Moreover, adherens junctions are Ca^{2+} channel dependent which are formed by several transmembrane proteins such as cadherins and VE-cadherin, which are cell junction whose cytoplasmic face is linked to actin cytoskeleton. These endothelial cell junctions are involved in regulating endothelial cell permeability to circulating blood cells according to the functional requirement of body organ (Yuan and Rigor, 2010). The permeability of ECs changes by the rearrangement of surface occludins and cadherins, leading to activation of matrix metalloproteinases or endopeptidases that degrade extracellular matrix (ECM) proteins (Alexander and Elrod, 2002). Impairment of function of these endothelial cell junctions may lead to edema (an increase in the interstitial volume). Some endothelial cell stimuli such as arterial natriuretic factor (ANF), thrombin or histamine provoke a fast but temporary rise of vascular permeability, whereas vascular endothelial growth factor (VEGF) and cytokines trigger a prolonged response. The majority of these agonists are released inflammatory mediators (Mitchell and Niklason, 2003). Thus, ensuring endothelial cell permeability when conducting *in vitro* assays, is key to ensure that any endothelial monolayer is behaving similarly to its native counterpart. In addition, ECs also synthesise and releases a number of paracrine substances acting on cells of the blood. By secreting

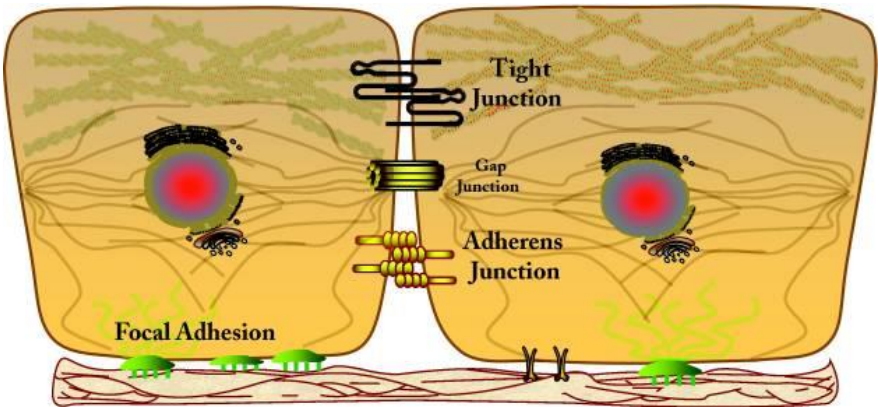

Figure 1.4 - Shows endothelial cell-cell junctions that control permeability of blood cells (Yuan and Rigor, 2010).

specific molecules like NO and PGI_2, endothelial cells inhibit platelet activation and prevent thrombus formation as detailed above.

Following blood vessel injury, ECs are lost from the site of vascular injury and so expose the subendothelial matrix triggering the activation of the haemostatic system. In addition, ECs surrounding the damaged blood vessel wall exhibit local activation induced by inflammatory cytokines. This shifts the balance from its normal inhibitory towards favouring platelet aggregation and thrombus formation. This shift occurs as ECs start to increase the production and expression of pro-aggregatory or pro-coagulant molecules and suppressing the normal anticoagulant mechanisms, facilitating activation of platelets and the blood coagulation system (Gross and Aird, 2000; Preissner et al., 2000). There are two main pro-aggregatory mediators released by activated ECs that support platelet aggregation - platelet-activating factor (PAF) and vWF. PAF is a strong platelet activator which is produced by ECs promoted by thrombin, histamine and cytokines. vWF is normally stored within Weibel–Palade bodies of ECs and constitutively released into the plasma (Denis et al., 2011). The action of thrombin causes the release of vWF from their stores. Additionally, vWF has a function in stabilising factor VIII, involved in coagulation. This coagulation factor is necessary for binding of platelets to TF during vessel wall injury (Ruggeri et al., 1999). Interference with the anti-aggregatory function of the endothelial lining evokes a regulatory mechanism that maintains a physiological blood flow.

1.5.2.2. Medial layer and the associated extracellular matrix

The middle layer of the blood vessel, the *tunica media*, is composed of SMCs that provide structural support, mechanical strength and contractility to the blood vessel wall. SMCs are arranged helically, surrounded by elastin and collagen fibres that form a strong, elastic extracellular matrix. A major function of the vascular SMCs in medium to large vessels is to synthesize and organize the unique ECM responsible for the mechanical properties of the wall, these include elastin and collagen. Hence the ability of SMCs in providing these key proteins is essential to maintain mechanical

properties of the wall. The production of a functional ECM requires the coordinated expression of complex sets of genes that encode ECM proteins as well as the enzymes responsible for their secretion and assembly (Wagenseil and Mecham, 2009). Elastin is an ECM protein that is at least 5 fold more extensible compared to a conventional rubber (Alberts et al., 2002). This astonishing property of elastin enables large arteries to expand during each heartbeat, storing mechanical energy to help ensure a continuous pressure gradient driving blood flow through the circulation between each cardiac cycle. In addition, the mechanical properties of arteries are controlled by the activity of SMCs. Collagen is less extensible compared to elastin, but offers mechanical strength to the vessel to protect it from aneurysm (Guthold et al., 2007). Collagen is found in the arteries of which type I, III, and V collagens are fibril-forming, with types I and III being mainly responsible for imparting strength to the vessel wall (Stuart and Panitch, 2009).

Under physiological conditions, SMCs possess a contractile phenotype and control the dilatation and constriction of blood vessels thus regulating blood flow. Under certain pathological conditions, SMCs convert to a synthetic and non-contractile phenotype (Patel et al., 2006). This synthetic phenotype results in proliferation and increased matrix production in the tunica media. In contrast to the endothelial cell layer, the subendothelial matrix within the medial layer normally provides a pro-thrombotic surface to trigger the activation of circulating platelets. Blood vessel damage leads to the platelets exposure to collagen within this layers hence their adhesion and activation (Patel et al., 2006). Due to its central role in triggering activation of the haemostatic system, the molecular basis of platelet-collagen interaction has been a major focus of research, especially its structure and its influence on platelet activation (Shinohara et al., 2013; Stinson et al., 1979). The role of collagen in platelet activation will be explained later in detail. The medial layer is separated from the adventitia (outer layer) by a dense elastic membrane called the *external elastic lamina*.

1.5.2.3. Adventitial layer

The adventitia consists of connective tissue sheath without a distinct external border. It has a function of anchoring the blood vessel to ECM. Thus, this layer has a role in tethering the blood vessel to surrounding tissues. Fibroblasts are the major cell component found in the adventitia, but in larger arteries this may also possess network of smaller vessels called the vasa vasorum which supply the blood vessel wall with oxygen and nutrients as the diffusion distance is too long from the arterial lumen. It may be possible that the ECs of the vasa vasorum secrete vasoactive substances such as NO to the surrounding adventitial compartment which can influence its function (Kleschyov et al., 1998; Lin et al., 2004). Others have shown that the vasa vasorum may be involved in several vascular diseases such as atherosclerosis (Plante, 2002; Scotland et al., 2000). Some have suggested that NO may be produced by mast cells and neurons present in the adventitia (Laine et al., 2000; Yoshida et al., 1993). Other cell types that are found within the adventitia include pericytes and perivascular adipocytes. Pericytes functions to stabilise blood vessels and angiogenesis but there are some evidence suggesting a role in calcification which is commonly associated with atherosclerosis (Shao et al., 2006). Although perivascular adipocytes have been mentioned, but these types of cells are not morphologically counted as part of the adventitia itself but rather presents anatomically close to blood vessels (Auger et al., 2007). The adventitia also contains sympathetic nerve terminals that control vessel diameter. Vasoconstriction is achieved by the action of noradrenaline released from these sympathetic nerve endings, hence regulating blood flow through the artery (Levick et al., 2010).

1.5.3. Current vascular tissue engineering strategies

In the past 40 years, there have been considerable efforts in producing tissue-engineered blood vessels as an alternative vascular graft which maintain a high patency rate. Scientists attempted to improve synthetic grafts in number of ways such as; (i) seeding with ECs, (ii) embedding cells with anti-thrombotic drugs and (iii) development of new biomaterials. Herring *et al* (1978)., first

reported the successful isolation and seeding of ECs onto synthetic grafts (Herring et al., 1978). This study demonstrated an improved patency rate of the blood vessels when using 6 mm diameter synthetic grafts than when compared with unseeded grafts. However, the graft failed to show retention of the ECs under flow conditions, highlighting the limitation of using such approach. Therefore, a significant focus of research has been on improving ECs adhesion to biomaterial surfaces. This includes investigating the use of natural ECM proteins such as collagen, fibrin, fibronectin and laminin (Cooper and Sefton, 2011; Pankajakshan and Agrawal, 2010). However, this approach has been limited by the potential for development of a chronic inflammatory response targeted at the synthetic support.

Tissue engineered blood vessels have generally been designed to be utilised for vascular grafting as a substitute for autologous transplantation in those patients lacking a suitable graft tissue. There are certain requirements that have to be met to achieve a highly functional blood vessel model. These requirements include: biocompatibility, non-thrombogenicity, non-immunogenicity as well as confluent and quiescent EC layer (Hasan et al., 2014). Also, it should have appropriate mechanical properties such as withstand the high pressure and haemodynamic stress found within the arteries in long term. In addition, it should also fulfil all the physiological requirements such as being able to constrict and relax and should be indistinguishable from the native blood vessel. Thus, creating a construct that meets these requirements represents a significant challenge.

There are three main components that are needed to allow realistic tissue formation using tissue engineering techniques. Firstly, the use of an appropriate cell source that can maintain the cellular phenotype found i*n vivo* to sustain tissue function. Secondly, the use of bioreactive mediators and an appropriate culture environment to help maintain the normal cellular phenotype. Lastly, the use of a scaffold that acts as temporal extracellular matrix to hold cells together in the normal patterns found inside the body. Current tissue engineering techniques involve the use of layer-by-layer fabrication technique (Wilkens et al., 2016), scaffold free constructs (Jung et al., 2015), plastic

compression of collagen hydrogels (Braziulis et al., 2012; Levis HJ, 2010) and angiogenesis, the process where new blood vessels form from existing vasculature (LaValley and Reinhart-King, 2014). A recent review have discussed *in vivo* generation of TEBVs using the host reaction to an implanted biomaterial (Geelhoed et al., 2017). To be exact, this approach intends to make use of the body's foreign body response to biomaterials, and exploits the host environment as a bioreactor for the generation of new tissues, essentially allowing for the re-construction of the entire vascular graft within the patient's body.

1.5.3.1. Scaffolds

Scaffolds may be biological or synthetic (Fernandez et al., 2014; Goonoo et al., 2013; L'Heureux et al., 1998). At present, there are 4 main strategies used to create scaffolds that allow the formation of tissue that meets the criteria highlighted in the previous section. This includes the use of (1) decellularised tissues (2) synthetic polymer scaffolds (3) tissue self-assembly approach to create cell sheets and (4) hydrogels or biopolymer scaffolds. Each of these approaches have their advantages and disadvantages and relevant methods will be described in the next section, except for the decellularised tissues approach as it is beyond the scope of this project.

1.5.3.1.1. Synthetic polymer scaffolds

Various vascular models using biodegradable polymer scaffolds have been studied. This simply implies seeding cells onto degradable polymer to aid cell growth and remodelling. Cellularisation is achieved by cell seeding techniques used to optimise their distribution (Kim et al., 1998). Preferably, the polymer will be gradually absorbed in culture, yielding the tissue produced by the cells. These polymers are beneficial as they have tailorable mechanical properties, degree of resorption and micro/nano-structure, which can be manipulated by changing the chemical makeup in an effort to improve cell growth and tissue remodelling. Another benefit of these polymer scaffolds is that they have early mechanical function supporting the scaffold, until the cells produce enough ECM.

1.5.3.1.2. Nanofiber scaffolds

Nanofibers provide a high surface area to volume ratio with microporous structures that support cell adhesion, proliferation, migration, differentiation and alignment (Ma et al., 2005). Fabrication of nanofibers has been adopted for use in vascular tissue engineering for reasons that some of these being biocompatiple, biodegradable and provide mechanical strength to the vessel replica (Agarwal et al., 2008). At present, there are three different methods available for creating nanofibers which include: (i) electrospinning, (ii) self-assembly and (iii) phase separation. Electrospinning is the most commonly studied method and shown to be potential for tissue engineering. The resulted nanofiber can be used to make synthetic biodegradable scaffolds that provide a suitable structure for cell proliferation, adhesion and differentiation.

There are two main limitations of using synthetic polymers for vascular tissue engineering. Firstly, degradation of these polymers causes the formation of by-products such as lactic acid and glycolic acid. Although these compounds are naturally produced by the human body, when high local concentrations of these by-products are produced they can become toxic to cells due to their ability to trigger a drop in pH of the microenvironment. The second problem lies in the imbalance in the relative rate of polymer degradation and tissue remodelling. Generally, the synthetic polymer degrades more rapidly than the time taken for a full ECM to be developed by the seeded cells. Hence, the construct can become weakened and incapable to sustain the high arterial pressure of the blood – potentially resulting in aneurysm. Therefore, these methods will need to be further optimised to be able to be used in creating a transplantable vessel graft.

1.5.3.1.3. Scaffold-free culture-cell sheets

This methodology was developed by Jung *et al.*, (2015) which is based on using cultured human cells, without using additional synthetic or exogenous materials (Jung et al., 2015). Briefly, sheets of SMCs were cultured on culture plates with high levels of ascorbic acid (to generate high levels of collagen synthesis), this produced an organised cellular sheet. The cell sheet was then detached

and placed on a tubular support to produce the medial layer. In the same way, a sheet of fibroblasts was cultured and wrapped around the media to form the adventitial layer. After 14 days, the two sheets were fused together to produce a cohesive structure. Finally, ECs were seeded on the luminal surfaces from the 2 ends and distributed through the vessel by rotating the sheet overnight. This has shown a well-defined, multi-layer arrangement with an apparent ECM, though the ECM did not display a circumferential alignment as found in the native blood vessel. The SMCs re-expressed desmin which is a marker that was lost during culture and is indicative of a contractile phenotype. In addition, the ECs could be seen to possess a physiological phenotype as shown by their expression of vWF, production of PGI_2, uptake of acetylated LDL and inhibition of platelet adhesion to their surface. The construct produced using this methodology had a burst strength above 200 mmHg, after three weeks of sequential culture in a rotating wall bioreactor and perfusion at 6.8 dynes/cm^2, which is comparable to human vessels. However, cell sheet grafts have shown to be stiffer than the vessel being bypassed, this could lead to intimal hyperplasia (Jung et al., 2015). The stiffness of this construct is perhaps due to inadequate elastin deposition by the SMCs. Nevertheless, results from transiently grafting this type of blood vessel in canines demonstrated that it was able to function *in vivo* (L'Heureux et al., 1998).

1.5.3.1.4. Hydrogel and biopolymer scaffolds

Tissue engineering using hydrogels was first developed by Weinberg and Bell in 1986. This involved seeding ECs on the luminal surface of a tubular structure composed of type I collagen hydrogels filled with SMCs (Serbo and Gerecht, 2013). Type I collagen is a major component of the subendothelail matrix, and is a highly-abundant protein found throughout the human body, including the blood vessel wall (Xu and Shi, 2014). Fibrin can also be used as a biopolymer instead of collagen to form the basis of the blood vessel structure. Collagen and fibrin cause cells to entrap during gelation (fibrillogenesis) of the hydrogel allowing direct cellularisation within the construct. The advantages of using hydrogels are: (1) high degree of circumferential SMC alignment and (2)

direct cellularisation of the construct. However, these characteristics were not enough in the study by Weinberg & Bell (1986) to produce the mechanical properties found in native arteries since it could not withstand perfusion with arterial blood pressures (Weinberg and Bell, 1986).

1.5.3.1.5. Cell source

Differentiated primary cells and cell lines have also been used as cell sources for fabricating tissue engineered constructs (Sankaran et al., 2014; Sundaram and Niklason, 2012; Wilkens et al., 2016). The cellular components required to build stable blood vessels include ECs which line the inner surface of blood vessels and SMCs and lie in the subendothelial matrix of the medial layer. A commonly used primary cell type, human umbilical vein endothelial cells (HUVECs), play a role in endothelial layer formation, preventing platelet adhesion (Kelm et al., 2010). In addition, HUVECs are routinely cultured from readily available tissues in a reproducible manner. Syedain et al., (2011) demonstrated capability to fabricate tissue engineered arteries like native arteries by entrapment of human neonatal dermal fibroblasts in a fibrin gel (Syedain et al., 2011). The construct was subjected to a bioreactor to convey both transmural flow and cyclic distension ultimately leading to the formation of circumferentially aligned collagen and other ECM using a burst pressure of 1,400–1,600 mmHg. A period of 7-9 weeks of culture is required for this method with notable mechanical properties of the grafts generated using this method make this approach extremely interesting for grafting (Syedain et al., 2011). Creating a tissue engineered vascular construct requires integration of SMCs and ECs to be able to form a tubular structure that mimics the native blood vessel (Nerem and Ensley, 2004).

Various stem cell sources have been used to generate a viable vascular tissue engineered constructs that includes adult stem cells (Krawiec and Vorp, 2012). The inherent ability of stem cells to self-renew and proliferate rapidly makes them a viable cell source addressing limitations of other approaches. These cells have been widely used in vascular tissue engineering applications (Krawiec and Vorp, 2012; Samuel et al., 2015). After extraction using Ficolle-Paque density centrifugation method these cells are subjected to a differentiation culture period, of which a graft can be created

comprising of SMCs and ECs that mimics a native blood vessel. These rich populations of progenitor cells are heterogeneous including endothelial precursor cells (EPCs), early-outgrowth EPCs, mature ECs, mesenchymal stem cells (MSCs), hematopoietic stem cells, monocytes, CD4+ T-cells, CD8+ T-cells, B cells, natural killer cells, among others (Roh et al., 2010). In order to make a more feasible vascular engineered construct, researchers have used EPCs isolated from adult peripheral blood in place of HUVECs. These cells regressed in 3 weeks whereas it took HUVECs more than 4 months. Various factors such as soluble growth factors, mechanical stimulation, cell-cell contact, and extracellular matrix substrate proteins are recognised to have an effect on the differentiation of MSCs (Sundaram and Niklason, 2012).

1.5.3.1.6. Mediators

General mediators that are used to examine tissue engineered blood vessels (TEBVs) include bioreactors, mechanical stimulation and the application of growth factors. Various studies have reported the use of TEBVs in physiological pulsatile flow yielding an enhanced tissue formation, ECM production, cellular alignment and the retention of cellular morphology (Zhang et al., 2009). These also include computer-controlled bioreactors (Song et al., 2012), which allow precise adjustment of physiological pressure. Figure 1.5, shows a dual-loop bioreactor providing physiological pulsatile flow conditions for TEBVs culture. Niklason and colleagues have designed a bioreactor which uses a distensible silicone tube, carrying a pulsatile flow of culture medium (Niklason and Langer, 1997; Niklason et al., 2002, 1999). Interestingly, some of these pulsatile bioreactors are able to incorporate multiple seeded vascular constructs in parallel. This provides a physiologically relevant strain to the synthetic polymer scaffold seeded with vascular cells. An increase in ECM formation and vessel strength were observed compared with scaffolds cultured in static conditions. Additionally, administration of a cyclic strain has shown an improved tissue organization and significantly increase the strength of collagen gel-based TEBVs (Ye et al., 2000). Other scientists have reported that mechanical preconditioning benefited the generation of 3D

TEBVs culture systems (Nerem and Seliktar, 2001; Niklason et al., 1999). The sporadic stretch mediated by bioreactors increases the contractile nature of SMCs, increases synthesis and secretion of ECM and facilitates cellular proliferation. For these reasons, studies have focused in using pulsatile fluid flow exposure to guide the development of TEBVs (Pandit, 2005).

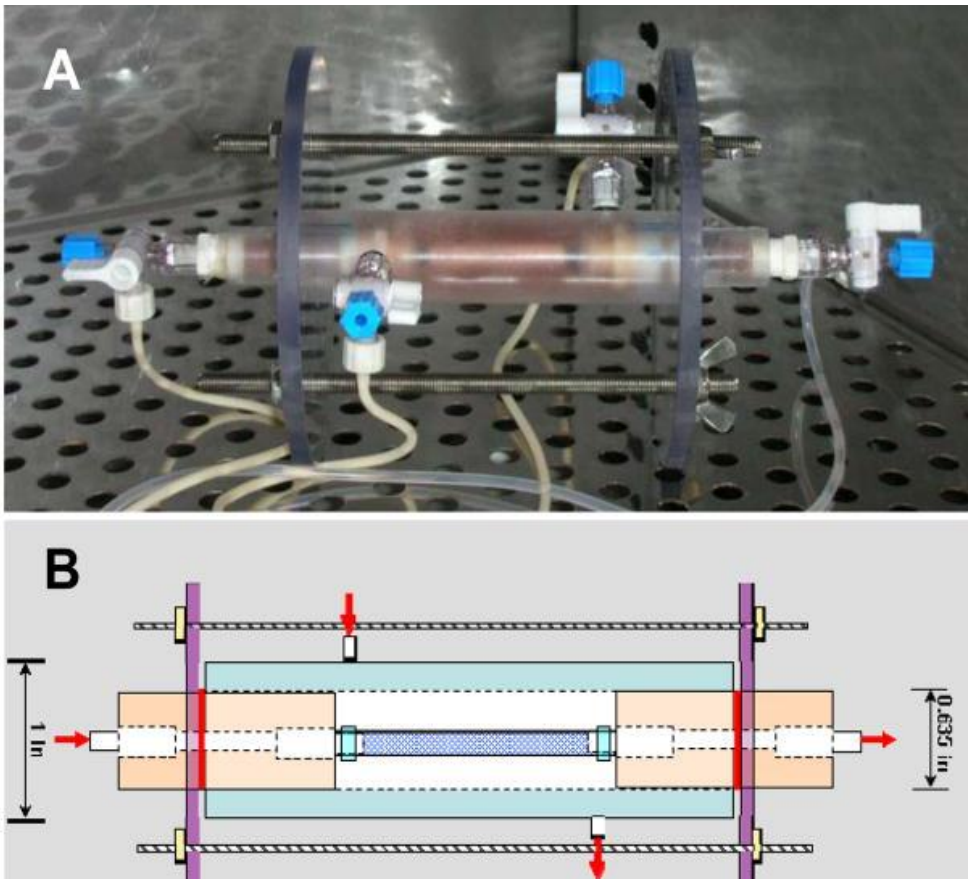

Figure 1.5 - Dual-loop bioreactor for tissue-engineered blood vessel graft culture. (A) Image of vascular bioreactor with electrospun silk fibroin vascular graft in culture; (B) Schematic diagram of the vascular bioreactor with indication of dual flow directions (Zhang et al., 2009).

Numerous research have been conducted in applying dynamic mechanical conditioning to improve mechanical properties of TEBV constructs composed of living cells embedded in a collagen-gel scaffold (Seliktar et al., 2000). This approach attempts to provoke a unique response from the embedded cells so as to rearrange their surrounding matrix, thus improving the overall mechanical stability of the constructs. This technique uses a cyclic strain resulting in an increased contraction,

mechanical strength and circumferential orientation (Seliktar et al., 2000). Other mediators that are used in vascular constructs include the application of growth factors (Bertanha et al., 2014). This study has applied endothelial inductor growth factor obtained from human platelet lysate to differentiate mesenchymal stem cells into functional endothelial cells. These cells were shown to acquire morphologic characteristics of endothelial cells and secrete high levels of vWF compared with the untreated cells.

By utilising some of the above techniques it is possible to produce a blood vessel model that mimics the native artery to study platelet activation status. An arterial construct for use in basic studies haemostasis will have different requirements to those intended for use in transplantation. In transplantable constructs where a lack of immunogenicity, stable cell integration and an ability to withstand arterial pressures over a long timeframe is important however, these are lesser considerations for a construct to be used for haemostasis as their intended lifespan is much shorter.

1.5.4. Characterisation of 3-dimensional (3D) models

There are various 3D models that have attempted to replicate the native structure of the vessel wall which were designed to be mainly utilised for grafting (Dorweiler et al., 2006; Hoenig et al., 2005; Hoerstrup et al., 2001; Sankaran et al., 2014). There are certain requirements that have to be met to achieve a functional blood vessel model. These requirements include non-thrombogenicity and a quiescent EC layer (Hasan et al., 2014).

1.5.4.1. Characterisation of endothelial cell function

To create a 3D tissue-engineered blood vessel model, the endothelial cell lining should be fully confluent, anti-thrombotic and possess no signs of the pathological inflammatory phenotype observed in some conditions. The mean life span for HUVECs is 10 serial passages, subsequently the cells become giant, multi-nucleated and eventually dies (Bouis et al., 2001). Therefore, no long term *in vitro* studies can be established with HUVECs.

ECs are characterised by their phenotypic features which include the presence of Weibel-Palade bodies (Weibel and Palade, 1964). These are large rod-shaped organelles that are specific feature for ECs. These Weibel-Palade bodies store vWF and are worthwhile observing to confirm the cells being cultured are ECs. vWF is a widely used endothelial cell marker that can be used to confirm endothelial cells origin, as explained in earlier sections (Zanetta et al., 2000). This marker along with the cell-surface marker, CD31 (also known as Platelet endothelial cell adhesion molecule- 1;PECAM-1), have been widely used to assess endothelial cell phenotype. In addition, a common method is to ensure that the endothelial cells possess the normal cobblestone cell morphology through using fluorescence and scanning electron microscopy (Thomas and Nair, 2013).

It is also important that the endothelial cell layer does not express inflammatory markers in a resting state, as these are not normally seen in healthy blood vessels exposed to physiological flow conditions. These inflammatory markers, such as intercellular adhesion molecule-1 (ICAM-1) and vascular cell adhesion molecule-1 (VCAM-1) have been used in numerous studies (Kim et al., 2001). ICAM-1 and VCAM-1 are inflammation markers normally expressed at low levels on the endothelial cell and are able to be enhanced by TNF-α (tumour necrosis factor-α). This parameter is essential for examining the inflammatory condition of the generated TEBV. In addition, the endothelial cells should be able to enhance the expression of inflammatory markers in response to exposure of inflammatory cytokines, such as TNF-α (Kjaergaard et al., 2013).

Another vital characteristic that must be investigated is the endothelial cell permeability. If the endothelial layer is not complete then this could allow platelets and the coagulation system to be inappropriately exposed to the subendothelial matrix triggering unwanted clotting responses. Disruptions of the endothelial cell barrier integrity can possibly occur from incorrect seeding ability or due to manipulations during handling of construct. This may have significant effect on platelets adhesion and activation and to avoid such problem, permeability of the TEBV must be tested. The use of fluorescently labelled-high molecular weight dextran to test the permeability of the inter-endothelial cell junctions is a simple approach of which has previously been used *in* vitro using cell

culture inserts. FITC-dextran is added on top of the cells, allowing it to permeate through the cell monolayer. The extent of permeability can be determined by measuring the fluorescence of the plate-well solution. However, permeability testing of 3D TEBV constructs using dextran cannot be achieved using this technique, due to the requirement of seeding HUVECs in the insert. Alternatively, the trans-epithelial electrical resistance can also be used to quantify the permeability of the endothelial junctions, by assessing how easy it is for electrical charge to transfer paracellularly through the endothelial layer. However, like the fluorescent techniques this has principally been applied to cellular monolayer. Thus, there is a need to develop new methodologies to assess the permeability of the endothelial layer in a 3D TEBV construct.

However, very few studies have used platelets as a tool for measuring the influence of the tissue-engineered vessels on platelet activity. The method most commonly used in determining the thrombogenicity of TEBV models is to use scanning electron microscopy to examining platelet adhesion upon the surface of the construct after perfusion (Boccafoschi et al., 2005; L'Heureux et al., 2001). For instance, if the TEBV model is lacking an intact endothelial monolayer, then the subendothelial matrix would promote platelet adhesion or aggregation due to the gaps present between endothelial cells. In contrast, an intact and well cultured endothelial cell monolayer would not promote platelet adhesion, due to the lack of exposure of the subendothelial matrix to the bloodstream as well as endothelial secretion of inhibitory substances such as NO and PGI_2, as mentioned previously.

1.5.4.2. Characterisation of platelet activation

Despite the requirement for TEBV to prevent the activation of the haemostatic system only few of these studies have fully investigated platelet responses to these models (Boccafoschi et al., 2005; L'Heureux et al., 2001). Therefore, there is a need for new methodologies to fully test platelets activation and inhibition upon exposure to TEBVs. The methods commonly used by platelet biologists to characterise platelet activation are discussed in following section.

1.5.4.2.1. Adhesion

Platelet adhesion to the subendothelial matrix is the first step of the haemostatic mechanism. The simplest method is to label washed platelets with the fluorescent cell membrane dye $DiOC_6$ – these can then be perfused over the surface of the construct (Navarro-Núñez et al., 2015; Van Kruchten et al., 2012). $DiOC_6$ can be used to detect adhesion of these fluorescently-labelled platelets using fluorescence or confocal microscopes. In addition, fluorescently-labelled antibodies to platelet-specific cell surface markers such as CD41 have also been used to visualise platelets in *in vivo* studies using intravital microscopy (Furie and Furie, 2008). However, platelet adhesion is not a very sensitive test as platelets can transiently bind to many surfaces, whereas the irreversible binding that underlies platelet aggregation is not distinguishable from these tests.

1.5.4.2.2. Granule Secretion

Platelets contain 3 classes of secretor granules which are rapidly released upon agonist-stimulation – the lysosome, and the α- and dense granules. These granules contain distinct cargos which may play a number of roles in haemostasis and inflammation. For instance, the dense granules contain autocrine signalling molecules such as ATP, ADP and serotonin which are responsible for the recruitment of other circulating platelets, whilst the α-granules contain haemostatic proteins (e.g fibrinogen and vWF) as well as mediators of angiogenesis (e.g. VEGF). Therefore, assessing platelet granule secretion is a useful method for sensitively assessing platelet activation status. However not all platelet agonists effectively trigger granule secretion – with only "strong" platelet agonists such as collagen and thrombin being able to effectively trigger secretion, whilst "weak" agonists such as ADP and 5-HT are not able to (Lages and Weiss, 1988).

There are various tests that can be used to evaluate agonist-evoked platelet granule release, including quantitative or semi-quantitative assays to measure release of granule components into the extracellular medium or increase in surface expression of markers of the platelet granule membrane (Saboor et al., 2013). Secreted granule contents may be measured in the platelet

supernatant at a single time point after stimulation and then compared to the total platelet content to determine the secreted fraction of granule contents. Alternatively, granule contents can be measured over a time course to determine the kinetics of secretion. Platelet secretion may also be evaluated by measuring increases in the surface expression of markers of the platelet granule membrane, such as *P*-selectin to measure α-granule release (Saboor et al., 2013). Measurement of platelet surface *P*-selectin is usually performed as a semi-quantitative test, in which the proportions of *P*-selectin positive platelets are compared before and after agonist stimulation (Tschoepe et al., 1990).

Another commonly used method to test platelet granule secretion is to indirectly measure ATP secretion from dense granules via luminescence from a bioluminescent reaction catalysed by firefly luciferase (Harper et al., 2009; Mumford et al., 2015). This test measures ATP release into the extracellular medium from the dense granules. The released ATP is able to react with luciferin and luciferase (firefly extracts) added to the external medium resulting in light emission. Other tests include the detection of PF-4 which is secreted during platelet activation and can be measured using ELISA, to evaluate α-granule release from platelets after agonist stimulation.

To date, these tests have not yet been performed in platelets that has been exposed to tissue-engineered constructs but rather utilised in basic and clinical research to assess experimental and clinical defects *in vitro* or in platelets perfused over immobilised agonists or drugs (Dovlatova, 2015; Merten et al., 2000; Mumford et al., 2015).

1.5.4.2.3. Aggregation

Platelet aggregation through platelet-platelet cohesion mediated via fibrinogen through the activated integrin $\alpha_{IIb}\beta_3$ is the key step in the development of a thrombus. LTA is a widely-used technique used by basic and clinical scientists to monitor agonist-evoked platelet aggregation *in vitro* in platelet rich plasma or washed platelet suspensions (Gibbins and Mahaut-Smith, 2004). LTA is considered the 'gold standard' for platelet function testing and so it is nearly universally used in

clinics as well as platelet research labs (Michelson, 2004). Readings are recorded using an aggregometer, indicating several features of platelet activation such as: (i) shape change, (ii) reversible primary aggregation and (iii) irreversible secondary aggregation. The basis of the test is to monitor the relative amount of light passing through the platelet suspension compared to a platelet free blank (e.g platelet-poor plasma or saline solution). At rest, discoid platelets are homogenously distributed through the platelet suspension and so can deflect lots of light. However, upon activation, platelets change into a larger, spherical form that is able to block more light transmission – this is known as the shape change phase. Finally, after a short lag period platelet aggregation starts to occur and platelets clump together allowing more light to pass through the sample. The latency and the extent to which aggregation occurs can be observed in real-time and can be quantified allowing effective comparison between multiple experimental conditions. However, such method can only measure up to 8 samples at one time restricting the throughput of the system. In addition, there is a need for reasonably large volumes of platelet suspension. An alternative microplate-based assay has recently been developed which can measure platelet responses to a broad range of agonists at any given time using a 96-well plate read through a standard plate reader (Armstrong et al., 2009; Chan and Warner, 2012).

However, whilst aggregometry is a good test for studying platelet function, aggregation requires strong platelet activation to occur to be observed. Therefore, studies examining platelet aggregation either *in vitro* or on the surface of a blood vessel construct may not observe the low-level platelet activation that may be occurring in response to contact with these constructs.

1.5.4.2.4. Phosphatidylserine exposure

Prolonged, strong platelet activation causes the exposure of negatively charged phosphatidylserine (PS) at their outer surface (Heemskerk et al., 1997). PS is normally located on the cytoplasmic face of the resting platelet membrane but appears on the plasma-oriented surface of discrete membrane vesicles that derive from activated platelets. The transbilayer migration of PS to the

outer membrane leaflet binds to the activated coagulation factor V, hence promoting Ca^{2+}-dependent binding of activated factor X to the platelet surface, resulting in localised assembly of the prothrombinase complex that accelerates the generation of thrombin at the site of thrombus formation (Bevers et al., 1982). Platelet procoagulant activity is most commonly measured by flow cytometry using fluorescently-labelled annexin V which binds strongly to the exposed PS groups (Furman et al., 2000). However other groups also perform similar experiments assessing the binding of fluorescently-labelled coagulation factors to the platelets (Dörmann et al., 1998).

Whilst these assays are an effective method for assessing the ability of platelets to assist in the activation of the blood coagulation cascade, it is unlikely to be effective to assess platelet activation in response to a tissue-engineered construct as PS exposure requires strong, prolonged activation of platelets – which may therefore miss cells that are only marginally activated.

1.6. Measurement of cytosolic calcium concentration ($[Ca^{2+}]_{cyt}$)

An increase in cytosolic calcium concentration is a crucial step in all stages of thrombus formation – with Ca^{2+} rises being obligatory for platelet adhesion, secretion, aggregation and phosphatidylserine exposure. These range from small Ca^{2+} rises observed in adherent platelets to the large, prolonged Ca^{2+} signals observed in pro-coagulant, PS-exposing cells. Therefore an assessment of platelet $[Ca^{2+}]_{cyt}$ represents a sensitive method for assessing platelet activation. In addition, agonist-evoked rises in $[Ca^{2+}]_{cyt}$ are also strongly sensitive to endothelial derived inhibitors such as NO and PGI_2 – therefore assessment of this parameter should allow us to sensitively assess both platelet activation and inhibition in response to exposure to the blood vessel construct.

Measurements of agonist-evoked changes in $[Ca^{2+}]_{cyt}$ can be determined in platelets loaded with the high-affinity fluorescent calcium-sensitive indicator, Fura-2 (Harper et al., 2009). The loading of this fluorescent indicator is performed using the acetoxymethyl (AM) ester derivative of the Fura-2. The AM esters shield the negative charges of the indicator allowing it to be cell-permeable. However once inside the AM esters are hydrolysed by non-specific esterases to yield anionic Fura-

2 which becomes trapped inside the cytosol where it can be used to measure the Ca^{2+} concentration inside the cytosol. Fura-2 is a ratiometric calcium indicator, meaning that the Ca^{2+} concentration is assessed through changes in the emission from two different excitation wavelengths (340 and 380 nm). The use of ratiometric dyes is advantageous as this help to eliminates many of the artefacts that can affect fluorescence readings. This include artificial changes in fluorescence intensity caused by factors such as variations in cell loading, photobleaching, differences in dye leakage from the cell, changes in cell thickness and volume, and difference in optical path length. In addition, the use of ratiometric dye will also have the advantage of preventing artefactual signals caused by loss of platelets from the suspension as they adhere to the blood vessel construct.

1.7. Aims and objectives of the current research project

In a construct to be used for studies of haemostasis, the prime considerations must be for the construct to be able to prevent platelet activation prior to vessel injury, adequately replicate the normal *in vivo* clotting response upon injury and be simple enough to make repeatable, to be able to elicit a reproducible platelet response across batches of the construct. The overall aim of this project is to:

- Fabricate and characterise a tri-layered 3D TEBV generated using a layer-by-layer fabrication approach. By using human primary cell source in both the intimal and medial layers, these two layers will be separated with high density aligned nanofibers to align the endothelial cells and aid in the production of an aligned, low permeable ECs layer. Thus, preventing cross-migration of both cell types between the layers at the same time, allowing cell-cell communication between the ECs and the SMCs. In contrast to the approaches used to produce artificial blood vessels for grafting and transplantation, where lack of immunogenicity, high mechanical strength and appropriate cell integration is important, the key design parameters in this construct will be to achieve a functional EC layer that prevents platelet adhesion prior to injury, and a functional media layer that can

trigger platelet activation once the vessel wall is damaged. Fully recapitulating the well-organized vessel wall structure is important for proper functioning of tissue engineered blood vessels and so it is vital to define regional cellular localisation within TEBVs post its culture period.

- This thesis evaluates pro- and anti-thrombotic properties of the created blood vessel model that has the correct vessel wall layered structure found *in vivo.* Hence, the first aim of this thesis is to fabricate functional tissue engineering blood vessels which possess required the pro- and anti-thrombotic properties.
- Design a unique *ex vivo* method in which it is possible to assess platelet activation sensitively and in real-time, in response to exposure to the produced blood vessel constructs. This method tests the activation level of platelets in response to the 3D human blood vessel constructs via quantifying changes in the platelets' $[Ca^{2+}]_{cyt}$ in real-time using a fluorescence spectrophotometer. Through exposing the constructs to washed human platelet suspension labelled with Fura-2, we will be able to assess in real-time the activation status of the platelet suspension, or modulation of platelet responsiveness to soluble agonists.
- Investigate the functionality of the 3-dimensional tissue-engineered blood vessel using the newly developed methodology. In particular, we aim to develop a TEBV construct which inhibit platelet activation and resist platelet adhesion due to the presence of endothelial cell lining, whereas the TEML construct show a pro-aggregatory feature that promote platelet activation consistent with the known properties of the subendothelial matrix. Other conventional methods will also be used to validate the pro- and anti-aggregatory properties of the constructs. These include platelet aggregometry, aggregation on the surface of the constructs using $DiOC_6$-labelled platelets visualised under fluorescence microscopy and dense granular secretion using luciferin-luciferase assay which detects the amount of ATP secreted from platelets' dense granules post exposure to the fabricated

constructs. The endothelial cell function will be assessed by inhibiting its anti-thrombotic nature using specific inhibitors that inhibit NO and PGI_2 production. The endothelial cell layer will be subjected to the inflammatory cytokine, TNF-α, to produce a diseased model. The surface platelet aggregation and monitoring of $[Ca^{2+}]_{cyt}$ of platelets incubated with the diseased model will be investigated. Establish a lesioned blood vessel model under fluid dynamic condition in order to study the effect of anaesthetics on platelet responses to the construct. This will be done to establish an alternative to intravital microscopy. We intend to do this by using the tissue-engineered human blood vessel construct developed in this project to create an *ex vivo* ferric chloride arterial injury model by recreating physiological blood flow conditions inside a commercially-available parallel flow chamber. Given the potential impact of general anaesthetics on platelet function, experiments were also performed to assess if preincubation with ketamine into the developed arterial injury model could alter the response observed in this system.

Chapter 2

Fabrication and characterisation of human 3D blood vessel constructs

1. Introduction

Cardiovascular disease is one of the primary causes of morbidity and mortality worldwide. Each year, thousands of people die from acute cardiovascular events caused by abnormal blood clotting responses. This includes disorders such as myocardial infarction, ischaemic stroke and pulmonary embolism. Due to the prevalence of these vascular diseases, there is a need for us to better understand the cellular and molecular mechanisms underlying blood clotting so that we can try and design better techniques to prevent unwanted clotting that occurs in these disorders.

In vivo study of haemostasis in mice has provided a number of valuable results on mechanisms underlying thrombus formation (Bellido-Martín et al., 2011b; Falati et al., 2002; Sachs and Nieswandt, 2007). However, there are potential limitations of the animal models used which may limit the insight that the models may reveal about these disorders in humans (Janssen et al., 2004; Rowley et al., 2011; Weinberg and Ross Ethier, 2007). Therefore, these factors should be considered before attempting to apply results obtained from *in vivo* mouse models to human clotting pathways.

Tissue engineering of human blood vessel replicas has emerged as a promising alternative approach to the use of autologous grafts in coronary artery bypass grafts. The existing diverse and advanced techniques used in current tissue engineering field enable us to mimic the anatomic, biological and physical features of a native blood vessel into tissue engineered counterpart. The central target of this thesis is to establish a highly reliable human blood vessel model in which we can better study the processes underlying haemostasis. This model should be able to overcome the technical limitations faced with current *in vivo* animal models and *in vitro* models. However, there are limitations in current tissue engineered blood vessel models which involve cellular, anatomical or functional limitations. Some of the current vascular models lack the multi-layered structure which lack the physiologically relevant 3D structures and the interactions of the different cell types normally present (Lopez and Zheng, 2013). Other scientists have created TEBV models that do not

show the anatomical similarities that are found *in vivo* human blood vessels such as the use of rolled cell sheets (Ren et al., 2014). Further existing limitations include the use of synthetic hydrogel which do not fully replicate the *in vivo* ECM environment (Geckil et al., 2010; Liu et al., 2009). Also, the use of a tubular structure vascular models which do not fully enable the visualisation of platelet-endothelial cell interactions (Peck et al., 2012). Although these models may provide useful information, these do not fully address the current challenges that are faced in tissue engineered blood vessel models. Hence, it is crucial to address these limitations, through the introduction of multiple optimisation steps using currently available tissue engineering techniques.

Current methods that are widely used to create scaffolds to produce these tissue engineered blood vessels include hydrogels and nanofiber scaffolds (Hu et al., 2010; Subramanian et al., 2012; Yang et al., 2011). Aligned nanofibers can promote effective cell adhesion and proliferation, and provide a construct with mechanical properties of the native coronary artery (Mo et al., 2004). Nanofiber scaffolds can be fabricated using an electrospinning technique to generate highly dense and aligned nanofibers on which cells can be seeded. Synthetic biodegradable polymers such as PLA, polycaprolactone (PCL) or polylactic-co-glycolic acid (PLGA) are now commonly used in tissue engineering of scaffolds (Subramanian et al., 2012; Yang et al., 2011). PLA is widely used in the biomedical field due to its biodegradability, biocompatibility, thermal plasticity and suitable mechanical properties. Previous studies have shown that endothelial cells respond to their topographical microenvironment, aligning and elongating themselves along the direction of the nanofibers (Sankaran et al., 2014). This adhesion and spreading of cells can also be further enhanced by coating nanofibers with endogenous extracellular matrix molecules such as fibronectin, which have been shown to increase endothelial cell survival (Cooper and Sefton, 2011). Aligned nanofibers could therefore be used to provide mechanical support for HUVECs growth and adhesion, to produce an endothelial cell lining that can extend in the direction of blood flow, to mimic the cellular arrangement found in the tunica intima *in vivo*.

HUVECs have been previously grown atop of PLA nanofibers however, these studies lack underlying layers that support platelets' thrombogenicity. In addition, the SMCs function has been shown to be modulated by the composition of the ECM (Chan-Park et al., 2009). A suitably timed SMC phenotype modulation is thought to be the key to success: a synthetic phenotype is required initially for vessel remodelling, whereas a contractile phenotype is required ultimately for vasoactivity (Reidinger and Rolle, 2014). The surrounding ECM has been shown to influence the mechanical properties of SMCs, in particular, collagen. Current tissue engineered constructs identified issues relating to low densities of SMCs and collagen, limiting construct performance (Chan-Park et al., 2009). Thus, existing research is focusing in mimicking this environment by seeding SMCs into collagen hydrogels using various tissue engineering techniques. To the best of our knowledge, currently used artificial tissues cannot replicate all the functions of the real tissues and do not have the essential layered structure that are effectively characterised for platelet studies. The structural integrity of the TEBV model is essential as cells should not migrate through the layers during culture. Thus, the main objective for this chapter is to fabricate and characterise a tri-layered TEBV generated using a layer-by-layer fabrication approach.

2. Methods

2.1. Electrospinning of PLA nanofibers

For the fabrication of Poly-L,D-lactic acid (PLA) nanofibers, a 2% solution was prepared for electrospinning. Initially, PLA granules ($96\%_L/4\%_D$; Purac biochem BV, Gorinchem, Netherlands) were dissolved in chloroform, followed by addition of dimethylformamide (7:3 ratio). The solution was left to mix overnight at room temperature with continuous magnetic stirring. Once the solution is fully blended, it was loaded into a 5 mL glass syringe (KR Analytical, Sandbach, UK) with 18-gauge blunt tip needle (11.7 mm, KR Analytical, Sandbach, UK) and connected to a syringe pump (KR Analytical, UK) in a horizontal mount. The solution was pushed through the syringe into a capillary blunt steel needle at a constant speed of 0.025 mL/min and a total volume of 0.2 mL. The steel needle was connected to an electrode of a high-voltage power supply (SpellmanHV, UK) feeding though the positive electrode +6 kV. The solution then formed aligned PLA nanofibers which deposited onto the negatively charged collector (30 ×10 cm) -6kV, with 2 sheets of thin steel 'blades' arranged in parallel and 4 cm apart. The collector was electrically connected to a static copper plate. The distance between the tip of the needle and the collector was at all times kept at 15-20 cm (Figure 2.1). The electrospinning parameters are shown in table 2.1.

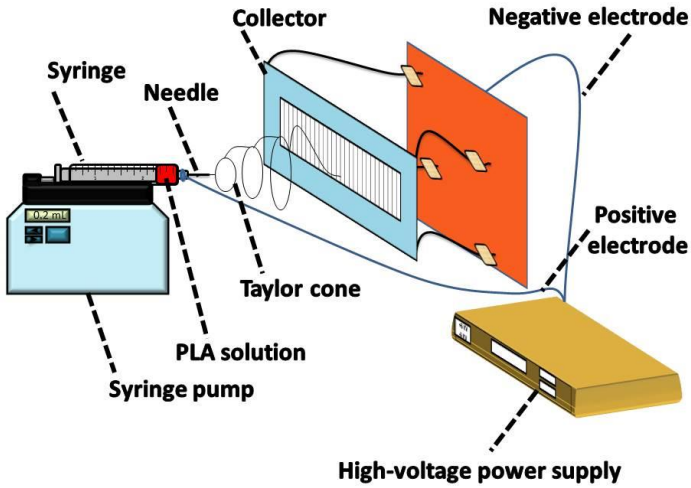

Figure - 2.1 Experimental set-up of the electrospinning system.

A densifier, constructed from metal steel, was used to carefully collect the deposited PLA nanofibers. Following the densification of the PLA nanofibers, these fibers were transferred carefully onto a portable cellulose acetate frames (16 cm^2) to enable for cell culture usage. After collection, all samples were placed in a vacuum at room temperature for 20 minutes to ensure that residual solvents were removed. They were sterilised under ultraviolet light for 90 seconds, three times before usage. To facilitate visualisation of the nanofibers, Rhodamine B has been added to the PLA solution at a final concentration of 0.1% *(w/v)* in 2% solution for fabrication of fluorescently-labelled nanofibers (Figure 2.2).

Solution *(w/v)* %	**Voltage (kV)**	**Flow rate (mL/min)**	**Tip-Collector Distance (cm)**	**Volume (mL)**	**Time (min)**
PLA 2%	6	0.025	15 - 20	2	10

Table 2.1 Electrospinning parameters.

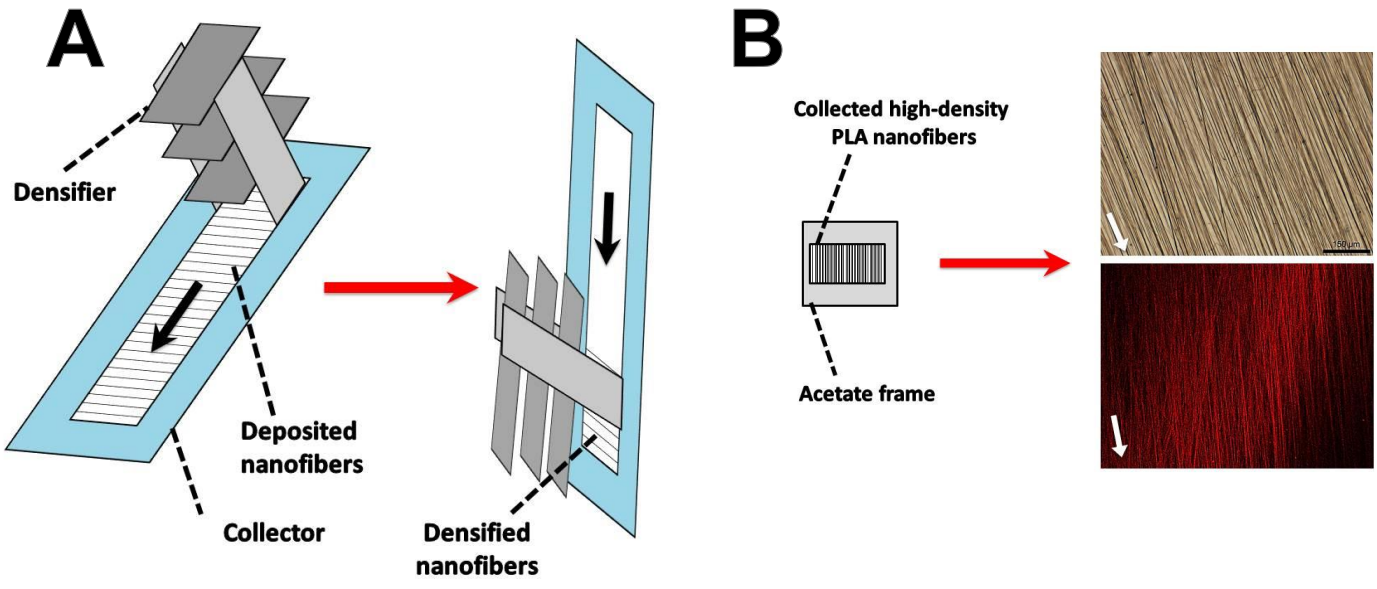

Figure - 2.2 Shows aligned nanofiber collection and imaging. A) Illustrates the manual densification process of nanofiber collection; B) Visualisation of transferred nanofibers under bright field and fluorescence microscopy. Arrows = direction of nanofibers.

2.2. Culture of primary cells

Human coronary artery smooth muscle cells (HCASMCs; Life Technologies, UK) and human umbilical vein endothelial cells (HUVECs; Life Technologies, UK) were cultured according to the supplier's recommendations. HUVECs were cultured in medium 200 (Life Technologies, UK) supplemented with low serum growth supplement (LSGS; Life Technologies, UK) whereas HCASMCs were cultured in medium 231 (Life Technologies, UK) supplemented with smooth muscle growth supplement (SMGS; Life Technologies, UK). The cells were placed in a humidified incubator at 37°C and 5% CO_2 with medium exchanged every other day, until confluent. In the present study, both HCASMCs and HUVECs were used until passage 5.

2.3. Construction of a 3D tissue engineered medial layer (TEML)

Type I collagen from rat tail was used to form the ECM for smooth muscle cells and construct a 3D TEML construct. All reagents were kept pre-chilled on ice to prevent unnecessary gelation during preparation. These reagents include: 10x αMEM, 1M NaOH, dH_2O and rat tail type I collagen (BD biosciences, California, USA). HCASMCs pellet were mixed at a density of 5 x 10^5/mL into a neutralised solution of 3 mg/mL type I collagen, according to the manufacturer's protocol shown below, and using αMEM in place of phosphate-buffered saline:

$$\frac{Final\ solution\ volume}{10} = \boldsymbol{volume\ of\ 10\ x\ \alpha MEM}$$

$$\frac{(final\ solution\ volume)\ x\ (final\ conc.of\ collagen\ desired)}{stock\ conc.of\ collagen} = \boldsymbol{volume\ of\ collagen}$$

$$volume\ of\ collagen\ x\ 0.023 = \boldsymbol{volume\ of\ 1M\ NaOH}$$

$$final\ solution\ volume - (volume\ of\ 10x\ DMEM + volume\ of\ collagen + volume\ of\ 1M\ NaOH) = \boldsymbol{volume\ of\ dH2O}$$

Where final solution volume is 0.2 mL x (number of samples), final concentration of collagen desired is 3 mg/mL and the stock concentration of collagen (which is subject to batch variation). 0.2 mL of the mixture was then loaded onto a 1 cm^2 square shaped filter paper frame with

underlying non-adherent PTFE plates, and the collagen-cell mixture was left to set for 40 minutes at 37˚C, 5% CO_2. The PTFE plates were removed and the gels were transferred into 24 well-plates. The formed gel was then covered with supplemented medium and the medium was changed every 48 hours. HCASMCs were subsequently allowed to grow in the TEML.

Another method was used to fabricate the TEML construct by fine-tuning of the above protocol. Instead of using HCASMCs pellet, the required number of cells were thoroughly suspended in a small volume of supernatant medium that was aspirated after centrifugation. This leads to a change in the final equation where the volume of media is subtracted from the final solution volume as shown below:

$$\frac{Final\ solution\ volume}{10} = \boldsymbol{volume\ of\ 10\ x\ \alpha MEM}$$

$$\frac{(final\ solution\ volume)\ x\ (final\ conc.of\ collagen\ desired)}{stock\ conc.of\ collagen} = \boldsymbol{volume\ of\ collagen}$$

$$volume\ of\ collagen\ x\ 0.023 = \boldsymbol{volume\ of\ 1M\ NaOH}$$

$$final\ solution\ volume - (volume\ of\ 10x\ DMEM + volume\ of\ collagen + volume\ of\ 1M\ NaOH + \boldsymbol{volume\ of\ media}) = \boldsymbol{volume\ of\ dH2O}$$

Primarily, the collagen reagents were mixed together prior to adding the cell suspension. 0.2 mL of the mixture was then loaded onto a 1 cm^2 square shaped filter paper frame with underlying non-adherent PTFE plates, and the collagen-cell mixture was left to set for 40 minutes at 37˚C, 5% CO_2. The PTFE plates were removed and the gels were transferred into 24 well-plates. The formed gel was then covered with supplemented medium with changing the medium every 48 hours. HCASMCs were subsequently allowed to grow in the TEML until they were observed to possess an elongated spindle-shaped morphology.

2.4. Construction of a 3D tissue engineered intimal layer (TEIL)

0.2 mL of a neutralised 3 mg/mL BD type I collagen solution was loaded upon a square frame made by filter paper with an area of 1 cm^2 to form an acellular collagen gel base first. An aligned, portable PLA nanofiber mesh previously fabricated (section 2.1) was coated with fibronectin (10 ng/mL). The coating was performed by placing the portable nanofiber mesh atop of a non-adhesive PTFE plate. A 1 mL of the fibronectin solution with a concentration of 10 ng/mL was applied on these nanofibers and allowed to incubate for 1 hour at room temperature. Following incubation, the fibronectin solution was removed, and the nanofiber was dried and used for construct fabrication. The coated nanofiber was placed atop of the constructed collagen gel. The fibronectin coating is a standard step in all fabricated TEIL constructs, unless or otherwise stated. The corners were then carefully sealed using a freshly prepared rat tail type I collagen solution. The sample was then placed in the incubator programmed at 37˚C, 5% CO_2 until the collagen was set. A sterile scalpel blade was used to cut the outer corner and remove the acetate frame. After successful attachment of the nanofibers to the collagen hydrogel, HUVECs (4 x 10^4 cells per sample) were carefully seeded in two separate occasions using small 10 µL volumes on top of the nanofibers. This is to prevent the cells from leaking over the confined area and eventually cell loss. The cells were allowed to attach at 37˚C, 5% CO_2 for 1 hour. Samples were then topped up with supplemented 200 medium and subsequently allowed to be cultured for 4 days at 37˚C and 5% CO_2, with a single media change on day 2.

2.5. Construction of a 3D multi-layered tissue engineering blood vessel (TEBV)

A 3D multiple layered TEBV construct was fabricated by using the methods explained above combining both TEIL and TEML constructs. A layer-by-layer methodology was used to fabricate the TEBV construct. Initially HCASMCs were seeded in type I collagen to make the primary base of the TEBV construct, creating TEML. Mainly, the collagen reagents were mixed together prior to adding the cell suspension. 0.2 mL of the mixture was initially loaded onto 1 cm^2 square

shaped filter paper frame with underlying non-adherent PTFE plates for optimisation, and the collagen-cell mixture was left to set for 40 minutes at 37˚C, 5% CO_2. The PTFE plates were removed and the gels were transferred into 24 well-plates. The formed gel was then covered with supplemented medium with changing the medium every 48 hours. HCASMCs were subsequently allowed to grow in the TEML until they were observed to possess an elongated spindle-shaped morphology.

Once the HCASMCs acquired a spindle-shaped morphology within the TEML, the media was removed. The TEML sample was placed on PTFE plates and PLA nanofiber mesh coated with fibronectin (10 ng/mL) was placed to create the second layer, acting as an *internal elastic lamina*. The fibronectin coating is a standard step in all fabricated TEBV constructs, unless or otherwise stated. The corners were then carefully sealed using a freshly prepared rat tail type I collagen solution. The sample is then placed in the incubator programmed at 37˚C, 5% CO_2 until the collagen is set. A sterile scalpel blade was used to cut the outer corners, removing excess nanofibers and the outlining acetate frame. After successful attachment of the nanofibers to the collagen hydrogel, HUVECs (4 x 10^4 cells per sample) were carefully seeded in two separate occasions using small 10 µL volumes on top of the nanofibers. Once HUVECs were attached, samples were topped up with the mixture supplemented medium 200 and 231 at the ratio of 7:3, and subsequently allowed to be cultured for 4 days at 37˚C and 5% CO_2, with a single media change on day 2. In such way, a tri-layered construct was fabricated composed of medial and intimal layers separated by PLA nanofibers.

2.6. Nanofiber coating

An experiment was designed to examine the effect of nanofiber coating on HUVECs attachment and growth over the course of 10 days (Table 2.2). The fabricated nanofiber scaffolds were coated with various materials such as soluble form of Horm-collagen (HC; 1 µg/mL) or dual coating of fibronectin (10 ng/mL) and Horm-collagen (1 µg/mL), previously discussed in section

1.4.1.1. The coating was performed by placing the portable nanofiber mesh atop of a non-adhesive PTFE plate. A 1 mL of the various solutions were applied on these nanofibers and allowed to incubate for 1 hour at room temperature. Following incubation, the solutions were removed, and the nanofibers were dried and used for TEIL fabrication. All samples including an uncoated control sample were imaged 4 and 10 days of culture using brightfield inverted microscope (Olympus, Japan).

Nanofiber coating	Sample 1	Sample 2
Horm collagen	✓	✓
Fibronectin	-	✓
Foetal calf serum	-	-

Table 2.2 shows the various nanofiber coating combinations used to attain a greater HUVECs coverage.

2.7. HUVECs seeding density

Various HUVECs densities on fibronectin coated nanofibers were investigated to observe the optimum cell seeding density. TEIL constructs were fabricated as stated in section 2.4 with two different HUVECs densities of $2.5x10^4/cm^2$ and $6.25x10^4/cm^2$. The cells were seeded on fibronectin (10 ng/mL) coated PLA nanofibers. A control sample was also prepared without underlying nanofibers to observe HUVECs coverage without alignment using a cell density of $2.5x10^4/cm^2$. The samples were cultured up to 14 days and images of the constructs were taken at 10 and 14 days of culture.

2.8. TEBV characterisation

2.8.1. Fluorescent visualisation of TEBVs

To observe the overall multi-layered structure of TEBV, the cells in each layer was stained with a cell tracker. HCASMCs were labelled with 5(6)-CFDA, SE; CFSE (5-(and-6)-Carboxyfluorescein Diacetate, Succinimidyl Ester), mixed isomers (CFDA, SE; 80 µM; Life Technologies UK) for 15 minutes at 37˚C and 5% CO_2 prior to seeding into the hydrogel (Boucher et al., 2015). The cells

were washed and re-suspended with a fresh medium to remove the excess dye after the end of incubation. This dye is a fixable-cell-permeant, green fluorescein-based cell tracker used for labelling cultured cells. HUVECs were labelled with 7-amino-4-chloromethylcoumarin (CMAC) cell tracker blue (20 µM; Life Technologies, UK) for 30 minutes and incubated at 37˚C and 5% CO_2 before seeding atop of the nanofiber. The cells were washed and re-suspended with a fresh medium to remove the excess dye after the end of incubation and prior to seeding. The fibronectin-coated nanofiber separating both of the layers was labelled with rhodamine b as stated in section 2.1. The TEBV was cultured as previously stated above. At the end of the culture period, the sample was imaged using a confocal microscopy and *z*-stacked with 15 µm steps. CFDA, SE was imaged at an excitation of 492nm and an emission of 517nm. Whilst, CMAC was imaged at an excitation of 353nm and an emission of 466nm. Rhodamine b was recorded at an excitation of 554nm and an emission of 627nm. The 3 layers were reconstructed in a 3-dimensional image to define the locations of the cells post-culture.

2.8.2. Endothelial cell permeability assay

Two different methods were used in determining permeability of the endothelial lining the TEIL construct. In the first method, 150 kDa Fluorescein isothiocyanate-dextran (Sigma Aldrich, USA) solution (1 mg/ mL in PBS) was applied on top of the cultured 3D TEBV samples and incubated for 60 minutes at 37˚C and 5% CO_2 (Chetprayoon et al., 2015). The fluorescently-labelled dextran was then removed and the samples were washed three times with PBS. The TEIL construct was examined in two different regions where HUVECs were confluent or non-confluent. This was determined by examining the construct by light microscopy for the underlying nanofibers. A *z*-stack (XYZ) scan from the luminal HUVECs surface through the TEBV was performed using confocal microscopy (Olympus, Japan). The slice step was set to 10 µm and 30 steps were recorded through the depth of the sample. Confluent and non-confluent regions of the TEIL sample were separately recorded on the same sample. The fluorescence intensity at the

different depths of the samples were measured using ImageJ software (National Institute of Health).

The second method uses the same principle by seeding a small volume of 5 µl 150 kDa FITC-labelled dextran solution on the centre of an inverted 3D TEBV construct. Prior to this, a 1.5 mL of PBS solution was added into a cuvette spectrophotometer. An aluminium foil with small openings was used to create a gasket to hold the construct above the PBS solution. The TEBV sample was overturned, in which the endothelial layer is facing downwards, and placed atop of the aluminium gasket. After the addition of dextran, the sample was immediately placed into the spectrophotometer holder to record the fluorescence. The permeability of the construct could then be measured via tracking the fluorescence in the PBS.

2.8.3. Immunostaining

2.8.3.1. Phenotyping HUVECs using CD31

To phenotypically assess whether HUVECs sustained its phenotype once applied on nanofibers, a CD31 (Dako, Glostrup, Denmark) immunostaining was performed (Cârţână et al., 2012; Fiedler et al., 2006). Initially, the TEIL (cultured for 4 days) was fixed with cold acetone for 5 minutes prior to staining. The acetone was discarded and the samples were washed with PBS. Following fixation, the TEIL samples were incubated with 10% FBS (Lonza, UK) diluted in PBS for 1 hour at room temperature, to block non-specific binding. The FBS solution was discarded and all the solution was removed without letting the samples to dry. Mouse anti-human CD31 monoclonal antibodies (1:20) was applied on the TEIL sample for 1 hour at room temperature. To avoid the evaporation of liquid during the incubation period, samples were stored in a closed box with placing wet paper inside the box to provide moisture. The samples were washed 3-times with PBS for 5 minutes, to remove any unbound primary antibodies. Subsequently, Alexa-Fluor 594 goat anti-mouse IgG_1 (H+L) secondary antibody (1:200, Life Technologies, UK) was incubated with the samples for 1 hour at room temperature, to detect the specific binding to CD31. The

samples were washed 3-times with PBS for 5 minutes, to remove any excess secondary antibodies. Samples were stained with DAPI-containing mounting medium. Non-aligned HUVECs monolayer was also prepared for comparison. These cells were cultured in an 8µ-well slide (Ibidi; Martinsried, Germany) with matching HUVECs density and stained for CD31 protein. Fluorescence images were obtained using a fluorescence inverted microscope (Nikon Eclipse Ti, Japan).

2.8.3.2. Intercellular adhesion molecule-1 (ICAM-1) expression of HUVECs

Immunofluorescence staining of ICAM-1 (Santa Cruz Biotech; Middlesex, UK) was performed on cultured TEBVs for 4, 10 and 14 days cultures. Initially, TNF-α (500 U/mL) was used as a positive control to stimulate ICAM-1 expression on the surface of HUVECs 24 hours prior to fixing, to mimic inflammation (Sawa et al., 2007; van Buul et al., 2010). Specifically, TNF-α was added at 3, 9 and 13 days to specific wells containing culturing TEBV samples. Unstimulated TEBV samples were prepared for controls. At the end of culture, samples were fixed overnight with 4% formalin solution. The samples were washed with PBS. Samples were blocked with 10 % goat serum (Santa Cruz Biotech; Middlesex, UK) for 20 minutes followed by incubation with mouse monocloncal anti-human ICAM-1 primary antibody (1:200) for 1 hour at room temperature. The samples were washed 3-times with PBS for 5 minutes, to remove any excess primary antibodies. This was followed by the incubation with Alexa-Fluor 594 goat anti-mouse IgG (H+L) secondary antibody (1:200, Life Technologies, UK). The samples were washed 3-times with PBS for 5 minutes, to remove any unbound secondary antibodies. These were then stained with DAPI-containing mounting medium. The samples were then visualised using fluorescence inverted microscope (Nikon Eclipse Ti, Japan) to obtain fluorescent images.

2.8.3.3. Cell viability assessment using live-dead cell staining assay

Cell viability was assessed using a live-dead cell double staining kit (Life Technologies, UK). Initially, the culture media was removed from the TEBV construct. The construct was washed once with PBS and a solution mixture containing calcein-AM (green) and ethidium homodimer-1 (red) was added. The kit contained Calcein-AM and Propidium iodide which fluorescently stained live and dead cells, respectively. The mixed dye solution was incubated with the TEBV construct for 30 minutes at 37°C and 5% CO_2 in the dark. After the incubation period, the solution was discarded to remove the unbound excess dye. PBS was added to the sample to keep the sample moist and avoid drying. The cells were immediately examined using a FV300 confocal microscope (Olympus, Japan). For 3D samples such as TEBV, confocal laser scanning microscopy has widely been applied (Gantenbein-Ritter et al., 2011). The primary advantage of this approach is its ability to produce optical sections through TEBV construct, by moving the focal plane of the instrument stepwise through the depth of the construct. A series of optical sections (stacks) were collected which was combined to produce a volume rendered 3D reconstructions of the TEBV construct.

2.8.3.4. Phalloidin staining of TEML constructs

TEML constructs cultured for 10 days were fixed with 4% paraformaldehyde in PBS for 20 minutes at room temperature. The samples were then washed with PBS and permeabilised with 500 µL of 0.1% TritonX-100 in PBS for 5 minutes at room temperature. Yet again, the samples were rinsed with PBS. 500 µL of tetramethylrhodamine-conjugated Phalloidin (10 µg/mL; Sigma-Aldrich, UK) was incubated with the TEML samples for 60 minutes at room temperature in the dark, to fluorescently stain actin filaments. Cell morphology was examined using confocal microscopy (Olympus, Japan).

3. Results

3.1 Optimising the intimal layer

In the initial part of the project, HUVECs were cultured on aligned nanofibers to generate an aligned endothelial cell layer, and experiments were performed to assess whether the cells change their phenotype with these culture conditions. Figure 2.3 shows a diagrammatic representation of parameters and variables that were tested to optimise and characterise the intimal layer.

3.1.1 HUVECs alignment

Since aligned electrospun PLA nanofibers have previously been shown to have beneficial effects on the attachment and alignment of other cell types (Sankaran et al., 2014; Yang et al., 2011), experiments were performed to examine the effect on the extent of orientation of HUVECs growth when cultured on PLA nanofibers. PLA nanofibers were fabricated and used to support HUVECs layer during cell culture to facilitate the production of a highly-aligned HUVECs layer. HUVECs were initially cultured in tissue culture flasks. HUVECs were not used after passage 5 as these cells are known to alter their phenotype with HUVECs spreading and migration decreasing at later passages (Liao et al., 2014). A TEIL was constructed by culturing HUVECs atop of an aligned PLA nanofiber mesh. These nanofibers were then transferred on top of collagen type I hydrogels and their ability to align HUVECs growth was tested against HUVECs seeded without nanofibers. The 2-dimensional endothelial cells are initially round when unattached to the tissue culture flask after attachment, and ultimately acquiring a cobblestone morphology a few hours after seeding (Figure 2.4A).

Once HUVECs became confluent, the cells were harvested and 2.5 x 10^4 HUVECs were seeded on top of a collagen hydrogel in the presence or absence of an uncoated PLA nanofiber scaffold (area = 1 cm^2). The underlying collagen gel provides sufficient mechanical strength to allow easy handling of the constructs. The samples were cultured for 2 days and optical image were taken (Figure 2.4B and C). HUVECs showed random orientation and similar morphology to the 2D

HUVECs monolayers as described above, however seemingly tightly packed due to the underlying collagen type I hydrogel (Figure 2.4B). In comparison, seeding the cells on top of the aligned nanofiber mesh supported with an underlying collagen type I hydrogel showed a high degree of cellular alignment, with an average angle of 6.3° orientation against the direction of the nanofibers. HUVECs were observed to be highly-aligned within an hour post-seeding (Figure 3.2C). Aligned nanofibers orient the HUVECs growth in one direction facilitating their growth in the desired direction. However, gaps between the HUVECs could be seen in places even when the constructs were cultured for over 14 days. HUVECs appeared to be unable to fully cover the surface of a construct with uncoated PLA nanofibers due to large spaces being visible between the cells. The diameter range of the nanofibers was determined by analysis of the representative images shown in Figure 2.2B, with an average diameter of 631 nm.

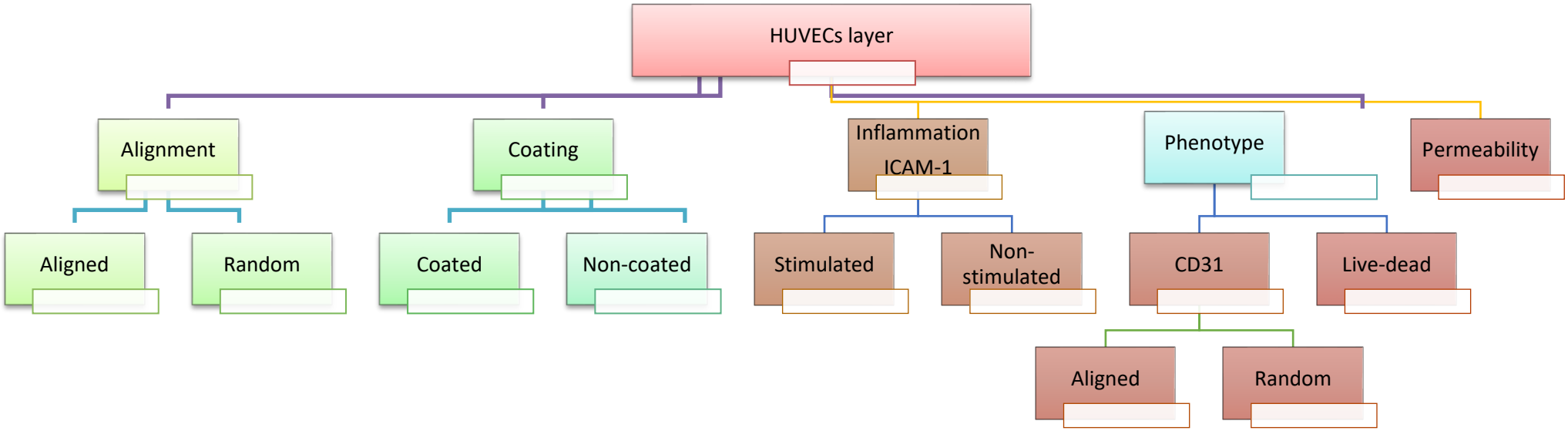

Figure 2.3 - Shows a simplified diagrammatic representation of the features that have been tested to optimise and characterise the HUVEC layer.

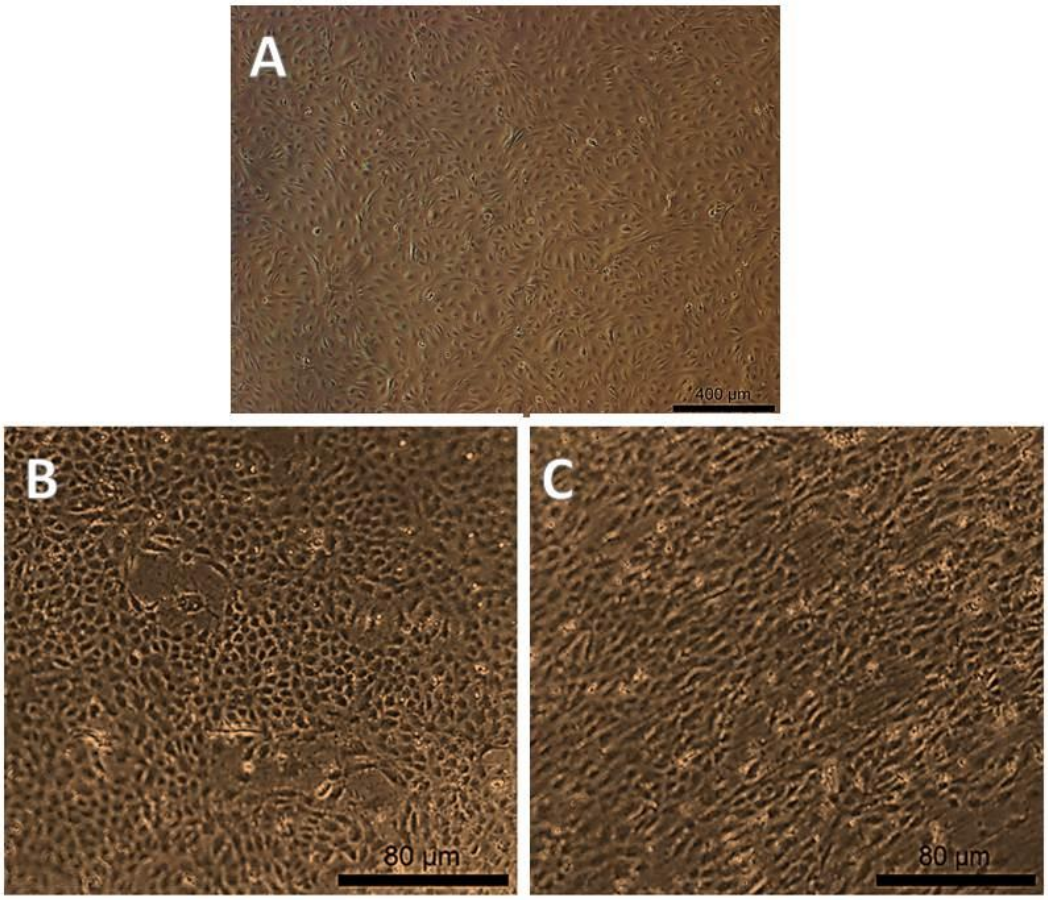

Figure 2.4 - **Shows morphology and orientation of cultured HUVECs in 2-dimensions and 3-dimensions.** Confluent HUVECs monolayer culture in cell culture flask (P2); tissue-engineered intimal layer showing HUVECs morphology cultured without (A) and with (B) highly aligned PLA nanofibers. Results are representative of 6 experiments (n=6). Scale bar A) = 200 µm and B,C) 80 µm.

3.1.2 The effect of nanofiber coating on HUVECs attachment and coverage

The effect on HUVEC cell attachment and growth of coating the PLA nanofibers with Horm collagen, and fibronectin was assessed. Firstly, nanofibers were coated with either Horm collagen alone (1µg/mL) or in combination with fibronectin (10 ng/mL). Horm collagen was used to coat the nanofibers as this is a key adhesive ligand for platelet binding to the subendothelial matrix after vascular damage. These coated nanofibers were then transferred on top of collagen hydrogels and their ability to facilitate HUVECs attachment and coverage were tested against HUVECs seeding on uncoated nanofibers. Preliminary experiments demonstrated that the optimal seeding density for

cell culture was 2.5 x 10^4 /cm^2, and this was initially used. Table 2.2 shows the different nanofiber coatings tested. These samples were cultured for 10 days to observe their growth over the culture period.

Figure 2.5, shows HUVECs seeded atop of the differentially-coated nanofibers. At day 4 of culture, none of the samples show a complete coverage by HUVECs, although this was observed to improve over the culture period in some samples. At day 10 of culture, Horm-collagen coated samples showed an increased HUVECs coverage compared to the uncoated sample, although some gaps between the HUVECs layer could still be seen. Dually-coated (fibronectin+Horm collagen) nanofiber sample showed a significantly enhanced surface coverage of HUVECs compared to the uncoated sample. At day 10, HUVECs had entirely covered the dually-coated nanofibers without visible gaps under light microscopy. Due to the enormous cost involved in using Horm-collagen for construct fabrication, fibronectin-coated nanofibers were used for subsequent samples to achieve a complete layer of HUVECs.

3.1.3 The effect of HUVECs density on fibronectin coated-nanofibers

The next experiment investigated the effect of varying HUVECs seeding densities and culture time to optimise the development of a complete HUVECs layer. Therefore, HUVECs were seeded atop of fibronectin-coated nanofibers attached on the surface of a collagen hydrogel to provide mechanical support. Two different seeding densities were used 2.5 x 10^4 cells/cm^2 and 6.25 x 10^4 cells/cm^2. Figure 2.6 shows that using a higher HUVECs density occupied a bigger surface area on the nanofibers and HUVECs eventually detached and left gaps that expose the underlying nanofibers. This is clearly shown at day 14 of culture with arrows pointing at the gaps between HUVECs (Figure 2.6B). However, using a lower HUVECs seeding density appears to be better as the HUVECs sustain a perfect coverage over 14 days of culture (Figure 2.6D). In contrast, HUVECs seeded directly onto a collagen gel do not appear elongated (Figure 2.6E-F). In these regards, we can conclude that a seeding density of 2.5 x 10^4/cm^2 is an ideal density to be used for construct generation. However,

14 days of cell culture would significantly limit the experimental throughput. Further assessment found that increasing the seeding density to 4 x 10^4/cm^2 and culturing for 4 days gives the same result with regards to an increased HUVECs coverage (Figure 2.7). For this reason, this seeding density and timeframe was used for subsequent experiments.

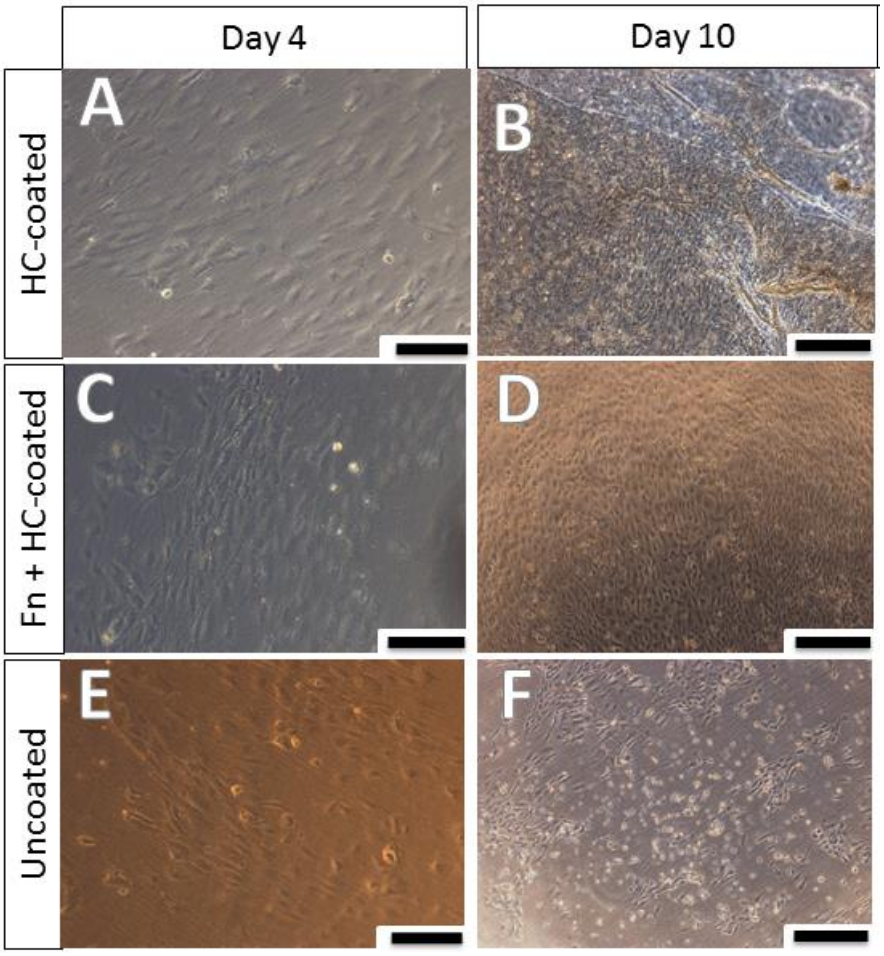

Figure 2.5 - Shows optical images of HUVECs growth atop of various coatings of nanofibers, at days 5 and 10 post seeding. A, B) Horm-collagen coated nanofibers; C,D) dual (Fn+HC)-coated nanofibers; E,F) Uncoated nanofibers. HC = Horm-collagen; Fn = Fibronectin; Scale bar A, C and E = 1500 µm; B, D and F = 400 µm. Results are representative of 3 experiments.

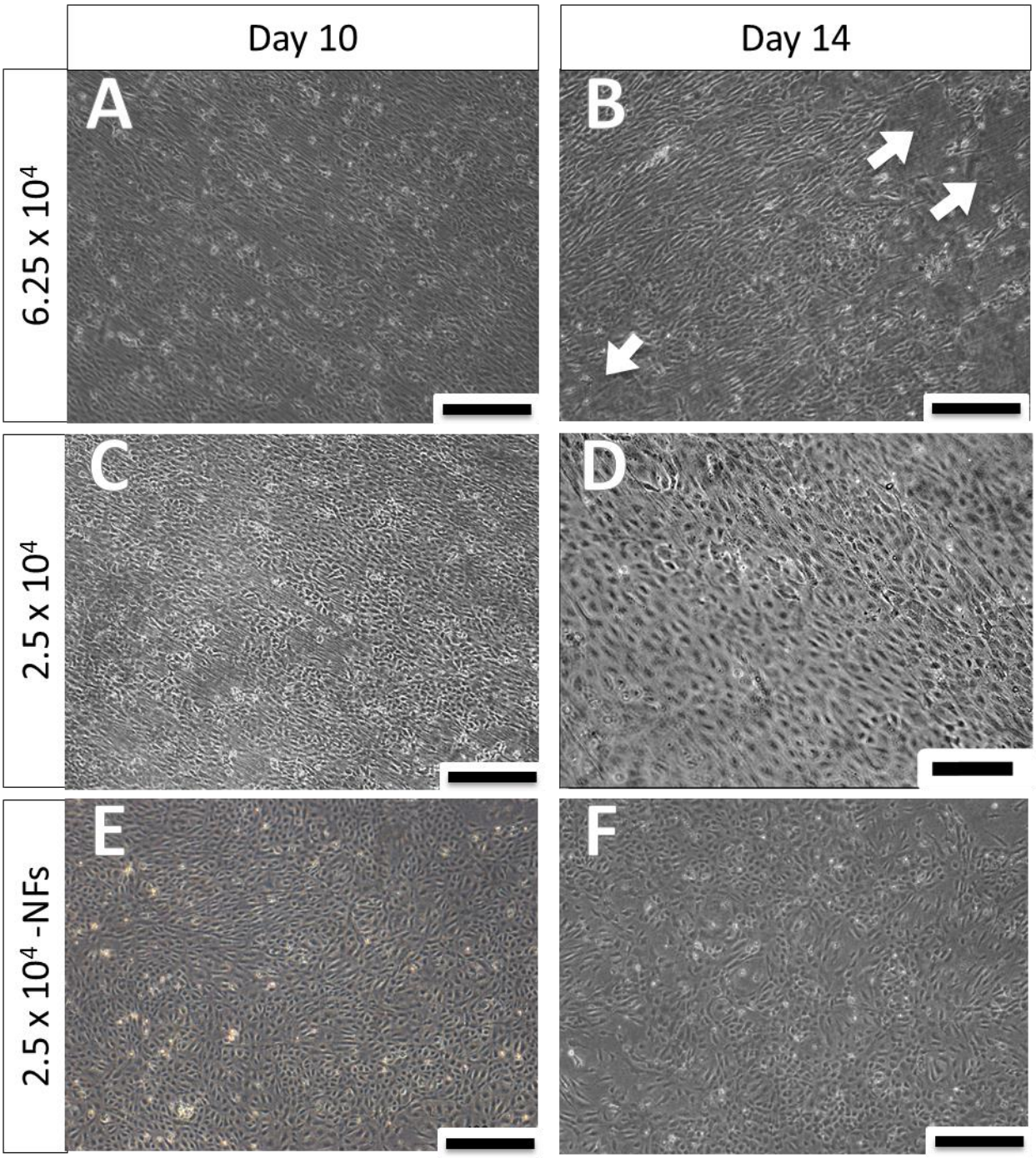

Figure 2.6 - Shows light microscopy images of different HUVECs densities seeded with and without nanofibers at 10 and 14 days of culture. A, B) with underlying fibronectin-coated nanofibers; C,D) with underlying fibronectin-coated nanofibers; E,F) without underlying nanofibers. Scale bar = 400 µm (except for D = 200 µm). Arrows show gaps between HUVECs. Results are representative of 3 experiments.

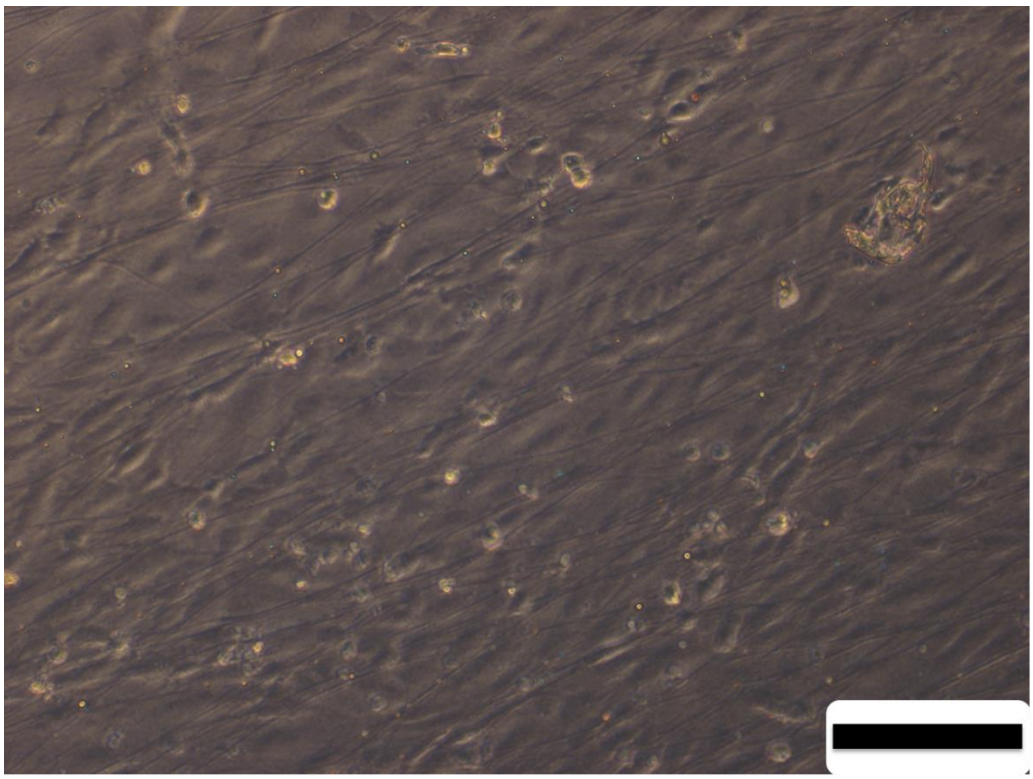

Figure 2.7 - **Shows light microscopy images of TEIL construct cultured for 4 days.** A cell density of 4 x10^4 was used to generate HUVECs monolayer with a high coverage. The cells were cultured on an underlying fibronectin-coated (10 ng/mL) nanofibers. Scale bar = 150 µm. Results are representative of 4 experiments.

3.1.4 CD31 immunostaining of HUVECs

Due to previous reports of changes in HUVECs phenotype when grown using different culture environment, experiments were performed to examine if HUVEC phenotype was stable in our culture system. ECs exhibit a number of unique cell specific markers, of which the expression of the platelet endothelial cell adhesion molecule (PECAM-1, CD31) is a widely accepted marker of normal HUVEC phenotype (Unger et al., 2002). Therefore, we examined whether the cell morphological changes observed upon culturing of HUVECs elicited any alteration in their basic endothelial phenotype by examining the expression of this endothelial cell marker.

Figure 2.8 shows the CD31 staining images of HUVECs grown on aligned PLA nanofibers or those allowed to grow randomly on an 8 µ-well culture plate. It can be observed that both HUVECs

populations strongly expressed CD31. Qualitative examination confirmed that the basic HUVECs phenotype does not change with changes in the cell alignment. This is in agreement with our findings that nanofibers-cultured HUVECs also maintain the normal elongated cobblestone morphology expected of ECs. There was no obvious difference observed between the aligned and non-aligned HUVECs in their CD31 expression with regards to phenotype.

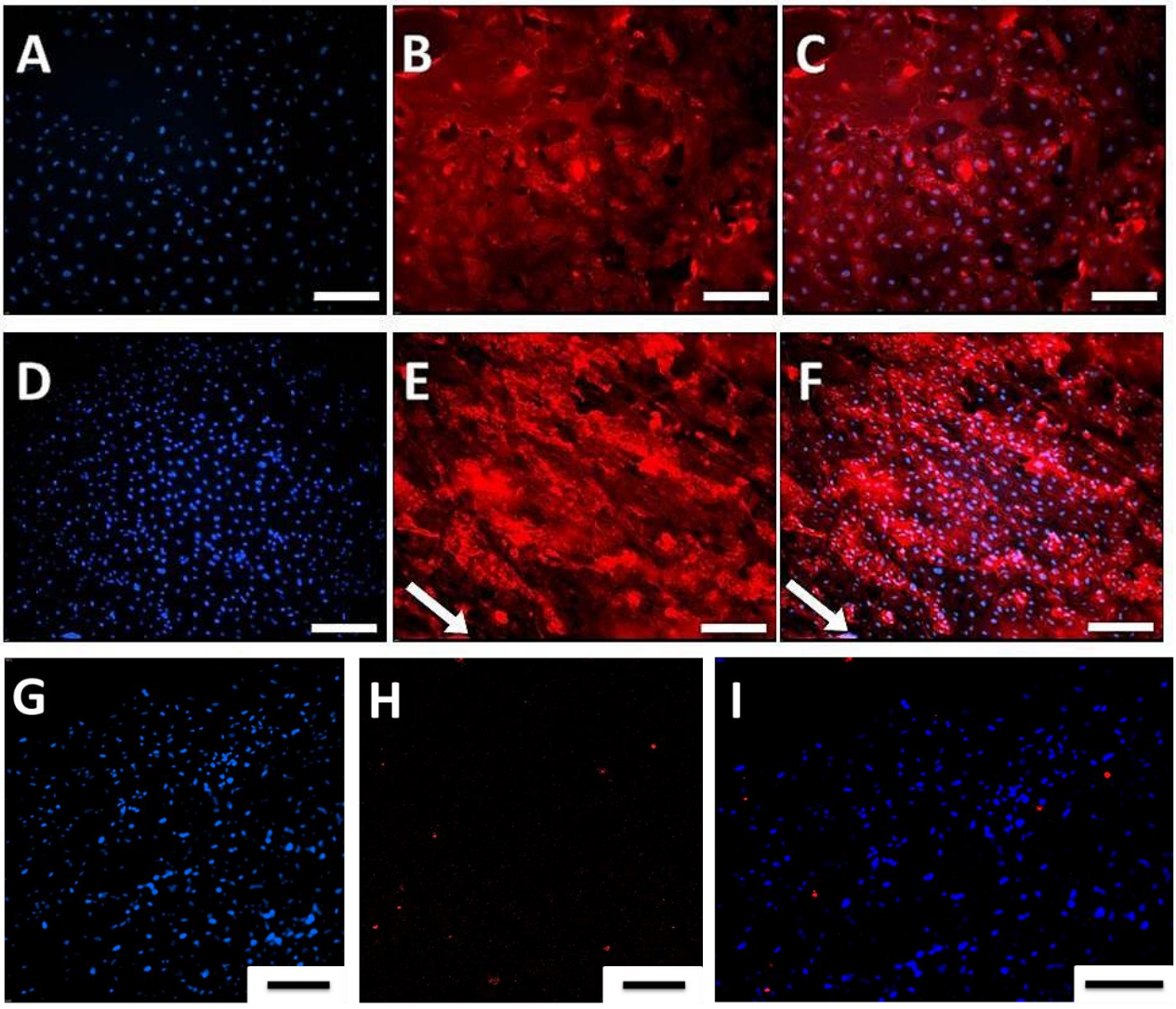

Figure 2.8 - Fluorescence images showing HUVECs CD31 expression. HUVECs were grown without (A-C) and with PLA nanofibers (D-F). Mesenchymal stem cells used as a negative control (G-I). A, D, G) DAPI channel, B, E, H) TRITC channel, C, F, I) Merged images of DAPI and TRITC channels. CD31 (HUVECs marker, Red); DAPI (nucleus marker, Blue), Scale bar = 200 µm.

3.1.5 ICAM-1 expression of HUVECs

Immunofluorescent labelling was performed to characterise HUVECs present on the surface of the TEBV construct. In healthy endothelial cells, these cells express limited amount of the ICAM-1 cell surface marker, however under pathological conditions HUVECs can be seen to express large amounts of ICAM-1 indicating a transition of these cells into an inflammatory phenotype which is linked to leukocyte adhesion and transmigration towards the trigger of inflammation. Therefore, a high expression of ICAM-1 protein on HUVECs would indicate their adoption of this pro-inflammatory phenotype. ICAM-1 is present at low levels on the surface of healthy HUVECs, but its expression can be increased by treatment with pro-inflammatory cytokines. Therefore, TNF-α was used to stimulate expression on the surface of HUVECs to determine whether our samples showed a pro-inflammatory phenotype. To define stimulatory conditions in which endothelial cells express elevated levels of ICAM-1, we treated TEBVs with the prototypic inflammatory cytokine TNF-α for 24 hours. ICAM-1 expression was increased for samples stimulated with TNF-α as assessed by confocal microscopy imaging (Figure 2.9). Subsequent confocal microscopy analysis showed that the surface of the endothelial cell membrane forms small filopodia-like protrusions on TNF-α stimulated samples. The untreated samples show a minimal expression of ICAM-1 surface markers, suggesting that our TEBV cells possess a physiological, non-inflammatory phenotype.

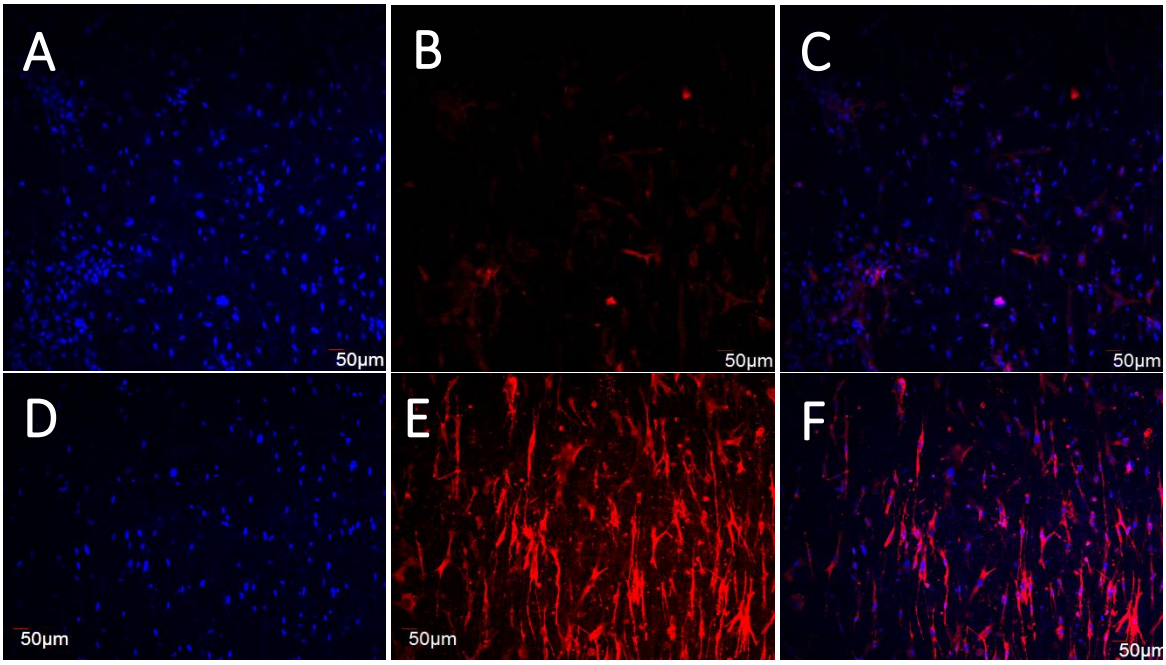

Figure 2.9 - Fluorescence images showing ICAM-1 protein expression of TEBVs. ICAM-1 expression of unstimulated tissue-engineered blood vessel (A-C) compared with 24-hour TNF-α-activated tissue-engineered blood vessel (D-F) cultured for 4 days. Results are representative of 4 experiments (n=6). ICAM-1 (HUVECs inflammatory marker, Red); DAPI (nucleus marker, Blue), Scale bar = 50 µm.

3.2 Optimising the medial layer

3.2.1. Morphology of smooth muscle cell monolayers

HCASMCs seeded onto cell culture plates possess round shape morphology with a bright centre under the light microscope, until they become attached. Once the cells are fully attached to the bottom of the cell culture plate, the cells stretch and acquire a spindle-shaped morphology (Figure 2.10). Confluency of the plate can be achieved within 4 days of culture when seeded at a density of 0.5 x 10^6 cells in T75 flasks.

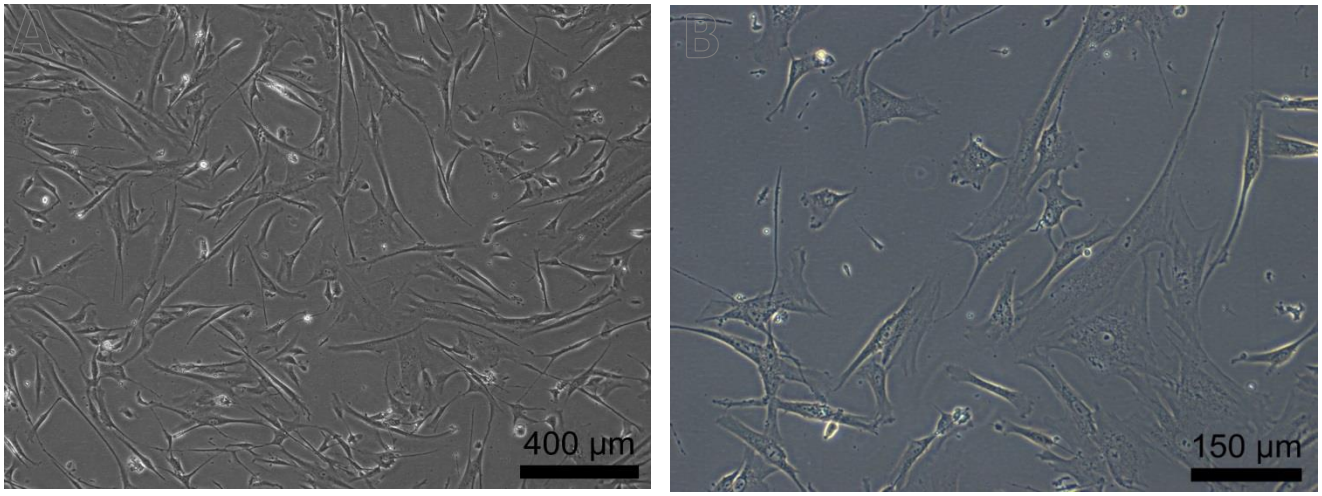

Figure 2.10 - Shows optical images of the morphology of human coronary artery smooth muscle cells 24 hours post seeding on cell culture flask. A) low magnification; B) high magnification.

3.2.2. HCASMCs morphology within the collagen hydrogel

To accurately replicate the medial layer of the blood vessel, we seeded HCASMCs within type I collagen hydrogels to mimic the composition of the native medial layer. Experiments were performed to optimise the culture and processing conditions for the HCASMCs grown within the TEML construct. Initial work optimised the mixing order of the HCASMCs pellet with collagen gel components. The cells were harvested from cell culture plates and seeded into type I collagen hydrogels using two different forms involving the addition of collagen mixture onto (i) cell pellet or (ii) cell suspension. Using the former method, the majority of the HCASMCs are round and do not seem to be spreading within the hydrogel after 2 days of culture (Figure 2.11A). After 6 days of culture the HCASMC morphology had not significantly changed (Figure 2.11B). In contrast, when collagen mixture was added to a cell suspension, the seeded HCASMCs show successful spreading within the hydrogel. HCASMCs initially show a rounded morphology that change over time. Subsequently the cells started to acquire an elongated, spindle-shaped morphology with elongated cell body. The cells rapidly regained their original spindle-shaped morphology within 24 hours of

seeding within the collagen hydrogels (Figure 2.12). The TEML was then cultured and cell morphology was monitored for up to 10 days. Therefore, the mixing of HCASMCs with a cell suspension was used for culturing the TEML in all subsequent experiments.

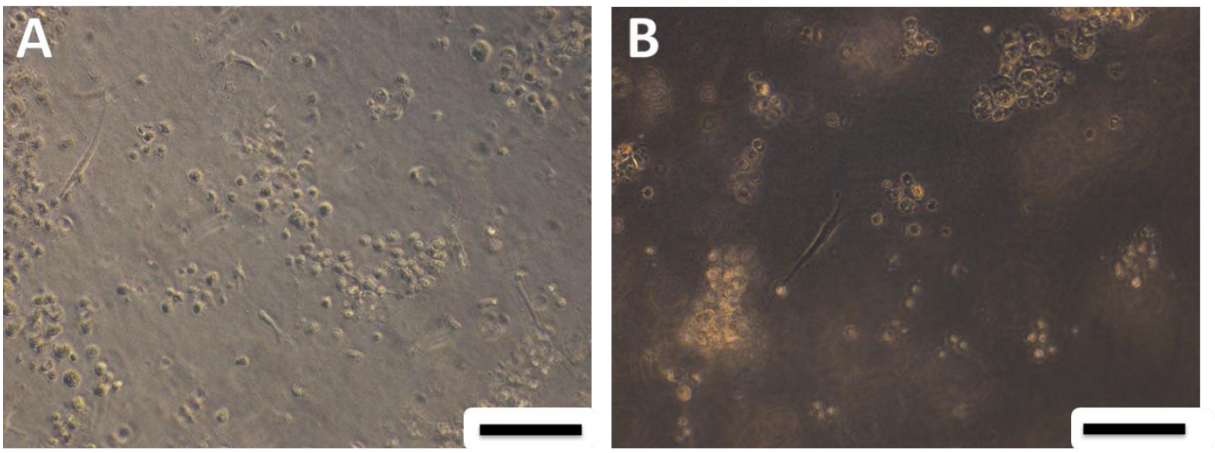

Figure 2.11 - Shows light microscopy images of the morphology of human coronary artery smooth muscle cells seeded within type I collagen hydrogel using the pellet method. A) HCASMCs morphology 2 days post collagen type I seeding; B) 6 days post type I collagen seeding. Scale bar = 150 µm

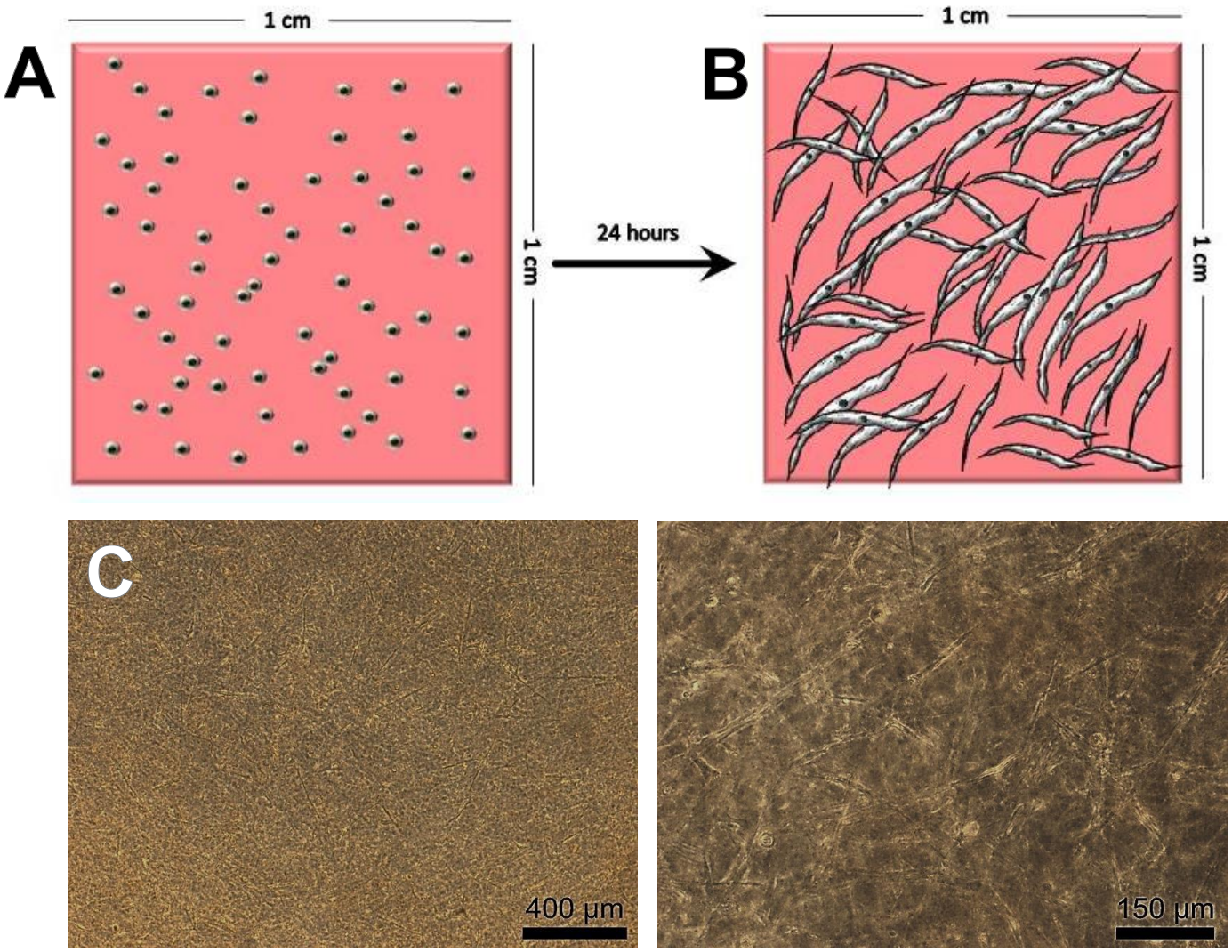

Figure 2.12 - Shows the morphology of Human Coronary Artery Smooth Muscle Cells 24 hours post seeding in type I collagen. A,B) An illustration of HCASMCs morphology 0 and 24 hours post collagen type I seeding; C) A low magnification of bright field image of HCASMCs morphology 24 hours post type I collagen seeding. D) A high magnification of bright field image of HCASMCs morphology 24 hours post type I collagen seeding Scale bar = C) 400 µm; D) 150 µm.

3.3 Assembly of TEBVs

Once majority of the HCASMCs were elongated (at around day 10 of culturing), the TEML construct could be seeded with HUVECs. To accurately replicate the physiological vessel wall layers, HUVECs were seeded atop of aligned PLA nanofibers supported with the previously

constructed TEML to create a 3D TEBV model (as shown in Figure 2.13). The HUVECs were observed to show alignment on top of this construct within an hour of seeding.

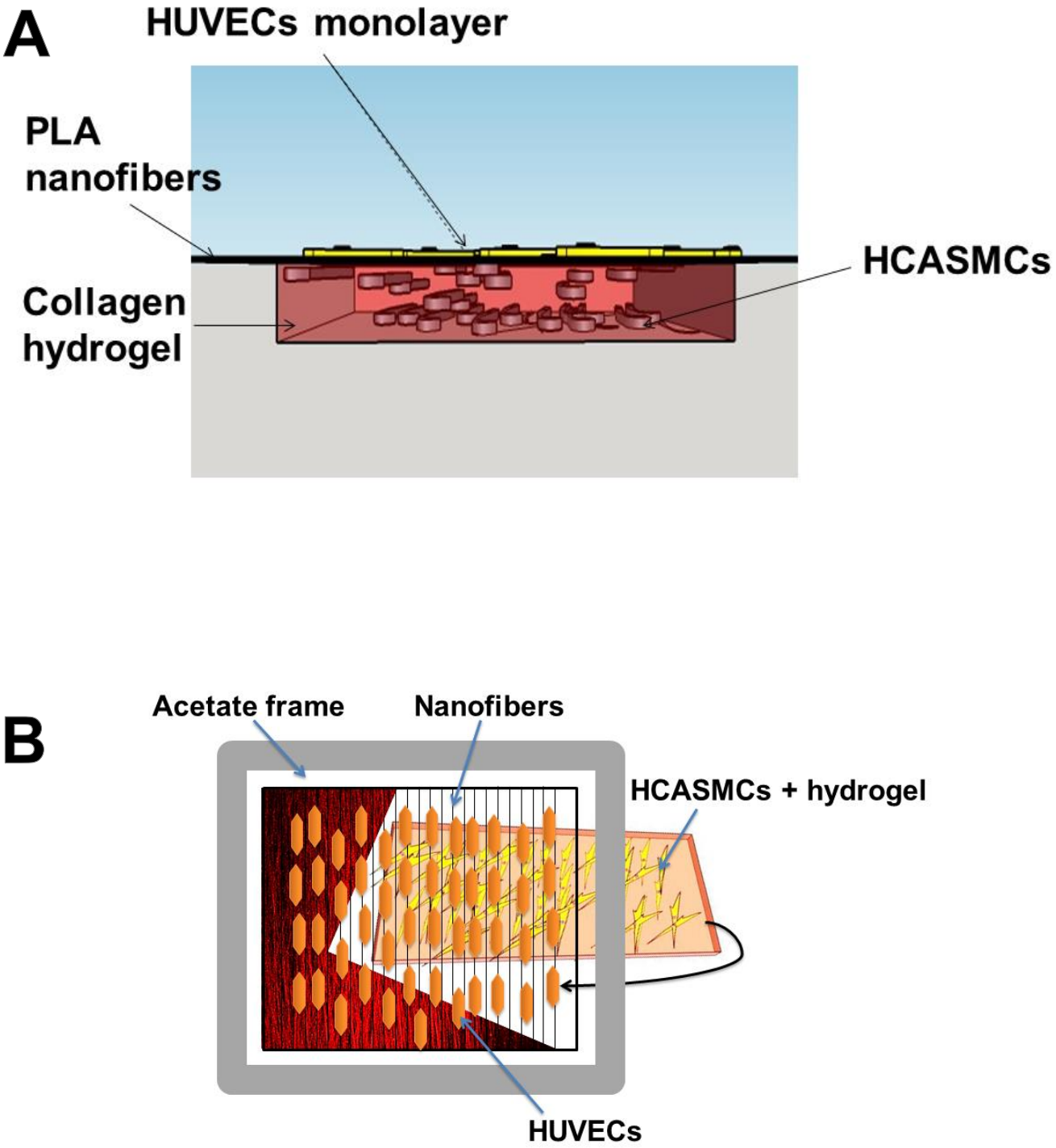

Figure 2.13 - Diagrammatic representation of a (A) top view of a multi-layered TEBV construct and its assembly; (B) Side view sketch of the TEBV construct showing the locations of the cells within the construct.

3.3.1. Defining regional cellular localisation within TEBVs

To observe whether the cells stably stayed within their seeding region or migrate between layers of the co-culture, HUVECs and HCASMCs were tracked using cell tracker dyes. TEBVs were cultured for 4 days and imaged using confocal microscopy to show cellular locations. As shown in Figure 2.14, HUVECs remained in the upper region where they were initially seeded, and no cells migrated to the below layer. Alternatively, HCASMCs also remained within the TEML and no cells migrated into the other regions too. This layer made up majority of the construct due to the thickness of the collagen hydrogel. From these tracking experiments of the TEBV in co-culture, it was demonstrated that this technique has allowed us to reproducibly generate a tri-layered vessel model which stably maintained defined intimal and medial layers throughout the culture period.

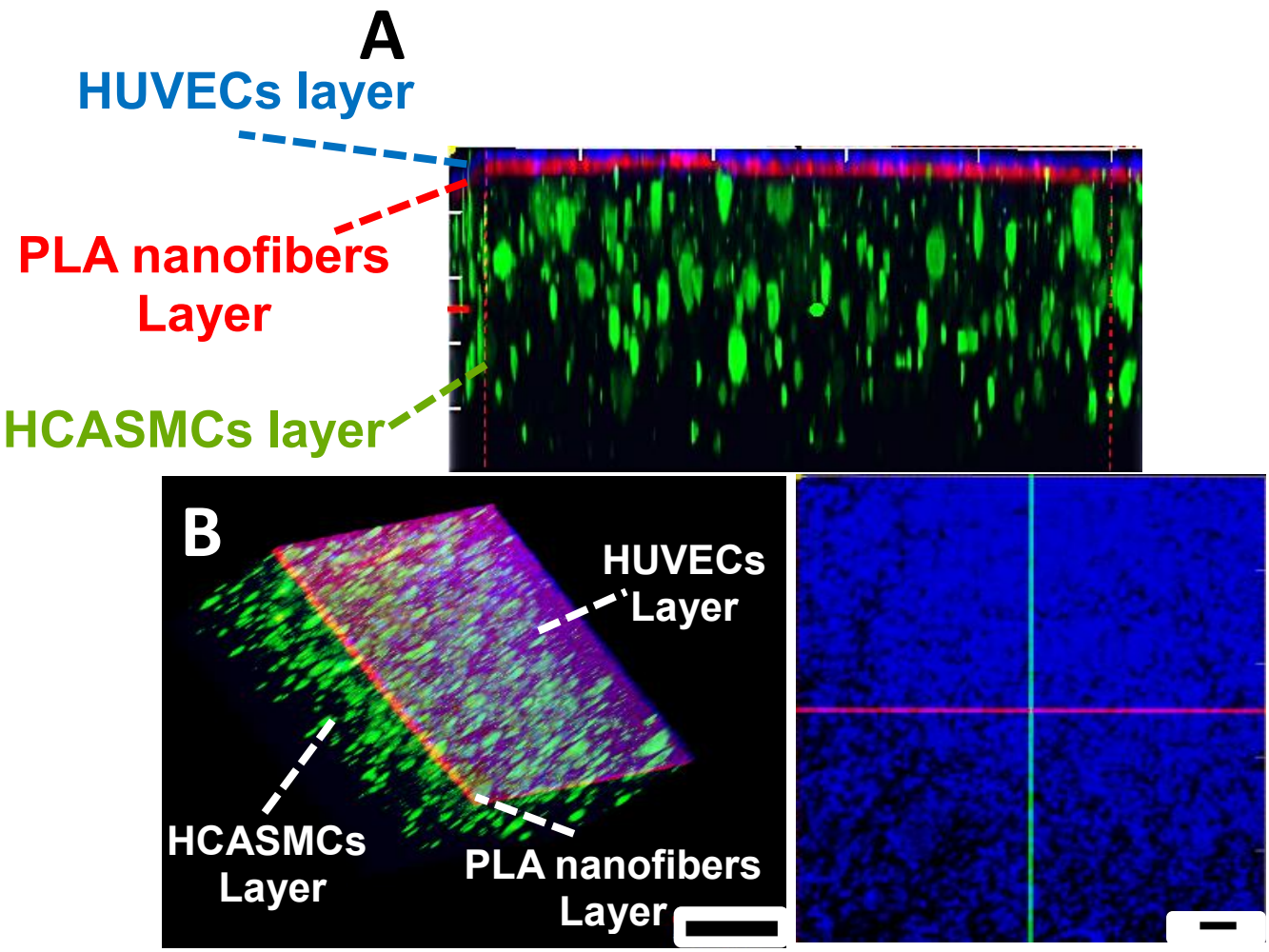

Figure 2.14 - Fluorescent 3D image of *z*-stack TEBV highlighting the integrated tri-layered construct. A) Side view of a multi-layered TEBV construct; B) Angle view of the TEBV construct showing the locations of the cells within the construct. C) Top view of the TEBV construct. Blue = HUVECs; Red = nanofibers; Green = HCASMCs. Scale bar = C) 30 µm.

3.3.2. Cell viability staining of TEBV using live-dead assay

Cell viability is an important parameter in tissue engineering to evaluate the effect of environmental conditions on cell viability. To assess cell viability within TEBV layers, live-dead staining was used. Using this technique viable cells show predominantly green fluorescence whereas dead cells appear to mainly emit red fluorescent light. HCASMCs within the TEBV can be observed to be viable as shown by the strong green fluorescence from these cells displaying spindle-like morphology as observed previously in section 3.2.2 (Figure 2.15). No dead HCASMCs were detected for the first 10

minutes of imaging. Similarly, for HUVECs, the number of dead cells was zero at the start of imaging. In addition, HUVECs show a strong green fluorescence showing almost complete coverage across the surface of the TEBV construct, indicating the creation of a viable, confluent intimal layer in agreement with our previous findings, these cells are also found to be highly-aligned indicating the underlying nanofibers are serving to provide contact guidance to the HUVECs (Figure 2.15H). Although the endothelial layer appears to be complete, the potential for paracellular transport at a molecular level remains, therefore the permeability of the endothelial cell layer required investigation.

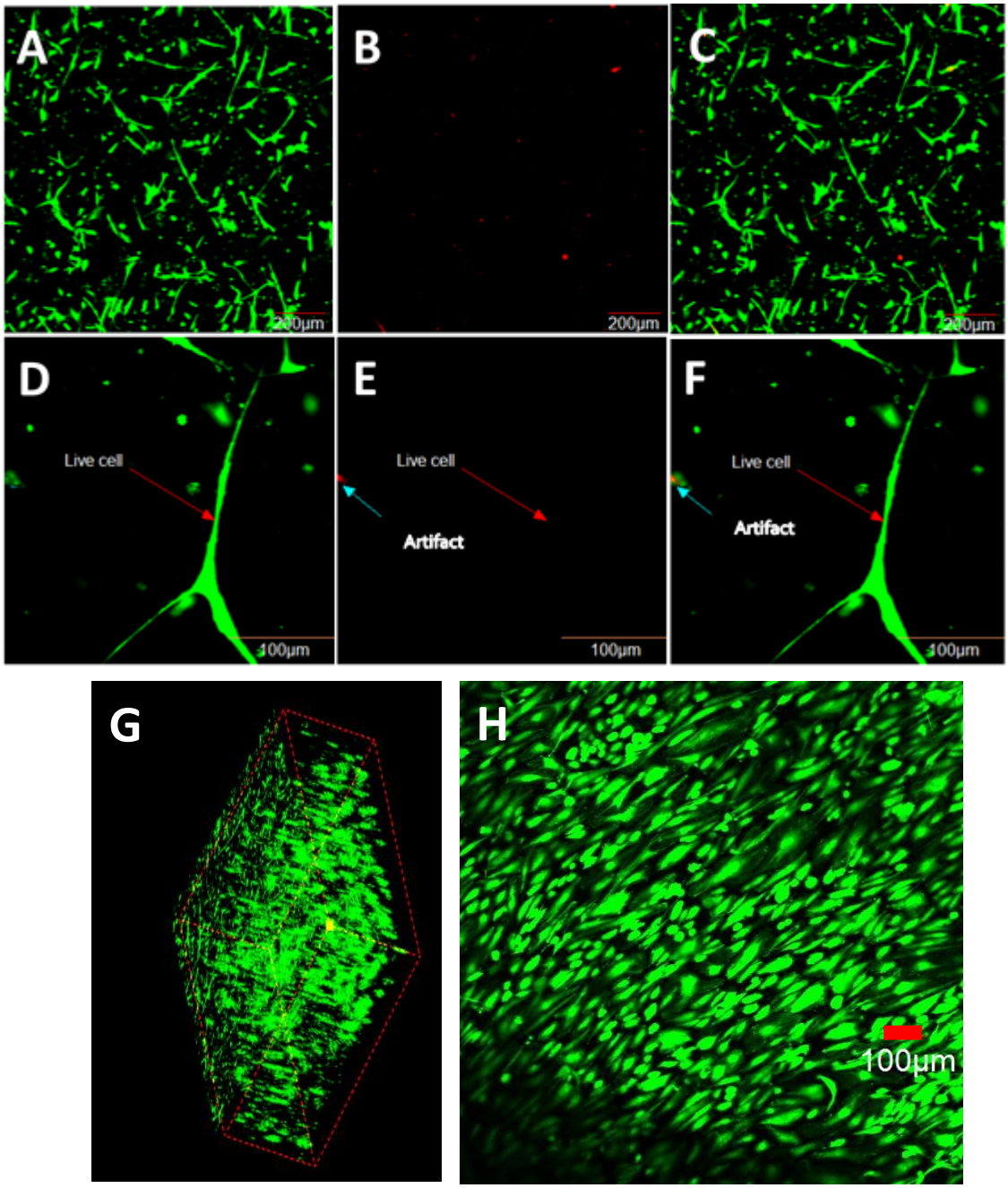

Figure 2.15 - Shows fluorescence live-dead staining fluorescent images of TEBV layers cultured for 4 days using calcein-AM and ethidium homodimer-1. Live-dead staining of HCASMCs within TEBV (A-C); High magnification image of a live smooth muscle cell (D-F); 3-dimensional *z-stack* image of combined TEML section planes (G); Live-dead staining of the top upper layer of TEBV construct (H). A, D) FITC channel; B, E) TRITC channel and C, F) Overlay of FTIC and TRITC channels. Scale bar = 200 µm for A-C, H and 100 µm for D-F. Results are representative of 4 experiments (n=6). Calcein-AM (live cell marker, Green); ethidium homodimer-1 (dead cell marker, Red).

3.3.3. Permeability of the TEBV

Initial permeability experiments were performed to test whether confluent sections of the HUVECs layer of TEBV was able to create effective intercellular junctions to resist the transfer of plasma proteins across the endothelial lining. The permeability of the intimal model was tested by examining the ability of a fluorescently-labelled high molecular weight dextran molecule to permeate across the endothelial lining. To do this the constructs were exposed to a solution containing high molecular weight FITC-dextran (1mg/mL) on the luminal surface of the construct, for 1 hour at 37˚C and 5% CO_2 (n = 3). Using confocal microscopy, 30 z-stack sectioned images (slice thickness = 10 µm) were recorded for each sample, to observe the extent of FITC-dextran infiltration across the luminal surface of complete and non-complete regions of the HUVECs layer. The start of the z-stack was determined by focusing on the HUVECs layer and starting to set the Z-stack settings to slice from this focal plane (0) to 300 µm depth. By using the ImageJ software package, it was possible to analyse the amount of FITC dextran fluorescence found in each of the individual images from the Z-stack collection.

These data were then used to plot a graph of FITC dextran intensity against the sample thickness (depth) for the different regions of the construct. These data are shown in Figure 2.16, and showed that at the same depth of the sample, FITC-dextran intensity was higher in non-complete regions of the construct than in regions where HUVEC growth has reached high coverage. Thus, complete regions of HUVECs seeded on nanofibers showed a better ability to reduce the penetrance of the fluorescent dextran into the underlying collagen hydrogel than in non-confluent regions of the same construct. However, the confluent HUVECs layer does not completely block translocation of the fluorescent dextran. Further experiments were required to consider whether this is due to an inability of the HUVECs to form tight intercellular junctions or whether this is due to FITC dextran diffusing laterally through the gel from areas underlying non-confluent regions of the sample to the areas of the gel underneath areas of confluent HUVEC growth. It could also be the selected slice

thickness for the z-scan is too large, and so the observed fluorescence is actually collected from the applied dextran solution above the cell layer. Also, HUVECs layer in covered and non-covered regions do not start from the same fluorescent point. Namely, non-complete regions start from a higher fluorescent point compared to a complete region. Therefore, the experimental set-up was not a valid method to test for permeability. Hence, another technique was pursued to test for a 3-dimensional permeability test to accurately measure dextran movement across the endothelial cell layer.

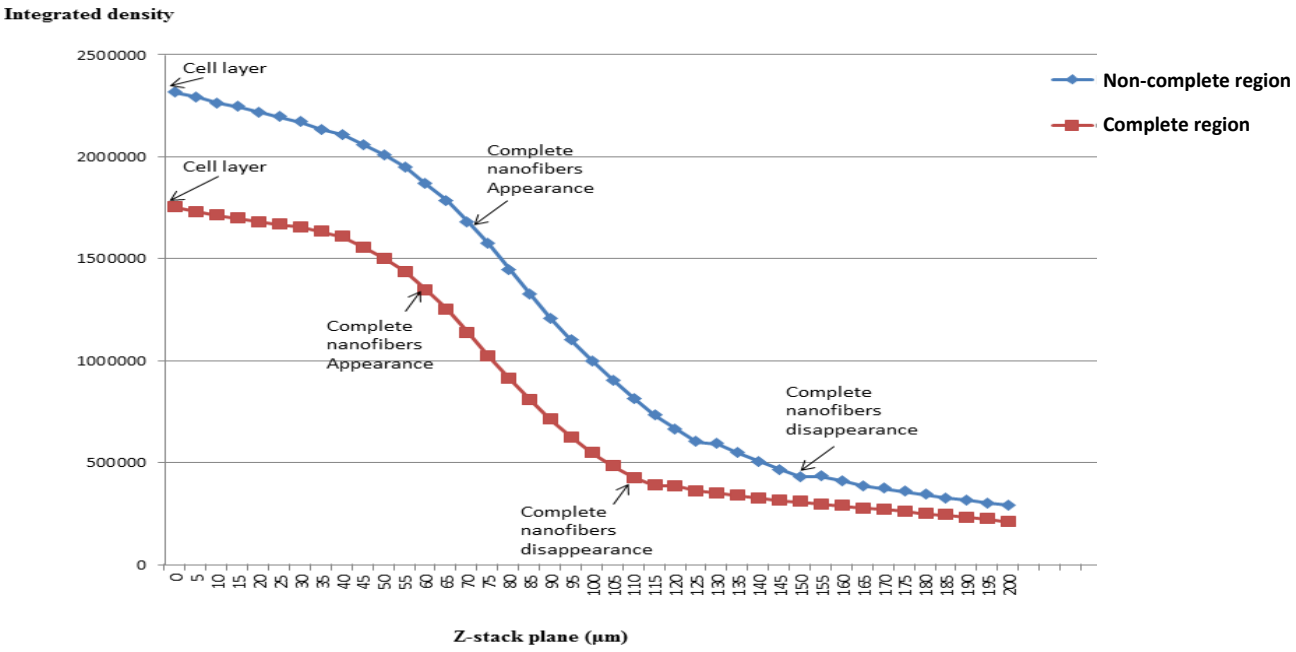

Figure 2.16 - A line graph of FITC-dextran intensity against the sample depth in different HUVECs complete regions.

Due to concerns that dextran could be artefactually permeating into the construct via leaking down the sides, another method was devised to measure permeability using fluorescently labelled-high molecular weight FITC-dextran permeation through TEBV constructs (Figure 2.17). For this 1.5 mL of PBS was added into a spectrophotometer cuvette and aluminium foil was placed atop of the solution with small openings to create a mask to allow a 5 µl sample of the dextran solution to only come into contact in central regions of the construct. After addition of the dextran, the sample was

immediately placed into the spectrophotometer holder to record the fluorescence. The permeability of the construct could then be measured via tracking the fluorescence in PBS. The more dextran solution flowing into the PBS solution, the higher the fluorescence reading detected by the spectrophotometer, indicating a greater permeability of the TEBV construct. All samples were compared against the permeability of a collagen hydrogel without any cellular elements included (maximum fluorescence). TEBV and collagen hydrogel (control) samples were both cultured for a total of 14 days and placed in a cuvette as shown in Figure 2.17. A percentage of maximum fluorescence was plotted as shown in the equation below:

$$\text{Percentage of maximum fluorescence (\%)} = \frac{fluorescence\ of\ the\ sample}{maximum\ fluorescence}\ x\ 100$$

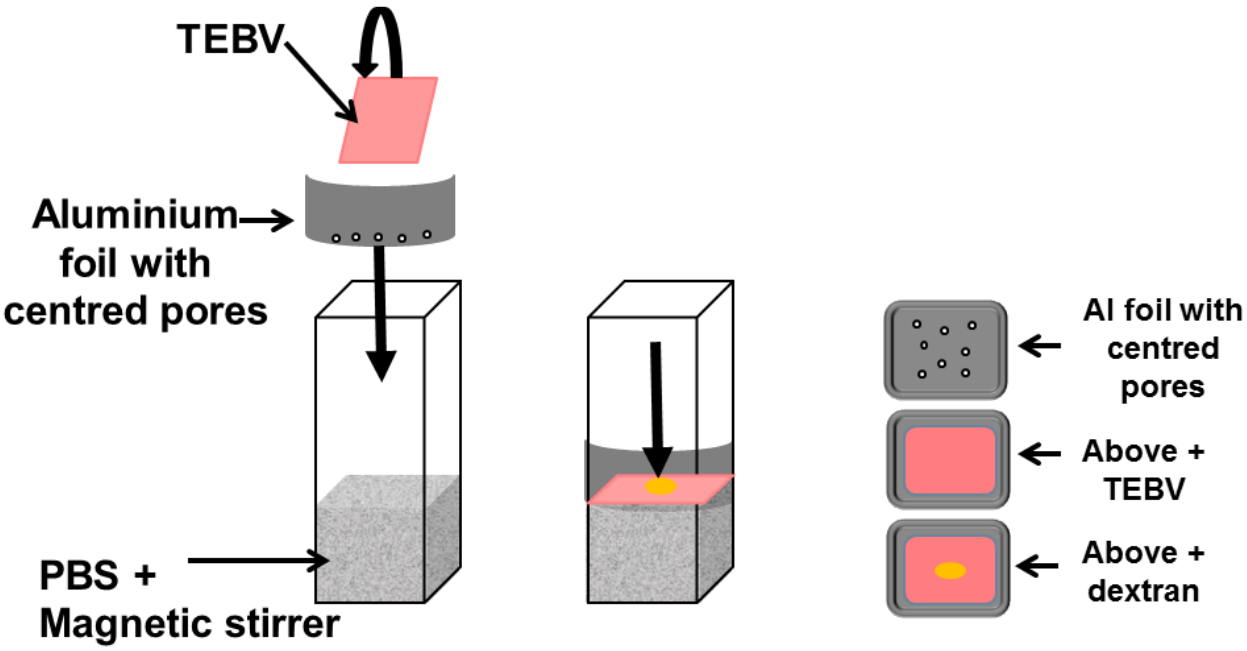

Figure 2.17 - A permeability design used to measure the dextran permeation through the construct. A porous aluminium foil was used to hold the construct in place followed by placing the gel on the aluminium foil. The dextran was then placed atop of the construct and recorded for 10 minutes.

The fluorescence of the sample was determined in real-time via fluorescence spectrophotometer. The signal was triggered by the migration of dextran into the PBS solution and through the construct (if permeable). The maximum fluorescence is measured by freely adding the dextran solution into the PBS wherethe signal is detected by the fluorescence spectrophotometer. Figure 2.18 shows the dextran solution permeation through the collagen hydrogel and TEBV constructs. At the beginning, there is no dextran permeated through both of the constructs. With time, more and more dextran is flowing through the collagen hydrogel compared to TEBV. At 10 minutes of recording the dextran is still flowing through the collagen hydrogel without levelling off. Dextran permeation is reduced in TEBV constructs by almost 20% at the end of the run compared to the collagen hydrogel sample. In general, dextran permeation through the TEBV construct show no change in fluorescence compared to the collagen hydrogel – thus suggesting that the TEBV is largely impermeable to the dextran. However, there are few limitations associated with the design of the methodology which will be discussed in detail in the discussion.

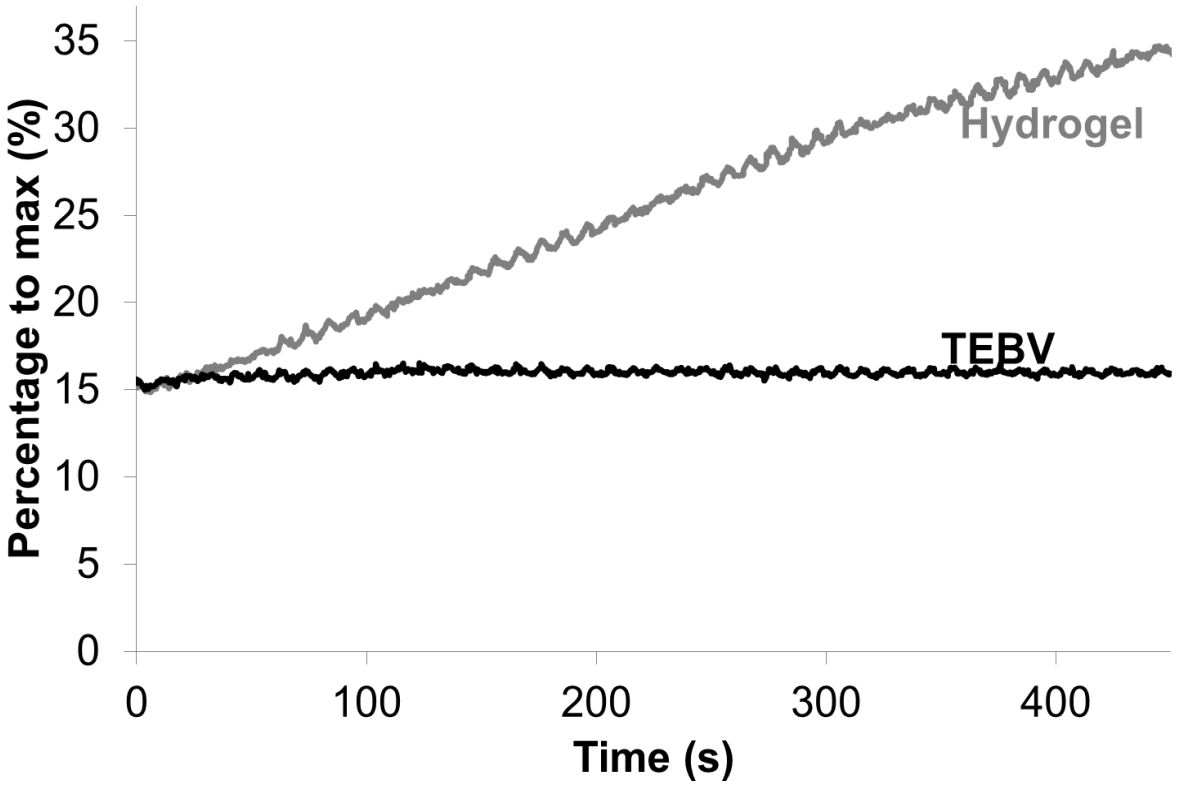

Figure 2.18 - **High-molecular weight dextran permeation through TEBV and collagen hydrogel cultured for up to 14 days.**

3.3.4. HCASMCs within the medial layer express F-actin

Phalloidin staining has been most frequently used to study cytoskeletal structures within cells. HCASMCs are characterised by the presence of actin fibres, including "α-smooth muscle actin (α-SMA), which help to convey contractile properties of the cell. The use of fluorescently labelled toxins which bind to F-actin such as phalloidin have been widely used in the research field to image cytoskeletal structure. In this experiment, HCASMCs within our TEML have been stained for F-actin filaments using Phalloidin-TRITC dye (Figure 2.18). The cells show a strong expression of F-actin filaments especially concentrated in the periphery of the cell surface and also in cellular protrusions to regulate cellular structure and movement of these highly contractile cells. However, this is not specific to SMCs but also ubiquitously expressed in other types of cells and therefore further work will be required to fully phenotype the HCASMCs.

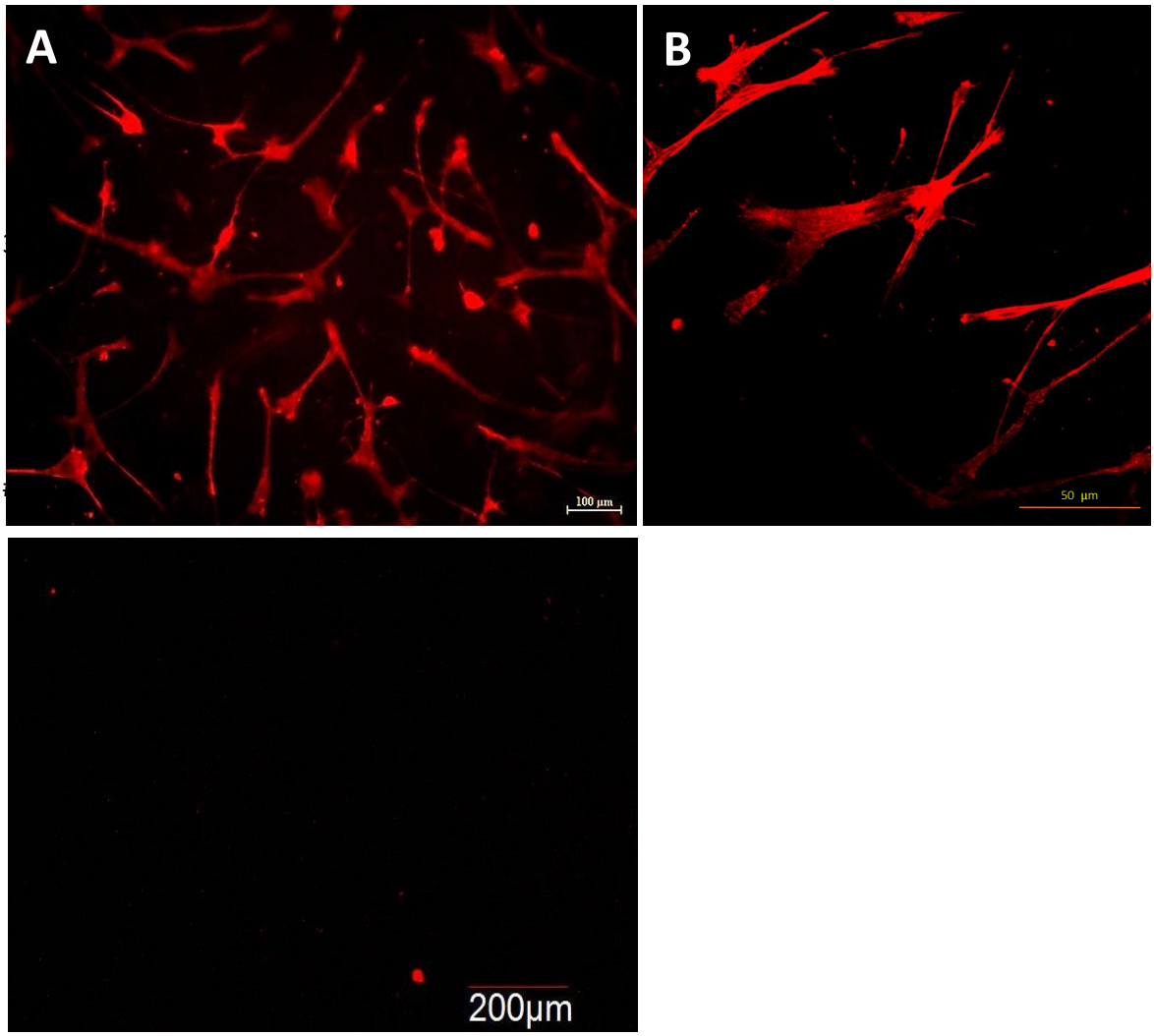

Figure 2.19 - HCASCMs within the TEML express F-actin. TEML was cultured for 10 days and stained with TRITC-Phalloidin. A) Low magnification of HCASMCs expressing F-actin. B) High magnification of HCASMCs expressing F-actin. C) F-actin stained collagen gel without HCASMCs. Results are representative of 3 experiments.

4. Discussion:

In this study, the methods for fabricating a tissue-engineered blood vessel construct were optimised. The aim of these studies was to produce a tissue-engineered blood vessel construct with structural properties of the native artery, which could be stably maintained during co-culture. The work shown in this chapter has established the feasibility of producing a biological TEBV exclusively from primary human cells using appropriate nanofiber and hydrogel scaffolds.

Experiments were performed to optimise the culture conditions for the production of TEML. Initial attempts of seeding HCASMCs within collagen hydrogels were unsuccessful as these cells failed to regain their normal cellular morphology. The cells were observed to be rounded even after a week of culture. This is most likely due to the order of adding components of the collagen hydrogel to the cells. In fact, mixing all the collagen reagents first and then adding the cell suspension is the most reliable and reproducible method as this ensured neutralisation of the pH of the solutions before its addition to the cells (Figures 2.11 and 2.12).

Subsequent experiments assessed and optimised HUVECs attachment and growth upon PLA nanofibers in attempt to create a confluent, low-permeability endothelial layer that was able to maintain a normal cellular phenotype (Figures 2.4 and 2.5). Initial experiments found that HUEVCs attached poorly to the uncoated nanofibers, however upon coating the nanofibers with fibronectin, HUVECs attachment and coverage on the surface of nanofibers was markedly improved. These observations are consistent with previous findings which have shown that fibronectin is able to increase HUVECs survival (Cooper & Sefton, 2011). In addition, they are also supported by a recent study that examined human aortic endothelial cells (HAECs) growth on a fibronectin-modified hydrogel surface (Shinohara et al., 2013). These studies revealed that HAECs adhered to and grew better on the fibronectin-modified hydrogel surface compared to other modified hydrogel surfaces.

In the native artery, ECs are found to orient themselves in response to the shear stresses exerted by blood flow. A number of previous studies have shown that aligned nanofiber scaffolds can be used to orient the growth of endothelial cells, neurite and mesenchymal stem cells (Chew et al., 2008; Laco et al., 2013; McCullen et al., 2007). In this report, we have shown that HUVECs alignment can be artificially achieved by growing them upon aligned PLA nanofiber scaffolds (Figure 2.4). The response of human endothelial cells to the topographical features of nanofibers has been previously described in a comprehensive review of the topic by Nisbet et al (Nisbet et al., 2009). This includes cellular responses such as endothelial cells growth in the direction of an arranged surface pattern and significant elongation along the nanofibers. Cellular orientation and migration is subject to surface pattern and geometry (Liliensiek et al., 2010). This enables the production of an intimal construct that is highly-aligned and provides a near-complete layer that could act as an effective barrier between the blood and subendothelial matrix. To assess whether the endothelial lining was as impermeable as its native counterpart it was necessary to devise a new methodology to test this in our 3D TEBV, as current techniques are based around assessment of the permeability of 2D monolayers using electrical resistance or permeability of fluorescent compounds. In this chapter, experiments assessed fluorescent dextran permeation through the construct. Although dextran transmigration assay has been used on endothelial cell monolayer using filter transwells or cell culture inserts there are limited studies addressing its use in 3D constructs (Chetprayoon, Matsusaki, & Akashi, 2015; Grainger & Putnam, 2011; Hordijk et al., 1999; Varma et al., 2002). Our initial strategy appeared to suggest that the dye may be able to permeate through the TEBV when it was placed atop the whole of the construct – however there were concerns about whether this was due to the dye leaking down the sides of the construct. Here we have stablished a new method that uses a spectrophotometer to measure dextran permeation through tissue-engineered vascular constructs, as shown schematically in Figure 2.17. By comparing the permeability of dextran through the TEBV with that of an acellular collagen hydrogel, it was possible to observe that more dextran permeated through the collagen hydrogel compared with the TEBV indicating that the cells

within the TEBV construct are preventing dextran permeation. Although this methodology has produced some encouraging results, there are some potential limitations to this technique that will require further refinement. These include difficulties in placing the construct inside the cuvette, and due to the uneven surface of the aluminium foil this may accidentally damage the construct. Dye leakage can still occur since the sides of the construct are not sealed, if not carefully placed on top of the construct, the dye can escape through the sides and travel into the PBS solution being measured. Further work will be required to refine this methodology to provide better reproducibility.

In addition to these features immunofluorescent analysis of the cellular phenotype of the TEIL has also shown that the HUVECs stably retain their healthy endothelial cell phenotype throughout the culture period. This was demonstrated by the maintained expression of the CD31 marker on the surface of HUVECs and low ICAM-1 inflammatory marker expression (Figures 2.9 and 2.18). These data therefore suggest that the HUVECs phenotype is not significantly altered by the culturing conditions used to create the TEBV.

Confocal imaging of the TEBV have shown distinct zonal organisation in 3D TEBV constructs after being maintained in co-culture (Figure 2.14). These cells are localised where they had been seeded originally after 4 days of culture, confirming that the cells do not shift across between layers within the construct. During the experiments presented here, it was possible to see that the fluorescent nanofibers sustained their fluorescence intensity for the entire experimental period, suggesting that they are not subject to significant photobleaching and thus can be used to facilitate the visualisation of the adherent HUVECs layer. Additionally, a live-dead staining of the TEBV have shown that the cells are finding the culturing conditions favourable with all the cells being alive within the first 10 minutes of confocal imaging.

4.1. Conclusion

In summary, a layer-by-layer fabrication technique has been successfully developed to fabricate a tri-layered human 3D tissue engineered blood vessel model composed of primary cell sources. Using a highly dense PLA nanofiber scaffold, we were able to generate a unidirectional, impermeable endothelial cell layer. The TEBV model can be observed to mimic the structure and cellular phenotype of native human counterpart. Using this 3D tissue engineered blood vessel model, it may be possible to create a model system in which to study the molecular and cellular events of haemostasis.

Chapter 3

Establishment and optimisation of a real-time monitoring system to assess human platelet activation upon exposure to tissue-engineered blood vessel constructs

1. Introduction

This central role for platelet activation in thrombus formation has led to scientists using a variety of *ex vivo* platelet function assays to try to understand how these cells are normally regulated inside the body. However thrombus formation is further regulated by chemical and physical interactions between platelets, endothelium and leukocytes, as well as the blood flow conditions in the vicinity of the developing thrombus (Kim et al., 2013). Thus, whilst *ex vivo* study of isolated human platelet suspensions stimulated with soluble agonists or monolayers of extracellular matrix proteins or cells isolated from the blood vessel wall, creates a simple experimental system in which to assay platelet activation mechanisms, they are unlikely to adequately replicate responses observed *in vivo*.

This has led to a growing interest in studying platelet activation *in vivo*. The most commonly used methodology is the use intravital microscopy to examine thrombus formation induced by artificial damage to the blood vessel during the course of the experiment. A number of mouse models of thrombosis have been studied including studies using ferric chloride-induced oxidative damage, Rose Bengal-induced photo-oxidative damage, laser injury and a variety of mechanical injuries (Bonnard and Hagemeyer, 2015; Furie and Furie, 2005, 2005; Rosen et al., 2001). However, each of these models has limitations that may affect the direct translation of these data into obtaining information regarding the human *in vivo* environment (Janssen et al., 2004; Rowley et al., 2011; Weinberg and Ross Ethier, 2007). Hence due to the inability to perform *in vivo* experiments on humans due to ethical concerns, there is a need to develop an *in vitro* system which can better assess human platelets' reaction to intact, damaged or diseased human blood vessels. Developing such a system will greatly enhance our understanding physiological haemostatic processes and pathological responses occurring *in vivo* in humans.

An intact blood vessel could be acquired through unwanted surgical tissue collected during vascular graft – however underlying cardiovascular pathologies in these patients may not make these tissues reliable indicators of normal haemostasis. In addition, the complexities of obtaining sufficient

quantity of such tissues to facilitate wide-spread use of this technique is a significant limiting factor of this approach. Therefore, tissue engineering has emerged as a promising approach to address these shortcomings. The construction of such a human tissue-engineered blood vessel construct that could be used to improve the physiological relevance of current *in vitro* studies has been described in chapter 2. However, we require methodologies to allow us to assess the physiological relevance of our constructs. Previous studies examining artificial tissue-engineered blood vessel models examine the ability of constructs to withstand or facilitate platelet aggregation upon their surface, however as aggregation requires strong activation of platelets, low-level activation of platelets may be missed. Similarly, examination of the production of anti-aggregatory properties of the grafts usually assays the production of endothelial-derived inhibitors without directly examining their effect on platelet activation. Hence, there is a need for a monitoring method that allows us to assess the pro- and anti-aggregatory properties of the blood vessel constructs. An ideal method should allow real-time monitoring of platelets activation, with a sensitive readout for platelet activation that can measure both pro- or anti-aggregatory properties of either intact or damaged blood vessel wall. Monitoring of platelet Ca^{2+} signalling is widely used as a sensitive method for monitoring platelet activation – this is because rises in cytosolic Ca^{2+} concentration play a key role in all stages of platelet activation, with higher Ca^{2+} signals tending to enhance the ability of platelets to form thrombi (Gresele et al., 2017). In addition, endothelial derived inhibitors such as NO and prostacyclin are known to significantly inhibit thrombin-evoked rises in $[Ca^{2+}]_{cyt}$. Therefore, designing a system that allows us to measure cytosolic Ca^{2+} concentration from platelets exposed to the blood vessel construct would allow us to assess how interaction with our blood vessel constructs developed in chapter 2 can influence the activation state of human platelets. Thus, the main aim for this chapter is to develop and optimise a novel methodology for assessing the effect of our constructs on platelet function by creating a system that allows us to make real-time fluorescence spectrophotometry measurements of $[Ca^{2+}]_{cyt}$ from suspensions of washed human platelets.

2. Methods

2.1. Fabrication of tissue-engineered blood vessel constructs

2.1.1. Generation of TEML constructs

To prepare TEML constructs, HCASMCs were mixed at a density of 5 x 10^5/mL into a neutralised solution of 3 mg/mL type I collagen obtained from BD biosciences, according to the manufacturer's protocol. 0.2 mL of the mixture was then loaded onto a 1 cm^2 square shaped filter paper frame, and the collagen-cell mixture was left to set for 40 minutes at 37˚C, 5% CO_2. The formed gel was then covered with supplemented medium and with changing the media every 2 days. HCASMCs were subsequently allowed to grow in the TEML until they were observed to possess an elongated spindle-shaped morphology.

2.1.2. Generation of TEBV constructs

TEBV construct was fabricated by placing a PLA nanofiber mesh coated with a 10 µg/mL fibronectin solution on the 3D TEML, to create the initial layer of the luminal surface. After successful attachment of the nanofibers to the TEML hydrogel, HUVECs (at a density of 4 x10^4 cells/cm^2) were then seeded on top of the nanofibers to create a full TEBV construct. The HUVECs density is a standard seeding process unless or otherwise stated.

2.2. Ethical approval

This project was approved by the Keele University Research Ethics Committee and all work was performed in accordance with the Declaration of Helsinki.

2.3. Preparation of platelet-rich plasma (PRP) and washed Fura-2-loaded human platelet suspensions

Human platelets were used to test platelets activation and aggregation. A standard method of extraction was used. Blood was obtained by venepuncture from healthy volunteers who had given informed written consent. 5 mL blood was mixed with 1 mL acid citrate dextrose (ACD) anticoagulant (85 mM sodium citrate, 78 mM citric acid and 111 mM d-glucose). Platelet-rich

plasma (PRP) was then obtained by centrifuging at 1500 g for 8 minutes, and was then treated by the addition of 100 µM aspirin (ASA) and 0.1 U/mL apyrase) unless otherwise stated. PRP was then incubated with 2.5 µM Fura-2/AM for 45 minutes at 37°C. Platelets were then collected by centrifugation at 350 g for 20 minutes. Washed platelets were re-suspended into supplemented HEPES –Buffered Saline (HBS) to a final cell density of to $2x10^8$ cells/mL. To make supplemented HBS, HBS (pH 7.4, 145 mM NaCl, 10 mM HEPES, 10 mM d-glucose, 5 mM KCl, 1 mM $MgSO_4$), was supplemented on the day of the experiments with 1 mg/mL Bovine Serum Albumin (BSA), 10 mM glucose, 0.1 U/mL apyrase and 200 µM $CaCl_2$ (supplemented HBS). $CaCl_2$ concentration of the supplemented HBS was adjusted to 1 mM prior to individual sample analysis.

2.3.1. Preparation of PRP using prostacyclin

To examine whether preparation with aspirin significantly alters the platelet response to our blood vessel constructs, experiments were performed in which PRP was prepared using either ASA or PGI_2 to prevent platelet activation. To prepare prostacyclin-treated, Fura-2 labelled washed human platelet samples, the PRP was treated with 10 µM PGI_2 and 0.1 U/mL apyrase. PRP was incubated with 2.5 µM Fura-2/AM for 45 minutes at 37°C. Prior to centrifugation, the PRP was treated again with 10 µM PGI_2 to further inhibit unwanted platelet activation. The platelet pellet was re-suspended with supplemented HBS as described above for ASA-treated cells.

2.4. Designing and constructing a real-time monitoring system to assess platelets' response to blood vessel construct by measurement of platelets' cytosolic Ca^{2+} concentration ($[Ca^{2+}]_{cyt}$)

2.4.1. Sample holder design

To position the construct in contact with the human platelet suspension within the cuvette, an acetate frame was designed to act as a sample holder. This comprised of two regions including a central region holding the blood vessel construct and permitting exposure to the platelets with two flanking sides enabling easy handling (Figure 3.1). The central part was designed to facilitate

construct interaction with platelet suspension cut to a 1 cm length and 1 cm width square, to enable correct fitting on to the spectrophotometer cuvette. Within this square, another 0.5 cm x 0.5 cm square was cut in the middle to create a window for construct interaction with the platelets. The second part consists of two flanking sides extended from the central region 'hook'. These were 4 cm in length, to allow lowering and uplifting of the central region containing the construct. The length of the 'hook' can be adjusted depending on the volume of platelets used to ensure this could facilitate optimal contact of construct with platelets.

2.4.2. Sample assembly

Once tissue engineered blood vessel constructs were fabricated, the upper side of the construct (region of interest), was overturned upside down on an acetate frame, with the centre part permitting direct exposure to the platelet suspension. By slowly combining the construct with the central part of the acetate frame, this composite (sample holder and construct) is slowly lowered down into the cuvette containing platelets and levelled just above the platelet suspension. The sides of the acetate frame was bent around the cuvette to secure the composite. A magnetic stir bar was also added at the bottom of the cuvette to mix the washed platelet suspension and facilitate dynamic interaction between of platelet suspension with the construct.

2.4.3. Real-time monitoring of $[Ca^{2+}]_{cyt}$ of washed human platelet suspension

Fluorescence was recorded from stirred aliquots of Fura-2-loaded washed human platelet suspensions in contact with the blood vessel constructs at 37°C using Cairn Research Spectrophotometer with excitation of 340 and 380 nm and emission of 515 nm. Changes in $[Ca^{2+}]_{cyt}$ were monitored using the 340/380 nm fluorescence ratio. Data were calibrated using the method of Grykiewicz *et al*., (1985) (Grynkiewicz et al., 1985). Agonist-evoked changes in $[Ca^{2+}]_{cyt}$ were quantified by integration of the change in fluorescence records from basal with respect to time from 5 -15 minutes after agonist addition.

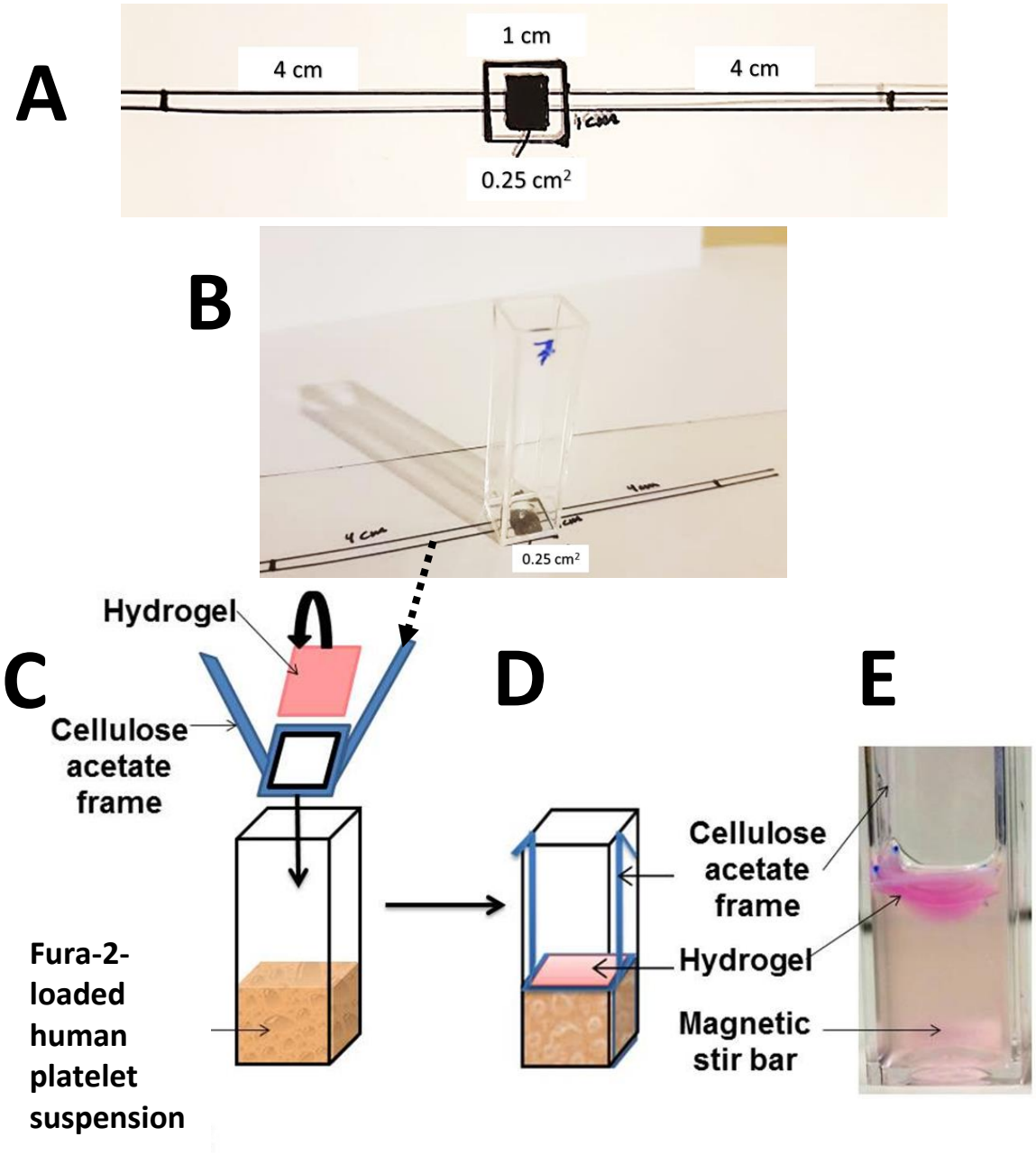

Figure 3.1 - **A picture showing the novel testing platform to assess the pro-aggregatory capacity of acellular collagen hydrogel or tissue-engineered vessel constructs in *ex vivo* platelet Ca^{2+} signaling assay.** (A and B) are showing the measurements drawn on a cellulose acetate prior to cutting the frame. (C) The 3D sample to be tested was placed on a cellulose acetate frame with the centre part permitting direct exposure to Fura-2- and $DiOC_6$-co-labelled washed human platelet suspension. (D) The sample was lowered down allowing contact with the platelet suspension. (E) The picture of the assembled test sample with the presence of constant stirring of platelet suspension using a magnetic stir bar shown at the bottom. Platelet Ca^{2+} signaling in the platelet suspension was measured in real-time through Fura-2 fluorescence intensity, whilst platelet adhesion and aggregation on the surface of the samples were assessed by the imaging of $DiOC_6$-labeled platelets after removal of the sample from the cuvette. Dashed arrow = sample holder.

2.5. Assessment of the new monitoring system

2.5.1. The effect of sample holder on platelet activation

The sample holder generated from cellulose acetate frame was placed in a cuvette containing 1.2 mL of Fura-2-loaded human platelet suspensions. The sample was introduced onto the new monitoring system explained in section 2.3. The $[Ca^{2+}]_{cyt}$ was measured with initial recording of a basal reading for 1 minute followed by 4 minutes following stimulation with 0.2 U/mL thrombin.

2.5.2. The effect of different platelet preparations on platelet activation

To investigate whether using two different PRP preparations would influence platelets response to TEML constructs, an experiment was conducted comparing the effect of TEML construct on potentiating $[Ca^{2+}]_{cyt}$ increase in platelets compared with acellular hydrogel (n=6). 10 µM PGI_2 or 100 µM ASA treated PRP preparations were used from the same donor at any given time. 1.5 mL of washed platelet samples from these preparations were used incubated with TEML constructs. The sample incorporated with either cellular or acellular hydrogels were placed into the cuvette holder of the spectrophotometer machine. Fluorescence recording was commenced 1 minute prior to construct addition to the platelets, of which a basal reading was taken from stirred aliquots of platelet suspension at 37°C using Cairn Research Spectrophotometer.

2.5.3. The effect of time dependent TEBV incubation on platelet activation

TEBV construct was incubated with 1.2 mL of washed platelet suspension at different times 1, 5, 10 and 15 minutes and introduced onto the new monitoring system explained in section 2.3 (n = 4). $[Ca^{2+}]_{cyt}$ basal reading was measured for 1 minute followed by 4 minutes following stimulation with 0.2 U/mL thrombin

2.5.4. The effect of various HUVECs densities on $[Ca^{2+}]_{cyt}$

TEBV constructs were fabricated at various HUVECs densities, 5 $x10^3$, 4 $x10^4$ and 8 x 10^4 cells/cm^2. These 3 different samples were cultured for 4 days. These samples were then individually assessed

using a 1.2 mL of platelet suspension and the new method explained in section 2.3 (n = 3). $[Ca^{2+}]_{cyt}$ basal reading was measured for 1 minute followed by 4 minutes reading post thrombin (0.2 U/mL) stimulation.

2.6. Statistics

Values stated are mean ±SEM of the number of observations (*n*) indicated. Analysis of statistical significance was performed using a paired student's t-test. $P < 0.05$ was considered significant.

3. Results

3.1. Designing a real-time monitoring system to assess the effect of tissue-engineered blood vessels constructs on activation state of human platelets

To detect the activation status of platelets upon exposure to tissue-engineered blood vessel constructs, we have constructed a system to allow real-time monitoring of platelets activation (Figure 3.1). $[Ca^{2+}]_{cyt}$ was quantitatively measured using human platelets loaded with Fura-2, a high-affinity fluorescent Ca^{2+} indicator. The fluorescence signal from these platelets can be measured in real time using a fluorescence spectrophotometer. The construct can be removed after sufficient time was allowed for interaction with platelets. By pulling the flanking side of the acetate frame of which the construct is resting on, the remaining platelet suspension is put inside the cuvette holder to resume the recording.

3.1.1. Thrombin-evoked response of platelets $[Ca^{2+}]_{cyt}$ incubated with the sample holder

Prior to using the method for testing tissue engineered constructs, a typical experiment was set-up to assess if pre-incubation with the acetate sample holder could artificially alter Ca^{2+}. To do this, the $[Ca^{2+}]_{cyt}$ of platelets was monitored following incubation with the sample holder as well as following thrombin stimulation. These initial experiments showed that there appeared to be no apparent activation of platelets following pre-incubation. In addition, a robust Ca^{2+} signal which was similar to those previously reported in the literature suggesting no inhibition of platelet function elicited by the sample holder. These data therefore suggest that the acetate sample holder does not significantly alter the responsiveness of platelets exposed to it.

3.2. Testing variables

To assess and optimise the effectiveness of methodology described above, experiments were undertaken to examine the effect of altering a number of variables which might alter the results

seen. This included investigating the effects of different methods for producing the tissue-engineered blood vessel constructs, changing HUVECs densities and time of incubation of the vessel construct with platelet suspension. The testing parameters and variables tested in this chapter are summarised in Figure 3.2.

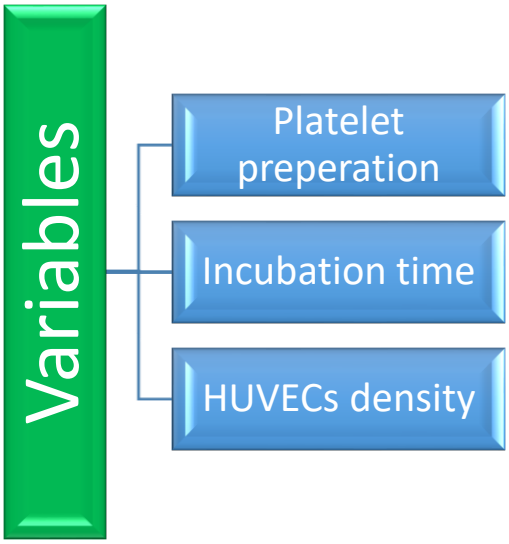

Figure 3.2 - Testing variables for platelets' calcium signalling using tissue engineered blood vessels to assess the sensitivity of the model.

3.2.1. TEML activates platelets in a manner that is independent of the platelet preparation method

It was predicted that exposure of platelets to the subendothelial matrix of the TEML should elicit platelet activation, and thus a rise in $[Ca^{2+}]_{cyt}$. However, the response observed may also depend upon the method of platelet preparation. Both ASA and PGI_2 have been widely used to prevent unwanted platelet activation during the preparation of washed platelet samples (Dorsam et al., 2005; Heemskerk, Farndale, & Sage, 1997; S. Kim et al., 2013; McCloskey et al., 2010; Rosado, Brownlow, & Sage, 2002). PGI_2 inhibits platelets aggregation by activating cell surface prostacyclin receptors (IP) linked to activation of adenylate cyclase (AC), leading to the conversion of ATP to cAMP. This rise in cAMP prevents platelet activation and aggregation by inhibiting agonist-evoked

rises in $[Ca^{2+}]_{cyt}$ (Paul et al., 1990). In contrast, the use of aspirin is common in platelet signalling studies to remove autocrine activation of platelets by thromboxane A_2 production and therefore remove any confounding influence of this autocrine signalling molecule in studying the primary activation mechanisms of platelets by soluble or adhesive agonists. Its inclusion here permits examining how various constructs alter primary platelet activation in the absence of secondary autocrine mediators of platelet activation. To assess this, we examined the effect of pre-incubating Fura-2-loaded washed human platelets prepared with either ASA or PGI2 as a platelet inhibitor during the washing process, with either the TEML construct or a control collagen hydrogel. As can be seen in Figure 3.3, the TEML constructs causes an increase in $[Ca^{2+}]_{cyt}$ prior to thrombin stimulation which was not observed in platelets exposed to the collagen hydrogel. These data therefore suggest that the TEML is able to trigger platelet activation which is not supported by the collagen hydrogel alone. This result was observed in both platelet preparation methods, with the Ca^{2+} signal being potentiated to 180.3 ± 43.3% and 174.6 ± 51.3% of control, collagen hydrogel for PGI_2- treated and ASA-treated- samples respectively ($P < 0.05;$ n = 4). The construct-evoked rises in the two preparation methods were found not to be statistically significant ($P > 0.05$). Therefore, platelet preparation by either method produced similar results, hence all further experiments used washed platelets prepared using ASA.

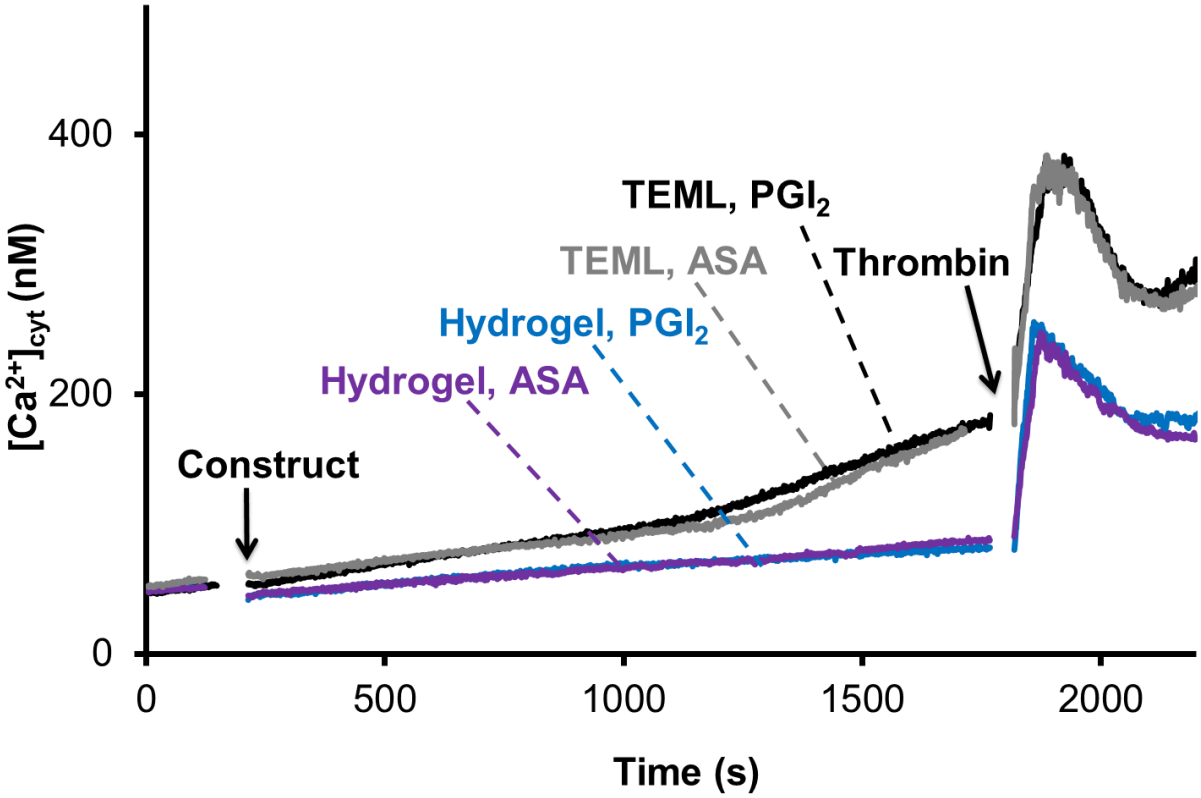

Figure 3.3 - $[Ca^{2+}]_{cyt}$ measurement of fluorescently-labelled human platelets exposed to the luminal surface of TEML or acellular hydrogel using two different methods for PRP preparation. The PRP preparation was split into half of which one was treated with prostacyclin (PGI_2, 10 µM) and the other with aspirin (ASA, 100 µM). The PRP preparations were then treated with Fura-2/AM (2.5 µM) for 45 minutes. PGI_2 treated PRP was treated yet once more with PGI_2 prior to centrifugation. Washed platelets (1.5 mL) from both preparations were individually incubated with TEML constructs for 15 minutes at 37˚C, under continuous magnetic stirring. The constructs were removed and the $[Ca^{2+}]_{cyt}$ in the remaining suspension was recorded and stimulated with 0.2 U/mL thrombin. Results are representative of 3 experiments (n=4).

3.2.2. Increasing HUVECs seeding densities reduces thrombin-evoked rises in $[Ca^{2+}]_{cyt}$ in washed human platelets

As endothelial cells play a key role in preventing platelet activation through releasing paracrine inhibitors of platelet function, experiments were performed to assess whether changes in the seeding densities of HUVECs used in the TEBV constructs could alter its inhibitory effect on platelet activation. Figure 3.4 shows thrombin evoked $[Ca^{2+}]_{cyt}$ rise in platelets pre-exposed to TEBVs with different HUVECs densities. TEBVs with various HUVECs densities showed to inhibit thrombin-evoked rises in platelet $[Ca^{2+}]_{cyt}$ in a manner that was dependent upon the HUVECs seeding density of the constructs. Seeding TEBVs with a high density of HUVECs (8 X 10^4 cells/cm^2) causes a significant reduction of thrombin evoked $[Ca^{2+}]_{cyt}$ rise in platelets upon pre-exposure compared with the collagen hydrogel (46.9 ±4.5 % of control; *n = 3; P < 0.05*). Moreover, using a lower density of HUVECs (4 X 10^4 cells/cm^2) on TEBVs also seems to cause a significant reduction in thrombin evoked $[Ca^{2+}]_{cyt}$ rise in pre-exposed platelets compared with collagen hydrogel (49.0 ± 3.7 % of control; *n = 3; P < 0.05*). Seeding even a lower HUVECs density of 5 X 10^3 cells/cm^2 likewise elicit a significant inhibitory effect on $[Ca^{2+}]_{cyt}$ of platelets pre-exposed to such construct (51.8 ± 9.3 % of control; *n = 3; P < 0.05).* These data demonstrate that the presence of more HUVECs on the construct elicits a greater inhibition of platelets pre-exposed to it. This is likely due to an increase in the inhibitory paracrine signalling molecules produced by the endothelial cells which are known to inhibit platelet activation. The use of a cell number of 4 x 10^4 cells/cm^2, for a culture period of 4 days can be seen to be sufficient in mediating a consistent, effective and reproducible inhibition of thrombin-evoked rise in $[Ca^{2+}]_{cyt}$ of platelets in this system. Therefore, this is the cell seeding density has been on the TEBV in all future experiments.

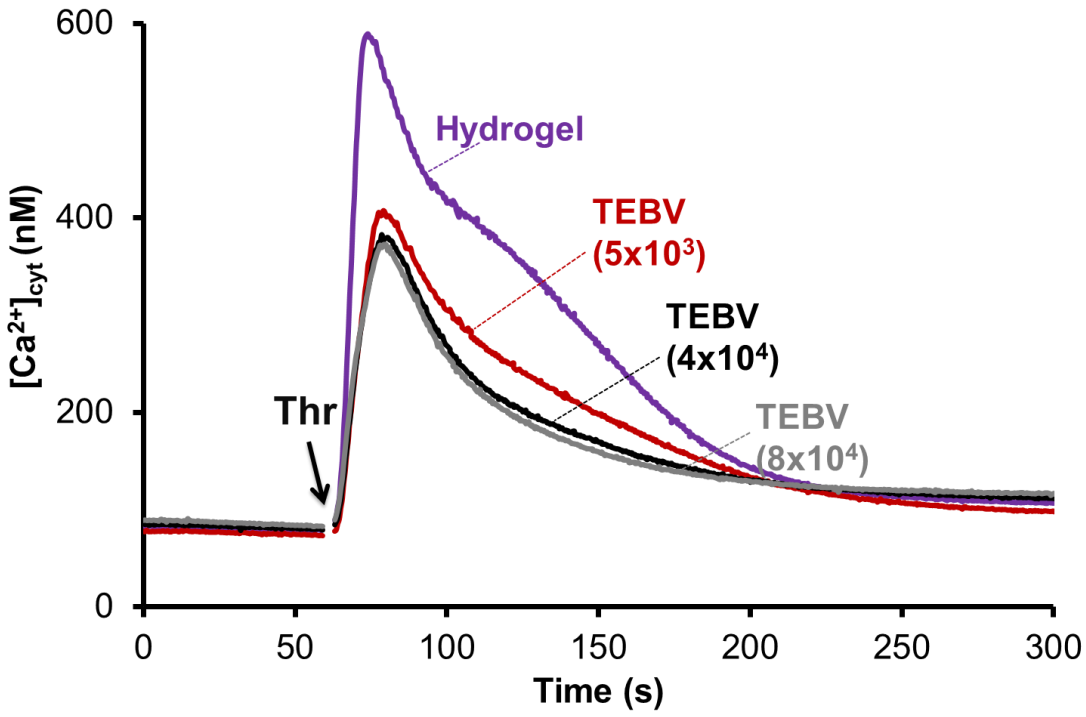

Figure 3.4 – A real-time measurement of thrombin-evoked cytosolic Ca^{2+} concentration increase in platelets pre-exposed to tissue-engineered blood vessels (TEBV) with various HUVECs densities. The constructs were cultured for 4 days and pre-incubated with 1.2 mL of washed human platelet suspension for 15 minutes prior to thrombin stimulation (0.2 U/mL). Hydrogel was used as a control to show a maximum stimulation. Results are representative of 3 experiments (n=3).

3.2.3. The effect of TEBV incubation period

Using the newly developed monitoring system, the effect of incubation period of TEBV with platelets was measured. In this experiment, TEBVs were seeded with 4 x 10^4 HUVECs/cm^2 and cultured for 72 hours. These constructs were subsequently placed atop of platelet suspension for 1, 5, 10 and 15 minutes. Changes in platelet $[Ca^{2+}]_{cyt}$ was measured for 1 minute at baseline and then for a further 4 minutes following stimulation with 0.2 U/mL thrombin. As shown in Figure 3.5, the addition of thrombin elicits an agonist-evoked increase in $[Ca^{2+}]_{cyt}$ with the highest reading for those platelets exposed to the hydrogel control. the inhibitory effect of pre-incubation with the TEBV was found to be time-dependent. The longer the incubation of platelets with TEBV, the more

inhibition of thrombin-evoked increase in $[Ca^{2+}]_{cyt}$. There is no significant difference observed in thrombin-evoked increase of $[Ca^{2+}]_{cyt}$ in platelet pre-incubated for 1 minute with TEBV compared with the collagen hydrogel (107.3 ±3.9 % of control; *n = 4; p > 0.05*). A similar result was found in platelets pre-incubated for 5 minutes as this shows insignificant difference compared with the collagen hydrogel (60.3 ±16.5 % of control*, n=4; p > 0.05*). However, a significant difference was detected with platelet samples pre-incubated with TEBV for 10 and 15 minutes compared with the collagen hydrogel (53.0 ±11.9 % of control and 39.0 ± 11.6% of control; *n = 4; p < 0.05,* respectively). This results show that pre-incubating platelet with the TEBV for 10 minutes or more is sufficient to produce a reproducible inhibitory signal that reduces the thrombin-evoked increase in platelet $[Ca^{2+}]_{cyt}$.

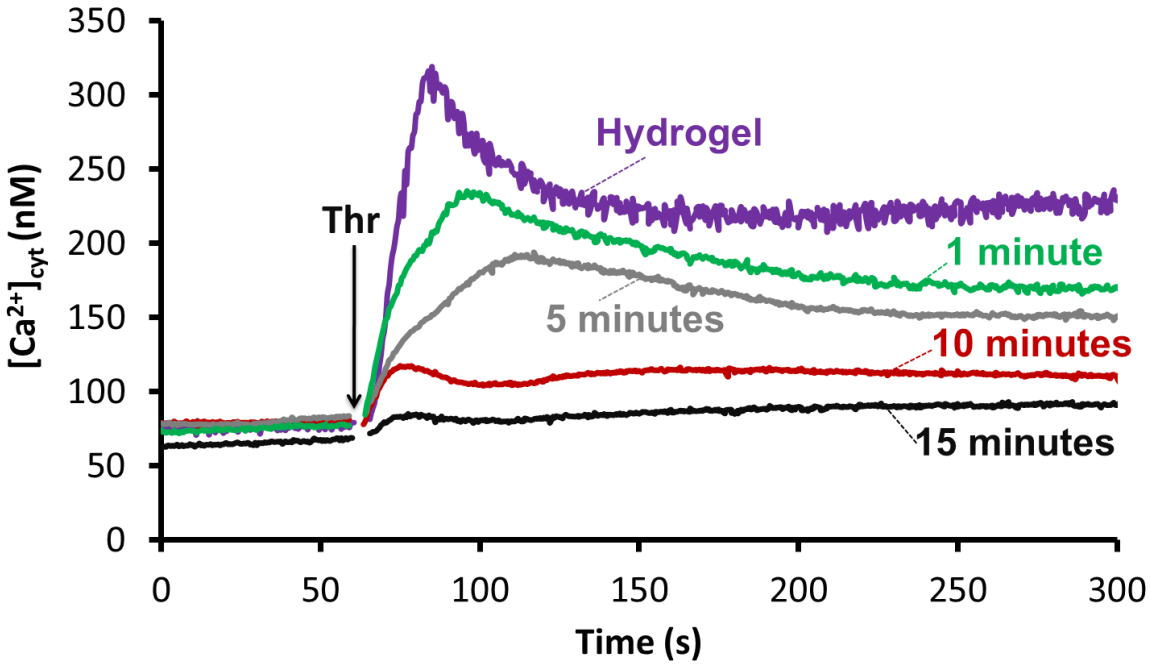

Figure 3.5 – Time dependent incubation of platelets pre-exposed to TEBVs. The constructs were cultured for 4 days and pre-incubated with 1.2 mL of washed human platelet suspension for 1, 5, 10 and 15 minutes prior to thrombin stimulation (0.2 U/mL). Hydrogel was used as a control to show a maximum stimulation. Results are representative of 3 experiments (n=4).

4. Discussion

This chapter demonstrated the development and optimisation of a new *in vitro* testing system to assess the effect of exposure to TEBVs on platelet activation status. Using this method, we were able to adapt traditional fluorescence spectrophotometric methods to detect the $[Ca^{2+}]_{cyt}$ of suspensions of Fura-2-loaded human platelets to allow a real-time assessment of changes in platelet activation. Methods previously used to assess human platelet function such as assessing aggregate formation of the surface of the construct (Boccafoschi et al., 2005; L'Heureux et al., 2001; Sankaran et al., 2014) are limited, as these assess platelet activation at specified time points and only detect the highly-activated platelets that form thrombi. It also cannot distinguish between a construct that is inert to platelets from those actively inhibiting platelet function. The methodology presented here is an improvement as it allows real-time assessment of platelet activation in response to the construct, as well as allowing an assessment of inhibitory signals produced by the construct through using post-construct stimulation with thrombin. Due to the known relationship between higher rises in $[Ca^{2+}]_{cyt}$ and greater adhesive and aggregatory potential of platelets (Sargeant and Sage, 1994; Varga-Szabo et al., 2009), it provides a valid method for quantitatively comparing the pro- and anti-aggregatory potential of tissue-engineered blood vessel constructs. This can be seen in the data demonstrating that platelet responses are sensitive to both HUVECs-seeding density and TEBVs pre-incubation period – demonstrating that the methodology has sufficient sensitivity to allow differences in the properties of the construct to be reliably assessed quantitatively.

Using this methodology, we can assess the ability of the construct to directly activate human platelets during the incubation period with the construct, as well as assessing the ability of layers of the construct to inhibit or sensitize platelets to other agonist through monitoring alterations in the thrombin-evoked signal. Through these tests, experiments in this chapter have demonstrated that the TEML construct is able to directly activate human platelets and the TEBV constructs can

inhibit this function – consistent with the physiological role of these constructs *in vivo*. These pro- and anti-aggregatory properties of the TEML and TEBV constructs will be examined in more detail in the next chapter.

The described experiments have been principally used to assess the optimisation of key variables of this technique, such as the platelet preparation method, HUVECs seeding density and the pre-incubation period with the constructs prior to stimulation with soluble agonists. From these studies, it has been possible to observe that platelet responsiveness to our construct is not dependent upon the formation of thromboxane A_2 as ASA preincubation does not significantly alter the response of platelets. This finding is consistent with previous findings that the main autocrine signal that potentiates collagen signalling is ATP secreted from platelet dense granules (Fung et al., 2012).

4.1. Conclusion

In this study, we have demonstrated a novel testing platform enabling analysis of the effect of tissue-engineered blood vessel constructs on platelets activation. Through exposing the constructs to washed human platelet suspension labelled with Fura-2, we are able to assess in real-time the activation status of the platelet suspension, or modulation of platelet responsiveness to soluble agonists. Through this method, we were able to optimise suitable HUVECs seeding densities and duration of incubation with tissue engineered constructs. This broad analysis of a range of different effects provides the potential for a simple, standardised and quantifiable method to directly compare the effects of a range of different tissue-engineered vessel constructs or biomaterials on platelet function. In addition, this methodology would also be accessible to simple modification to also potentially make it as a suitable *in vitro* testing system for studying healthy or diseased blood vessel models.

Chapter 4

Characterisation of pro- and anti-aggregatory characteristics of tissue-engineered blood vessel constructs

1. Introduction

Platelets are prevented from being activated through a complex series of physical and chemical interactions with flowing blood and vessel wall cells. The most significant of these is the role of the endothelial cell monolayer, which functions to create an anti-thrombotic layer of the native blood vessel (Vassalle et al., 2003). The endothelial layer does this via secretion of paracrine inhibitors of platelet function such as NO and PGI_2. PGI_2 and NO are main anti-platelet agents secreted by ECs (Bunting et al., 1983). In addition, cells possess proteins that interfere with the blood coagulation cascade such as tissue factor pathway inhibitor and thrombomodulin (Kurz et al., 1990).

NO and PGI_2 are continuously released from ECs, as previously discussed in chapter 1. However, their production by ECs can be increased in response to certain molecules involved in mediating inflammation or blood such as bradykinin and thrombin (Bartha et al., 1989). Aggregating platelets also release ATP which increases PGI_2 and NO production from ECs, allowing undamaged endothelial cell to limit the extent of thrombus formation at the site of vascular damage (Carter et al., 1988).This bi-direction communication between ECs and platelets play a key role in regulating haemostasis.

Upon damage to the vessel wall, the inhibitory effect of the endothelium is removed and the haemostatic system is activated. This removes endothelial-derived inhibitors of platelet function, and allows platelets to bind to pro-aggregatory ligands present within the subendothelial matrix, such as collagen, laminin, fibronectin and vitronectin, as well as recruited plasma components such as von Willebrand factor and thrombospondin-I (Ruggeri, 2007). Of these components, type I and III collagen are considered most able to support platelet adhesion and trigger strong platelet activation (Farndale, 2009; Kawamoto and Kaibara, 1990; Savage et al., 1999). In addition to the type of collagen present, studies have demonstrated that the structure of the collagen is also a key factor in influencing its thrombogenicity, as different collagen preparations vary widely in their ability to support their adhesion and trigger platelet aggregation. For example, fibrillar collagen is

much more potent in inducing platelet activation than the same type of acid-solubilised monomeric collagen (Savage et al., 1999). Other studies have demonstrated that cross-linking of collagen fibrils is also important in inducing platelet activation (Kawamoto and Kaibara, 1990). Platelet binds to collagen via glycoprotein VI and integrin $\alpha_2\beta_1$ receptors. This triggers Ca^{2+} signals through activation of phospholipase Cγ2 and subsequent cleavage of phosphatidylinositol 4,5-bisphosphate into inositol 1,4,5-trisphosphate and 1,2-diacylglycerol (Paul et al., 1990). Inositol 1,4,5-trisphosphate induces the release of calcium from the dense tubular system, whereas 1,2-diacylglycerol activates protein kinase C (Authi and Crawford, 1985). The collagen-induced inositol 1,4,5-trisphosphate-mediated increase in $[Ca^{2+}]_{cyt}$ is also accompanied by an influx of calcium from the extracellular milieu through both store- and receptor-operated channels (Gresele et al., 2017). 1,2-Diacylglycerol and calcium mediate the characteristic platelet activation responses such as shape change, granule secretion, and aggregation. These Ca^{2+} signals trigger the activation of adherent platelets which will begin to recruit other circulating platelets to build a thrombus through secretion and production of autacoids such as ATP, ADP, serotonin and thromboxane A_2 by the activated platelets. This recruitment of platelets to the surface of the damaged vessel wall, creates a thrombus which plugs the wound and prevents further blood loss.

The integrity of the endothelial lining acts dynamically to maintain haemostasis by balancing anti-aggregatory and pro-aggregatory factors of the blood vessel wall. Under normal conditions, an intact endothelial cell layer functions as a barrier between the blood vessel components and vascular wall, inhibiting platelets and clotting factors from interacting with the thrombogenic subendothelial matrix. However, upon damage to the endothelial lining the subendothelial matrix is exposed to the bloodstream triggering platelet activation. Therefore, a model of blood vessel must possess both these pro- and anti-aggregatory properties which can be differentially expressed depending on the confluency of the endothelial lining.

Tissue engineering offers the potential to create a human blood vessel replica that can be utilised for studying platelet activation and thrombus formation under *in vitro* condition. To be appropriate for this purpose, the produced tissue-engineered blood vessel should possess similar physiological properties of a native human blood vessel. Thus, the tissue-engineered blood vessel construct must possess an anti-aggregatory luminal surface to prevent thrombosis and a quiescent endothelial cell layer possessing an anti-platelet, anti-coagulant and pro-fibrinolytic surface (Torikai et al., 2008; Yu et al., 2008). In addition, the endothelial lining must be healthy and not demonstrate the inflammatory phenotype seen to contribute to the development and progression of an atherosclerotic plaque (Daniel and Sedding, 2011). However, upon damage of the blood vessel, the construct must also be able to switch from this anti-aggregatory phenotype to a pro-aggregatory condition which is able to support efficient but self-limiting thrombus formation as seen in the native vessel. Therefore, the main aim for this chapter is to assess and optimise the anti- and pro-aggregatory properties of the tissue-engineered blood vessel construct to match the known properties of the native vessel.

2. Methods

2.1 Tissue engineered blood vessel constructs fabrication

2.1.1 Generation of TEML constructs

To prepare TEML constructs, HCASMCs were mixed at a density of 5 x 10^5/mL into a neutralised solution of 3 mg/mL type I collagen obtained from BD biosciences, according to the manufacturer's protocol. 0.2 mL of the mixture was then loaded onto a 1 cm^2 square shaped filter paper frame, and the collagen-cell mixture was left to set for 40 minutes at 37˚C, 5% CO_2. The formed gel was then covered with supplemented medium and with changing the media every 2 days. HCASMCs were subsequently allowed to grow in the TEML until they were observed to possess an elongated spindle-shaped morphology. The formed gel was then covered with supplemented medium with changing the medium every 48 hours. HCASMCs were subsequently allowed to grow in the TEML.

2.1.2 Generation of TEIL constructs

0.2 mL of a neutralised 3 mg/mL BD type I collagen solution was loaded upon a square frame made by filter paper with an area of 1 cm^2 to form an acellular collagen gel base first. An aligned, portable PLA nanofiber mesh coated with fibronectin (10 ng/mL) was placed on the collagen hydrogel. HUVECs (4 x 10^4 cells per sample) were carefully seeded in two separate occasions using small 10 µL volumes on top of the nanofibers. This is to prevent the cells from leaking over the confined area and eventually cell loss. The cells were allowed to attach at 37˚C, 5% CO_2 for 1 hour. Samples were then topped up with supplemented 200 medium and subsequently allowed to be cultured for 4 days at 37˚C and 5% CO_2, with a single media change on day 2.

2.1.3 Generation of TEBV constructs

TEBV construct was fabricated by placing a PLA nanofiber mesh coated with a 10 µg/mL fibronectin solution on the 3D TEML, to create the initial layer of the luminal surface. After successful attachment of the nanofibers to the TEML hydrogel, HUVECs (at a density of 4 x10^4 cells/cm^2) were then seeded on top of the nanofibers to create a full TEBV construct. Once HUVECs were attached,

samples were topped up with the mixture supplemented medium 200 and 231 at the ratio of 7:3, and subsequently allowed to be cultured for 4 days at 37˚C and 5% CO_2, with a single media change on day 2.

2.1.4 Fabrication of control scaffolds (Horm collagen coating)

In some experiments, PLA nanofibers were coated with Horm collagen (1 µg/mL diluted in HBS; Chrono-log, USA) for 1 hour at room temperature. Unbound Horm collagen was washed away using HBS and nanofibers were left to dry. The coated nanofiber was carefully sealed onto collagen hydrogels using freshly prepared rat tail type I collagen solution. These were placed in the incubator programmed at 37˚C, 5% CO_2 until the collagen was set. A sterile scalpel blade was used to cut the outer corner and remove excess nanofibers.

2.2 Preparation of platelet-rich plasma and washed Fura-2-loaded human platelet suspensions

Human platelets were used to test platelets activation and aggregation. A standard method of extraction was used. Blood was obtained by venepuncture from healthy volunteers who had given informed written consent. 5 mL of blood was mixed with 1 mL of acid citrate dextrose anticoagulant (85 mM sodium citrate, 78 mM citric acid and 111 mM d-glucose). Platelet-rich plasma was then obtained by centrifuging at 1500 g for 8 minutes, and was then treated by the addition of 100 µM aspirin and 0.1 U/mL apyrase unless otherwise stated. PRP was then incubated with 2.5 µM Fura-2/AM for 45 minutes at 37°C. Platelets were then collected by centrifugation at 350 g for 20 minutes. Washed platelets were re-suspended into supplemented HEPES –Buffered Saline to a final cell density of to $2x10^8$ cells/mL. To make supplemented HBS, HBS (pH 7.4, 145 mM NaCl, 10 mM HEPES, 10 mM d-glucose, 5 mM KCl, 1 mM $MgSO_4$), was supplemented on the day of the experiments with 1 mg/mL BSA, 10 mM glucose, 0.1 U/mL apyrase and 200 µM $CaCl_2$ (supplemented HBS). $CaCl_2$ concentration of the supplemented HBS was adjusted to 1 mM prior to individual sample analysis.

2.3 Assessment of the pro- and anti-aggregatory potential of the tissue engineered constructs and conditioned media from the construct using real-time monitoring of platelet $[Ca^{2+}]_{cyt}$

PRP was incubated with 2.5 µM Fura-2/AM for 45 minutes at 37°C. Platelets were then washed by centrifugation and re-suspended in supplemented HBS to a final cell density of $2x10^8$ cells/mL. Fluorescence was recorded from stirred aliquots of Fura-2-loaded washed human platelet suspensions in contact with the blood vessel constructs at 37°C using Cairn Research Spectrophotometer, with excitation of 340 and 380 nm and emission of 515 nm. This methodology has been used to assess the impact of exposure of human washed platelet suspensions to a variety of components of our tissue-engineered blood vessel constructs. Changes in $[Ca^{2+}]_{cyt}$ were monitored using the 340/380 nm fluorescence ratio. Data were calibrated using the method of Grykiewicz *et al*., (1986). Agonist-evoked changes in $[Ca^{2+}]_{cyt}$ were quantified by integration of the change in fluorescence records from basal with respect to time from 5 - 15 minutes after agonist addition.

Conditioned media from cultured 3D TEML constructs and cultured 2D HCASMCs monolayer were collected, with matching of cell densities and culture duration. 1 mL of conditioned media was added to 1 mL of washed Fura-2-loaded human platelets obtaining a final platelet concentration of 2×10^8 cells/mL HBS and freshly supplemented medium (not exposed to cells) were used as controls. Changes in $[Ca^{2+}]_{cyt}$ of Fura-2-loaded human platelets was recorded using a Cairn Research spectrophotometer with excitation at 340 and 380 nm and emission at 515 nm for 10 minutes.

2.4 Assessment of tissue engineered constructs using conventional assays

2.4.1 Fluorescent imaging of Platelet adhesion and aggregation upon layers of the TEBV

To study aggregate formation upon the surface of the constructs, platelets were labelled with $DiOC_6$. In these experiments, 5 mL whole human blood was collected into 1 mL ACD anticoagulant

containing the fluorescent plasma membrane label, $DiOC_6$, to provide a final concentration of 1 µM (Metcalfe et al., 2016). The blood was mixed with anticoagulant and dye, and left to incubate for 10 minutes at room temperature prior to centrifugation to collect PRP. Washed human platelet suspensions were then prepared by centrifugation at 350 g for 20 minutes. Platelets were then resuspended into supplemented HBS to a final cell density of $2x10^8$ cells/mL. The TEBV, or layers of the TEBV, samples were then incubated with 1 mL of washed $DiOC_6$-labelled human platelet suspensions for 15 minutes at 37°C. Following the incubation period, the platelet suspension was discarded and the constructs were washed once with HBS. Images of adhered platelets were taken under fluorescence microscope using excitation wavelengths of 485 nm and emission of 501 nm (Nikon Eclipse *Ti,* Japan).

2.4.2 Aggregation studies

Platelet aggregation studies were conducted using two different techniques, a traditional light transmission aggregometer (Metcalfe et al., 2016) and a microplate-based absorbance assay (Lordkipanidzé et al., 2014). The TEML, TEBV and collagen hydrogel were individually pre-incubated with washed human platelet suspension for 15 min at 37˚C with continuous magnetic stirring using the sample holders developed in chapter 3. At the end of this incubation, the constructs were removed and the platelet suspension was transferred for use in these experiments as set out below.

2.4.3 Microplate-based absorbance assay

200 µL of the remaining washed platelet suspension were added to a 96-well plate. A baseline recording was taken following the incubation with the construct using a BioTek Synergy 2 microplate reader assessing absorbance at 600 nm. Platelets aggregation was then stimulated by addition of 0.2 U/mL of thrombin into each well and subjected to rapid agitation between readings. Absorbance was measured every minute for 6 minutes after agonist addition. The mean absorbance was then calculated and compared between experimental conditions.

2.4.3.1 Light Transmission aggregometry

Platelet aggregation was measured using a ChronoLog light transmission aggregometer according to the manufacturer's instructions. Following incubation with the blood vessel constructs, 0.5 mL of the platelet suspension was transferred into glass aggregometry tubes containing magnetic stir bars. Stirring was set to 1200 rpm and temperature of the aggregometry tube holder was maintained at 37°C. Prior to each reading, the baseline for full aggregation was set by comparison to a tube filled with 0.5 mL supplemented HBS. A baseline reading was then taken for 2 mins. Platelets were then stimulated by adding 0.2 U/mL thrombin. Changes in light transmission was recorded during constant stirring of the samples at 37°C. Aggregation responses were quantified and compared by measuring the maximum percentage aggregation for each sample, 8 minutes after thrombin addition.

2.4.3.2 Dense granule secretion

Platelet secretion was assayed using a luciferin-luciferase assay to quantify ATP release from the dense granules. The TEML, TEBV and collagen hydrogel were individually pre-incubated with washed human platelet suspension for 15 min at 37˚C with continuous magnetic stirring using the sample holders developed in chapter 3. Following this incubation period, 0.2 mL of platelets pre-exposed to tissue engineered constructs were transferred to a clean 96-well plate and incubated with 10% [v/v] luciferin-luciferase (Sigma Aldrich, USA). A basal reading was obtained at this stage by integrating light emission for 1-minute following luciferin-luciferase addition at 37°C using a BioTek Synergy 2 microplate reader. The samples were then stimulated with 0.2 U/mL thrombin for 1 min. Data were normalised to a maximum light emittance by treating all samples following thrombin stimulation with 10 µM of ATP (Sigma Aldrich, USA) which was added to each sample to obtain a maximum increase of ATP. Luminescence was quantified using a luminescence setting on Synergy 2 microplate reader.

2.4.4 Collagen morphology assessment

2.4.4.1 Reflectance microscopy

Acellular collagen hydrogels made from rat tail type I collagen and cultured TEML construct were transferred onto petri dishes with centrally located coverslips to enable visualisation with a PLAPON 60× oil immersion objective using FluoView FV1200 laser-scanning confocal microscope (Olympus, Japan). The collagen fibre morphology was imaged under reflection mode.

2.4.4.2 Scanning electron microscopy

For imaging using scanning electron microscopy (SEM), the same group samples were subjected to standard critical point drying first and mounted onto aluminium stubs with carbon tape for SEM/EDXA examination using a bench top Hitachi TM3000 system under 1.5-5 kV acceleration voltage.

2.5 Immunostaining of human type I and III collagens

The presence of type I and III collagens of the TEML constructs were examined using monoclonal antibodies specific to human type I and III collagen, respectively. TEML constructs cultured for 10 days were fixed for 40 mins at room temperature with 4% paraformaldehyde. Subsequent to fixing, the TEML constructs were incubated with Sudan Black B for 30 mins at room temperature. This was followed by blocking with 5% goat serum for 30 mins at room temperature. The cells were then incubated with either a primary antibody to human type I or type III collagen for 60 mins at room temperature. Both antibodies were used at a concentration of 1:200 [v/v] diluted in PBS with 0.1% [v/v] Tween 20 (PBST). Subsequently, the samples were incubated for 60 mins at room temperature with a 1:500 dilution in PBST of AlexaFluor-labelled goat anti-mouse secondary antibody. Fluorescence images were obtained using the confocal microscope (Olympus, Japan).

2.6 Platelet adhesion assay to TNF- α-treated HUVEC monolayers and blood vessel constructs

The HUVECs monolayer was seeded on a glass slide coated with 2% BSA (sigma Aldrich, UK) solution to prevent platelet activation on the glass surface. Tissue-engineered blood vessel constructs and HUVECs monolayers were incubated with either 100 U/mL or 1000 U/mL TNF-α (or an equivalent volume of its vehicle, HBS for 24 hours under standard culturing conditions. At the end of the incubation period, the media was removed and 1 mL of $DiOC_6$-labelled washed platelets were incubated with the constructs for 15 minutes at 37°C under continuous magnetic stirring. The platelet suspension was then removed and the constructs were washed once with HBS. The samples were imaged using a Nikon fluorescence microscopy.

2.7 Statistics

Values stated are mean ± SEM of the number of observations (n) indicated. Analysis of statistical significance was performed using a two-tailed Student's *t*-test. $P < 0.05$ was considered statistically significant.

3. Results

3.1 Analysis of pro- and anti-aggregatory properties of the constructs

In the previous chapter, we established a methodology for assessing pro- and anti-aggregatory properties of tissue-engineered blood vessel constructs through real-time monitoring of $[Ca^{2+}]_{cyt}$. Therefore, experiments were performed using this technique to simultaneously compare the pro- and anti-thrombotic properties of each of the produced blood vessel constructs (hydrogel, TEIL, TEBV and TEML). This was performed by measuring construct- and thrombin-evoked rises in $[Ca^{2+}]_{cyt}$ of platelets. Constructs were individually placed atop of washed Fura-2-loaded human platelet suspensions for 15 minutes at 37˚C with continuous magnetic stirring to assess whether any of the constructs could demonstrate a direct pro-thrombotic effect on the underlying platelet suspension. This was followed by the removal of the construct and addition of thrombin to assess the impact of any soluble agonists and inhibitors released from the 3D models on sensitizing or inhibiting the platelet response to this soluble agonist.

As shown in Figure 4.1, prior to thrombin stimulation, platelets exposure to the TEML were found to trigger a significant increase in platelet cytosolic Ca^{2+} concentration compared to collagen hydrogel prior to thrombin stimulation (179.3 ±42.7% of control; *n=6*). These data therefore indicate that exposure to the TEML alone could trigger activation of platelets, in line with our previous results shown in chapter 3. In addition, thrombin-stimulation also evoked a larger increase in the $[Ca^{2+}]_{cyt}$ of platelets exposed to the TEML when compared to the collagen hydrogel alone (169.2 ± 33.1% of control; n = 8; $P < 0.05$). This is consistent with the platelets aggregating on the surface of the construct able to increase the activation status of the underlying platelets in the suspension. These data therefore suggest that the TEML may provide a suitable pro-aggregatory surface on which to from thrombin when the endothelial lining has been damaged.

Thrombin-evoked rises in $[Ca^{2+}]_{cyt}$ in TEBV-exposed platelets were found to be significantly reduced compared to those in contact with the collagen hydrogel (24.0 ± 11.3% of control; n = 8; $P < 0.05$).

Similar to the TEBV, the exposure of washed platelets to the TEIL caused a significant reduction of thrombin-evoked $[Ca^{2+}]_{cyt}$ when compared to samples exposed to the acellular collagen hydrogel (24.9 ± 13.7% of control; $n = 8$; $P < 0.05$). Interestingly, platelets exposed to the TEIL constructs showed a smaller thrombin-evoked rise in $[Ca^{2+}]_{cyt}$ than those incubated with the TEBV, however this was not statistically significant (90.4 ± 30.4%; $n = 8$; $P > 0.05$). These data therefore demonstrate that both the TEBV and TEIL possess the anti-aggregatory effects of the native blood vessel. As the TEIL only contains endothelial cells, these data therefore suggest this inhibitory effect is coming from the HUVECs monolayer. Interestingly the presence of HCASMCs in both the TEML and TEBV, appear to enhance the thrombogenicity of the respective constructs lacking these cells (hydrogel for TEML and TEIL for TEBV). These data therefore suggested that the HCASMCs may possess pro-aggregatory properties.

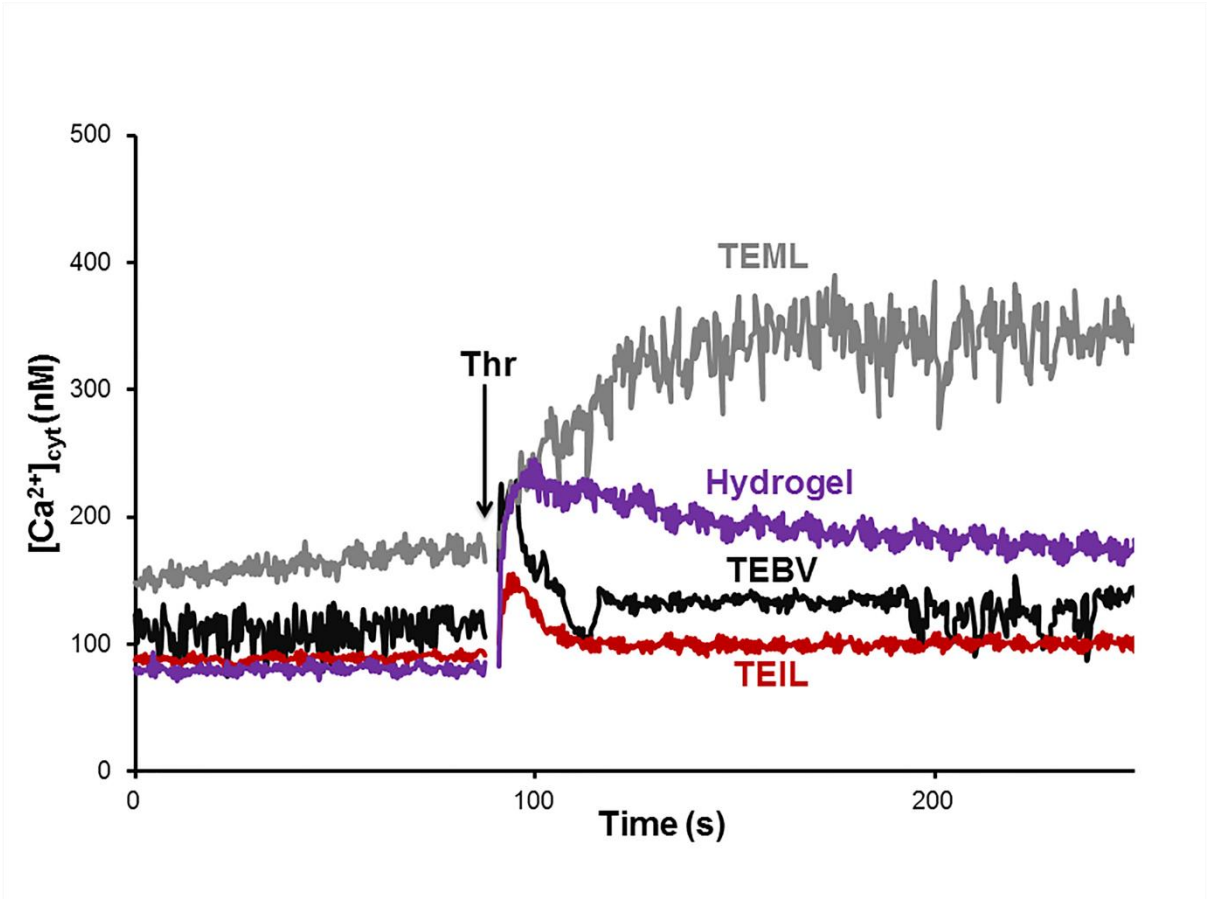

Figure 4.1 – Real-time measurements of $[Ca^{2+}]_{cyt}$ in platelet suspension exposed to tissue-engineered vessel constructs. Fura-2 loaded human platelets suspension was incubated in contact with hydrogel alone, TEML, TEIL and TEBV constructs for 15 minutes at 37˚C off-screen. The constructs were then removed and the remaining suspension was stimulated with thrombin (0.2 U/mL). Results are representative of 4 experiments (n=6). Thr, thrombin.

3.2 Platelet aggregometry experiments replicate the findings of the real-time platelet activation monitoring experiments

To validate the results from the calcium signalling studies, experiments were performed to assess platelet aggregation using a previously-developed microplate-based absorbance assay (Lordkipanidzé et al., 2014). In this assay, aggregation of the platelet sample was tracked as a reduction in the absorbance of the washed human platelet sample – since stimulated platelets

begin to clump and form aggregates within the cell suspension, this allows more light to pass through the sample and thus can be observed as a reduced absorbance of the sample.

A 15-minute pre-incubation of platelets in the presence of collagen hydrogel alone or TEBV triggered no change in the basal absorbance readings of the samples– in line with neither of these samples being able to trigger platelet activation by themselves (Figure 4.2A, 0 minutes prior to thrombin stimulation). However, upon stimulation of samples with thrombin, aggregation could be observed in both samples, although this was found to be significantly slower in samples exposed to the TEBV at the end of the reading (75.1 ±34.3% of control; $P < 0.05; n = 10$) – which demonstrates that TEBV possesses the anti-aggregatory effects of the native blood vessel. In contrast, after pre-incubation with the TEML it was possible to observe a significant reduction in the basal absorbance reading prior to thrombin stimulation (63.6 ±24.3 % of control; $P < 0.05; n = 10$). In addition, the percentage platelet aggregation was found to be more extensive at the end of the experiment (146.5 ±84.1 % of control; $P < 0.05; n = 8$). This was consistent with our other findings that TEML exposure caused platelet activation.

To further assess whether the TEBV was able to inhibit platelet function, further experiments using a conventional aggregometer were performed to assess the effect of preincubation with the blood vessel constructs on platelet aggregation. In these experiments aggregation is monitored by light transmittance. Upon platelet stimulation, this is typically a biphasic response in which an initial decrease in light transmittance caused by the platelet shape from a discoid to spherical form, followed by a secondary rapid increase in light transmittance, as the aggregated platelets are lost from the normal light path. As can be seen in Figure 4.2B, platelets exposed to the TEML showed a slow aggregatory response prior to thrombin stimulation – indicating that these cells were already subject to low-level activation prior to the addition of thrombin. After thrombin addition, the TEML-exposed platelets undergo a rapid aggregation without notable shape change response, which provides further evidence of their prior activation. At the end of the experiment, the TEML

construct shows a significantly higher average percentage of maximum aggregation compared with the collagen hydrogel (154.6 ±15.6 % of control; *P < 0.05; n = 4)*. These data are consistent with the Ca^{2+} signalling studies, and suggest that the TEML is a pro-aggregatory surface. In contrast, platelets exposed to the TEBV show no significant aggregatory response prior to stimulation and upon thrombin addition there is no notable aggregatory response following the initial shape change response of platelets. When compared with the collagen hydrogel, the TEBV significantly inhibits platelet aggregation with an average maximum percentage of aggregation of 6.15 ±6.15% of control; *P < 0.05; n = 4.*

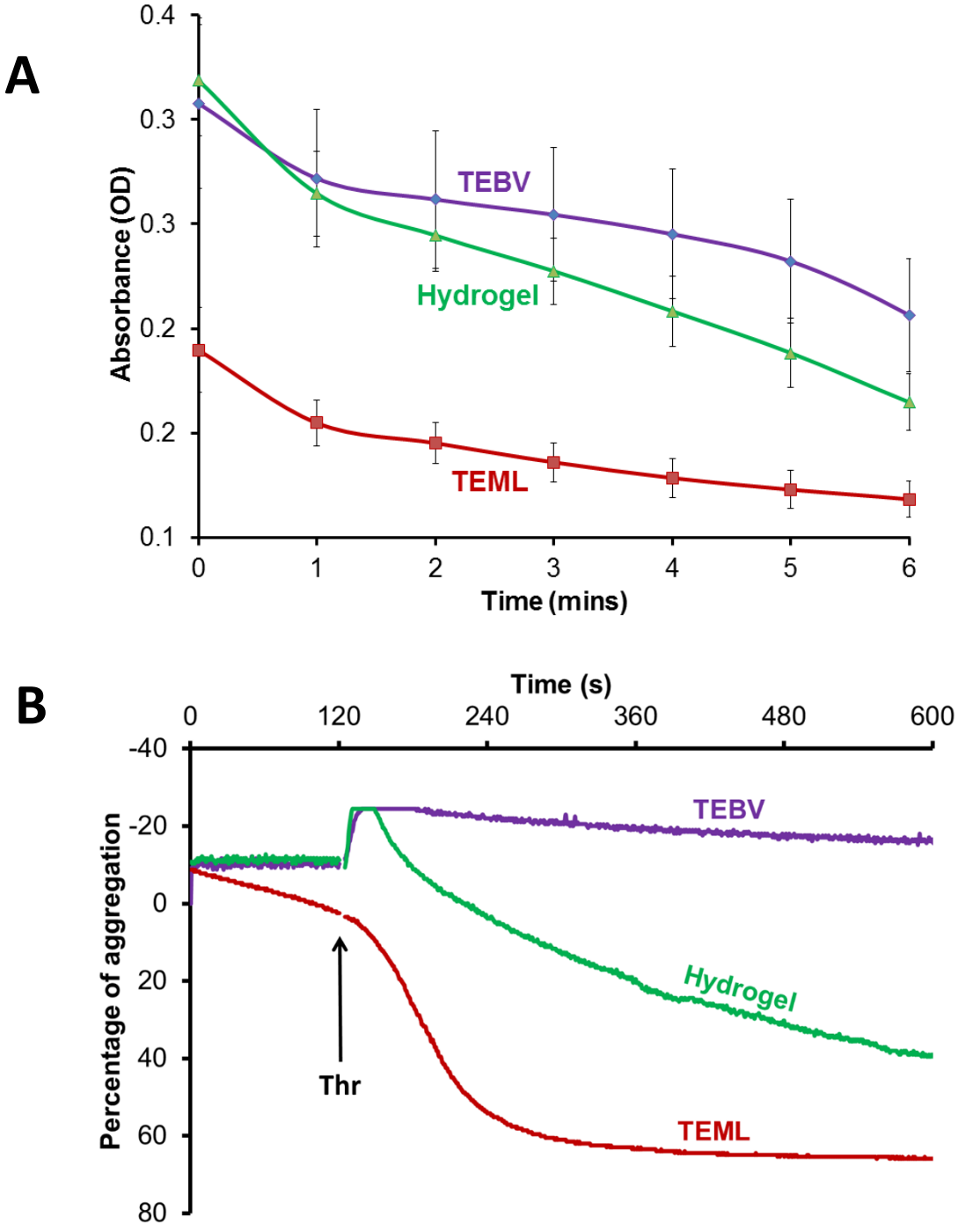

Figure 4.2 – Shows absorbance aggregation traces of platelets formerly incubated with tissue-engineered constructs. Platelets were incubated with hydrogel alone, TEML or TEBV constructs for 15 minutes, with dynamic stirring at 37˚C; A) Absorbance measured using a plate reader. B) Percentage aggregation measured using an aggregometer. A baseline value was obtained at 0 minutes, post construct incubation and prior to thrombin stimulation. Results are representative of 6 and 3 experiments, respectively.

3.3 Exposure to the TEML triggers platelet dense granule secretion, whilst pre-incubation with the TEBV inhibits this parameter

Another commonly used assay is to assess agonist-evoked secretion of platelet dense granules (a key step in thrombus formation) by measuring ATP released into the extracellular medium. This experiment uses the firefly luciferin-luciferase reagent to produce a light output proportional to the ATP concentration in the extracellular medium from platelet preparations (reaction is shown below).

$$ATP + \text{D-luciferin} + O_2 \rightarrow AMP + PP_i + \text{oxyluciferin} + CO_2 + \text{light}$$

The luminescence is measured on a plate reader to assay either relative or absolute ATP release. Platelets exposed to TEML construct display a significantly higher absolute increase of ATP secretion at baseline when compared to platelets exposed to TEBV or collagen hydrogel (140.8 ±23.3 RLU; Figure 4.3A; *P < 0.05; n = 6)*. This indicates a greater amount of ATP being secreted by these platelets which in turn binds to the readily available luciferin, yielding a high luminescence. Interestingly, this signified that exposure to TEML constructs triggers platelets secretion of ATP-containing dense granules prior to stimulation with thrombin, suggesting that the TEML constructs acting as an agonist. Whereas platelets exposed to TEBV or collagen hydrogel show a significantly reduced baseline when compared with those incubated with TEML constructs (60.2 ±6.6 RLU and 70.7 ± 7.2 RLU, respectively; *P < 0.05; n = 6)*. This result suggests that TEBV constructs inhibits ATP secretion from platelets pre-exposed to it.

To confirm this finding, the thrombin-evoked ATP secretion was assessed from both TEBV- and hydrogel-exposed platelets. For internal standardisation, a known amount of ATP was added at the end of the assay to measure a maximal response to ATP to compensate for any variation of firefly luciferase activity between samples to ensure these data represented differences in ATP secretion and not changes in the maximal luciferase light production potential. This percentage was calculated as shown below:

$$Percentage\ of\ maximum\ = \frac{Post\ thrombin\ stimulation - baseline}{Maximum\ luminescence - baseline} x\ 100$$

As shown in Figure 4.3B, platelets exposed to the TEBV constructs display a significant reduction in thrombin-evoked ATP secretion when compared with those exposed the collagen hydrogel (0.4 % and 1.4 % of maximum, respectively; *P < 0.05; n = 6).* This result suggests that the TEBV construct releases anti-aggregatory factors that opposes the stimulatory effect of thrombin.

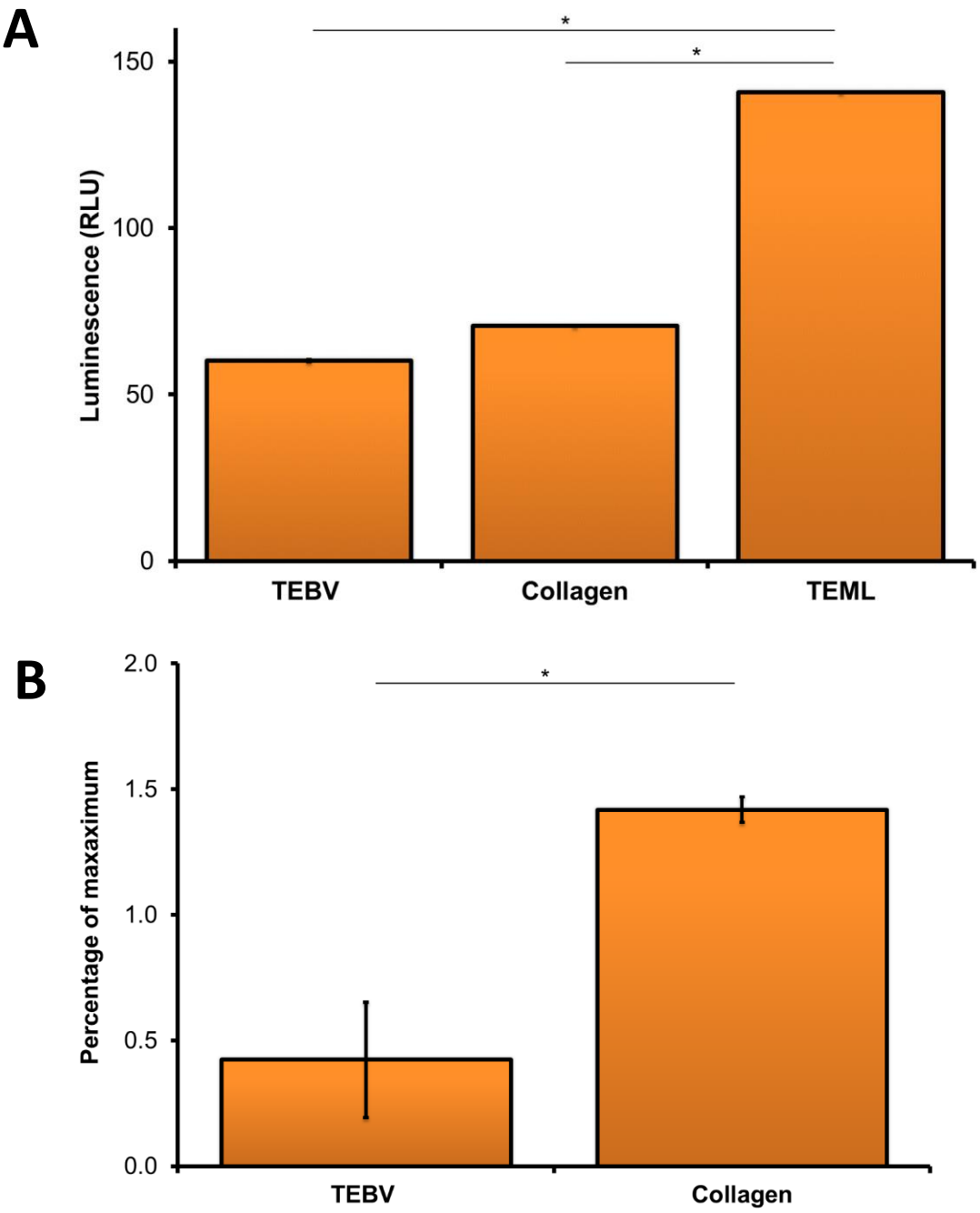

Figure 4.3 – ATP secretion of platelets incubated with tissue-engineered constructs. A) Absolute increase in luminescence of platelets incubated with either TEBV, collagen or TEML constructs, prior to thrombin stimulation. B) Percentage of maximum of platelets incubated with either TEBV, or collagen, post 0.2 U/mL thrombin stimulation. Constructs were incubated with either TEBV, collagen or TEML constructs for 15 minutes, with dynamic stirring at 37˚C. The constructs were removed and luminescence of the remaining platelets were measured using Luciferin-Luciferase assay. The absolute luminescence reading was recorded as baseline prior to thrombin stimulation. Followed by calculating the percentage of maximum ATP secretion upon 0.2 U/mL thrombin stimulation. Results are representative of 3 experiments (n=6). * *P < 0.05.*

3.4 Fluorescent imaging of the surface of the blood vessel constructs after incubation with fluorescently-labelled platelets confirms the pro-aggregatory capacity of the TEML and the anti-aggregatory capacity of the TEBV

To further assess the effect the thrombogenic properties of the acellular type I collagen hydrogel, TEML and TEBV, fluorescent imagining experiments were performed to assess thrombus formation on their surfaces. Washed $DiOC_6$-labelled platelet suspensions were allowed to interact with the acellular type I collagen hydrogel, TEML or TEBV constructs for 15 minutes at 37C. These samples were then washed and subject to fluorescent imaging. These experiments found that type I collagen hydrogel alone could only sporadic platelet adhesion on is surface, with no obvious signs of any platelet aggregates forming (Figure 4.4 A, B). These data are consistent with our previous findings that the type I collagen hydrogel is relatively inert to human platelets. In contrast, the inclusion of human coronary artery smooth cells within the TEML construct was found to support platelet adhesion as well as supporting the formation of some platelet aggregates (Figure 4.4 C, D). This is consistent with our real-time monitoring of platelet activation, and suggests that our TEML had pro-aggregatory properties that allow it to provide a valid replica of the subendothelial matrix upon which to study platelet activation. Lastly, the TEBV construct was found to be very resistant to platelet aggregation, however a few individual platelets could occasionally be observed to adhere to regions where HUVEC monolayer did not cover the medial layer (Figure 4.4 E, F). These areas could be identified by $DiOC_6$ fluorescence leaching from platelet suspension onto HUVECs, allowing to their identification for this fluorescent membrane label. Due to $DiOC_6$ being a non-specific fluorescent dye for cell membranes, the endothelial cells were also found to be labelled as excess dye from the platelet suspension appear to be associated with the nucleated endothelial cells under the fluorescence microscope. This labelling of the endothelial cells allowed identification of areas in which the HUVEC monolayer was incomplete. The average size of aggregates was quantified and TEML constructs generated a significant average number of platelet aggregates per 100 μm^2 compared with the TEBV (20 ±1.4 and 2 ±0.5; $P < 0.05$, respectively). There were no platelet

aggregates present on the collagen hydrogel alone, post platelet incubation period. These data therefore confirm the findings of our real-time monitoring system that the TEBV provides an anti-aggregatory surface, and supports the validity of the TEBV as a potential replica of the intact native blood vessel. However further work will be required to optimise the HUVEC coverage of the luminal surface to prevent unwanted artefacts.

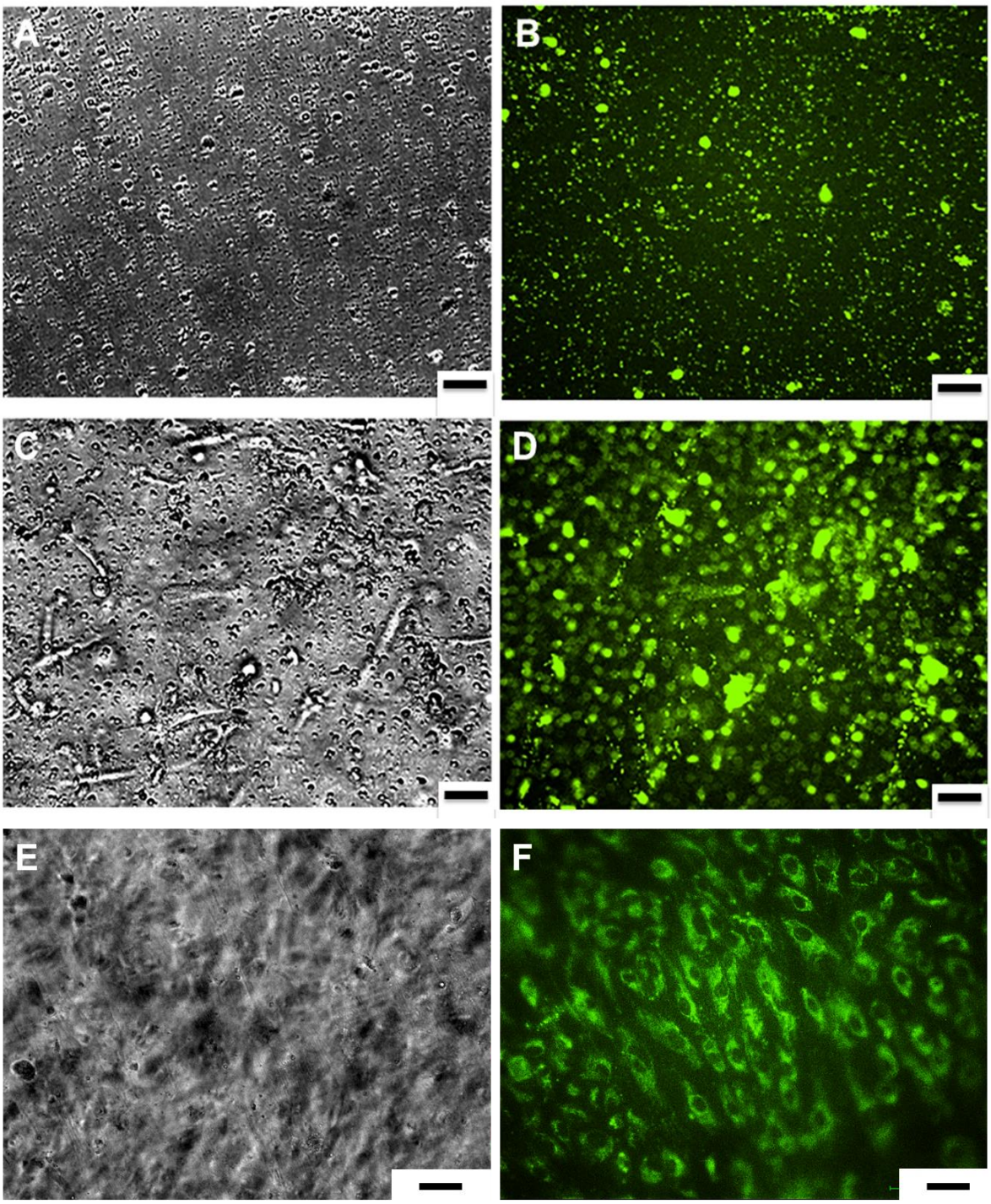

Figure 4.4 – Optical images of acellular collagen hydrogel, TEML and TEBV constructs after exposure to platelets. $DiOC_6$ labelled-human platelets suspension was incubated with type I collagen hydrogel (A,B), TEML (C,D) or TEBV (E,F) for 15 minutes at 37˚C with gentle agitation of samples. Platelet aggregation were recorded, after the samples were washed with HBS, in brightfield microscope (A,C,E) and fluorescence microscope (B,D,F). Results presented are representative of 4 experiments. Scale bar = 50 µm.

3.5 The pro-aggregatory properties of HCASMCs do not appear to be due to the release of a soluble agonist

The analysis of the pro-aggregatory properties of the blood vessel constructs indicated that the presence of HCASMCs increased their pro-aggregatory properties. The HCASMCs may be able to provide a pro-aggregatory property either through release of a soluble agonist or production of an adhesive ligand which triggers platelet activation. To assess whether a soluble agonist was released by the HCASMCs, experiments were performed to assess if conditioned media from these cells could trigger platelet activation. As platelet activation is dependent on rises in cytosolic Ca^{2+} concentration, changes in this parameter was monitored in Fura-2-loaded platelets exposed to conditioned culture media from TEML constructs. A concentrated suspension of Fura-2-loaded platelets (4×10^8 cells/mL) was mixed with an equal volume of either conditioned cultured media, basal media supplemented with growth factors which had not been used for cell culture, or HBS. HBS addition was used in these studies to assess the impact on the fluorescence of cell dilution. As can be seen in Figure 4.5, the dilution of the platelet suspension created a small but consistent artefactual drop in the basal fluorescent signals seen in all conditions. Interestingly, when basal media was added to the cells, a small, transient Ca^{2+} signal was observed suggesting that the growth factors in the media may have a small stimulatory effect on the cells. However when the conditioned culture media collected from the TEML construct was added to the platelet suspension it appeared to elicit no discernible increase in the $[Ca^{2+}]_{cyt}$ compared to the HBS control over the course of the monitoring period. These data therefore suggest that a soluble agonist released from the HCASMCs was responsible for its pro-aggregatory properties. The growth factors used in the basal media may not be accessible after binding to the target cells, thus explaining why there is no effect on cytosolic Ca^{2+} concentration observed in this experimental condition.

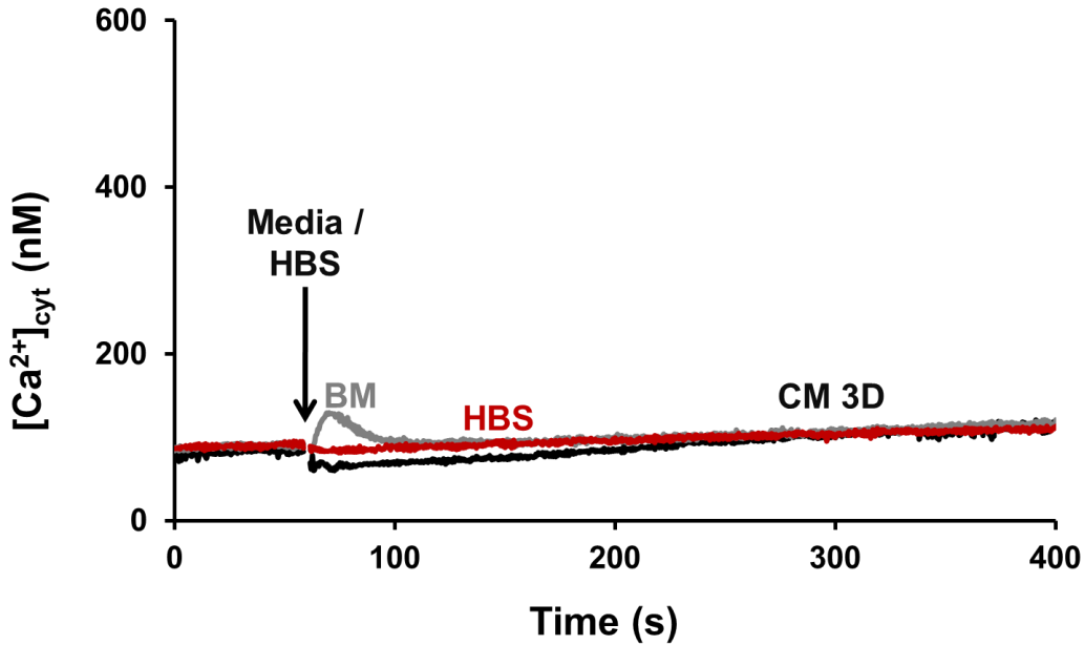

Figure 4.5 – Real-time measurements of cytosolic calcium concentration $[Ca^{2+}]_{cyt}$ in platelet suspension exposed to various culture media. M231 basal media, M231 culture media or HBS solutions were added to fura-2-loaded human platelets at 37˚C and measured for 6 minutes. Results are representative of 3 experiments.

3.6 Collagen morphology assessment

As no evidence could be found for a soluble agonist being secreted from the HCASMCs, experiments were performed to assess if these cells could affect the thrombogenicity of the constructs by altering the structure of the collagen hydrogel. Previous studies have demonstrated that fibrillary collagen is more able to support platelet adhesion and aggregation than monomeric forms (Farndale, 2009), therefore Reflectance confocal microscopy was utilised to examine whether the presence of HCASMC within the TEML could alter the collagen fibril morphology compared to that observed in the type I collagen hydrogel. As shown in Figure 4.6, distinct architectural differences could be observed in the TEML compared to the type I collagen hydrogel. The collagen fibrils observed in the type I collagen hydrogel exhibited a larger diameter (244.4 ±56.3 % of control; $P < 0.05$; $n = 3$) and a greater degree of shorter fibrils (40.6 ±16.9% of control; $P < 0.05$; $n = 3$) compared to hydrogels in which HCASMCs were cultured. Additionally, fibrils of the TEML construct appeared

more densely packed compared to those of the hydrogels without HCASMCs. These data therefore suggested that the HCASMCs may be altering the structure of the collagen in our constructs.

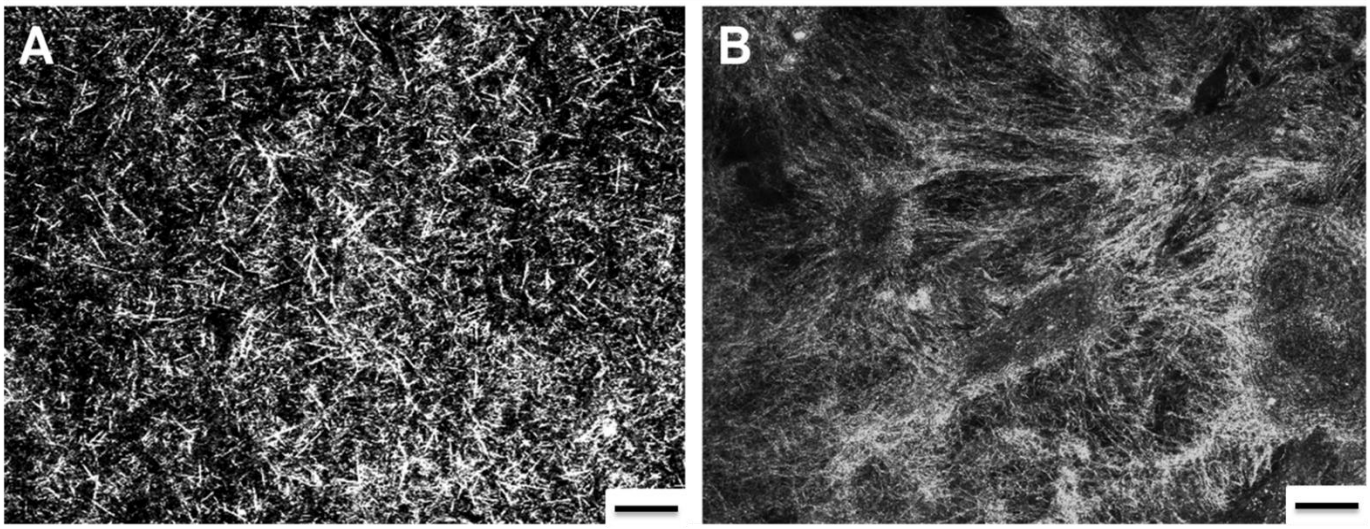

Figure 4.6 – Collagen fibrillar morphology in acellular collagen hydrogel and TEML. Confocal reflection images of acellular collagen hydrogel (A) and TEML construct (B) cultured for 10 days. Scale bar = 10µm. (C) SEM image of the same TEML sample. Scale bar 50 µm. Results are representative of 5 experiments.

Further examination of the TEML using scanning electron microscopy found that the HCASMCs appeared to have created a dense mesh of fibrils could be seen to be extending from the surface of the cell in an organised manner (Figure 4.7). This pericellular matrix of highly-arranged collagen fibrils emerging from the cells exhibited a different morphology in comparison to the fibrils of the type I collagen scaffold observed further away from the cell body. This can clearly be seen around the cell, where extensions of organised collagen fibrils merging with the cell membrane. These native collagen fibrils emerging from the cells appear to be denser compared with the surrounding collagen scaffold. The figure also shows a breakage of the cellular lamellipodia which was an

artefact created by the cell damage elicited by the standard critical point drying procedure required for sample preparation for the electron microscope.

To further examine this difference in collagen structure, the TEML constructs and collagen hydrogel were examined by confocal microscopy after being labelled with a fluorescently-tagged antibody to type I or type III human collagens. Due to the use of rat tail collagen in the type I hydrogel, the species specificity of these antibodies should allow the identification of neo-collagen forms produced by the HCASMCs. Whilst there was no binding of the antibody to the collagen hydrogel alone, there was a strong fluorescence found to occur around the HCASMCs within the hydrogel for both type I and type III collagen (Figure 4.8). Highly fluorescent thin fibrils extending from the cells are visible appearing for both types of collagen, some of which are away from the nucleus. Suggesting that collagen is being released from the cell. These secreted neo-collagens formed into a pericellular matrix around HCASMCs within the TEML layer. These data therefore suggest that neo-collagen secreted by the HCASMCs is likely to be responsible for the pro-aggregatory effects of these cells when included within our tissue-engineered blood vessel constructs (section (1.4.1.1).

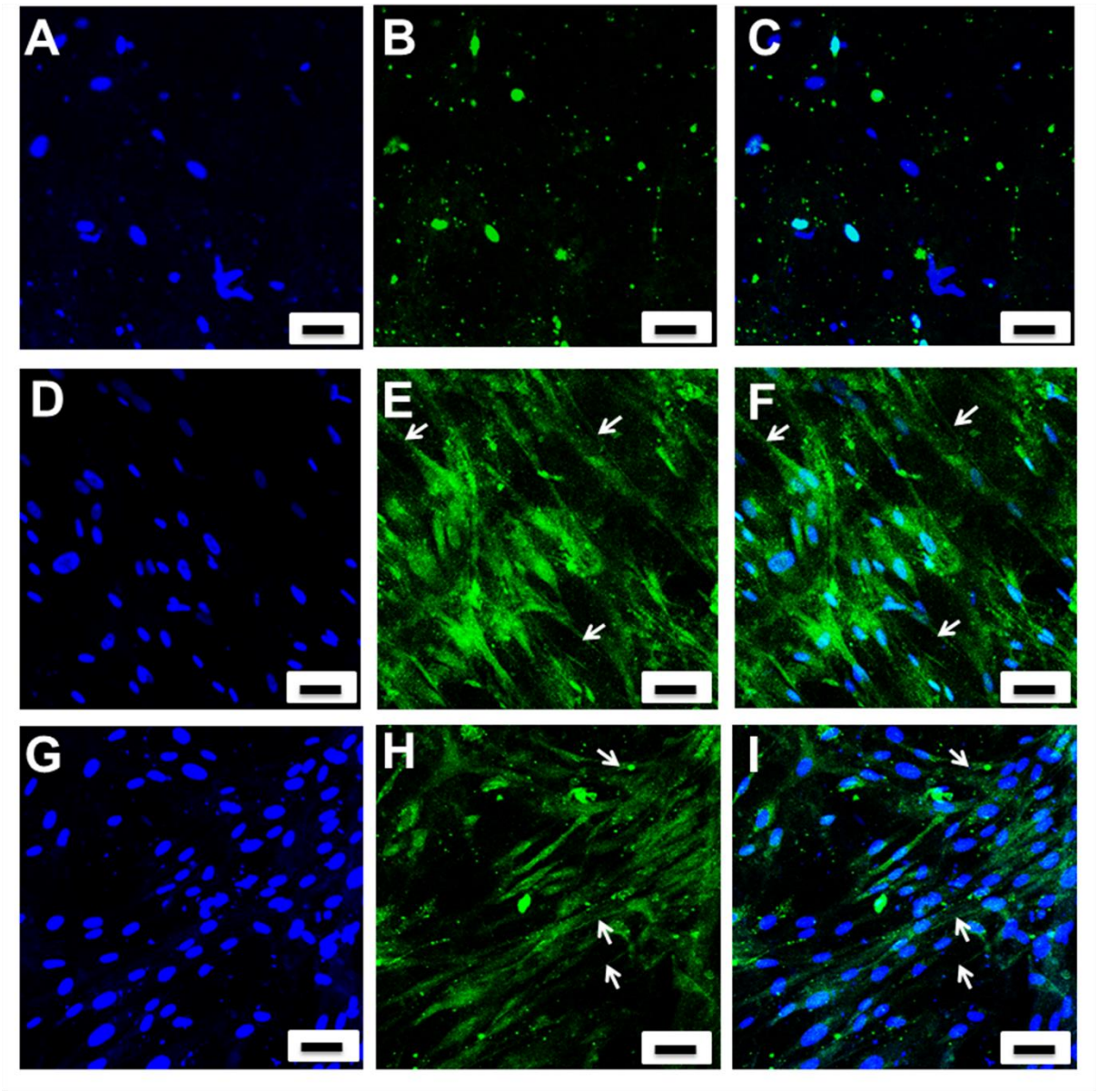

Figure 4.7 – Immunostaining of types I and III collagen within the TEML samples. Primary-free control (A-C); type I collagen in TEML sample cultured for 10 days (D-F); type III collagen in TEML sample cultured for 10 days (G-I). The results presented are representative of 4 experiments. Scale bar 50 µm. **Blue = DAPI; Green = Collagen**

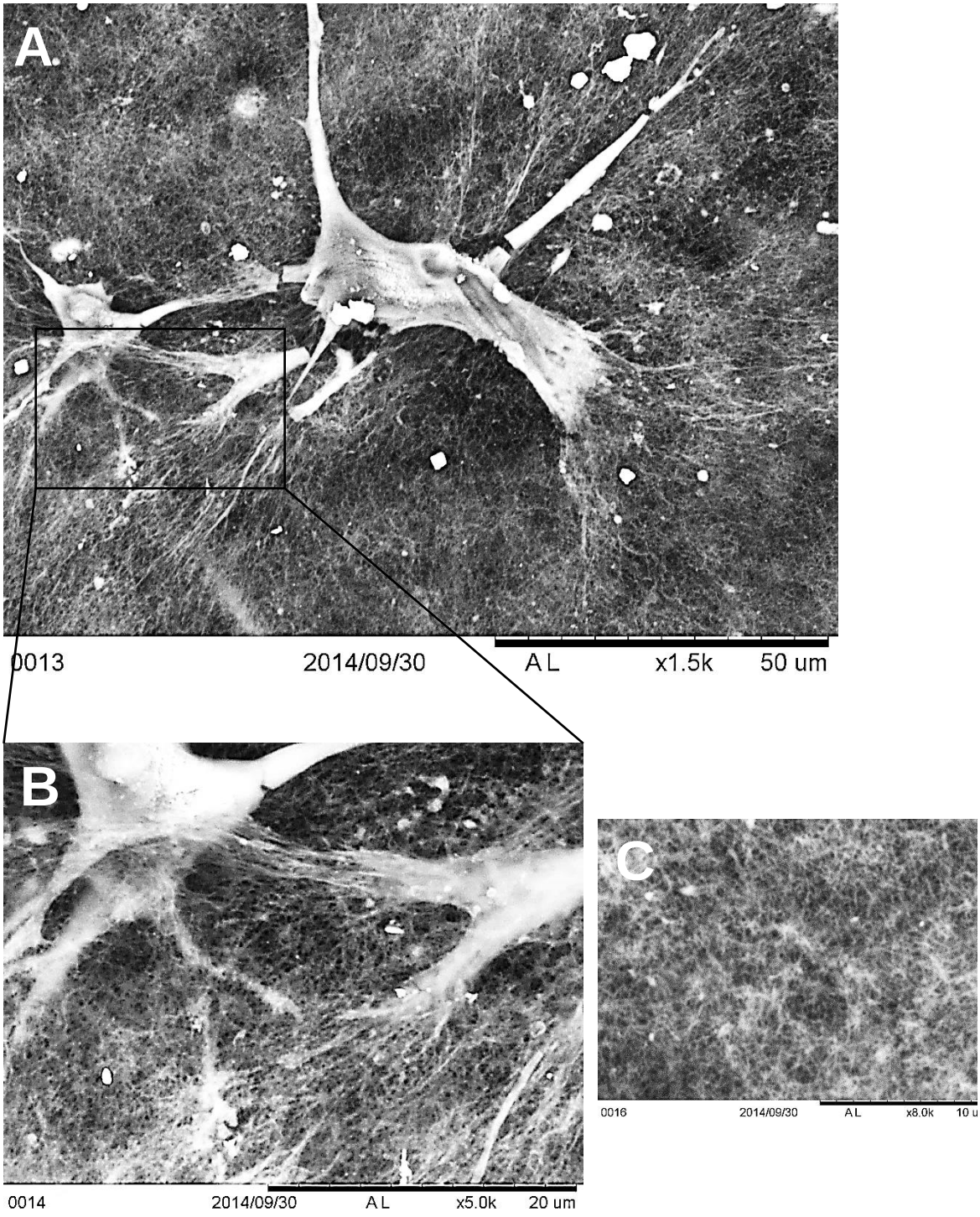

Figure 4.8 – TM3000 SEM images demonstrating the topography of collagen fibres emerging from HCASMCs seeded within rat tail type I collagen. HCASMCs were cultured for 10 days in type I collagen (A, B). Collagen hydrogel without HCASMCs (C).Self-assembly of the collagen matrix was conducted at collagen concentrations of 3 mg/mL with HCASMCs and then subjected to critical point drying to preserve ultrastructure and surface structure of the cells.

3.7 Coating the PLA nanofibers with native Horm collagen increases the thrombogenic potential of the collagen hydrogels

To assess if an increase of an intact collagen on the surface of the construct was able to enhance the thrombogenicity of our collagen hydrogels in a similar manner to the inclusion of HCASMCs, experiments were performed to assess the impact of including of native type I collagen from equine tendons (Horm collagen) on the surface of our construct. To do this we compared the effect of adding PLA nanofibers with and without Horm collagen coating on top of our collagen hydrogel. As can be seen in Figure 4.9, the exposure of Horm collagen-coated nanofibers does not cause a significant increase in $[Ca^{2+}]_{cyt}$ in platelets exposed to these constructs compared with those incubated with the uncoated nanofiber sample. However, platelets appeared to be sensitized to soluble agonists as thrombin-evoked rises in $[Ca^{2+}]_{cyt}$ could be seen to be potentiated by 135.7 ± 22.1 % of that observed in platelets exposed to the uncoated nanofibers ($P < 0.05;$ n = 6). These data therefore are suggestive of collagen-activated platelets secreting autocrine messengers from their dense granules which are then able to potentiate the thrombin-evoked Ca^{2+} signal as has been proposed by others (Fung et al., 2012; Harper et al., 2009; Sage, Pugh, Farndale, & Harper, 2013). These data therefore suggest that exogenous inclusion of neo-collagen could evoke some of the effects of the HCASMCs.

The discrepancy observed may be due to the restriction of collagen to the nanofibers, rather than all over the construct. This reduced density of platelet binding sites might reduce the pro-aggregatory potential of the construct, to assess this further we imaged platelet binding to the surface of hydrogels upon which PLA nanofibers with and without Horm collagen coating had been affixed. As seen in Figure 4.10, no platelet aggregation could be observed upon the uncoated PLA nanofibers, with only the occasional individual platelet observed binding to this structure, with average aggregate sizes of 2.0µm ±1.8 and 4.8µm ±2.1, 10 and 30 minutes post-agonist addition, respectively. In contrast, Horm collagen-coated nanofibers could be observed to have significant

platelet binding along the nanofibers with notable platelet aggregates and average aggregate sizes of 4.7µm ±1.9 and 11.0µm ±4.4, 10 minutes and 30 minutes post agonist addition, respectively. These data therefore confirm that inclusion of native collagen can replicate the thrombogenic effect on the surface of the construct. However, restriction of these aggregates to the surface of the nanofibers may prevent the activated platelets triggering as effective an autocrine activation of platelets in the underlying suspension.

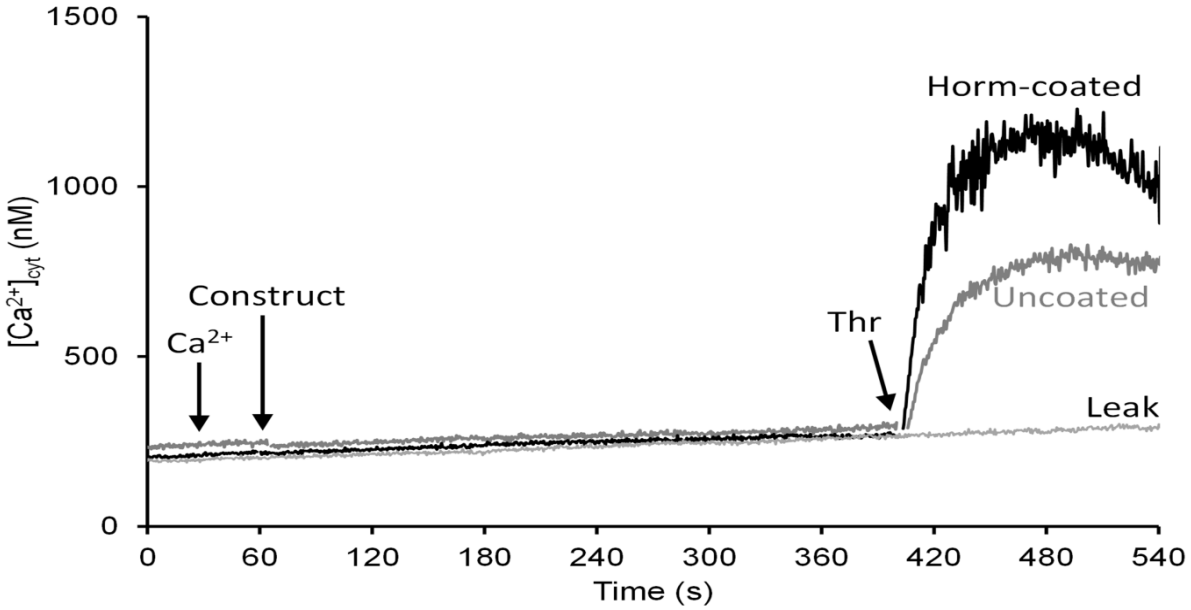

Figure 4.9 -Real-time measurements of cytosolic calcium concentration $[Ca^{2+}]_{cyt}$ in platelet suspension exposed to acellular collagen hydrogel and Horm-collagen coated nanofibers. Fura-2-loaded human platelets were exposed to the coated or uncoated nanofibers supported with collagen hydrogel for 7 minutes at 37˚C, then the samples were removed and the $[Ca^{2+}]_{cyt}$ in the remaining suspension was recorded and stimulated with 0.2 U/mL thrombin, to confirm platelet responsiveness. Arrows show Ca^{2+}, construct and thrombin (Thr) additions, respectively. Thrombin was added post-construct removal. Horm collagen Results are representative of 3 experiments (n = 6).

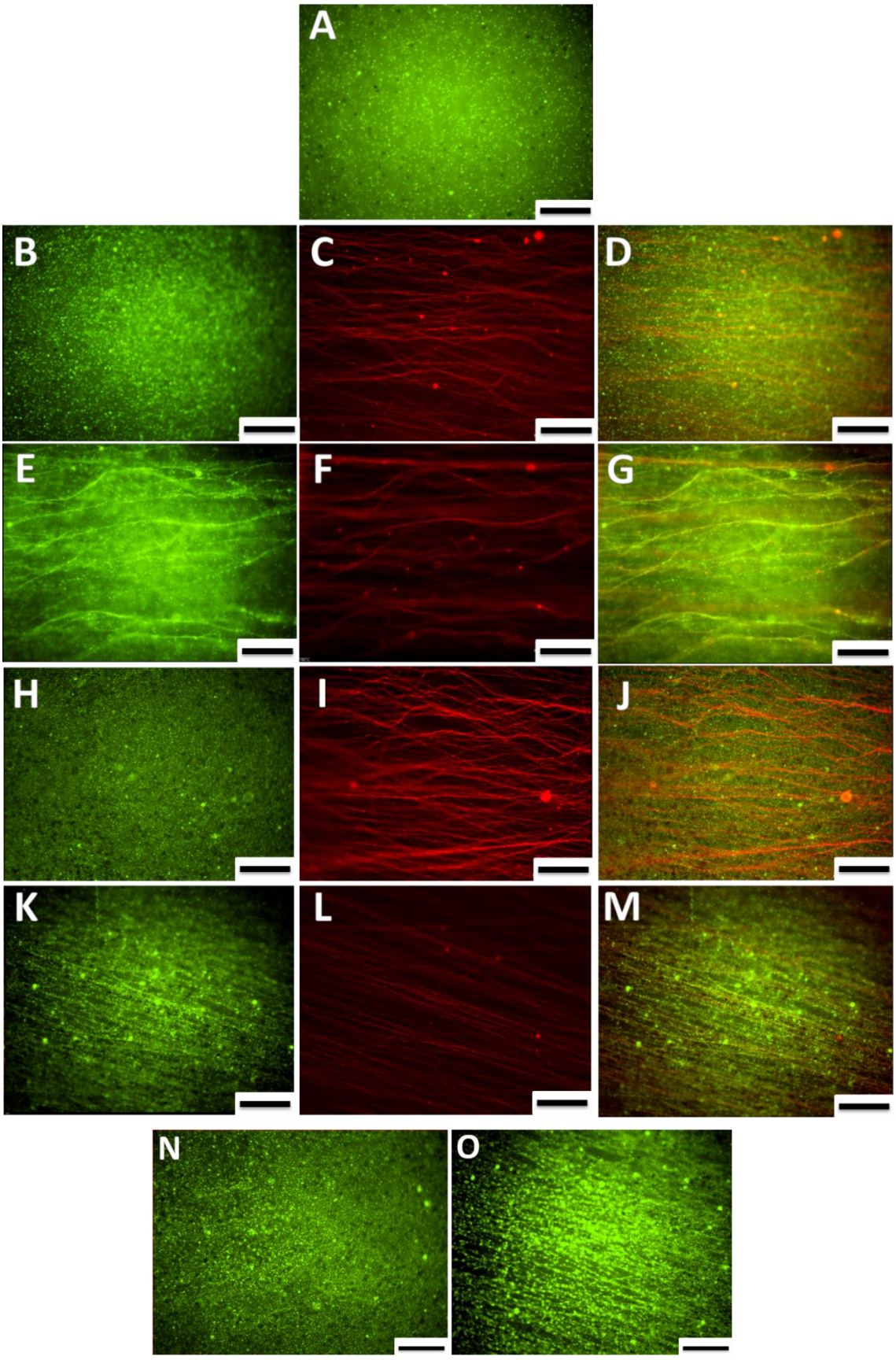

Figure 4.10 - Fluorescent images of Horm collagen coated and uncoated PLA nanofibers post exposure to human platelets. A) Baseline image of $DiOC^6$ labelled-human platelet suspension prior to start of the experiment. Platelets suspension incubated with uncoated nanofibers for 5 minutes (B-D), 10 minutes (H-J) and 20 minutes (O) at 37˚C with gentle agitation of samples; Platelets suspension incubated with immobilised collagen uncoated nanofibers for 5 minutes (E-G), 10 minutes (K-M) and 20 minutes (N) at 37˚C with gentle agitation of samples. Results presented are representative of 4 experiments (n = 4). Scale bar = 50 µm.

3.8 Horm collagen nanofibers do not reduce the anti-aggregatory properties of the TEBV

The earlier experiments demonstrated that the TEIL constructs could inhibit platelet activation more than TEBV. It was possible this might be due to an inhibitory effect of the neo-collagen on the HUVECs placed atop this layer. Experiments were therefore performed to examine if inclusion of native collagen can affect the inhibitory potential of the TEBV. Figure 4.11 shows Fura-2 ratio of platelets exposed of platelets to TEBV constructs incorporating fibronectin-coated or dually fibronectin- and Horm collagen-coated PLA nanofibers within TEBVs. These data show that there was no significant difference before or after thrombin stimulation in the fura-2 ratio of platelets exposed to TEBVs with the Horm collagen-coated compared to those without it (115.2 ± 42.1% of control; n = 3; $P > 0.05$). Thus, native collagen does not appear to impact on the inhibitory potential of the HUVECs. In addition, there is no additional pro-aggregatory effect of inclusion of this native collagen within the construct, as it is likely that platelets do not encounter this due to the endothelial cell coverage of the nanofibers.

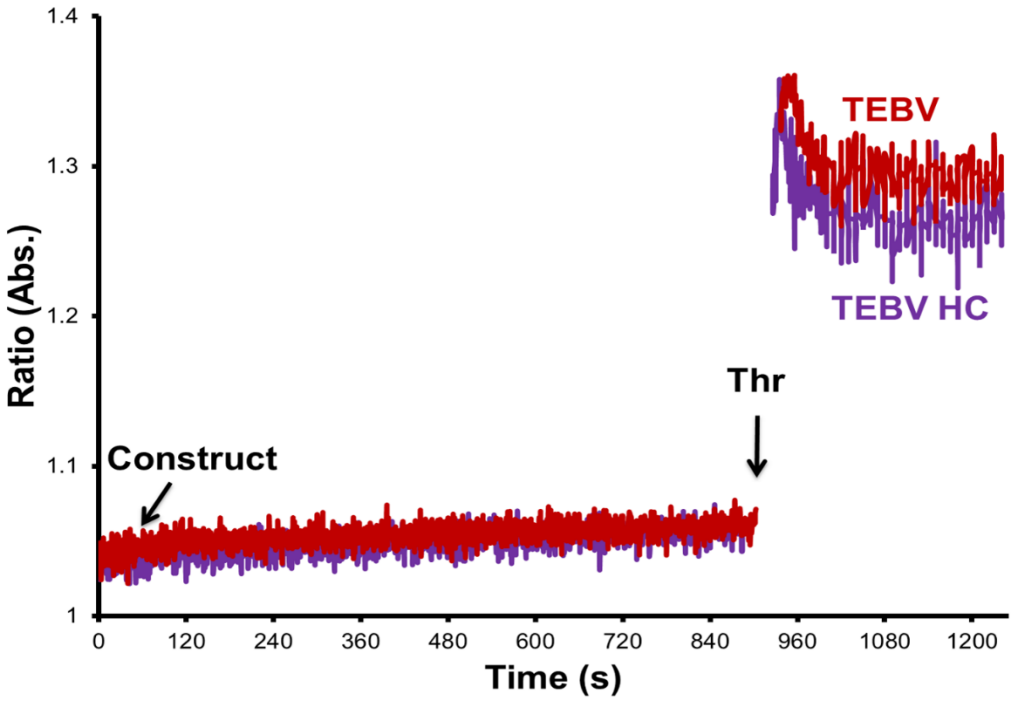

Figure 4.11 – Real-time measurements of 380/340 Fura-2 ratio in platelet suspension exposed to Horm collagen-coated PLA nanofibers within tissue-engineered vessel constructs. Fura-2 loaded human platelets suspension was incubated in contact with fibronectin coated or dually Horm collagen and fibronectin-coated PLA nanofibers of TEBV constructs for 15 minutes at 37˚C off-screen. The constructs were then removed and the remaining suspension was stimulated with thrombin (0.2 U/mL). Results are representative of 3 experiments (n=3). Thr, thrombin.

3.9 Assessment of endothelial cell layer of the TEBV construct

3.9.1 *Evaluation of the role of endothelial-derived inhibitors on anti-aggregatory properties of TEBV*

Our data demonstrates that the TEBV possesses a significant anti-aggregatory property. *In vivo* it is though that endothelial-derived inhibitors such as NO, PGI_2 and adenosine play a key role in keeping platelet quiescent inside the intact vasculature (Rumbaut, 2010). Therefore, experiments were performed to assess if the anti-aggregatory properties of the TEBV could be reversed by blocking the production of these endothelial-derived platelet inhibitors. Initial experiments examined the effect of inhibiting endothelial NOS by pre-treating the TEBV with L-NAME. These data showed that there was no difference in thrombin-evoked rises in $[Ca^{2+}]_{cyt}$ of platelet samples after incubation

with TEBVs treated with L-NAME to untreated TEBVs (Figure 4.12; 135.0 ± 52.3 % of untreated control; n = 9; $P < 0.05$). These data therefore indicated that NO from the TEBV may not be solely responsible for the inhibitory effect on platelet function.

3.9.1.1 Combination of L-NAME and indomethacin

As endothelial cells also produce prostacyclin using a COX-mediated pathway (Caughey et al., 2001), inhibition of NOS may not be sufficient to prevent the effect of the TEBV as there may be redundancy with either compound able to inhibit platelet function in the absence of the other. Therefore, experiments were performed to examine the effect of pre-incubating the TEBV with either 1 mM L-NAME, 300 μM indomethacin (a COX inhibitor), or a cocktail of both drugs. Either compounds or their vehicles were incubated with fabricated TEBV construct for 30 minutes in standard culture conditions. Following the incubation period, the sample was washed and placed atop of a 1.2 mL of platelet suspension for 15 minutes at 37°C with continuous magnetic stirring. The TEBV construct was then removed and platelets' $[Ca^{2+}]_{cyt}$ was recorded from the Fura-2-loaded platelet suspensions. Consistent with our previous data, preincubation with the untreated TEBV reduced thrombin-evoked signals to 24.0 ± 11.3% of that seen in the collagen hydrogel control sample (Figure 4.12A; n = 8; *P < 0.05).* Preincubation of the construct with L-NAME alone (18.1 ± 5.6% of control; n = 8; *P < 0.05*), indomethacin alone (13.9 ± 1.4% of control; n = 8; *P < 0.05*), or both compounds simultaneously (17.2 ± 3.2% of control; n = 8; *P < 0.05*). These data demonstrate that these interventions did not reverse the effect of exposure to the TEBV. These results were very surprising as NO and PGI_2 are the classic endothelial-derived inhibitors of platelet function (Banerjee et al., 2014; Menitove et al., 1984).

3.9.1.2 Treatment of the TEBV with L-NAME cannot reverse the inhibitory effect of this construct on platelet store-operated calcium entry

Endothelial cells are known to secrete a variety of proteins that interfere with the blood coagulation cascade. This includes thrombomodulin which is known to bind and restrain the activity of

thrombin (Esmon et al., 1982). Although this is an integral membrane protein, it can be released from cultured endothelial cells under conditions of inflammation or cell damage (Boehme et al., 2000; Ishii et al., 1991). Therefore, to ensure the inhibitory effect of TEBV incubation on platelet activation was not due to blockade of thrombin activity, experiments were performed to examine the effect of TEBV on an artificially-induced platelet Ca^{2+} signalling pathway. Store-operated Ca^{2+} entry (SOCE) is the major Ca^{2+} entry mechanism in human platelets (Gresele et al., 2017). This entry pathway is activated by depletion of the intracellular dense tubular Ca^{2+} stores. This can be artificially achieved using the sarco/endoplasmic reticulum Ca^{2+}-ATPasa (SERCA) inhibitor, thapsigargin. This allows passive leak of Ca^{2+} out of the stores triggering the activation of the store-operated channel (Tao and Haynes, 1992). Therefore, experiments were performed to assess the impact of TEBV preincubation on thapsigargin-evoked Ca^{2+} release from intracellular stores, as well as the effect on store-operated Ca^{2+} entry both in the presence and absence of antagonists of the endothelial-derived inhibitors, NO and PGI_2. Thapsigargin-mediated depletion of the intracellular stores was unaffected by TEBV compared with the collagen control (Figure 4.12B; 202.8 ± 76.9 % of control; n = 9; *P > 0.05*). This effect was not altered in samples exposed to TEBV treated with 1 mM L-NAME and 300 µM indomethacin (122.5 ± 14.2 % of control; n = 9; *P > 0.05*). These data therefore suggest that there is no difference in the filling state of the dense tubular stores for both untreated platelets and those that were treated with L-NAME and indomethacin. Upon re-addition of Ca^{2+} to the extracellular medium to trigger store-operated Ca^{2+} entry, it could be observed that preincubation with the TEBV significantly inhibits SOCE compared to that seen in cells incubated with the control collagen hydrogel (70.3 ±9.1 of control; n = 7; *P < 0.05*). This inhibitory effect was not reversed by preincubation of the TEBV with L-NAME and indomethacin (60.0 ± 8.0 of control; n = 7; *P < 0.05*). These data therefore suggest that the effect on thrombin-evoked Ca^{2+} signalling is not solely due to an effect of TEBV on downregulating thrombin activity, but is due to an alteration in the intracellular signalling pathways of the platelet.

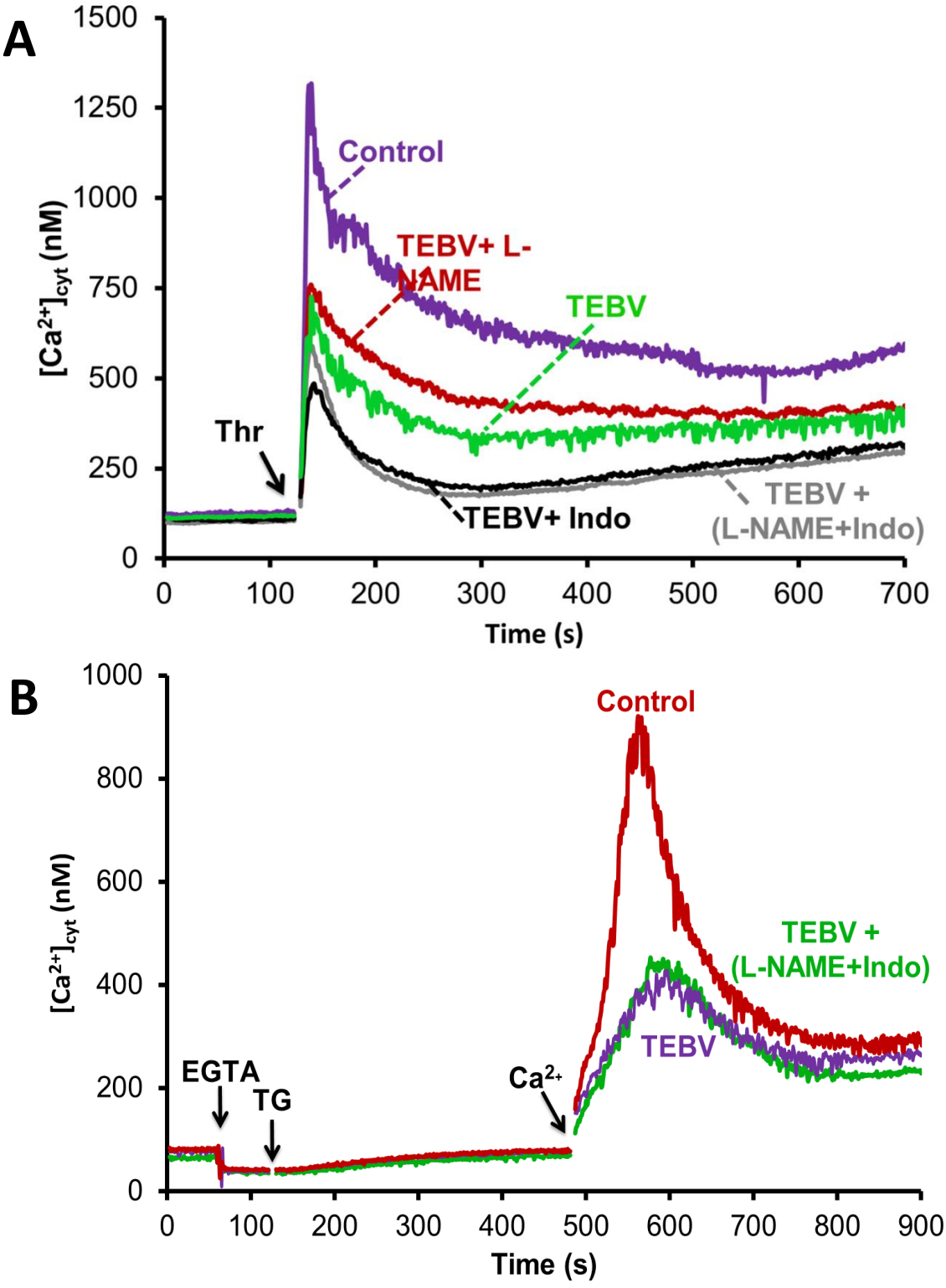

Figure 4.12 – Cytosolic calcium concentration $[Ca^{2+}]_{cyt}$ measurement in platelet suspension exposed to tissue-engineered blood vessel constructs with and without L-NAME and Indomethacin. Fura-2 loaded human platelets suspension was incubated in contact with hydrogel alone and TEBV constructs with and without L-NAME (1 mM) and Indomethacin (300 µM) for 15 minutes at 37˚C off-screen. The constructs were then removed and the remaining suspension was stimulated with 0.2 U/mL thrombin (A) and Ca^{2+} (B). EGTA (1 mM) was added 60 s after the start of recording, followed by 1 µM thapsigargin (TG) prior to 1 mM Ca^{2+} addition. Results are representative of 3 experiments. Thr, thrombin; L-NAME, NG-nitro-L-arginine methyl ester; Indo, indomethacin.

3.9.1.3 The TEBV releases a non-PGI_2, non-NO inhibitor of platelet activation

The previous results suggest that a non-classical inhibitor of platelets is produced by the TEBV. However, to confirm this finding it was important to rule out unexpected pharmacological issues. In particular, L-NAME is a reversible inhibitor of NOS – therefore transfer of the TEBV into a platelet solution without L-NAME may allow the re-establishment of NO production during the incubation. In addition, there was a previous publication describing L-NAME as an inactive pro-drug (Pfeiffer et al., 1996). Therefore, it is possible that our pharmacological interventions were not successful in preventing NO production. Hence, experiments were performed to assess if the use of a cocktail of a competitive inhibitor of NOS, L-NMMA, and an irreversible inhibitor, L-NIO, could reverse this effect. As shown in Figure 4.13A, platelets exposed to the untreated TEBV sample show a significant inhibition of thrombin-evoked rise in $[Ca^{2+}]_{cyt}$ compared to the collagen hydrogel (24.0 ± 11.3% of control; n = 8; *P < 0.05)*. Pretreatment of the TEBV with high concentrations of both L-NIO and L-NMMA still maintained a significant platelet inhibition (33.8 ±4.5% of control; n=6; *P < 0.05).* However, this showed a significant difference compared with the untreated TEBV construct (172.5 ±39.5% of control; n=6; *P < 0.05)*. This suggests that a partial reversal of the TEBV mediated inhibition can be achieved by the NOS inhibitors L-NMMA and L-NIO.

Indomethacin is considered to be a relatively non-selective inhibitor of COX-1 and COX-2, however there is a greater potency for COX-1 (Mitchell et al., 1993). Although controversial, there is some evidence that COX-2 may be an important mediator of PGI_2 production in humans (McAdam et al., 1999). Therefore, we considered whether remnant COX-2 activity might be responsible for this inhibitory effect. To confirm the presence of a non-PGI_2, non-NO inhibitor of platelet activation we therefore pre-treated our construct with a cocktail of inhibitors of PGI_2 and NO production including NS398, a selective COX-2 inhibitor. The TEBV constructs were preincubated with (L-NMMA, L-NIO, NS398 and Indomethacin for 1 hour at 37°C. The sample was then washed and incubated with washed platelets for 15 minutes. The construct was removed and the $[Ca^{2+}]_{cyt}$ was measured from the remaining platelet suspension. As shown in Figure 4.15B, platelets exposed to the untreated

TEBV sample show a significant inhibition of thrombin-evoked rise in $[Ca^{2+}]_{cyt}$ compared to the collagen hydrogel (20.6 ±6.2% of control; n=6; *P < 0.05).* When all four inhibitors collectively, L-NMMA, L-NIO hydrochloride, NS398 and Indomethacin, thrombin-evoked rises in $[Ca^{2+}]_{cyt}$ were still inhibited to 25.6 ±3.6% of control (n = 6; *P < 0.05)*. These data indicated that the inhibitory effects of TEBV are mediated at least in part by a non-NO, non-PGI_2 inhibitor of platelet function.

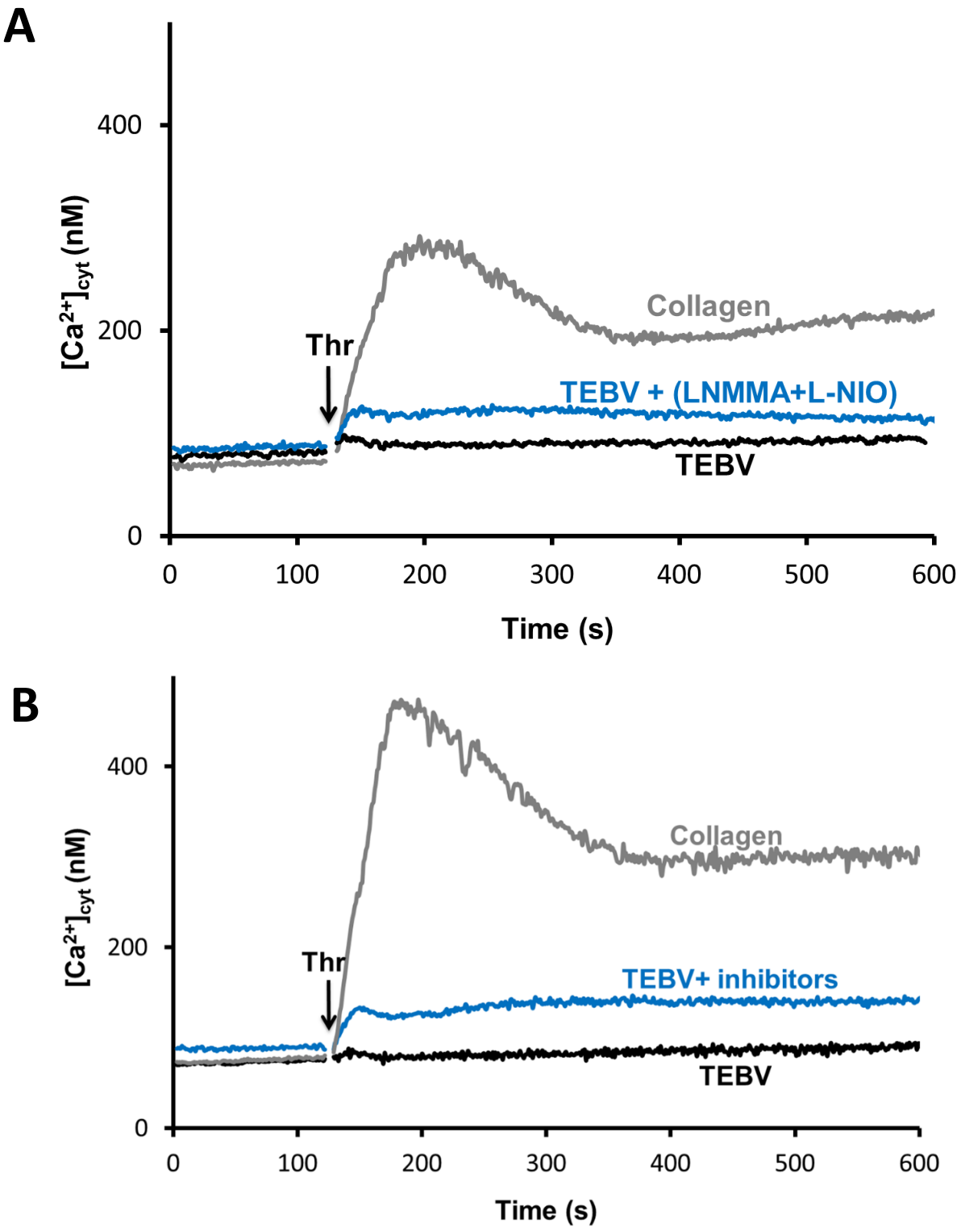

Figure 4.13 – Cytosolic calcium concentration $[Ca^{2+}]_{cyt}$ in platelet suspension exposed to tissue-engineered blood vessel constructs with and without a combination of NO synthase and PGI_2 inhibitors. Fura-2 loaded human platelets suspension was incubated in contact with hydrogel alone and TEBV constructs with and without (L-NMMA, L-NIO hydrochloride , ndomethacin and NS398) for 15 minutes at 37˚C off-screen. A) TEBV samples incubated with L-NMMA and L-NIO hydrochloride; B) TEBV samples incubated with L-NMMA, L-NIO hydrochloride, Indomethacin and NS398. The constructs were then removed and the remaining suspension was stimulated with thrombin (0.2 U/mL). Results are representative of 4 experiments. L-NMMA, N^G-Monomethyl-L-arginine, monoacetate salt; L-NIO, L-N^5-(1-Iminoethyl)ornithine; NS-398, N-[2-(Cyclohexyloxy)-4-nitrophenyl]methanesulfonamide.

3.9.2 Assessing the effect of inflammatory endothelial cell phenotype using induced by TNF-α

3.9.2.1 Platelet adhesion

In addition to haemostatic responses to the damaged endothelium, platelets are also known to modulate their function in response to inflammatory stimuli (Gawaz et al., 2005). To assess if triggering an inflammatory response alters platelet function in response to the TEBV, experiments were performed to examine the effect of inducing an inflammatory phenotype of our TEBV by treating it with TNF-α. Previous studies have shown that TNF-α induces changes in endothelial cell functions to change into a procoagulant phenotype, which in turn stimulates platelets adhesion and activation (Kirchhofer et al., 1994; Pircher et al., 2012; Wagner and Frenette, 2008). In addition, activated endothelial cells contract, increasing the distance between endothelial cells which increases the blood vessel permeability (Morgan BL, 2013). Activated endothelial cells also express proteins onto their surface that are adhesive such as ICAM-1. Therefore it would be expected that exogenous application of TNF-α might increase platelet adhesion to the TEBV, as well as sensitize platelets in the underlying suspensions (van Buul et al., 2010).

TNFα-treated TEBV was generated to study how platelets would react to an inflamed HUVECs. In this experiment, $DiOC_6$-labelled platelets were incubated with TEBV for 15 minutes at 37°C with continuous magnetic stirring. Figure 4.14 shows HUVECs monolayer, TEIL and TEBV constructs treated with two different concentrations of TNF-α, 100 and 1000 U/mL. The baseline image shows individually scattered discoid shaped platelets around the sample. Alternatively, the HUVECs monolayer shows ubiquitous platelet aggregation regardless of TNF-α treatment and concentration. Untreated TEIL sample shows no platelet aggregates on its surface after incubation, however a large number of aggregates are observed on TEIL samples treated with high and low concentrations of TNF-α. A similar observation can be made on the TEBV sample except that there are less platelets aggregates on the low TNF-α treated TEBV construct. These findings confirm that TNF-α increases platelet aggregation on the surface of TEIL and TEBV constructs.

3.9.2.2 Measurement of $[Ca^{2+}]_{cyt}$ of platelets exposed to TNFα treated TEBVs

To further assess whether the induction of an inflammatory phenotype in our HUVECs alters platelet activation, experiments were performed to assess if this treatment altered the ability of our TEBVs to modulate platelet Ca^{2+} signals. Fura-2-loaded platelet samples were pre-incubated with TEBV constructs treated either with or without 1000 U/mL TNF-α (Figure 4.15). No difference could be observed in the $[Ca^{2+}]_{cyt}$ in the treated and untreated TEBV constructs when they were incubated with Fura-2-loaded human platelet suspension for 15 minutes on-screen. Following this incubation period, the TEBV constructs were removed and the remaining platelet suspension was stimulated with 0.2 U/mL thrombin. Although there was a tendency to slightly increased thrombin-evoked rises in $[Ca^{2+}]_{cyt}$ in platelets exposed to the TNF-α-treated samples, the difference was found to be not statistically significant (98.3 ±19.5 % of control; n = 6; $P > 0.05$). These data highlight that although TNF-α influences platelet adhesion to the endothelial lining of our TEBV, it does not significantly affect either its ability to directly or indirectly influence platelet function in the underlying platelet suspension. Further studies will need to examine if other inflammatory stimuli can independently alter the effect of our TEBV on platelets either alone or in synergy with TNF-α.

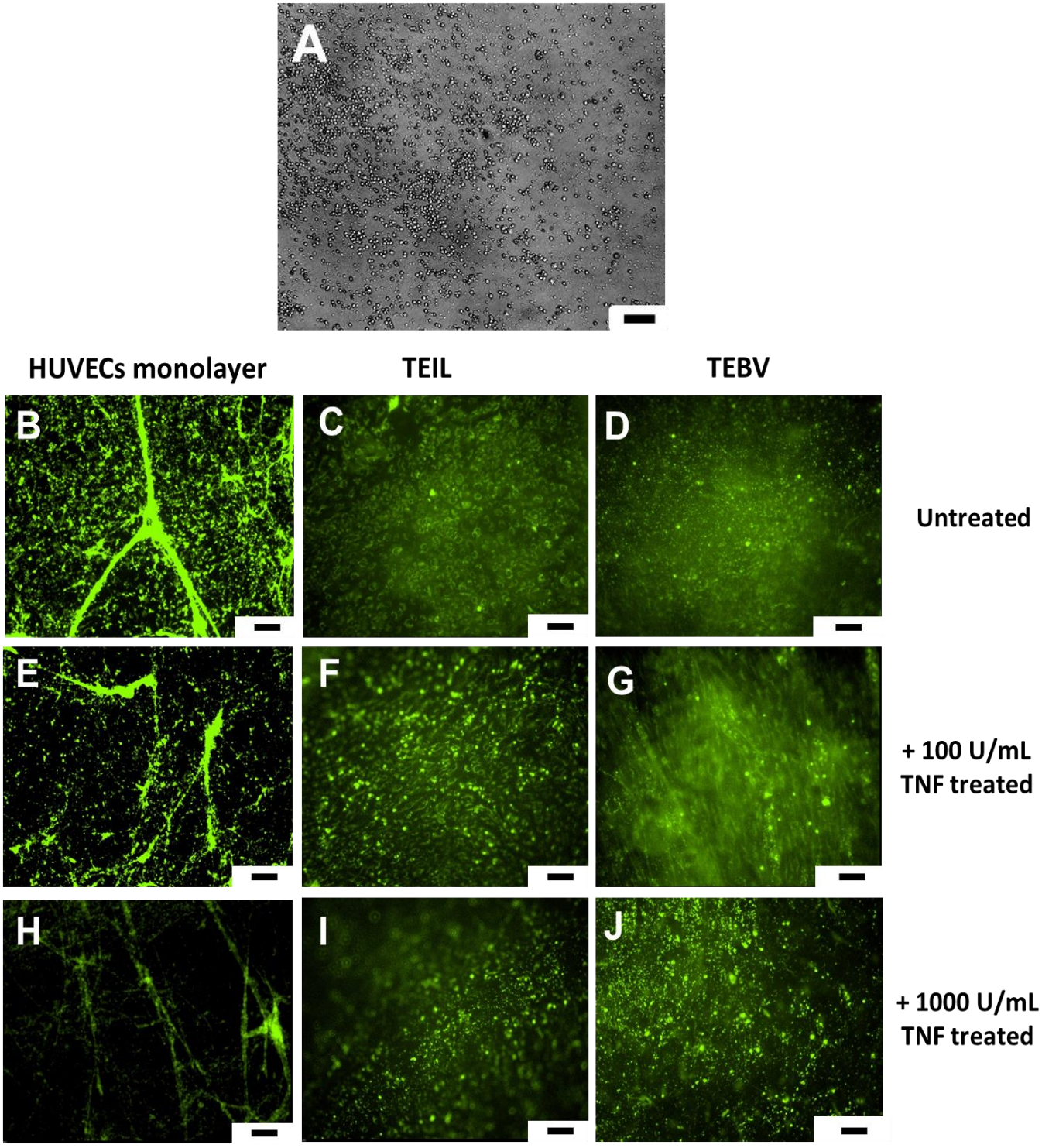

Figure 4.14 – Fluorescence images of TNF-α treated TEIL and TEBV constructs after exposure to platelets. $DiOC_6$ labelled-human platelets suspension was incubated with HUVECs monolayer (B, E, H) or TEIL (C, F, I) or TEBV (D, G, J) for 15 minutes at 37˚C with gentle agitation of samples. TNF-α was used at two different concentration 100 U/mL (E-G) and 1000 U/mL (H-J). A brightfield baseline (A) and untreated samples (B-D)-were imaged for comparison. Platelet aggregation was recorded, after the samples were washed with HBS. Results presented are representative of 4 experiments. Scale bar = 100 µm.

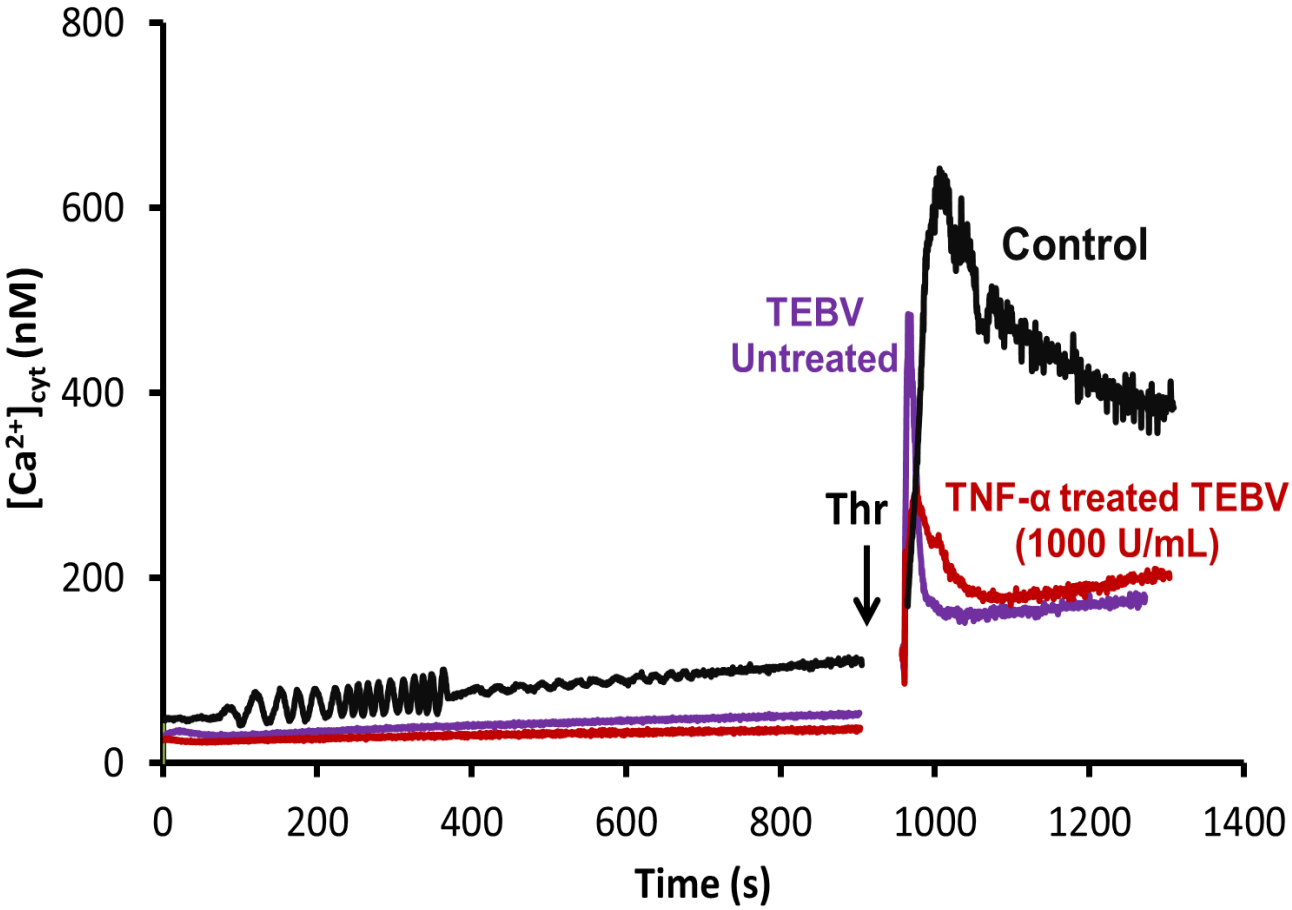

Figure 4.15 – Cytosolic calcium concentration of platelet suspension exposed to tissue-engineered blood vessel constructs treated and untreated with TNF-α. Fura-2 loaded human platelets suspension was incubated in contact with TEBV constructs with and without TNFα (1000 U/mL) for 15 minutes at 37˚C. The constructs were then removed and the remaining suspension was stimulated with thrombin (0.2 U/mL). Thr, thrombin.

4. Discussion

Physiologically, the endothelial cell layer acts as an inhibitor of blood clotting through preventing platelet interaction with the pro-thrombotic subendothelial matrix as well as producing and secreting a variety of anti-thrombotic molecules (e.g. NO, PGI_2 and Protein C). Therefore, to create a functional replica of the human blood vessel, the intimal layer of the construct should possess an appropriate anti-aggregatory property by both acting as a physical barrier to platelet interaction with the subendothelium, as well as via its secretion of paracrine inhibitors of platelet function. In contrast, the medial layer of our construct in the absence of the endothelial lining should be able to replicate the pro-aggregatory properties found *in vivo*.

In this chapter, experiments were performed to assess the pro- and anti-aggregatory factors arising from the fabricated tissue engineered constructs. By assessing platelet reactivity to the fabricated tissue-engineered constructs it was possible to validate the functionality of each layer. The pro- and anti-thrombotic properties of each of the blood vessel constructs have been assessed using the novel protocol established in chapter 3. These studies have demonstrated the similarity of these constructs to the equivalent structures found in native blood vessel, with the endothelial lining of the TEIL and TEBV found to strongly inhibit platelet activation, whilst the TEML was able to trigger platelet activation independent of further stimulation as well as potentiate thrombin-evoked Ca^{2+} signals. As far as we know, this is the first time that the strong pro-thrombotic effect from underlying neo-collagen can be demonstrated to be completely suppressed by the presence of an endothelial layer in a 3D human blood vessel model.

Platelet aggregometry is the most widely-used assay utilised for assessing platelet function in both research and clinical laboratories. Here we have used this technique to validate the results of our Ca^{2+} signalling studies. One of the notable results in this experiment is the basal absorbance of platelets exposed to TEML constructs is lower than that seen in collagen hydrogels prior to

thrombin stimulation. This indicates that some of the platelets has already aggregated in response to TEML exposure. Platelets exposed to the TEBV sample showed an initial higher absorbance with less light passing through the sample during the experiment. These opposing effects caused by TEML and TEBV, respectively reveals the expected ability of the TEML and TEBV to both activate or inhibit platelet function, consistent with the known physiological functions of the medial layer and intact blood vessel. Similar results were also observed using LTA, thus confirming this result through this well-established technique. As well as providing data on platelet aggregation, LTA is also able to monitor the initial discoid-to-sphere shape change as an initial rise in absorbance after agonist stimulation. Platelets exposed to the TEML constructs prior to observation in LTA do not show shape change after thrombin stimulation. This likely due to the pre-activation of these cells, by the neo-collagen in the TEML construct during the incubation period. In contrast, platelets exposed to the TEBV construct shows a prolonged shape change phase which only slowly turns into fully-fledged platelet activation indicative of the significant inhibitory effect of the TEBV on platelet activation. These findings are further confirmed by the data from our luciferin-luciferase-based assay of platelet dense granule which demonstrate that the TEML is able to trigger ATP secretion without further thrombin stimulation, whilst the TEBV is able to significantly inhibit thrombin-evoked ATP secretion.

The above data therefore all demonstrate the TEML and TEBV fulfil their physiological function as pro- and anti-thrombotic layers of the blood vessel. Further assessment of the pro-aggregatory potential of the TEML demonstrated that this was not due to the secretion of a soluble ligand but was instead associated with the laying down of a pericellular matrix of type I and III collagen to increase the thrombogenicity of the collagen hydrogel. It is well-established that cultured smooth muscle cells are able to produce and secrete both type I and III collagens (Hospers et al., 1996; Rocnik et al., 1998), which are key mediators of thrombus formation *in vivo* (Jung et al., 2012). Therefore, this was shown using SEM and confocal reflective images of TEML constructs verifying the generation of a solid form neo-collagen agonist that are possibly responsible for platelet

aggregation (Figures 4.6 and 4.8). These collagens represent the major collagen isoforms found physiologically within the native blood vessel (Lodish et al., 2000). Further analysis will be required to assess if other extracellular matrix components, such as elastin, can also be discovered to be synthesised by these cells. This work therefore suggests that alteration of the culture conditions of the TEML may further enhance the thrombogenicity of this layer – further research will be required to assess if the optimal culture conditions are being used.

The anti-aggregatory properties of our TEBV are likely related to the ability of the HUVECs to secrete paracrine inhibitors of human platelet function. The vascular endothelium secretes NO, which protects the vessel wall by inhibiting platelet aggregation, secretion and adhesion (Bredt and Snyder, 1994). Endothelial cells also produce PGI_2 which acts synergistically with NO in inhibiting platelet activation and opposing the pro-aggregatory properties of thromboxane A_2. Therefore, experiments were performed to assess if blocking the production of these paracrine regulators of platelet function could mitigate the significant inhibitory effects of our constructs on platelet function.

Although two different concentrations of L-NAME were used in an attempt to reverse the HUVECs inhibitory activity, both experiments were not able to demonstrate a reproducible ability to reduce the inhibitory effect of the TEBV on the platelet suspensions. This might be caused by two factors which relate to the actual drug itself or due to preparation or handling of the drug. It has been reported that L-NAME is an inactive prodrug which only inhibits the NOS enzyme following its hydrolysis to the free acid NG-nitro-L-arginine (L-NOARG) (Pfeiffer et al., 1996). If dissolved in buffer at physiological pH, L-NAME was non-enzymatically hydrolysed to LNOARG with a half-life of 6 hours at room temperature (Pfeiffer et al., 1996).The enzyme kinetic characterization of the inhibition of eNOS by L-NOARG revealed a reversible inactivation of the enzyme (Mayer et al., 1993). Therefore, it is possible that L-NAME was in an inactive form during the experiment. L-NAME

has also been shown to have a direct effect on platelets that will interfere with platelets ability to aggregate due to blocking platelet NOS enzyme (Banerjee et al., 2014). As L-NAME treated TEBV samples were washed prior to incubation with platelets to ensure cell culture media or L-NAME was not transferred into the platelet suspension, this may have caused the reversal of NOS inhibition by L-NAME. This could significantly confound our analysis, so alternative methods to inhibit NOS were investigated. The use of irreversible inhibitors of NOS, L-NMMA and the potent NOS inhibitor, L-NIO, did partially reverse the inhibitory effect of the TEBV on platelets exposed to it. However, when these NOS inhibitors were combined with PGI_2 synthesis inhibitors (Indomethacin and NS398), the inhibitory effect mediated by TEBV construct on platelets was apparently lost.

Although a minor reversal of HUVECs inhibition of platelet was achieved, there is a still a signification inhibition of platelet function mediated by TEBVs treated with the cocktail of inhibitors. This suggests that there are other mechanisms that may also be working to block platelet function in a non-NO-, non-PGI_2-dependent manner. One possible mechanism is EC-mediated production of 14,15-epoxyeicodatrienoic acid which has previously been shown to inhibit platelet aggregation (Heizer et al., 1991). Other possible methods may also involve adenosine production by the ecto-adenosine diphosphatase (ADPase) found in the plasma membrane of ECs. Its anti-platelet effect occurs via metabolising ADP, which is a potent stimulator of platelet aggregation, into the potent platelet inhibitor, adenosine (Marcus et al., 2005). This molecule is known to indirectly inhibit platelets aggregation in a manner distinct from NO and PGI_2. However further experiments will need to be conducted to understand and rule out the remaining platelet inhibition elicited by our NOS- and COX-inhibited TEBVs.

4.1. Conclusion

In summary, we have shown that the endothelial lining of the previously fabricated TEBV construct possess an anti-aggregatory characteristic. Investigation of these anti-aggregatory mediators using

NO and PGI_2 inhibitors revealed that additional mechanisms may also be responsible for mediating the inhibitory effect of our constructs on platelet function. In contrast, the previously fabricated TEML construct was shown to provoke a pro-aggregatory appearance on the surface of the construct caused by the neo-collagen generated by HCASMCs within the constructs. These results therefore suggest that our constructs possess anti- and pro-aggregatory properties of native blood vessels, however the molecular mechanisms by which the anti-aggregatory properties of our TEBV are produced may still be distinct. Therefore, further experiments will be required to investigate how this is elicited, and to characterise the efficacy of this mediator in the ability of native blood vessels to inhibit platelet function.

Chapter 5

Using tissue-engineered blood vessel constructs to recreate a ferric chloride arterial thrombosis model *in vitro*

1. Introduction

Ferric chloride ($FeCl_3$) induced vascular injury is the most commonly used *in vivo* model of arterial thrombosis (Bonnard and Hagemeyer, 2015). In this model, $FeCl_3$ is applied to the outer surface of an intact vessel, triggering vascular wall injury and denudation of the endothelium (W. Li et al., 2010). $FeCl_3$ causes vascular damage through triggering the generation of free radicals, which leads to lipid peroxidation and destruction of endothelial cells. This in turn triggers activation of circulating platelets and components of the coagulation cascade, which can then be monitored by intravital microscopy (Chen et al., 2011). This model has most commonly been performed on carotid and femoral arteries and venules in mice and rats, although other species such as guinea pigs and rabbits have also been used (Bonnard and Hagemeyer, 2015; Kurz et al., 1990; W. Li et al., 2013). However, $FeCl_3$ is not the only injury model with other methods of inducing vascular injuries have also been used to trigger arterial thrombosis, such as those triggered by laser, photochemical damage or mechanical abrasion (Rosen et al., 2001).

Although the application of these models in mice has significantly furthered our understanding of how thrombus and thrombosis formation may occur *in vivo*, there are potential limitations that could affect the interpretation of the data obtained. The first of which is the difference in clotting response seen between different injury models. For example, thrombosis in $FeCl_3$ model being primarily dependent upon collagen signalling, whereas the laser injury model relies mostly on thrombin signalling (Furie and Furie, 2007). In addition, the $FeCl_3$ model leads to variable clotting responses between labs, such that better standardisation of this technique is required to help ensure reproducibility (Owens et al., 2011). For example, the time from injury to complete vessel occlusion can range from 5 and 30 minutes after the $FeCl_3$ application in different studies in mice. Analysis of these data have suggested that there are number of variables that may account for the difference in the thrombotic response observed in this model such as $FeCl_3$ concentration applied, method of anaesthesia, surgical technique, mouse age and genomic background, method of

measuring blood flow, as well as other environmental variables (W. Li et al., 2013). In addition, the effects of $FeCl_3$ vary based on the vessel to which it is applied. For example, in a study in mice lacking the extracellular domain of glycoprotein Ibα (GPIbα), the $FeCl_3$ injury model results in occlusion of mesenteric venules but not in the carotid artery (Ciciliano et al., 2015). This wide variability makes it very difficult to compare studies from different groups and may make detection of subtle differences difficult.

Furthermore, given there is significant variation in these arterial thrombosis models observed between different mice strains (Westrick et al., 2007), there must be a question raised over whether results obtained from these animal models are indicative of the response seen in humans. Whilst there are similarities in the basis haemostatic processes between mice and human, there are also a number of differences including variations in blood haemodynamics (Weinberg & Ross Ethier, 2007), as well as differences in the mRNA and protein expression between human and mice platelets (Janssen et al., 2004). These factors should be considered before attempting to apply results obtained from *in vivo* mouse models to human clotting pathways. Therefore, an *ex vivo* human arterial thrombosis model is required to complement the work performed *in vivo* models to better understand mechanisms of *in vivo* in thrombus formation in humans.

Lastly, these *in vivo* experiments require the use of general anaesthesia which could interfere with the normal clotting responses observed. A previous survey of investigators performing intravital microscopy found that ketamine, xylazine and pentobarbital are the most common anaesthetics used to undertake the surgery (Janssen et al., 2004). However other studies have demonstrated that each of these anaesthetics can have an inhibitory effect on platelet function (Chang et al., 2004; Janssen et al., 2004; Nakagawa et al., 2002; Undar et al., 2004). Previous studies have reported that ketamine inhibited platelet aggregation through suppression of IP_3 formation (Nakagawa et al., 2002) as well as by inhibiting thromboxane synthase activity (Atkinson et al., 1985). Further research has also shown that ketamine can also interfere with endothelial NO

production (Ogawa et al., 2001), as well as smooth muscle Ca^{2+} signalling (Akata et al., 2001), thus suggesting this drug could have multifactorial effects on the normal biology of blood vessels. Therefore, the potential ability to conduct an *ex vivo* assessment of whether inclusion of general anaesthetics with ketamine might artificially alter the types of thrombotic response *in vivo*. If this is found, it may question the potential physiological relevance of studies on the effectiveness of drugs and platelet-specific gene knockouts on normal haemostatic responses. Hence, this chapter aims to establish an alternative to intravital microscopy using ferric chloride and assess the effect of ketamine anaesthetic on the TEBV responses to platelets.

2. Methods

2.1. TEML and TEBV constructs fabrication for spectrophotometer-based experiments

To prepare TEML constructs, HCASMCs were mixed at a density of 5 x 10^5/mL into a neutralised solution of 3 mg/mL type I collagen obtained from BD biosciences, according to the manufacturer's protocol. 0.2 mL of the mixture was then loaded onto a 1 cm^2 square shaped filter paper frame, and the collagen-cell mixture was left to set for 40 minutes at 37˚C, 5% CO_2. The formed gel was then covered with supplemented medium and with changing the media every 2 days. HCASMCs were subsequently allowed to grow in the TEML until they were observed to possess an elongated spindle-shaped morphology for up to 10 days.

TEBV construct was fabricated by placing a PLA nanofiber mesh coated with a 10 ng/mL fibronectin solution on the 3D TEML, to create the initial layer of the luminal surface. After successful attachment of the nanofibers to the TEML hydrogel, 4 x $10^4/cm^2$ of HUVECs were then seeded on top of the nanofibers to create a full TEBV construct. The TEBV constructed was covered with supplemented medium 200 and medium 231 (7:3) and with changing the media every 2 days. The TEBV construct was cultured for further 4 days after HUVECs attachment.

2.2 Platelet preparation

Human platelets obtained using the standard method of extraction described in chapter 3, however platelets were labelled with $DiOC_6$ to allow us to examine platelet adhesion and aggregation on the surface of the construct aggregation when exposed to the tissue-engineered blood vessel construct both under static or flow conditions. Blood was obtained by venepuncture from healthy volunteers who had given informed written consent. 5 mL of blood was mixed with 1 mL ACD anticoagulant (85 mM sodium citrate, 78 mM citric acid and 111 mM d-glucose). The ACD contained $DiOC_6$ to provide a final concentration of 1 µM. The blood was mixed with anticoagulant and dye, and left to incubate for 10 minutes at room. PRP was then obtained by centrifuging at 1500 g for 8 minutes. The collected PRP was then treated with 100 µM aspirin and 0.1 U/mL apyrase. In some

experiments, the samples were labelled with Fura-2 by preincubating the PRP with 2.5 µM Fura-2/AM for 45 minutes at 37°C. The PRP was then washed by centrifugation at 350 g for 20 minutes. The collected platelet pellet was then re-suspended into supplemented HEPES –Buffered Saline (HBS) to a final cell density of $2x10^8$ cells/mL. To make supplemented HBS, HBS (pH 7.4, 145 mM NaCl, 10 mM HEPES, 10 mM d-glucose, 5 mM KCl, 1 mM $MgSO_4$), was supplemented on the day of the experiments with 1 mg/mL Bsa, 10 mM glucose, 0.1 U/mL apyrase and 200 µM $CaCl_2$ (supplemented HBS). $CaCl_2$ concentration of the supplemented HBS was adjusted to 1 mM prior to individual sample analysis.

2.3 Ferric chloride model

2.3.1 Measurement of platelets' cytosolic Ca^{2+} concentration ($[Ca^{2+}]_{cyt}$) exposed to $FeCl_3$ induced TEBV and TEML constructs

TEBV and TEML constructs were pre-incubated with a piece of filter paper (0.25 cm^2) saturated with 10% ferric chloride solution and placed directly on the basal side of the constructs for 5 minutes, and following the removal of the medium (Figure 5.1). The filter paper was removed and the construct was washed three times with HEPES-buffered saline to remove excess ferric chloride solution. The $FeCl_3$-damaged or undamaged (exposed to HBS treated filter paper) constructs were placed in the sample holder developed in chapter 3, and then exposed to 1.2 mL of Fura-2 and $DiOC_6$-labelled human washed platelets under continuous magnetic stirring for 15 minutes at 37˚C. Each construct was treated just prior to incubation with platelets. The constructs were then removed and the fluorescence of platelets were continuously monitored using Cairn Research Spectrophotometer (Cairn Research, UK), using excitation wavelengths of 340 and 380 nm, and emission of 515 nm. Platelets were monitored for 1 minute followed by stimulation with 0.2 U/mL thrombin and observed for a further 4 minutes. Changes in $[Ca^{2+}]_{cyt}$ were calculated using the 340/380 nm fluorescence ratio and calibrated as previously described in chapter 3. Thrombin-evoked changes in $[Ca^{2+}]_{cyt}$ were quantified by integration of the change in fluorescence records

from the point of thrombin stimulation with a total recording of 5 minutes, including baseline measurement.

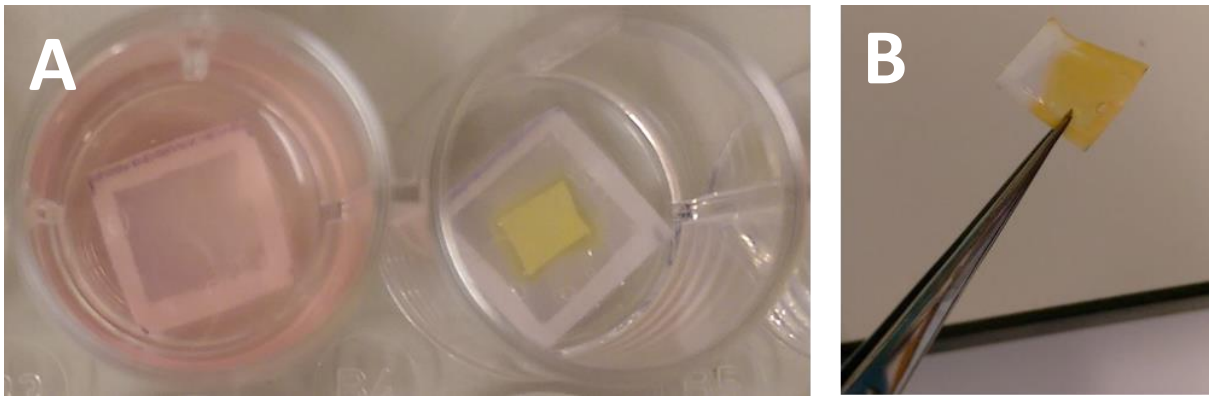

Figure 5.1 Optical images showing ferric chloride incubation with TEBV construct. A) The cell culture plate was taken out of the incubator and the media was removed. The construct was overturned and a filter paper saturated with 10% $FeCl_3$ was applied onto the basal side of the TEBV construct for 5 minutes. B) TEBV construct after applying $FeCl_3$ and washing three-times with HBS.

2.4 Perfusion system

A Watson-Marlow 505 series peristatic pump (Fluid technology, UK) was used for the perfusion assay to pump the labelled human platelet suspension through a PFC-1Proflow Chamber (Warner instruments, USA). A reservoir containing $DiOC_6$-labelled platelets was connected with the inlet of the parallel plate flow chamber via a polyethene (PE-90) tubing while the outlet was connected to the peristatic pump (Figure 5.2B). The chamber was assembled per manufacturer's instructions. Specifically, a 15-mm round cover glass and gasket were mounted onto the top plate of the chamber using a vacuum grease. This was followed by mounting a previously casted PDMS gasket with the desired area, in this case a rectangular cavity fitting the construct, to adjust the height of the flow channel. The preparation was left to set overnight and once solidified, the round shaped PDMS was cut into smaller circles of 2.8 cm in diameter, bearing a rectangular cavity shown in Figure 5.2A. In addition, spacers were generated from acetate cellulose with a window in the middle. These were placed inside the gasket cavity, to create a flow channel path of 300 µM depth through

which platelets can flow above the construct. TEML constructs were placed atop of the three spacers and the top and bottom plates were eventually assembled together, sealed with nylon screws. The chamber was put on a fluorescence dissection microscope stage for visualisation.

To prevent platelets adhesion to the perfusion system, prior to the start of experiment, the assembled perfusion system was perfused with 1% BSA solution for 1 hour with exclusion of the construct. In addition, the gasket and the spacers were coated overnight with 1% BSA solution.

2.4.1 Shear stress calculation

For a laminar flow within the perfusion chamber, wall shear stress τw was calculated using the following equation:

$$\tau_w = \frac{6Q\mu}{wh^2}$$

Where Q, refers to the volumetric flow rate; μ, indicates the solution viscosity (1.5Cp) and w and h refers to the width and height of the chamber, respectively. Flow rate was used at 0.077 cm^3/s. The width and height were measured to 5 mm and 30 μm, respectively to yield a shear stress of 15.4 dynes/cm^2.

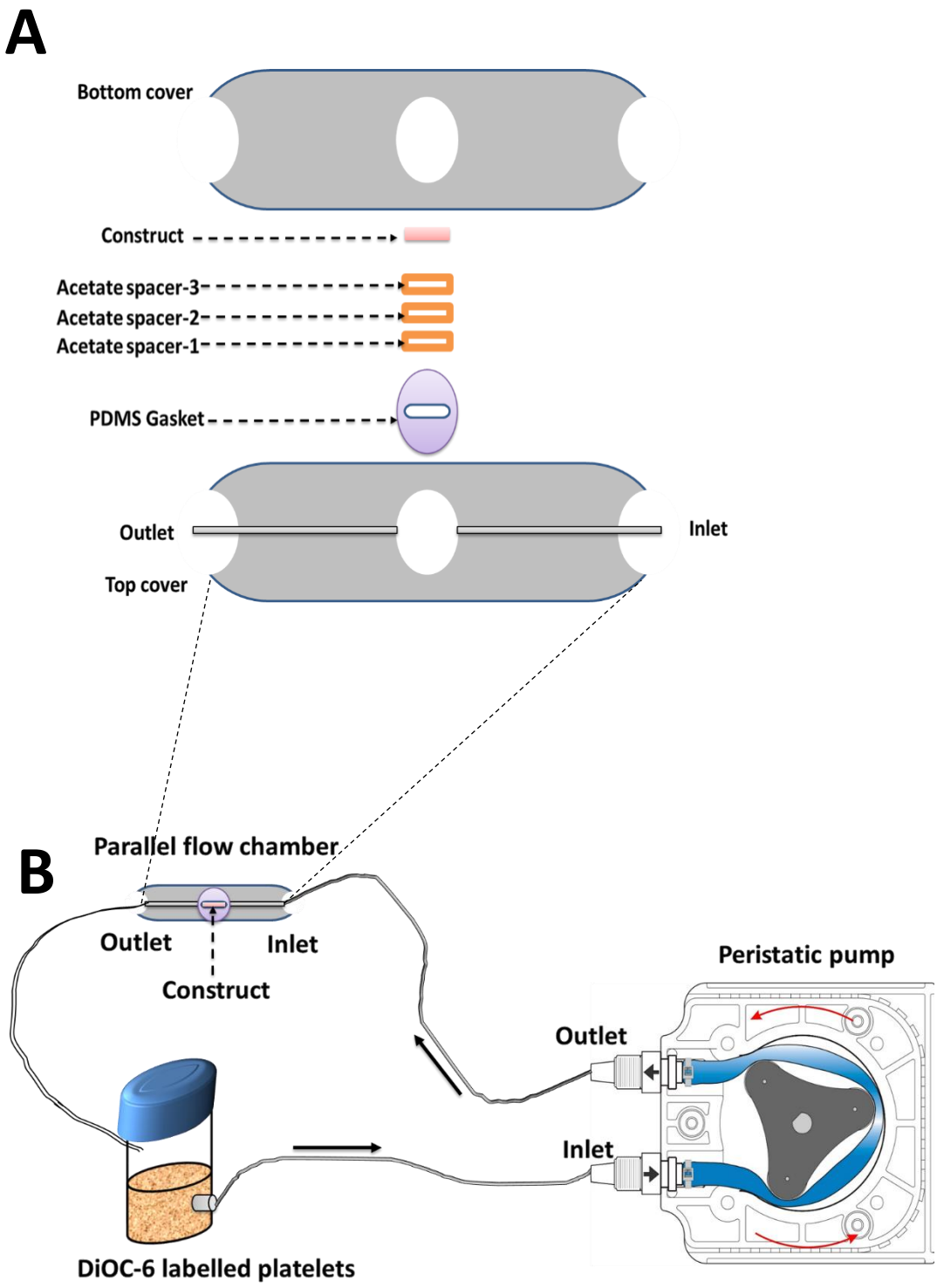

Figure 5.2 Schematic diagram showing perfusion chamber set-up. A) Parallel plate flow chamber assembly using a top and bottom plates with central gap fitting a PDMS gasket, 3x cellulose acetate frame spacers and a TEML construct. B) Perfusion chamber set-up enclosing a parallel plate flow chamber, peristatic pump and platelet suspension reservoir.

2.4.2 Real-time monitoring of $DiOC_6$-labelled platelet adhesion and aggregation on TEML constructs under physiological flow conditions

To avoid unwanted platelet activation, within the perfusion system, a 1% BSA solution was perfused into the system for 1 hour prior to construct inclusion. In addition, the gasket and 3x spacers were all coated with a 1% BSA solution overnight. Prior to the start of the experiment, 1.2 cm^2 TEML constructs were made to fit the perfusion chamber with proportionally adjusting the cell number and collagen volume which was inserted in the sample site in the parallel plate flow chamber. Washed $DiOC_6$-labelled human platelets were treated with either 100 µM ketamine hydrochloride (*P*fizer, USA) or HBS for 1 hour at 37°C, and then loaded into the perfusion system reservoir. Platelets were then perfused over the TEML constructs at a shear stress of 15.4 dynes/cm^2 for 15 minutes. Fluorescence images of platelet adhesion and aggregation were captured using CCD microscope camera (Leica Microsystems) using an excitation wavelength of 485 nm and emission of 501 nm for 0, 7 and 15 minutes.

2.4.3 Development of $FeCl_3$ arterial injury model using the TEBV construct.

To recreate the $FeCl_3$ arterial injury model, TEBV constructs were made to fit the perfusion chamber (1.2 cm^2) with proportionally adjusting the cell number and collagen volume which was inserted in the sample site in the parallel plate flow chamber. TEBV constructs was pre-incubated with a piece of filter paper saturated with 10% [v/v] ferric chloride solution and placed directly on the apical side of the construct for 5 minutes, following the removal of the medium (Similar to the image shown in Figure 5.1, but rectangular in shape). The filter paper was removed and the construct was washed with HEPES-buffered saline to remove the excess ferric chloride. The TEBV construct was assembled into the sample site of the parallel plate flow chamber. $DiOC_6$-labelled platelets were perfused over the damaged TEBV construct. Undamaged TEBV constructs were also perfused for comparison. At the end of perfusion, the TEBV constructs were removed for imaging under the fluorescence microscope. Overall, $FeCl_3$ damaged and undamaged TEBV constructs were imaged using an excitation wavelength of 485 nm and emission of 501 nm at 0, 7 and 15 minutes of perfusion.

2.5 Measurement of platelets' cytosolic Ca^{2+} concentration ($[Ca^{2+}]_{cyt}$) exposed to ketamine treated tissue engineered constructs

2.5.1 TEML constructs

1.7 mL of washed unlabelled human platelet suspension was pipetted into spectrophotometer cuvette and incubated with either 1 mM ketamine hydrochloride or HBS for 15 minutes at 37˚C, during the incubation with the constructs. Ketamine-treated TEML constructs were placed atop of washed platelets treated with ketamine whilst untreated TEML constructs were placed atop untreated platelet samples, using the sample holders previously described in chapter 3. Fluorescence was recorded from stirred aliquots of Fura-2-loaded washed human platelet suspensions in contact with the blood vessel constructs at 37°C using Cairn Research Spectrophotometer (Cairn Research, UK) with excitation of 340 and 380 nm and emission of 515 nm. Changes in $[Ca^{2+}]_{cyt}$ were monitored using the 340/380 nm fluorescence ratio. Data were calibrated using the method of Grykiewicz *et al*., (1986). Agonist-evoked changes in $[Ca^{2+}]_{cyt}$ were quantified by integration of the change in fluorescence records from basal with respect to 15 minutes after agonist addition.

2.5.2 TEBV constructs

TEBV constructs were incubated with ketamine (1 mM) or HBS for 1 hour at 37°C prior to the start of experiment. Solutions were discarded and constructs were washed with HBS. These TEBV samples were matched with corresponding 1 mM ketamine or HBS treated 1.2 mL platelets which were incubated together off-screen for 15 at 37°C. Following the incubation period, the constructs were removed and the remaining platelet suspension was monitored as described above using a spectrophotometer for 5 minutes post 0.2 U/mL thrombin stimulation.

2.6 Platelet aggregometry

Following the incubation period, the constructs were removed and 200 µl of the platelet suspension was transferred into a 96-well plate and then placed into a plate reader prewarmed to 37°C (BioTek Synergy 2 microplate, USA). Baseline absorbance readings were taken once at a wavelength of 600

nm, obtaining an absolute absorbance reading post construct incubation. In the present assay, the plate reader was set-up to use a fast shaking mode between absorbance readings to aid in sample mixing.

2.7 Dense granule secretion assay

Platelets from both ketamine treated and untreated samples, were collected following 15 minutes incubation period as described above. Subsequent to the incubation period, 200 µl of each platelet suspensions were transferred into a 96-well plate and then placed into a plate reader prewarmed to 37°C (BioTek Synergy 2 microplate, USA). ATP secretion from platelet dense granules was assessed by adding 10% [v/v] luciferin-luciferase reagent to the platelet sample. Baseline readings were obtained both prior to and following stimulation with 0.2 U/mL thrombin.

2.8 Statistics

Values stated are mean ± SEM of the number of observations (n) indicated. Analysis of statistical significance was performed using a two-tailed Student's t-test. $P < 0.05$ was considered statistically significant.

3 Results

Ferric chloride has been previously used to create artificial *in vivo* damage to the endothelial lining to induce arterial thrombosis. This effect is caused principally by the generation of free radicals, which triggers damage to the endothelial cells facilitating the exposure of the subendothelial matrix. The results presented in the previous chapters have demonstrated that the TEBV construct can prevent platelet aggregation on the surface of the construct, whilst a TEML construct lacking the endothelial lining can provide a substrate to support thrombus formation. In this chapter, experiments were performed to assess if experimental damage to the TEBV could also support the triggering of platelet activation, and as such provide initial evidence that the blood vessel construct could be used to provide an *ex vivo* human arterial thrombosis model in which to perform similar studies to those currently performed *in vivo*.

To initially examine this, experiments were performed to assess the effect of $FeCl_3$ damage on the anti-aggregatory properties of the TEBV. To do this, we assessed the effect of preincubating Fura-2-loaded platelets with either an untreated, intact TEBV or one damaged by application of $FeCl_3$. Following a 15 minutes incubation, the $FeCl_3$ damage elicited no significant change in the baseline $[Ca^{2+}]_{cyt}$ observed in these samples (89.4 ± 30.4 % of control; *P > 0.05; n = 6*). These data suggest that the presence of undamaged endothelial cells is still able to prevent significant activation of the platelets in suspension.

Following this, platelets were stimulated with thrombin to assess if the anti-aggregatory properties of the $FeCl_3$-damaged TEBV had been diminished. As can be seen in Figure 5.3, treatment of the TEBV with $FeCl_3$elicited a significant increase in thrombin-evoked rise of $[Ca^{2+}]_{cyt}$ in platelets compared with platelets pre-exposed to the undamaged TEBV construct (239.2 ±50.8% of control; *n = 6; P < 0.05*). These data therefore suggested that the anti-aggregatory properties of the TEBV had been diminished by the $FeCl_3$-induced endothelial damage.

To ensure this effect was due to endothelial cell damage and not due to a sensitising effect of the remaining $FeCl_3$ solution leaking into the platelet suspension, the $FeCl_3$ solution was applied using the same method onto a TEML construct. As the TEML lacks an endothelial lining, if the effect of $FeCl_3$ is through its leaching into the platelet suspension, a similar effect should be seen here. As seen in Figure 5.4, there is no significant increase in the baseline $[Ca^{2+}]_{cyt}$ (159.2 ±55.1 % of control; *P > 0.05; n = 3*) or thrombin-evoked rises in $[Ca^{2+}]_{cyt}$ in platelets exposed to $FeCl_3$-treated TEML constructs compared to their untreated controls (74.1 ± 17.6% of control; *n = 3; P > 0.05*). However, as this experiment was only performed 3 times, this may have prevented a significant finding from being observed due to a lack of statistical power. This experiment suggests that the effect of $FeCl_3$ on the TEBV model was due to $FeCl_3$ mediated injury of the endothelial lining. These data therefore indicate that the TEBV may be used to develop an alternative methodology to the *in vivo* $FeCl_3$ arterial thrombosis model.

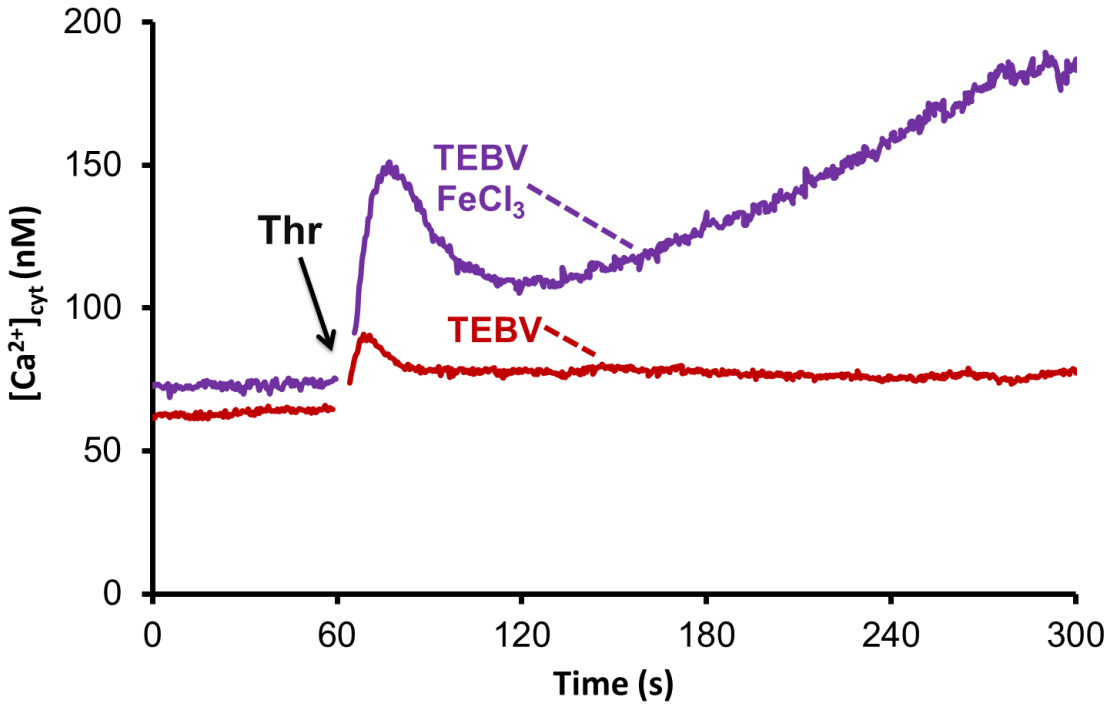

Figure 5.3 – Thrombin-evoked rise of $[Ca^{2+}]_{cyt}$ in platelets pre-exposed to $FeCl_3$ damaged TEBV construct. The tissue-engineered blood vessel construct (TEBV) was pre-incubated with a piece of filter paper saturated with 10% ferric chloride solution and placed directly on the basal side of the construct for 5 minutes. The filter paper was removed and the construct was washed 3x with HEPES-buffered saline to remove the excess ferric chloride. The $FeCl_3$ damaged or undamaged constructs were incubated with 1.2 mL of washed human platelets for 15 minutes at 37˚C. The constructs were then removed and the remaining platelets were exposed to thrombin (Thr) to measure the increase in cytosolic Ca^{2+} concentrations. Results are representative of 3 experiments (n=6).

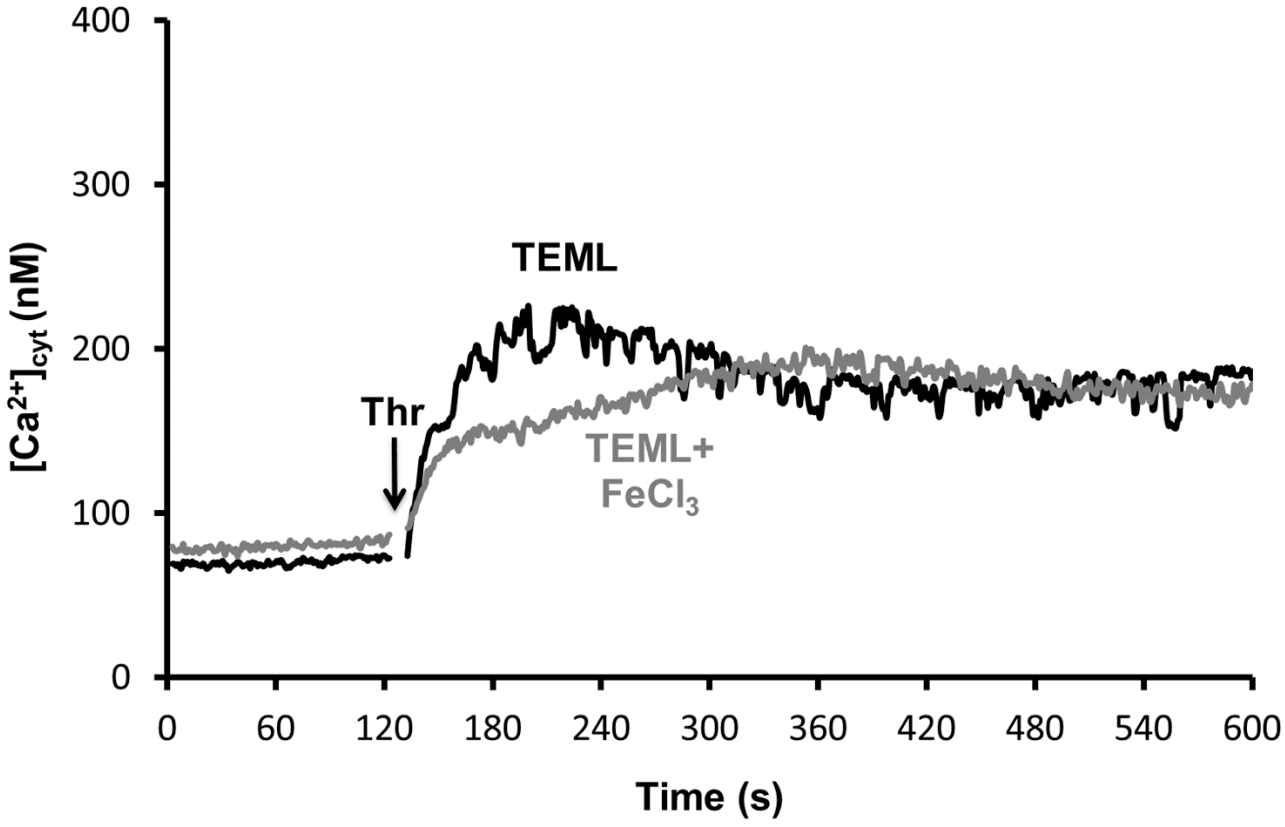

Figure 5.4 – Thrombin-evoked rise of $[Ca^{2+}]_{cyt}$ in platelets pre-exposed to ferric chloride damaged TEML construct. The TEML construct was pre-incubated with a section of filter paper saturated with 10% ferric chloride solution and placed directly on the basal side of the construct for 5 minutes. The filter paper was removed and the construct was washed 3-times with HEPES-buffered saline to remove the excess ferric chloride. The $FeCl_3$ damaged or undamaged TEML constructs were incubated with 1.2 mL of washed human platelets for 15 minutes at 37˚ off-screen. The constructs were then removed and the remaining platelets were exposed to thrombin to measure the increase in cytosolic Ca^{2+} concentrations. Results are representative of 3 experiments (n=3).

3.1 Assessment of Ferric chloride arterial injury model using platelets perfused over TEBV construct at arterial shear stresses

To allow assessment of thrombus formation under dynamic shear stress conditions found *in vivo,* the TEBV constructs were created in an elongated rectangular shape to allow their introduction into a commercially-available parallel plate flow chamber. This allowed labelled platelet suspensions to be perfused over the construct under physiological arterial shear rates – thus allowing us to

recreate the physical environment found *in vivo.* Experiments were performed to examine if application of $FeCl_3$ to the construct could elicit significant thrombus formation when perfused with $DiOC_6$-labelled human platelets under conditions of arterial shear stress for 15 minutes. In an untreated, intact TEBV construct, no platelet adhesion or aggregation on the surface of the construct could be observed (Figure 5.5A). This is consistent with the findings in chapter 4, that demonstrated that anti-aggregatory properties of the TEBV. In contrast, the $FeCl_3$-treateded TEBV construct showed significant platelet aggregation on the surface of the construct after 7 minutes of perfusion, which progressed further over 15 minutes (Figure 5.5B). These data suggest that our construct is able to support platelet aggregation after endothelial cell damage, and as such this provides a suitable system in which to recreate the $FeCl_3$ arterial injury model.

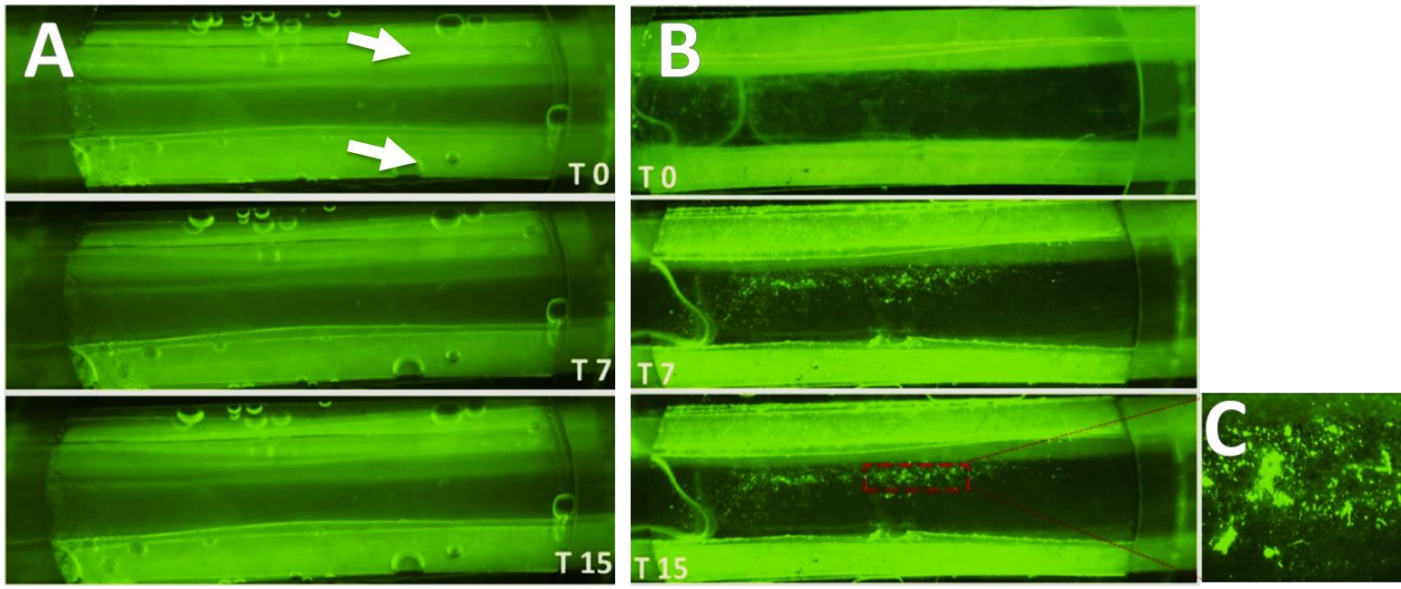

Figure 5.5 – Fluorescent images of perfused platelets aggregation on the surface of intact and $FeCl_3$- treated TEBV constructs under arterial flow conditions. $DiOC_6$-labelled human platelets were perfused over $FeCl_3$ damaged and undamaged endothelial lining of TEBV construct for 15 minutes using a parallel flow chamber at a shear stress (15.4 dynes/cm^2). Fluorescent images were recorded in real-time over the course of 15 minutes of perfusion using fluorescence microscopy. (A) Undamaged TEBV construct exposed to perfused platelets; (B) Lower magnification image of $FeCl_3$ damaged TEBV construct exposed to perfused platelets; (C) A higher magnification image showing surface platelets aggregation. (T0) Beginning of perfusion; (T7) 7 minutes post-perfusion; (T15) 15 minutes post-perfusion. Arrows indicate auto-fluorescent filter paper.

3.2 Ketamine has no significant effect on the anti-aggregatory properties of non-damaged TEBV constructs

Ketamine is commonly used to induce anaesthesia in mice undergoing the $FeCl_3$ arterial thrombosis assay (Denis et al., 2011). However previous studies have demonstrated that ketamine treatment can inhibit endothelial production of NO, contraction of smooth muscle cells and platelet activation (Akata et al., 2001; Chen et al., 2005; Nakagawa et al., 2002; Undar et al., 2004). To assess if the platelet responses in currently used *in vivo* models might be affected by ketamine treatment, experiments were performed to assess if either treatment of platelets or the TEBV could alter the responsiveness of platelets to this construct. Figure 5.6 shows thrombin-evoked changes in $[Ca^{2+}]_{cyt}$ of platelets pre-exposed to TEBV constructs with and without ketamine. Ketamine-treatment of both the TEBV construct and platelets does not provoke a significant effect on the thrombin-evoked rise in $[Ca^{2+}]_{cyt}$ in platelets elicited post-construct incubation compared with the untreated sample (89.3 ± 18.5% of control; *n = 6; p > 0.05*). Treatment of only the TEBV construct with ketamine causes no significant change to the thrombin-evoked rise in $[Ca^{2+}]_{cyt}$ of platelets elicited after incubation with the TEBV construct (124.1 ± 30.9% of control; *n = 6; P > 0.05*). Similarly, ketamine-treated platelets pre-exposed to untreated TEBV construct does not elicit a significant rise in thrombin-evoked changes in $[Ca^{2+}]_{cyt}$ when compared with the untreated sample (104.8 ±25.5% of control; *n = 6; P > 0.05*). All together these results suggest that ketamine does not influence the anti-aggregatory properties of the TEBV construct. It is possible that ketamine has an opposing effect on the EC and SMCs layers. Ketamine may reduce the anti-aggregatory capacity of ECs, but also reduce the pro-aggregatory capacity of SMCs. Although applying ketamine causes platelets inactivation, this makes the two effects cancelling each other with an overall $[Ca^{2+}]_{cyt}$ level similar to the untreated samples.

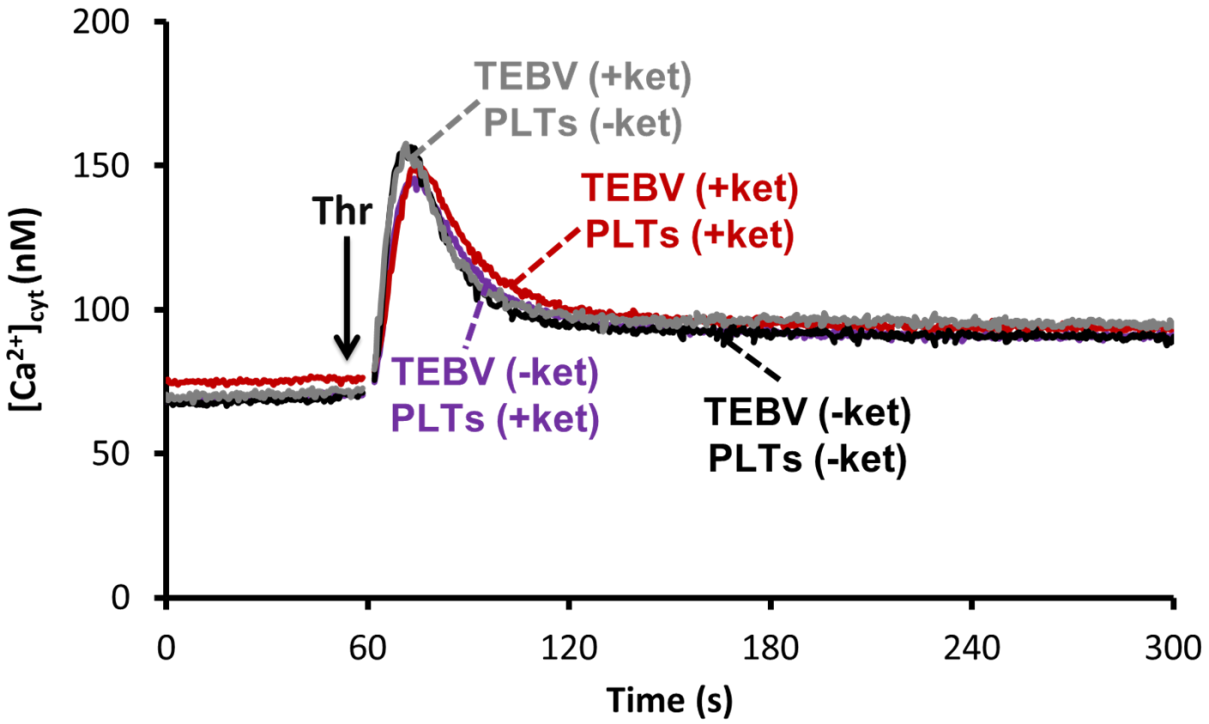

Figure 5.6 – A real-time measurement of the effect of ketamine on cytosolic Ca^{2+} concentration in human platelets pre-incubated with TEBV constructs. Tissue-engineered blood vessel constructs were incubated with and without 1 mM ketamine for 1 hour at 37˚C prior to start of experiment. Platelets were also treated with or without 1 mM ketamine for 15 minutes. Both corresponding TEBV construct and platelet suspensions were incubated together for 15 minutes at 37˚C off-screen, the constructs were removed and the remaining platelets were stimulated with thrombin (0.2 U/mL). Results are representative of 6 experiments.

3.3 Ketamine inhibits the pro-aggregatory properties of the TEML constructs

To investigate if ketamine pre-treatment of platelets or TEML constructs, could interfere with the pro-aggregatory properties of this construct, real-time monitoring of construct- and thrombin-evoked changes in $[Ca^{2+}]_{cyt}$ of platelets pre-incubated with TEML constructs with and without ketamine are shown in Figure 5.7. Prior to TEML construct removal, platelets exposure to TEML constructs did not cause a significant increase in the construct-evoked rise in cytosolic Ca^{2+} concentration compared to ketamine-treated sample. However, following TEML construct removal,

samples in which platelets and the TEML had been preincubated with ketamine were found not to elicit the same rise in $[Ca^{2+}]_{cyt}$ seen in control samples in which neither the platelets or TEML had been exposed to this general anaesthetic (40.2 ± 11.6% of control; *P < 0.05; n = 6*). The control sample did not show a Ca^{2+} rise post-TEML construct addition due to the higher volume of 1.7 mL used in the experiment when compared to the previous chapter where, lower volumes has been used. This may make the propagation of the activation signal insufficient due to the availability of more platelets that need to be stimulated. However, thrombin-evoked rises in $[Ca^{2+}]_{cyt}$ examined following construct removal were not significantly difference between the treated samples compared with the untreated control samples (90.9 ±16.7% of control; n=6; *P > 0.05*).

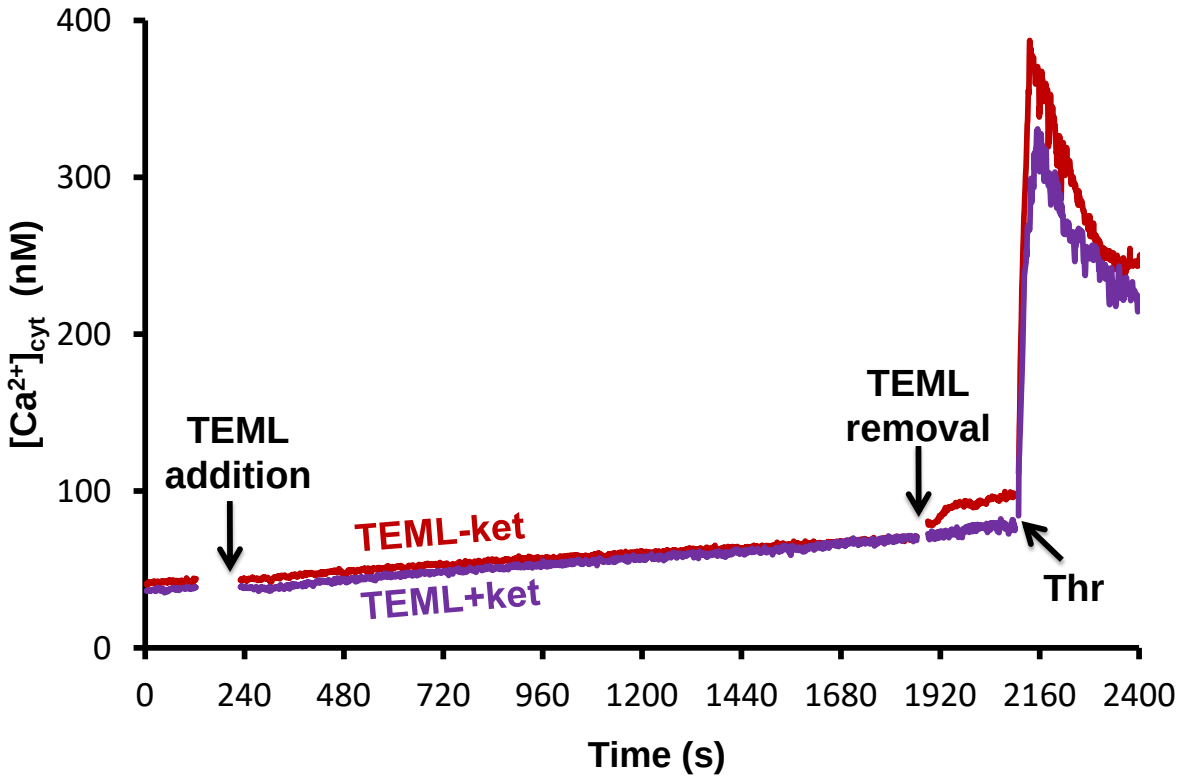

Figure 5.7– A real-time measurement of ketamine effect on the cytosolic Ca^{2+} concentration in human platelets incubated with TEML. Tissue-engineered medial layers were incubated with and without ketamine (1 mM) for 1 hour at 37˚C prior to start of experiment. TEML constructs were incubated with corresponding platelets suspensions with and without ketamine on-screen. After 15 minutes, the TEML constructs were removed and 2 minutes later the remaining platelets were stimulated with thrombin (0.2 U/mL). Results are representative of 3 experiments (n=6).

The failure of ketamine-treated samples to demonstrate a rise in platelet $[Ca^{2+}]_{cyt}$ after TEML construct removal suggests that ketamine may inhibit local signalling events between the platelets in the suspension and the platelets or vascular cells on the surface of the construct. This may be due to ketamine influencing the dense granule secretion of the platelets activated on the surface of the construct. The autocrine signalling molecules released from these platelets upon construct removal could be mixed in the bulk platelet solution upon construct removal – triggering this small Ca^{2+} signal.

To investigate whether ketamine affects platelet's dense granule secretion, ATP release was measured as described previously in chapter 4. The TEML and washed platelets were both either treated with or without ketamine were pre-incubated together for 15 mins at 37°C. Following this, ATP release into the extracellular was measured using the luciferin-luciferase luminescence assay. As shown in Figure 5.8, the ketamine treated samples reduced ATP secretion from platelets granules compared with untreated samples (*P < 0.05)*. These data suggest that ketamine can interfere with TEML-induced dense granules secretion.

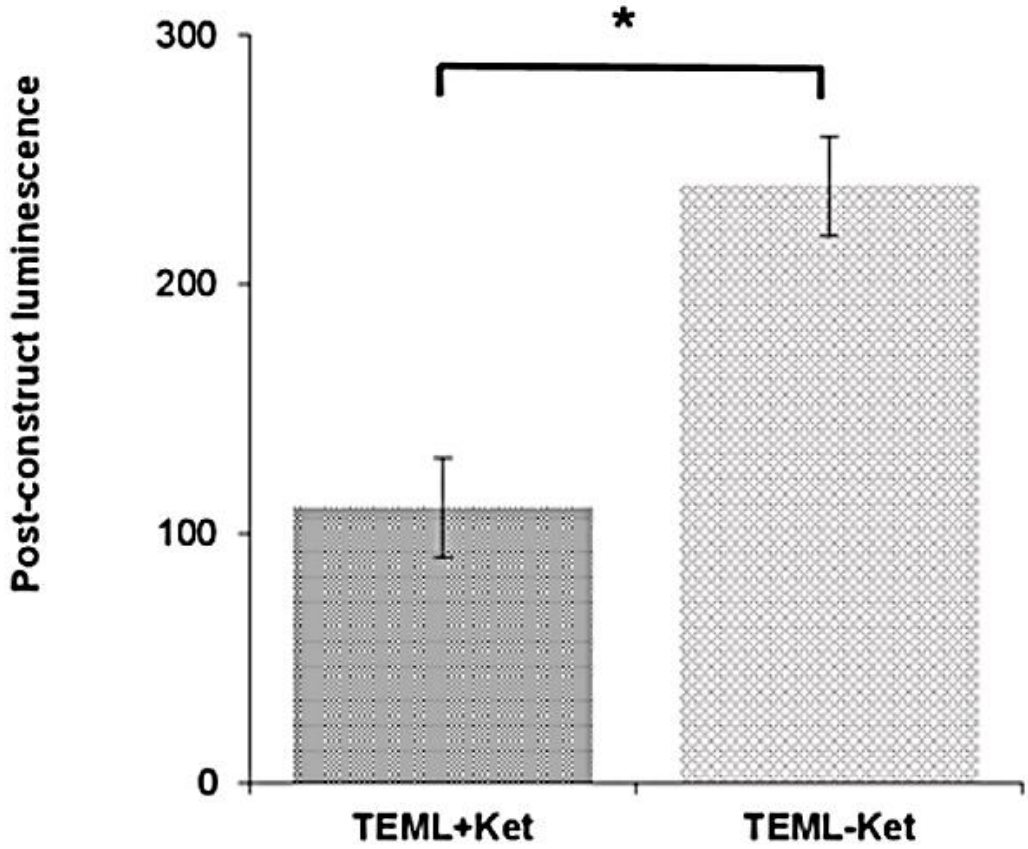

Figure 5.8 – Platelets dense granule secretion post TEML construct incubation with and without ketamine. Platelets treated or untreated with 1 mM ketamine were incubated with corresponding 1 mM ketamine treated or untreated TEML constructs for 15 minutes at 37˚C, with dynamic stirring. Luminescence of platelet suspension was measured using 10% Luciferin-Luciferase reagent. Results are representative of 6 experiments (n=13).

3.3.1 Inhibition of conventional PKC isoforms does not prevent the Ca^{2+} signal induced by TEML removal

To investigate if this ketamine-induced interference with dense granule secretion could be the cause of the construct removal-induced Ca^{2+} signals, experiments were performed to investigate the effect of the convention PKC isoform inhibitor, GÖ6976, on this parameter. This compound has previously been shown to completely inhibit collagen-evoked dense granule secretion when used at concentrations of 3 μM and above (Gilio et al., 2010). As shown in Figure 5.9, pre-treatment of platelets with 3 μM GÖ6976 did not affect Ca^{2+} signals evoked by TEML removal (90.4 ±16.8% of control; *P > 0.05; n = 4)*. Neither did it significantly alter Ca^{2+} signals evoked by the addition of the construct (105.3 ± 21.9 % of control; *P > 0.05; n = 4).* However, as the experiment was only repeated 4 times, which is considered further replication will need to be conducted to confirm these preliminary findings. These results indicate that the construct removal-induced Ca^{2+} signals was not caused by dense granule secretion from platelets.

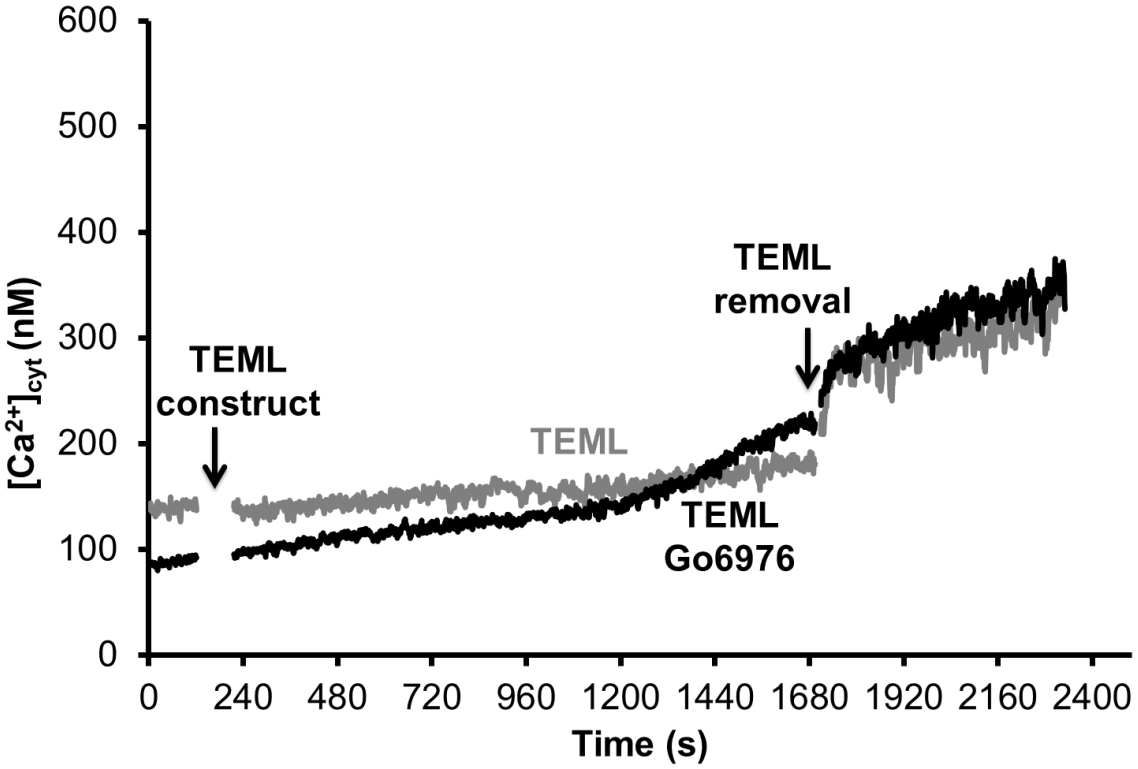

Figure 5.9 – Cytosolic Ca^{2+} concentration measurement of human platelets treated with GÖ6976. Fura-2-loaded human platelets were treated with or without GÖ967 (3 µM) for 10 minutes at 37˚C prior to start of experiment. Tissue-engineered medial layers were incubated with treated or untreated platelets for 15 minutes at 37˚ on-screen. Following the incubation period, the constructs were removed and the $[Ca^{2+}]_{cyt}$ was measured for a further 5 minutes. Results are representative of 3 experiments (n=4).

3.3.2 Ketamine inhibits TEML-induced platelet aggregation

Following the establishment of ketamine presence influencing the pro-aggregatory capacity of the TEML constructs, we assessed whether this could be seen to inhibit the aggregation of the platelet solution. Ketamine treated and untreated TEML constructs were incubated with corresponding platelet samples for 15 minutes at 37°C. Following the incubation period, the TEML constructs were removed and the remaining platelet suspension was analysed for changes in TEML-evoked platelet aggregation using a previously characterised plate reader assay (Lordkipanidzé et al., 2014). Ketamine significantly suppressed aggregation of platelet after 15 mins of incubation in the treated sample compared with untreated sample as the absorbance of the sample was significantly higher

(169.4 ±29.5; *P < 0.05*, n = 11; Figure 5.10). These results suggest that ketamine Interferes with the pro-aggregatory capacity of the TEML construct.

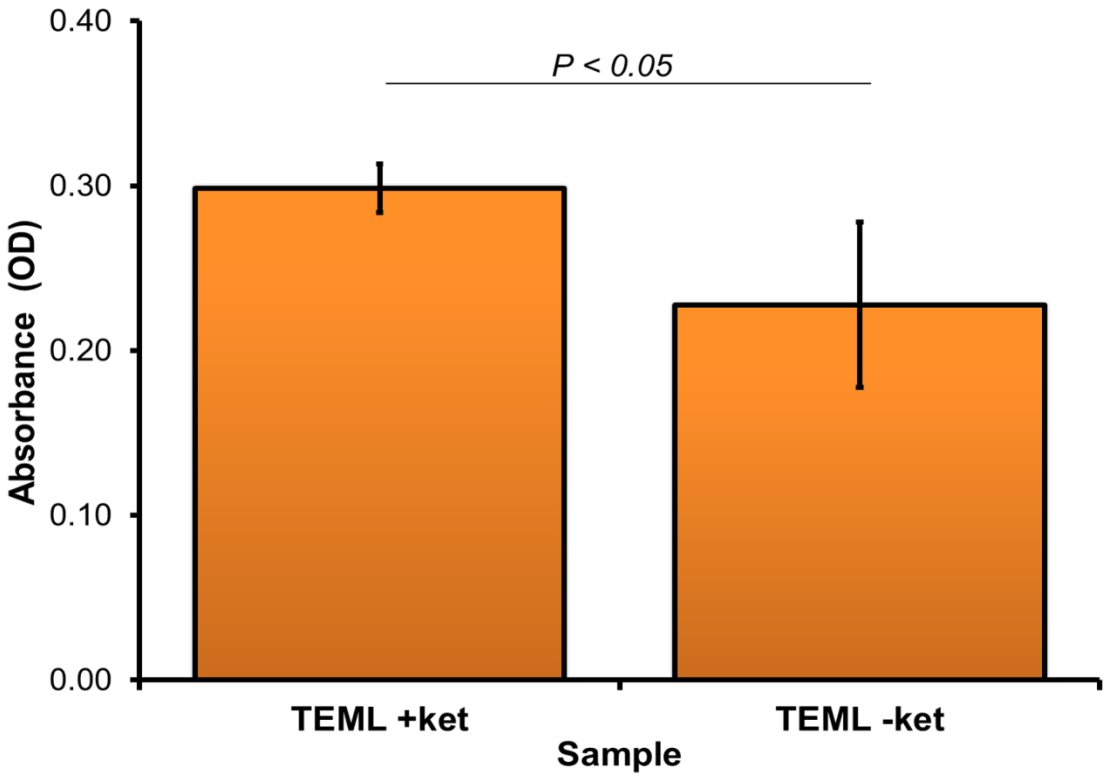

Figure 5.10 – Bar chart absorbance of platelets formerly incubated with ketamine treated tissue-engineered medial layer constructs. TEML constructs were incubated with or without ketamine (1 mM) for 1 hour prior to the start of experiment. The TEML samples were incubated with corresponding ketamine treated or untreated platelet samples for 15 minutes with dynamic stirring at 37˚C. Absorbance was measured post TEML construct incubation using a plate reader. Results are representative of 5 experiments (n=11).

3.3.3 *Ketamine inhibits platelet aggregation on the surface of the TEML construct*

To assess if the inhibitory effect of washed $DiOC_6$-labelled platelet suspensions treated or untreated with ketamine, these platelets were allowed to interact with corresponding TEML construct pre-treated with or without ketamine (Figure 5.11) in cuvette holders under continuous magnetic stirring. Fluorescence imaging of the $DiOC_6$-labelled platelet-exposed surface of the TEML

constructs revealed that ketamine-treated sample exhibits very few platelet aggregates forming on the surface of the TEML construct (Figure 5.11D-F). In contrast, the untreated sample show to provide a greater platelet adhesion as well as the formation of multiple platelet aggregates, consistent with our previous findings in chapter 4 (Figure 5.11A-C). These data therefore showed that ketamine could significantly inhibit the normal aggregatory potential of platelets

3.3.4 *Ketamine inhibits thrombus formation in platelets perfused over the TEML at arterial shear stresses*

Finally, to assess if the use of ketamine has the potential to interfere with the structure of thrombi induced in arterial thrombosis assays in mice, experiments were performed to see if ketamine treatment of platelets could prevent thrombus formation when perfused across the TEML. As shown in Figure 5.12, perfusion of untreated platelets at arterial shear stresses stress (15.4 dynes/cm^2) over an untreated TEML construct elicited significant platelet aggregation upon the surface of the construct, consistent with our previous findings in this and the previous chapter. However, when the platelets were treated with ketamine, no platelet aggregation could be observed on the surface of the TEML construct with only occasional, isolated adherent platelets being observed. These data highlights that ketamine treatment can significantly impair platelets adhesion and aggregation upon the subendothelial matrix. Therefore, it raises questions about the potential for the anaesthetic regime used to create artefactual findings in *in vivo* studies of arterial thrombosis. However, to confirm this conclusion, similar experiments will also need to be performed on the $FeCl_3$-injured TEBV.

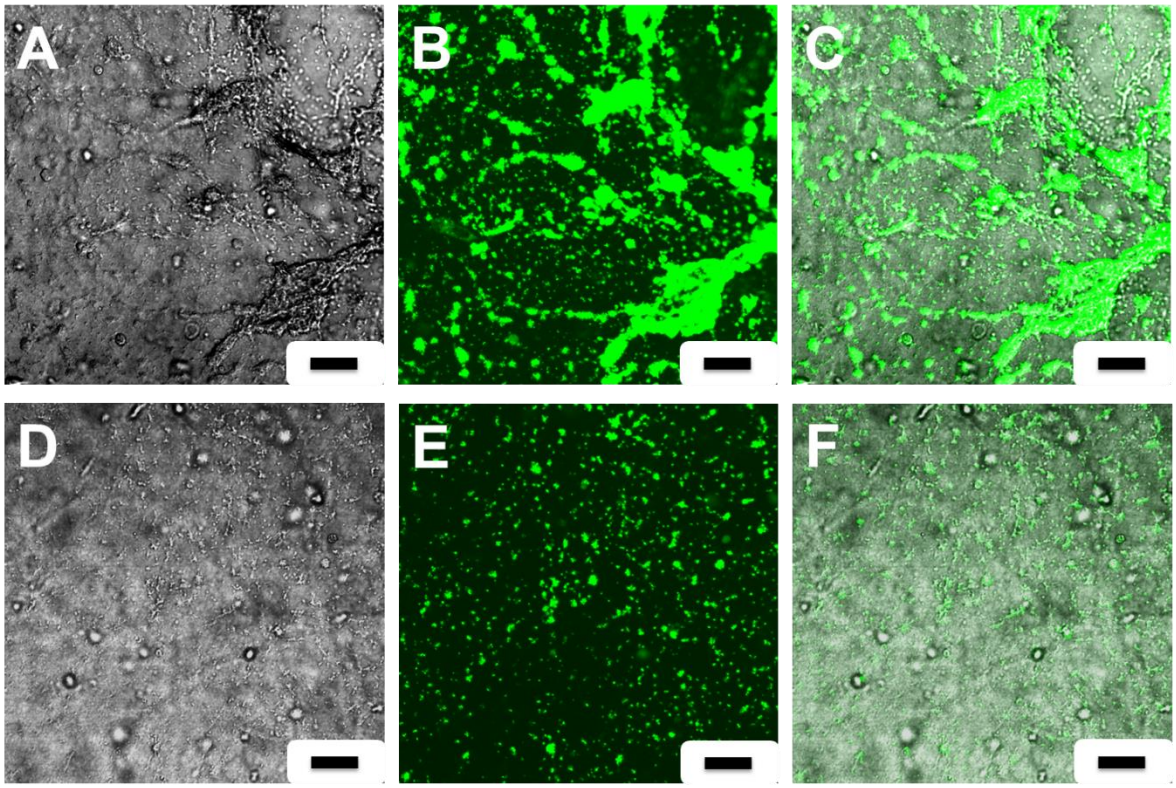

Figure 5.11 – Fluorescent and brightfield images of platelets aggregation to the surface of tissue-engineered medial layer incubated with and without ketamine. Tissue-engineered medial layer was incubated with ketamine (1mM) for 1 hour at 37˚C followed by incubation with 1 mL of washed platelets treated with ketamine (1mM) for 15 minutes at 37˚C. The constructs were then washed and the adhered platelet aggregates on the surface of the construct were imaged using fluorescence microscopy. (A-C) untreated sample; (D-F) Ketamine treated sample. Left panel: brightfield image, middle panel: $DiOC_6$, left panel: overlay. Results are representative of 4 experiments (n=6).

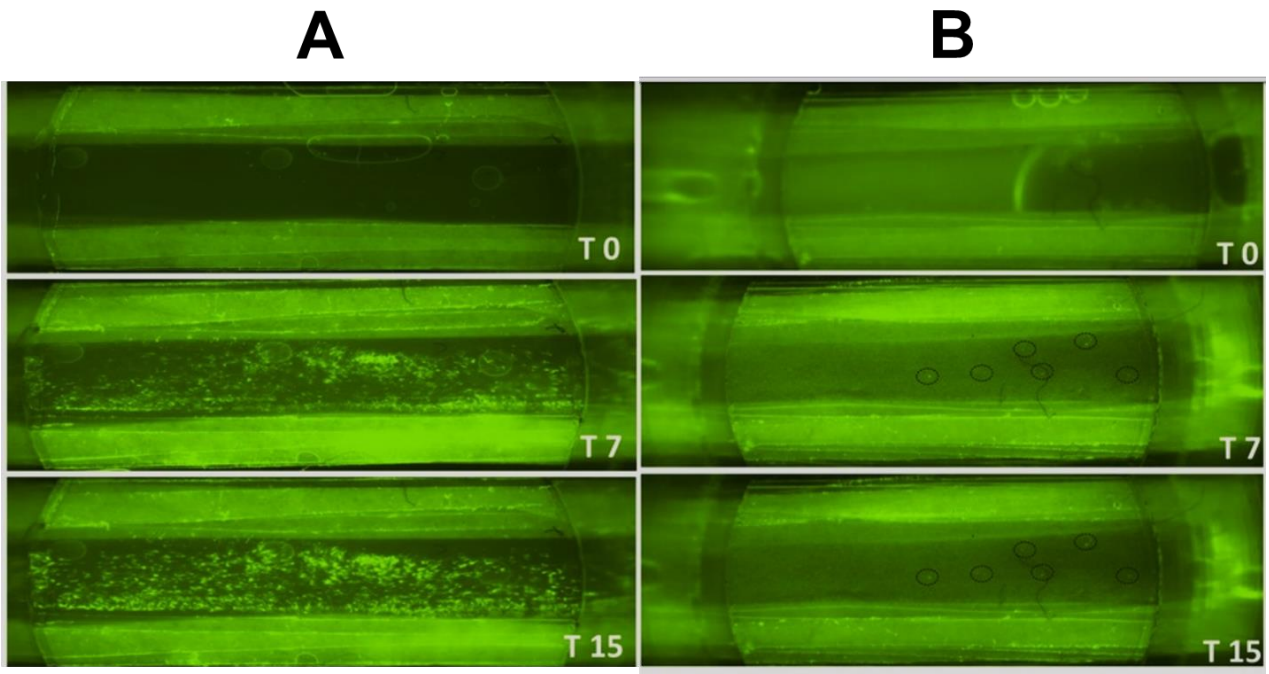

Figure 5.12 – Fluorescent images of perfused platelets aggregation to the surface of tissue-engineered medial layer incubated with and without ketamine using high shear stress. Ketamine treated (300 μM) and untreated platelets were perfused over tissue-engineered medial layer for 15 minutes using a parallel flow chamber at a shear stress (15.4 dynes/cm^2). Fluorescent images were recorded in real-time over the course of 15 minutes of perfusion using fluorescence microscopy. (A) Untreated sample; (B) Ketamine treated sample. (T0) Beginning of perfusion; (T7) 7 minutes post-perfusion; (T15) 15 minutes post-perfusion. Circles, indicate individual platelets adherence.

4 Discussion

In this chapter, we have developed a human *ex vivo* ferric chloride arterial injury model using our TEBV constructs. Through monitoring the $[Ca^{2+}]_{cyt}$ of platelets exposed to the $FeCl_3$ damaged TEBV constructs, we were able to show that this treatment reduces the inhibitory effect of the endothelium on the platelet sample. In addition, platelets aggregation could be observed upon the $FeCl_3$-injured construct under flow, where it was prevented in the untreated construct. This result was found regardless of where on the construct the solution was applied. The data also demonstrates that effect is due to the damage caused by the action of $FeCl_3$ on the endothelial cells, as the ability of $FeCl_3$ to enhance platelet activation was not replicated in TEML constructs treated with this solution. The data in chapter 4 demonstrate the pro-aggregatory effect of the TEML construct is mediated by native collagen synthesised and secreted by the human coronary arterial smooth muscle cells. Therefore, a traditional explanation of this model would suggest that $FeCl_3$-mediated oxidation induces endothelial cell denudation and subsequent exposure to neo-collagen which activates the platelets. Dubois *et al.* 2006., have examined the influence of the extent of collagen exposure in thrombus formation in $FeCl_3$ damaged vessel. The study found differences in the rapidity of collagen exposure in mild $FeCl_3$ injury compared with severe $FeCl_3$ injury (Dubois et al., 2006). After mild $FeCl_3$ vascular injury, the appearance of collagen was considerably reduced in comparison with severe $FeCl_3$ injury. However, the mechanism of $FeCl_3$ induced thrombus formation remains incompletely understood. In particular, the relative importance of collagen-dependent platelet adhesion via GPVI and integrin $\alpha_2\beta_1$ in this model remains controversial (Cheli et al., 2008; Dubois et al., 2006a; Konstantinides et al., 2006; Kuijpers et al., 2007; Massberg et al., 2003). Whereas some groups reported severe inhibition of $FeCl_3$-induced thrombus formation in GPVI-immunodepleted mice (Bender et al., 2011), others concluded that GPVI deficiency did not impair thrombosis in this model (Eckly et al., 2011). These different results are difficult to interpret as the vascular lesions were not examined in these studies and the

differences could arise from differences in experimental conditions, such as the $FeCl_3$ concentration (7–20%), the method (filter paper or drop) and time (2–5 min) of $FeCl_3$ application, or the vessel bed targeted (carotid or mesenteric artery). Such differences in experimental conditions can cause variations in the depth and extent of the vascular lesions, which consequently may modify the exposure of specific proteins to blood flow. Therefore, these discrepancies might be reconciled via using our model system to provide a standardised testing system in which to identify if these key variables could alter the relative importance of GPVI in these experiments.

Although previous studies have identified collagen-mediated activation as important in mediating platelet activation in the $FeCl_3$ injury model, more recently this interpretation has been challenged by the work of Eckly et al. (2011). This group identified spherical bodies filled with iron originating from endothelial cells exposed to $FeCl_3$ (Eckly et al., 2011). These spheres were surrounded by a bilayer characteristic of a plasma membrane budding off from the endothelium. Platelets appeared to adhere to the rough material present on the endothelial-derived spheres, suggesting that $FeCl_3$ might activate platelets through presentation of endothelial cell microparticles. Therefore, investigations into whether similar endothelial-derived microparticles can be observed to trigger platelet activation in our system may provide a basis for better understanding the $FeCl_3$ vascular injury model.

In this chapter, data is also presented showing that the effect of ketamine alters platelets ability to activate in response to TEML or TEBV constructs. However, ketamine does not have a significant effect on untreated TEBVs. These results therefore suggest that ketamine inhibits platelet ability to activate upon the subendothelial matrix as thrombus formation upon the TEML construct is inhibited by ketamine both under static conditions as well as under physiological flow. This failure to aggregate upon the surface is also linked with a reduced aggregation of platelets exposed to these constructs – suggesting that the absorbance difference is due to a failure to form thrombi upon the subendothelial matrix. However individual platelets are able to adhere to the surface as can be seen in both static and flow conditions. These data therefore suggest that ketamine does

not prevent collagen-mediated platelet adhesion but interferes with a process that helps recruit platelets to the subendothelial matrix. This effect is therefore is likely mediated by the ability of ketamine to inhibit dense granule secretion, as the ability of autocrine signalling molecules released from here are known to be critical to recruit circulating platelets to the surface of the forming thrombi (Stalker et al., 2012). Previous studies have demonstrated that ketamine can block platelet aggregation both by inhibiting thromboxane synthesis (Atkinson et al., 1985) or by suppressing agonist-evoked rises in $[Ca^{2+}]_{cyt}$ (Chang et al., 2004; Nakagawa et al., 2002). As all studies were treated in aspirin-treated platelets, it is unlikely that the effect on thromboxane synthesis is responsible for the inhibitory effects observed and thus the effect on Ca^{2+} signalling appears to be the most likely explanation. Previous studies have suggested that ketamine can inhibit platelet Ca^{2+} signalling by inhibiting inositol triphosphate formation (Chang et al., 2004; Nakagawa et al., 2002). This would explain the ability to prevent platelet granule secretion and aggregation. However, Ca^{2+} signalling is not significantly inhibited in response to exposure to the construct alone or stimulation with thrombin post-construct removal. The only effect observed is after construct removal - this may be due to improved signal propagation within the platelet sample from activated platelets which mixed freely in response to TEML construct removal. Previous studies have shown that ketamine reduces NO biosynthesis in endothelial cells by down-regulating endothelial NO synthase expression and intracellular calcium levels (Chen et al., 2005). A reduction in the production of NO would be expected to reduce the inhibitory effect of the TEBV on human platelets. However, this effect was not observed, with inhibition of thrombin-evoked Ca^{2+} rises in human platelet incubated with the construct found not to be significantly inhibited by ketamine treatment. These results therefore suggest that in this 3D system that ketamine is not able to significantly inhibit NO production, or that NO is not a significant inhibitor of platelet activation in our system. This latter effect may be due to the inhibitory effect of NO being redundant with another endothelial-derived platelet inhibitor such as prostacyclin. Further work will be required to assess these possibilities.

4.1 Conclusion

In summary, we have successfully generated a ferric chloride injury model using our TEBV construct which mimics the results previously reported in *in vivo* mice models. This model offers a number of advantages including the replacement of animal models, removal of the requirement for expensive intravital microscopy equipment, and are likely to be cheaper to produce than the costs of housing a colony of mice. In addition, data is presented which demonstrates that the lack of need to introduce anaesthetics such as ketamine into the blood sample could improve the physiological relevance of the clotting responses seen. The ability of ketamine to inhibit thrombus formation on the surface of the construct could play an important role in artefactually altering the size and structure of thrombi seen, and may lead to overestimation of the effective of putative anti-platelet therapies observed in these systems. However, as experiments were performed using high concentrations of ketamine further studies will be required to more adequately assess the extent to which this anaesthetic may interfere with the aggregatory response observed.

Chapter 6

Discussion and Conclusions

1. Discussion

The layers of the native human blood vessel create a complex tissue with intricate and unique biochemical and mechanical properties (Boland et al., 2004). These structural and functional properties represent incredible challenge for those scientists aiming to tissue engineer an arterial replica for use as an alternative to autologous vascular grafting. Such an artificial blood vessel would have to be mechanically strong to withstand the high pressures and fast, pulsatile flow rates of arterial blood similar to the native artery, as well as provide a non-immunogenic and non-thrombogenic surface that will not activate the immune, primary or secondary haemostasis systems (Isenberg et al., 2006; Lopez and Zheng, 2013; Sankaran et al., 2014). In this thesis, we have adapted some of these previously developed techniques to produce a viable 3D human tissue engineered blood vessel model which can be used to replicate the *in vivo* physical, chemical and cellular environment within human blood vessels as a tool to study haemostasis.

This study aimed to develop a tri-layered 3D tissue engineered blood vessel model generated from commercially-available human primary cells fabricated using a layer-by-layer methodology. Utilising this method, it has been possible to use tissue engineering techniques to manipulate the individual layers of our blood vessels alone and in co-culture. This has led to four major collections of work in this thesis; (i) establishing and optimising culture conditions for each layer of the construct individually as well as together in co-culture, (ii) developing a real monitoring system to test the physiological relevance of the fabricated tissue-engineered vessel constructs, (iii) investigating the pro- and anti-aggregatory capacities of medial and intimal layers of the construct and (iv) using the TEBV to recreate the $FeCl_3$ arterial thrombosis model.

1.1 Establishing and optimising culture conditions for each layer of the construct individually and when assembled together

Endothelial cells play a key role in haemostasis through maintaining platelets and the coagulation cascade in a quiescent state. Therefore, it is important that in the developed blood vessel model

the endothelial cells possess and maintain these anti-haemostatic characteristics. In culture, HUVECs grew as a homogenous monolayer of cells with distinct cell boundaries. These cells also display a cobblestone appearance during culture. These results were in agreement with those reported by other articles on the morphology of these cells in culture (Unger et al., 2002). HUVECs show a well spread morphology on fibronectin coated nanofibers indicating excellent compatibility of cells with the fibronectin coated PLA scaffold. Further, the images show that the cells were specifically orientated in the direction of the nanofibers, thus demonstrating that the nanofibers are able to direct HUVECs growth in the construct. Further, experiments demonstrated that the generated HUVECs monolayer of the completed TEBV was found to maintain itself separately from other layers of construct as well as stably maintain its endothelial phenotype as shown by the continually high CD31 expression of these cells in the fabricated TEBV. The cobblestone morphology displayed by the cultured HUVECs and their high CD31 expression were consistent with previous findings (Sankaran et al., 2014; Unger et al., 2002). In addition, endothelial cell alignment using underlying PLA nanofibers did not influence CD31 expression on these cells as a high fluorescence expression was observed in both aligned and randomly orientated HUVECs, as was also reported by Sankaran *et al.,* (2014). These data therefore demonstrate that HUVECs within the 3D culture system does not adversely affect the cellular phenotype of these cells.

HCASMCs cultured within TEML were found to express F-actin which is associated with a contractile phenotype of these cells (Gutierrez-Pajares et al., 2015). Typically, vascular SMCs can play two distinct physiological roles changing between synthetic or contractile phenotypes (Rensen et al., 2007). Following an injury to the smooth muscle layer, SMCs switch their phenotype to become more proliferative and migratory and producing more ECM proteins. Therefore, vascular SMCs are plastic cells that may undergo reversible phenotypic changes in response to local growth factors, reactive oxygen species, mechanical forces, and alterations in ECM (Crosas-Molist et al., 2015). The use of phalloidin to visualise F-actin expression can give crucial information such as fibre orientation and distribution (Na et al., 2007). This was reported in a study using cultured HCASMCs in

poly(ethylene glycol)-conjugated fibrinogen (Peyton et al., 2008). However, as F-actin is ubiquitously present in all cells, phalloidin staining is not a specific marker of a contractile smooth muscle phenotype, and so further experiments will be required to more fully assess other phenotypic markers such as smooth muscle α-actin (Beamish et al., 2010; Yuan, 2015).

Live-dead staining was performed for both HUVECs and HCASMCs to ensure their viability within individual layers as well as within the assembled TEBV construct. HUVECs seeded on PLA scaffolds and HCASMCs within the medial layer were both shown to be viable throughout the culture period (up to 14 days). Sankaran *et al.,* (2014) have previously shown that HUVECs cultured on electrospun PLA nanofibers maintain high cellular viability, as we have similarly observed here (Sankaran et al., 2014). Previous studies of HCASMCs cultured within a fibrin gel have found them to be fully viable with no dead cells reported for up to 3 weeks in culture (Gundy et al., 2008). Experiments performed in this thesis have similarly demonstrated a high viability of HCASMCs when cultured in type I collagen hydrogel. These data demonstrate that there is no impact on the viability of either cell type of culture within the TEBV.

Fluorescence imaging studies using cell tracker dyes has shown that the layer-by-layer fabrication technique yielded a TEBV construct that displayed a layered tissue with anatomic similarities to its native counterpart. The construct was observed to maintain distinct intimal and medial layers separated by the PLA nanofibers (mimicking the internal elastic lamina). These cells were also observed to remain in the layer of which they were initially seeded and do not migrate through the different layers – thus demonstrating that our TEBV construct can create a stable structure which mimics the anatomy of the native blood vessel. In this project, we have also shown that dextran permeation was reduced in TEBV constructs by almost 20% at the end of the run compared to the collagen hydrogel sample. In general, dextran permeation through the TEBV construct showed no change in fluorescence compared to the collagen hydrogel – thus suggesting that the TEBV was largely impermeable to the dextran. However, there are some limitations associated with the

design of the methodology that needs to be altered to make it more reliable. This includes modifying the design of the gasket and better sealing of the sides of the construct to prevent artefactual results caused by leak of dextran down the sides of the construct rather than its permeation through the TEBV. Overall, the initial characterisation has demonstrated that the human cells were able to maintain their viability and cellular phenotype when cultured within the TEBV, to produce a construct with anatomical similarity to its native arterial counterpart.

1.2 Developing a real-time monitoring system to test the physiological relevance of the fabricated tissue-engineered vessel constructs

The second aim of this thesis was to assess the functional properties of the fabricated blood vessel construct through assessing their ability to trigger or inhibit the activation of the primary haemostatic system. To do this, a novel real-time monitoring system to assess human platelet activation in response to exposure to our constructs was developed to test the haemostatic functionality of the fabricated tissue engineered vessel models. This method utilised the universal role of rises in $[Ca^{2+}]_{cyt}$ to trigger all aspects of platelet activation including platelet shape change, α- and dense- granule release, TXA_2 formation, integrin $\alpha_{IIb}\beta_3$ activation and platelet aggregation. Due to the ability of all platelet agonists to signal via a rise in $[Ca^{2+}]_{cyt}$ this system provides a sensitive system to monitoring pro-thrombotic functions of the construct. In contrast, endothelial-derived platelet inhibitors such as NO and PGI_2 also significantly inhibit agonist-evoked rises in $[Ca^{2+}]_{cyt}$, therefore post-exposure measurements of thrombin-evoked rises in $[Ca^{2+}]_{cyt}$ can be used to monitor the anti-thrombotic nature of the construct. This method therefore has a number advantages over currently-used methods including sensitive and dynamic measurements of both platelet activation and inhibition by the endothelial layer as well as allowing for analysis of platelet activation in the underlying platelet suspension. By utilising this method, it has been possible to perform a number of experiments investigating pro- and anti-aggregatory phenotypes of the fabricated medial and intimal layers of the construct individually as well as when assembled together as a full TEBV.

1.3 Investigating the pro- and anti-aggregatory capacities of medial and intimal layers of the construct

1.3.1 *The TEML possesses a pro-aggregatory phenotype due to the production of a neo-subendothelial matrix*

Using the real-time monitoring system it was possible to observe that the TEML was able to activate human platelets in the absence of any exogenous stimuli – with a small rise in $[Ca^{2+}]_{cyt}$ being observed in the underlying platelet suspension exposed to the TEML compared to that seen in those cells exposed to the collagen hydrogel. However, this Ca^{2+} signal is small in amplitude and therefore took much of the 10-minute incubation to become apparent from that seen when platelets were incubated with the hydrogel. This correlated with the results from analysis of $DiOC_6$-labelled platelets that had adhered to the surface of the construct that demonstrated significantly enhanced platelet aggregation on the TEML over that observed for the collagen hydrogel. The slow activation could represent the small proportion of the platelets in the suspension actually in contact with the surface of the construct at any one time. The volume of the platelet suspension used in the experiment was restricted to a minimal volume required to ensure the blood vessel construct was not positioned in the path of the excitation light which would interfere with the ability to make fluorescence readings from the platelet suspensions. Thus, having a large volume of platelet suspension not in continuous contact with the subendothelial matrix could dilute the pro-aggregatory signals being released from this surface. Further refinement of the spectrophotometer set-up to reduce this volume may help demonstrate a stronger activation signal. Alternatively, the accessibility of collagen at the surface of the construct may be limited – a mechanical injury may help us better expose more of the collagen within the medial layers to the platelets, which would provide a more realistic replica of blood vessel injury found *in vivo*.

The activation potential of our TEML was more clearly observed after exogenous thrombin addition, where those platelets exposed to the TEML had a significantly enhanced thrombin-evoked rise in $[Ca^{2+}]_{cyt}$. Activated platelets release a variety of autocrine signals which trigger the activation of

other circulating platelets to help recruit them to the growing thrombus. The ability of thrombin to potentiate the Ca^{2+} signal elicited by platelets co-stimulated with collagen is well known, and has been shown to be a critical factor in helping platelets expressing procoagulant phenotype in which phosphatidylserine is expressed on the extracellular face of the platelet plasma membrane (Kulkarni and Jackson, 2004). In this study, we have used washed platelet suspensions and therefore not examined the ability of the construct to trigger the activation of the coagulation system and natural thrombin production from plasma. Future experiments will be needed to examine whether the medial layer-evoked Ca^{2+} signals can be further enhanced by the activation of the extrinsic coagulation cascade when they are exposed to clotting factors present in platelet-rich plasma or whole blood.

This thesis has also demonstrated that platelet aggregation upon the surface of our construct is dependent on the presence of neo-collagen created within the TEML. The data shown in this thesis demonstrate that platelets failed to aggregate on the surface of the type I collagen hydrogel used for construct fabrication, whereas the use of other forms of collagen such as Horm collagen or type I and III collagen produced by the HCASMCs, supported platelet aggregation. Examination of type I collagen hydrogel used in construct fabrication only elicits minimal platelet adhesion to the surface of the construct and presents no ability to trigger Ca^{2+} signalling in the underlying platelet suspension – suggesting that platelets are inert to this form of collagen. This is supported by previous studies that have shown that type I collagen films made from rat tail's possess low thrombogenicity and can only support cell spreading but not aggregation (Boccafoschi et al., 2005). A potential reason for this is the difference in the structure of the soluble collagen used within the hydrogel and the mature neo-collagen forms produced by the HCASMCs. Previous studies have highlighted the importance of collagen structure in eliciting platelets aggregation, with different collagen preparations varying in their ability to aggregate platelets and support their adhesion, due to the structure of the collagen contained within them (Farndale, 2009; Farndale et al., 2008). For example, a previous study by Jaffe & Deykin (1974) showed that microfibrillar collagen purified from

rat skin is a potent initiator of platelet aggregation, whereas soluble, monomeric collagen from the same source was not (Jaffe and Deykin, 1974). This has been supported by further studies that have shown that fibrillar collagen is much more potent in inducing platelet activation than the same collagen type presented in its acid-soluble form (Farndale, 2009; Savage et al., 1999). Type I collagen used in creating the hydrogels for the TEML is a monomeric collagen solution dissolved in acetic acid – which according to these previous studies would have limited thrombogenic potential. The collagen was reconstructed in the laboratory to form the desired hydrogel constructs. Although the gelation process creates microfibrils of collagen, which are more effective initiators of platelet aggregation – this format was still found to be ineffective at eliciting platelet activation in these studies. The formed collagen microfibrils may be inefficient at triggering platelet aggregation due to the lack of critical tertiary and quaternary structures of collagens found in native collagen samples. For example, most native collagens are mixtures of different collagen isoforms, which can elicit alterations in the final collagen structure. For example, previous studies have shown that the presence of type III collagen alongside type I collagen has been shown to alter fibrillogenesis, as type III collagen has been shown to regulate the diameter of type I collagen fibrils (Liu et al., 1997; Stuart and Panitch, 2009). This difference in fibril diameter might explain the heightened pro-aggregatory capacity of the HCASMC-produced neo-collagen. In addition, the produced neo-collagen may also be cross-linked which is also known to increase platelet reactivity to collagen (Kawamoto and Kaibara, 1990). Further work will be required to assess which of these factors are important for mediating the enhanced pro-aggregatory capacity of the TEML.

1.3.2 *The TEBV replicates the anti-aggregatory phenotype of the native artery*

In contrast to the data obtained from the TEML, analysis of the haemostatic function of the TEIL and TEBV constructs have found them to be anti-aggregatory, consistent with the role of the tunica intima in the native artery. Both the TEBV and TEIL had no effect on platelet $[Ca^{2+}]_{cyt}$ during the incubation period, but significantly inhibited thrombin-evoked Ca^{2+} signals in a manner dependent

on HUVECs seeding density upon the construct. In addition, there was minimal platelet adhesion observed to the surface of the TEBV, and platelets exposed to the TEBV displayed significant inhibition of both thrombin-evoked dense granule secretion and aggregation, demonstrating that platelets preincubated with the TEBV has a reduced capacity to activate than those exposed to the collagen hydrogels. These anti-platelets effects of the TEBV were likely to be mediated by the ability of HUVECs to create endothelial-derived platelet inhibitors. NO and PGI_2 are widely considered to be the main endothelial-derived platelet inhibitors – however despite many attempts to block the effects of both of these paracrine regulators, we were only able to elicit a small partial reversal of this inhibition. These data will therefore need to be further investigated to examine whether this was due either to an inability of our drug cocktails to completely inhibit the action of either or both of these platelet inhibitors, or due to the TEBV producing a non-NO, non-PGI_2 platelet inhibitor which was able to mediate the same anti-platelet effects of these compounds. The next stage of work would be to characterise the effect of the inhibitor cocktails on construct NO and PGI_2 formation to address this question. Whilst there may be differences in the mediator of these anti-platelet effects, it is clear that the TEBV does possess appropriate anti-aggregatory properties of the native blood vessels.

1.4 Using the TEBV to recreate the $FeCl_3$ arterial thrombosis model

Whilst the real-time monitoring system provided a useful system for characterising the haemostatic properties of tissue-engineered blood vessel constructs, the stirring conditions used in the spectrophotometer did not recreate the physical environment found *in vivo*. In this thesis, experiments were performed to assess the ability of our TEBV to provide normal haemostatic function under physiological flow conditions when incorporated within a commercially-available parallel flow chamber. As shown in chapter 5, these data demonstrated that under arterial flow conditions the TEBV could resist platelet aggregation for to the entire 15 minutes perfusion period. In contrast, when the TEML was used, this could support significant platelet aggregation upon the

surface of the construct. These results therefore suggest that our construct may provide a more physiologically-relevant substrate to use in place of 2D monolayers of either endothelial cells or components of the subendothelial matrix currently used as part of flow chamber assessments of human platelet activation.

Further experiments also demonstrated that our construct could be used to replicate the *in vivo* $FeCl_3$ arterial thrombosis model, which is commonly used to assess haemostatic function in rodents. This work therefore provides a proof-of-concept that our TEBV could be developed further to create an *ex vivo* system in which to recreate and study the cellular events of human haemostasis. This new methodology provides advantages over the mouse and rat models currently used. For instance, these TEBVs could also be used in place of animal models providing a viable route to replace and reduce the number of rodents currently used in platelet research. In addition, the use of human cells over rodent cells provides a humanised system to perform preclinical testing of new anti-platelet drugs. Due to differences in the signalling pathways of mouse and human platelets- this might provide a platform for better predicting the potential benefit of any developed anti-platelet agent. Further, the design of microfluidic flow chambers that incorporate our TEBV could be used to support high-throughput testing of anti-platelet agents.

However, for other researchers to adopt such a system it is important to demonstrate the potential advantages of this model over the currently used *in vivo* system. One potential issue in current intravital microscopy studies is the need to anaesthetise the mice with general anaesthetics during the experiments to minimise their suffering. Commonly used anaesthetics for *in vivo* arterial thrombosis experiments include ketamine, xylazine and pentobarbital (Denis et al., 2011)– all of which are known to have anti-platelet effects (Bergqvist et al., 1974; Chang et al., 2004; Dwyer and Meyers, 1986; Sato et al., 2003). In this thesis, experiments were performed to assess whether ketamine could impact upon the ability of our TEML to support platelet aggregation under both static and physiological flow conditions. Both when the platelet suspensions were treated with the

anaesthetic alone or together with the constructs, ketamine inhibited platelet surface aggregation. The main motive for treating both samples was to replicate *in vivo* models where ketamine is injected and exposed to both platelets and the vessel wall simultaneously through the bloodstream (Akata et al., 2001). Treating the tissue engineered constructs alone becomes irrelevant since ketamine is not only exposed to the vessel wall but also exposed to platelets. From the results obtained here it appears that this effect of collagen-platelet interaction was inhibited due to the presence of ketamine and this suppression was stronger than the pro-aggregatory effect caused by the TEML. Thus, these results therefore question the potential whether the results of intravital microscopy experiments may be altered by the use of differing anaesthetic regimens. However, the dose of ketamine used is high and so full pharmacological characterisation of this drug alone and in combination with xylazine to properly assess its potential to alter the results of intravital microscopy experiments are required (Akata et al., 2001; Dubois et al., 2006b; Falati et al., 2002; Furie and Furie, 2008).

1.5 Future work

Numerous novel techniques have been developed throughout this project which have allowed us to develop and characterise a functional tissue engineered blood vessel construct for use in the study of haemostasis. However, whilst the work provides an experimental basis for developing and characterising tissue-engineered blood vessels, further work will be required to complete the development of the construct.

The most imminent question that remains to be answered is the mechanism by which the TEBV can elicit its anti-platelet effects even when treated with inhibitor cocktails to attempt to prevent production of NO and PGI_2. The most likely explanation is the inability of the inhibitor cocktails to fully inhibit both NO and PGI_2 production. Therefore, it would be interesting to investigate NO production of the TEBV in which HUVECs have been loaded with the fluorescent NO sensor, DAF-FM, both in the presence and absence of the NOS inhibitor-containing cocktails used in chapter 4.

This compound is essentially non-fluorescent until it reacts with NO to form a fluorescent benzotriazole (Figure 6.1; Mainz et al., 2012). Therefore, monitoring increases in DAF fluorescence will allow us to identify any residual NO production that may account for the remaining anti-platelet effects of our construct. Additionally, another useful experiment would be to examine total VASP and phosphorylated- vasodilator-stimulated phosphoprotein (P-VASP) proteins using western blot platelet samples exposed to TEBV, TEIL and TEML constructs. When platelets are exposed to endothelial derived inhibitors which elevate cAMP and cGMP respectively, such as PGI_2 and NO, VASP protein becomes phosphorylated (Wentworth et al., 2006). Thus, assessing the degree of P-VASP in platelet cell lysates exposed to the TEBV constructs in both the presence and absence of our cocktails could also indicate the likely presence of any residual NO, PGI_2 and/ or non-NO, non-PGI_2 mechanisms working through inhibitory cyclic nucleotide signalling pathways. If no residual activity is found this would necessitate a search for a non-NO, non-PGI_2 signalling pathway which may require a chemical analysis of substances released into conditioned culture medium used to co-culture the TEBV. This system will hopefully help us identify the signalling pathways preventing platelet activation in our construct, and allow us to adapt this to become similar to the effects observed in the native artery.

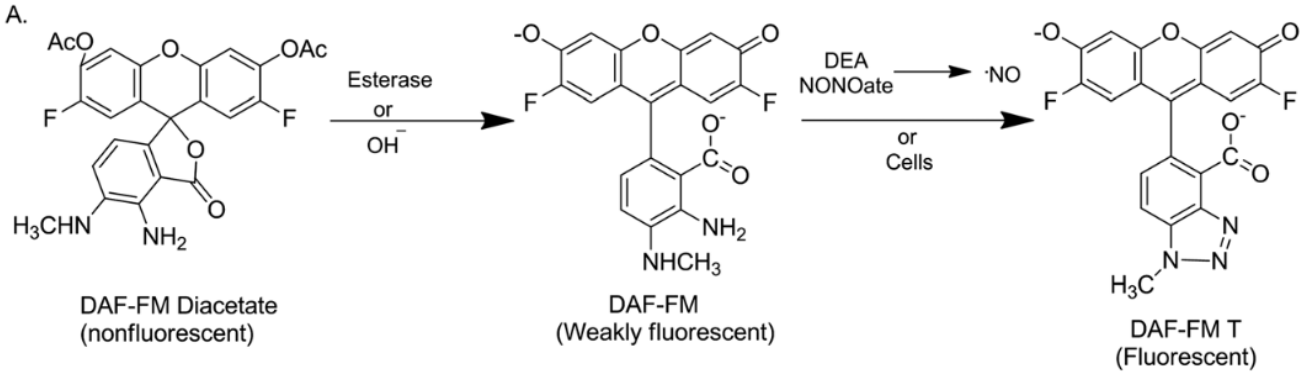

Figure 6.1 – Shows reaction scheme for DAF-FM diacetate (Mainz et al., 2012).

In addition to refining the biochemical characteristics of the construct, there are also structural aspects of the construct which can also be refined. For instance, the TEML constructs can be further modified by aligning HCASMCs to resemble the architecture of native SMCs where cells are seen aligned in the medial layer to provide a robust vasoconstrictive response when stimulated appropriately, as seen in native arteries. In addition, an adventitial layer can be introduced to form a blood vessel which fully replicates the native arterial structure. The inclusion of an adventitial layer would increase the mechanical properties of the construct and could potentially alter the ability of the construct to activate the extrinsic coagulation system, as adventitial fibroblasts are known to be a significant source of tissue factor in the subendothelial matrix (Butenas et al., 2009).

Furthermore, the biocompatibility of the PLA nanofiber could be improved by incorporating other native proteins beyond fibronectin onto them. This could improve cell retention whilst maintaining the mechanical strength of vascular constructs. Collagen and elastin are major extracellular matrix proteins found in the subendothelial matrix, and the use of these natural vessel wall components for fabricating electrospun nanofibers has been described previously in literature (Boland et al., 2004; Buttafoco et al., 2006). These electrospun nanofibers could therefore also be used to mimic the native extracellular matrix whilst further improving the mechanical strength and elasticity of the construct.

Lastly, another way to increase the mechanical properties of the constructs is via plastic compression of collagen hydrogel scaffold for media layer in the presence of HCASMCs, which will increase collagen density and strengthen the mechanical properties of the TEML (Braziulis et al., 2012; Hu et al., 2010). This process has also been demonstrated to improve collagen fibres alignment in cultured limbal epithelial cells grown in collagen hydrogel where the fibres within the compressed gel were densely packed and more evenly arranged (Levis, 2010). This may assist in better aligning HCASMCs within the medial layer. An attempt of compressed type I collagen hydrogel is shown in Figure 6.2. It is evident that the acellular collagen hydrogel incorporated with

PLA nanofiber sheath showed a mechanical stability compared with the hydrogel of which the inner lining is incorporated with high density PLA nanofiber. These nanofiber sheaths were primarily produced by electrospinning 5-times of 0.2 mL of PLA solution to produce a thick nanofiber scaffold on the collector. This was then sealed atop of a compressed acellular collagen hydrogel using a collagen solution. Once this was set, the construct was rolled using a metal rod. This improved mechanical strength also makes it possible to create a tubular vessel model – therefore better replicating the normal arterial geometry than the basic sheet model used throughout this thesis. Therefore, structure improvements to the TEBV may not also improve the stability and biological functionality of the construct, but could also be used to better replicate its native structure. The creation of a tubular TEBV with realistic lumen diameter could have significant impact in replicating the normal blood flow conditions that occur through the TEBV – thus further improving the biological validity of our constructs.

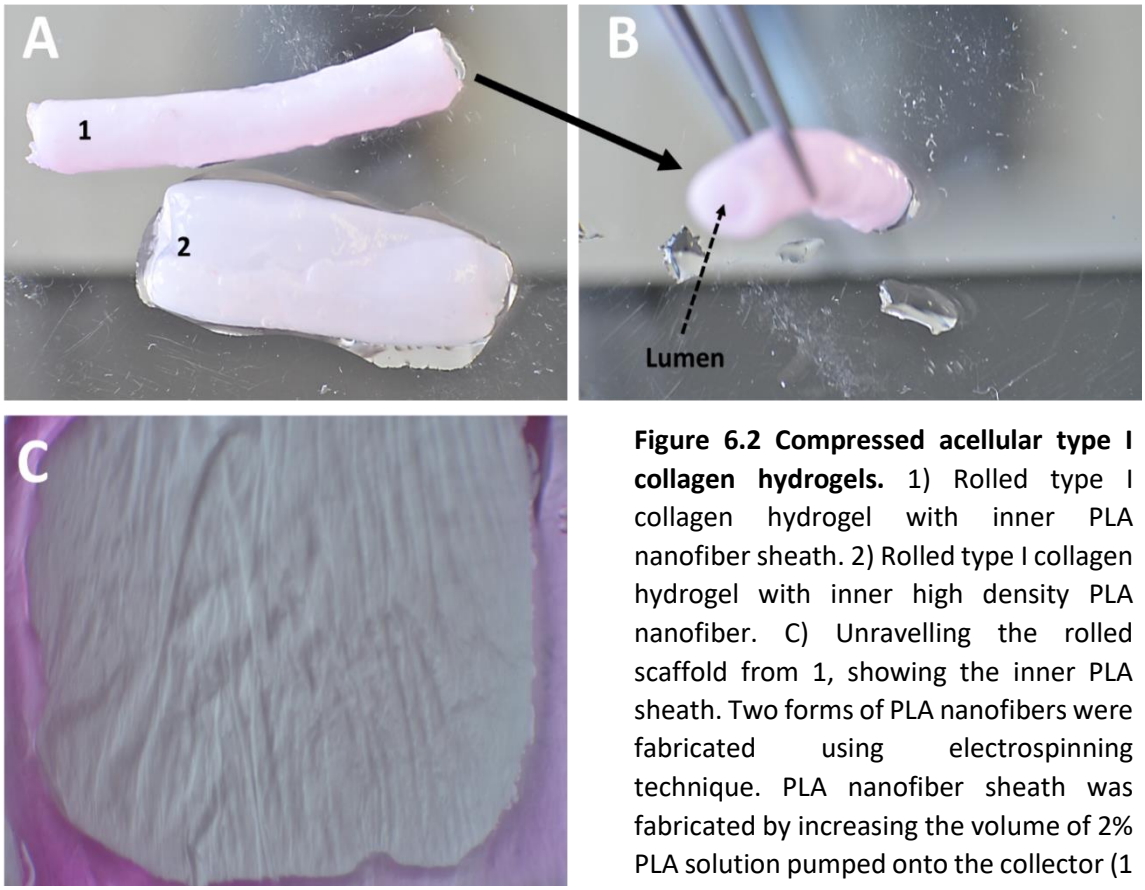

Figure 6.2 Compressed acellular type I collagen hydrogels. 1) Rolled type I collagen hydrogel with inner PLA nanofiber sheath. 2) Rolled type I collagen hydrogel with inner high density PLA nanofiber. C) Unravelling the rolled scaffold from 1, showing the inner PLA sheath. Two forms of PLA nanofibers were fabricated using electrospinning technique. PLA nanofiber sheath was fabricated by increasing the volume of 2% PLA solution pumped onto the collector (1 mL) whereas the high-density PLA nanofiber was generated using a lower 2% PLA solution volume (0.2 mL).

1.6 Conclusions

In this thesis, a successful fabrication and characterisation of a tri-layered TEBV was generated using a layer-by-layer fabrication approach. In addition, it was demonstrated the ability to create a novel testing platform to enable analysis of the effect of tissue-engineered blood vessel constructs on platelets activation. Through exposing the constructs to washed human platelet suspension labelled with Fura-2, we are able to assess in real-time the activation status of the platelet suspension, or modulation of platelet responsiveness to soluble agonists. Through this method, we were able to optimise suitable HUVECs seeding densities and duration of incubation with tissue engineered constructs. We have also shown that the endothelial lining of the fabricated TEBV construct possess an anti-aggregatory characteristic. Investigation of these anti-aggregatory

mediators using NO and PGI_2 inhibitors revealed that additional mechanisms may also be responsible for mediating the inhibitory effect of our constructs on platelet function. In contrast, the fabricated TEML construct was shown to provoke a pro-aggregatory appearance on the surface of the construct caused by the neo-collagen generated by HCASMCs within the constructs. These results therefore suggest that our constructs possess anti- and pro-aggregatory properties of native blood vessels.

In addition, we have successfully created an *ex vivo* ferric chloride arterial injury model that uses the fabricated TEBV construct by recreating physiological blood flow conditions inside a commercially-available parallel flow chamber. Using this model, we have demonstrated the ability of ketamine to inhibit platelet aggregate formation on the surface of the construct which could play an important role in artefactually altering the size and structure of thrombi seen *in vivo* mice models. In summary, although this project has reached a milestone in fabricating a new TEBV model and investigating its functionality using a newly designed testing platform, these findings require further investigations to more adequately assess how the anti-aggregatory properties of the TEBV model functions to inhibit platelet activation.

Chapter 7

References

Adams, R.L.C., Bird, R.J., 2009. Review article: Coagulation cascade and therapeutics update: Relevance to nephrology. Part 1: Overview of coagulation, thrombophilias and history of anticoagulants. Nephrology 14, 462–470.

Agarwal, S., Wendorff, J.H., Greiner, A., 2008. Use of electrospinning technique for biomedical applications. Polymer 49, 5603–5621.

Akata, T., Izumi, K., Nakashima, M., 2001. Mechanisms of direct inhibitory action of ketamine on vascular smooth muscle in mesenteric resistance arteries. Anesthesiology 95, 452–62.

Alberts, B., Johnson, A., Lewis, J., Raff, M., Roberts, K., Walter, P., 2002. The Extracellular Matrix of Animals.

Alexander, J.S., Elrod, J.W., 2002. Extracellular matrix, junctional integrity and matrix metalloproteinase interactions in endothelial permeability regulation. J. Anat. 200, 561–574.

Armstrong, P.C.J., Dhanji, A.-R., Truss, N.J., Zain, Z.N.M., Tucker, A.T., Mitchell, J.A., Warner, T.D., 2009. Utility of 96-well plate aggregometry and measurement of thrombi adhesion to determine aspirin and clopidogrel effectiveness. Thromb. Haemost. 102, 772–778.

Atkinson, P.M., Taylor, D.I., Chetty, N., 1985. Inhibition of platelet aggregation by ketamine hydrochloride. Thromb Res 40, 227–34.

Auger, F.A., D'Orléans-Juste, P., Germain, L., 2007. Adventitia contribution to vascular contraction: Hints provided by tissue-engineered substitutes. Cardiovasc. Res. 75, 669–678.

Auger, J.M., Kuijpers, M.J.E., Senis, Y.A., Watson, S.P., Heemskerk, J.W.M., 2005. Adhesion of human and mouse platelets to collagen under shear: a unifying model. FASEB J. Off. Publ. Fed. Am. Soc. Exp. Biol. 19, 825–827.

Authi, K.S., Crawford, N., 1985. Inositol 1,4,5-trisphosphate-induced release of sequestered Ca2+ from highly purified human platelet intracellular membranes. Biochem. J. 230, 247–253.

Banerjee, D., Mazumder, S., Sinha, A.K., 2014. The role of inhibition of nitric oxide synthesis in the aggregation of platelets due to the stimulated production of thromboxane A2. Blood Coagul. Fibrinolysis Int. J. Haemost. Thromb. 25, 585–591.

Bartha, K., Müller-Peddinghaus, R., Van Rooijen, L.A., 1989. Bradykinin and thrombin effects on polyphosphoinositide hydrolysis and prostacyclin production in endothelial cells. Biochem. J. 263, 149–155.

Bates, S.M., Weitz, J.I., 2005. Coagulation Assays. Circulation 112, e53–e60.

Beamish, J.A., He, P., Kottke-Marchant, K., Marchant, R.E., 2010. Molecular Regulation of Contractile Smooth Muscle Cell Phenotype: Implications for Vascular Tissue Engineering. Tissue Eng. Part B Rev. 16, 467–491.

Bellido-Martín, L., Chen, V., Jasuja, R., Furie, B., Furie, B.C., 2011a. Imaging fibrin formation and platelet and endothelial cell activation in vivo. Thromb. Haemost. 105, 776–782.

Bellido-Martín, L., Chen, V., Jasuja, R., Furie, B., Furie, B.C., 2011b. Imaging fibrin formation and platelet and endothelial cell activation in vivo. Thromb. Haemost. 105, 776–782.

Bender, M., Hagedorn, I., Nieswandt, B., 2011. Genetic and antibody-induced glycoprotein VI deficiency equally protects mice from mechanically and FeCl3-induced thrombosis. J. Thromb. Haemost. 9, 1423–1426.

Bergqvist, D., McKenzie, F.N., Arfors, K.E., 1974. Influence of various anaesthetic agents on the formation and stability of haemostatic plugs in the rabbit mesentery. Ups. J. Med. Sci. 79, 39–44.

Bertanha, M., Moroz, A., Almeida, R., Alves, F.C., Acorci Valério, M.J., Moura, R., Domingues, M.A.C., Sobreira, M.L., Deffune, E., 2014. Tissue-engineered blood vessel substitute by reconstruction of endothelium using mesenchymal stem cells induced by platelet growth factors. J. Vasc. Surg. 59, 1677–1685.

Bevers, E.M., Comfurius, P., van Rijn, J.L., Hemker, H.C., Zwaal, R.F., 1982. Generation of prothrombin-converting activity and the exposure of phosphatidylserine at the outer surface of platelets. Eur. J. Biochem. 122, 429–436.

Bianchini, M., Jamasbi, J., Weber, C., Siess, W., Megens, R.T., 2015. High-resolution optical imaging modalities for atherothrombosis research (Abstract). Presented at the Focus on Microscopy 2015, FOM, Germany.

Boccafoschi, F., Habermehl, J., Vesentini, S., Mantovani, D., 2005. Biological performances of collagen-based scaffolds for vascular tissue engineering. Biomaterials, Dedicated to Canadian Biomaterials ResearchDedicated to Canadian Biomaterials Research 26, 7410–7417.

Boehme, M.W., Raeth, U., Scherbaum, W.A., Galle, P.R., Stremmel, W., 2000. Interaction of endothelial cells and neutrophils in vitro: kinetics of thrombomodulin, intercellular adhesion molecule-1 (ICAM-1), E-selectin, and vascular cell adhesion molecule-1 (VCAM-1): implications for the relevance as serological disease activity markers in vasculitides. Clin. Exp. Immunol. 119, 250–254.

Boland, E.D., Matthews, J.A., Pawlowski, K.J., Simpson, D.G., Wnek, G.E., Bowlin, G.L., 2004. Electrospinning collagen and elastin: preliminary vascular tissue engineering. Front Biosci 9, 1422–32.

Bonnard, T., Hagemeyer, C.E., 2015. Ferric Chloride-induced Thrombosis Mouse Model on Carotid Artery and Mesentery Vessel. JoVE J. Vis. Exp. e52838–e52838.

Boucher, J., Simard, É., Froehlich, U., D'Orléans-Juste, P., Grandbois, M., 2015. Using carboxyfluorescein diacetate succinimidyl ester to monitor intracellular protein glycation. Anal. Biochem. 478, 73–81.

Bouis, D., Hospers, G.A., Meijer, C., Molema, G., Mulder, N.H., 2001. Endothelium in vitro: a review of human vascular endothelial cell lines for blood vessel-related research. Angiogenesis 4, 91–102.

Braziulis, E., Diezi, M., Biedermann, T., Pontiggia, L., Schmucki, M., Hartmann-Fritsch, F., Luginbuhl, J., Schiestl, C., Meuli, M., Reichmann, E., 2012. Modified Plastic Compression of Collagen Hydrogels Provides an Ideal Matrix for Clinically Applicable Skin Substitutes. Tissue Eng. Part C-Methods 18, 464–474.

Bredt, D.S., Snyder, S.H., 1994. Nitric oxide: a physiologic messenger molecule. Annu. Rev. Biochem. 63, 175–195.

Bunting, S., Moncada, S., Vane, J.R., 1983. The prostacyclin--thromboxane A2 balance: pathophysiological and therapeutic implications. Br. Med. Bull. 39, 271–276.

Butenas, S., Orfeo, T., Mann, K.G., 2009. Tissue Factor in Coagulation: Which? Where? When? Arterioscler. Thromb. Vasc. Biol. 29, 1989–1996.

Buttafoco, L., Kolkman, N.G., Engbers-Buijtenhuijs, P., Poot, A.A., Dijkstra, P.J., Vermes, I., Feijen, J., 2006. Electrospinning of collagen and elastin for tissue engineering applications. Biomaterials 27, 724–34.

Carpenter, S.L., Mathew, P., 2008. Alpha2-antiplasmin and its deficiency: fibrinolysis out of balance. Haemoph. Off. J. World Fed. Hemoph. 14, 1250–1254.

Cârţână, T., Săftoiu, A., Gruionu, L.G., Gheonea, D.I., Pirici, D., Georgescu, C.V., Ciocâlteu, A., Gruionu, G., 2012. Confocal Laser Endomicroscopy for the Morphometric Evaluation of Microvessels in Human Colorectal Cancer Using Targeted Anti-CD31 Antibodies. PLOS ONE 7, e52815.

Carter, T.D., Hallam, T.J., Cusack, N.J., Pearson, J.D., 1988. Regulation of P2y-purinoceptor-mediated prostacyclin release from human endothelial cells by cytoplasmic calcium concentration. Br. J. Pharmacol. 95, 1181–1190.

Caughey, G.E., Cleland, L.G., Gamble, J.R., James, M.J., 2001. Up-regulation of Endothelial Cyclooxygenase-2 and Prostanoid Synthesis by Platelets ROLE OF THROMBOXANE A2. J. Biol. Chem. 276, 37839–37845.

Chan, M.V., Warner, T.D., 2012. Standardised optical multichannel (optimul) platelet aggregometry using high-speed shaking and fixed time point readings. Platelets 23, 404–408.

Chang, Y., Chen, T.-L., Wu, G.-J., Hsiao, G., Shen, M.-Y., Lin, K.-H., Chou, D.-S., Lin, C.-H., Sheu, J.-R., 2004. Mechanisms involved in the antiplatelet activity of ketamine in human platelets. J. Biomed. Sci. 11, 764–772.

Chan-Park, M.B., Shen, J.Y., Cao, Y., Xiong, Y., Liu, Y., Rayatpisheh, S., Kang, G.C., Greisler, H.P., 2009. Biomimetic control of vascular smooth muscle cell morphology and phenotype for functional tissue-engineered small-diameter blood vessels. J Biomed Mater Res A 88, 1104–21.

Chapin, J.C., Hajjar, K.A., 2015. Fibrinolysis and the control of blood coagulation. Blood Rev. 29, 17–24.

Cheli, Y., Jensen, D., Marchese, P., Habart, D., Wiltshire, T., Cooke, M., Fernandez, J.A., Ware, J., Ruggeri, Z.M., Kunicki, T.J., 2008. The Modifier of hemostasis (Mh) locus on chromosome 4 controls in vivo hemostasis of Gp6-/- mice. Blood 111, 1266–1273.

Chen, K., Li, W., Major, J., Rahaman, S.O., Febbraio, M., Silverstein, R.L., 2011. Vav guanine nucleotide exchange factors link hyperlipidemia and a prothrombotic state. Blood 117, 5744–5750.

Chen, R.-M., Chen, T.-L., Lin, Y.-L., Chen, T.-G., Tai, Y.-T., 2005. Ketamine reduces nitric oxide biosynthesis in human umbilical vein endothelial cells by down-regulating endothelial nitric oxide synthase expression and intracellular calcium levels. Crit. Care Med. 33, 1044–1049.

Chetprayoon, P., Matsusaki, M., Akashi, M., 2015. Three-dimensional human arterial wall models for in vitro permeability assessment of drug and nanocarriers. Biochem Biophys Res Commun 456, 392–7.

Chew, S.Y., Mi, R., Hoke, A., Leong, K.W., 2008. The effect of the alignment of electrospun fibrous scaffolds on Schwann cell maturation. Biomaterials 29, 653–61.

Chung, B.J., Robertson, A.M., Peters, D.G., 2003. The numerical design of a parallel plate flow chamber for investigation of endothelial cell response to shear stress. Comput. Struct., K.J Bathe 60th Anniversary Issue 81, 535–546.

Ciciliano, J.C., Sakurai, Y., Myers, D.R., Fay, M.E., Hechler, B., Meeks, S., Li, R., Dixon, J.B., Lyon, L.A., Gachet, C., Lam, W.A., 2015. Resolving the multifaceted mechanisms of the ferric chloride thrombosis model using an interdisciplinary microfluidic approach. Blood 126, 817–824.

Clemetson, K.J., Clemetson, J.M., 2001. Platelet collagen receptors. Thromb. Haemost. 86, 189–197.

Cooper, T.P., Sefton, M.V., 2011. Fibronectin coating of collagen modules increases in vivo HUVEC survival and vessel formation in SCID mice. Acta Biomater 7, 1072–83.

Crosas-Molist, E., Meirelles, T., López-Luque, J., Serra-Peinado, C., Selva, J., Caja, L., Gorbenko del Blanco, D., Uriarte, J.J., Bertran, E., Mendizábal, Y., Hernández, V., García-Calero, C., Busnadiego, O., Condom, E., Toral, D., Castellà, M., Forteza, A., Navajas, D., Sarri, E., Rodríguez-Pascual, F., Dietz, H.C., Fabregat, I., Egea, G., 2015. Vascular Smooth Muscle Cell Phenotypic Changes in Patients With Marfan SyndromeSignificance. Arterioscler. Thromb. Vasc. Biol. 35, 960–972.

Daniel, J.M., Sedding, D.G., 2011. Circulating smooth muscle progenitor cells in arterial remodeling. J Mol Cell Cardiol 50, 273–9.

de Wit, C., Hoepfl, B., Wölfle, S.E., 2006. Endothelial mediators and communication through vascular gap junctions. Biol. Chem. 387, 3–9.

Denis, C.V., Dubois, C., Brass, L.F., Heemskerk, J.W.M., Lenting, P.J., Biorheology Subcommittee of the Ssc of the Isth, 2011. Towards standardization of in vivo thrombosis studies in mice. J. Thromb. Haemost. 9, 1641–1644.

Dong, J., Moake, J.L., Nolasco, L., Bernardo, A., Arceneaux, W., Shrimpton, C.N., Schade, A.J., McIntire, L.V., Fujikawa, K., López, J.A., 2002. ADAMTS-13 rapidly cleaves newly secreted ultralarge von Willebrand factor multimers on the endothelial surface under flowing conditions. Blood 100, 4033–4039.

Dörmann, D., Kardoeus, J., Zimmermann, R.E., Kehrel, B., 1998. Flow cytometric analysis of agonist-induced annexin V, factor Va and factor Xa binding to human platelets. Platelets 9, 171–177.

Dorweiler, B., Torzewski, M., Dahm, M., Ochsenhirt, V., Lehr, H.A., Lackner, K.J., Vahl, C.F., 2006. A novel in vitro model for the study of plaque development in atherosclerosis. Thromb Haemost 95, 182–9.

Dovlatova, N., 2015. Current status and future prospects for platelet function testing in the diagnosis of inherited bleeding disorders. Br. J. Haematol. 170, 150–161.

Dubois, C., Panicot-Dubois, L., Merrill-Skoloff, G., Furie, B., Furie, B.C., 2006a. Glycoprotein VI-dependent and -independent pathways of thrombus formation in vivo. Blood 107, 3902–3906.

Dubois, C., Panicot-Dubois, L., Merrill-Skoloff, G., Furie, B., Furie, B.C., 2006b. Glycoprotein VI-dependent and -independent pathways of thrombus formation in vivo. Blood 107, 3902–3906.

Dwyer, S.D., Meyers, K.M., 1986. Anesthetics and anticoagulants used in the preparation of rat platelet-rich-plasma alter rat platelet aggregation. Thromb. Res. 42, 139–151.

E. Niklason, L., S. Langer, R., 1997. Advances in tissue engineering of blood vessels and other tissues. Transpl. Immunol. 5, 303–306.

Eckly, A., Hechler, B., Freund, M., Zerr, M., Cazenave, J.-P., Lanza, F., Mangin, P.H., Gachet, C., 2011. Mechanisms underlying FeCl3-induced arterial thrombosis. J. Thromb. Haemost. 9, 779–789.

Esmon, C.T., Esmon, N.L., Harris, K.W., 1982. Complex formation between thrombin and thrombomodulin inhibits both thrombin-catalyzed fibrin formation and factor V activation. J. Biol. Chem. 257, 7944–7947.

Falati, S., Gross, P., Merrill-Skoloff, G., Furie, B.C., Furie, B., 2002. Real-time in vivo imaging of platelets, tissue factor and fibrin during arterial thrombus formation in the mouse. Nat Med 8, 1175–81.

Farndale, A.H.& W., 2009. Structural Insights into the Interactions between Platelet Receptors and Fibrillar Collagen. J Biol Chem 284, 19781–19785.

Farndale, R.W., Lisman, T., Bihan, D., Hamaia, S., Smerling, C.S., Pugh, N., Konitsiotis, A., Leitinger, B., de Groot, P.G., Jarvis, G.E., Raynal, N., 2008. Cell-collagen interactions: the use of peptide Toolkits to investigate collagen-receptor interactions. Biochem Soc Trans 36, 241–50.

Fernandez, C.E., Achneck, H.E., Reichert, W.M., Truskey, G.A., 2014. Biological and engineering design considerations for vascular tissue engineered blood vessels (TEBVs). Curr. Opin. Chem. Eng. 3, 83–90.

Fiedler, U., Christian, S., Koidl, S., Kerjaschki, D., Emmett, M.S., Bates, D.O., Christofori, G., Augustin, H.G., 2006. The sialomucin CD34 is a marker of lymphatic endothelial cells in human tumors. Am. J. Pathol. 168, 1045–1053.

Förstermann, U., Schmidt, H.H., Pollock, J.S., Sheng, H., Mitchell, J.A., Warner, T.D., Nakane, M., Murad, F., 1991. Isoforms of nitric oxide synthase. Characterization and purification from different cell types. Biochem. Pharmacol. 42, 1849–1857.

Franchini, M., Mannucci, P.M., 2008. Venous and arterial thrombosis: Different sides of the same coin? Eur. J. Intern. Med. 19, 476–481.

Freedman, J.E., Loscalzo, J., Barnard, M.R., Alpert, C., Keaney, J.F., Michelson, A.D., 1997. Nitric oxide released from activated platelets inhibits platelet recruitment. J. Clin. Invest. 100, 350–356.

Freedman, J.E., Sauter, R., Battinelli, E.M., Ault, K., Knowles, C., Huang, P.L., Loscalzo, J., 1999. Deficient platelet-derived nitric oxide and enhanced hemostasis in mice lacking the NOSIII gene. Circ. Res. 84, 1416–1421.

Fung, C.Y., Jones, S., Ntrakwah, A., Naseem, K.M., Farndale, R.W., Mahaut-Smith, M.P., 2012. Platelet Ca(2+) responses coupled to glycoprotein VI and Toll-like receptors persist in the presence of endothelial-derived inhibitors: roles for secondary activation of P2X1 receptors and release from intracellular Ca(2+) stores. Blood 119, 3613–21.

Furie, B., Furie, B.C., 2008. Mechanisms of thrombus formation. N Engl J Med 359, 938–49.

Furie, B., Furie, B.C., 2007. In vivo thrombus formation. J Thromb Haemost 5 Suppl 1, 12–7.

Furie, B., Furie, B.C., 2005. Thrombus formation in vivo. J Clin Invest 115, 3355–62.

Furman, M.I., Krueger, L.A., Frelinger, A.L., Barnard, M.R., Mascelli, M.A., Nakada, M.T., Michelson, A.D., 2000. GPIIb-IIIa antagonist-induced reduction in platelet surface factor V/Va binding and phosphatidylserine expression in whole blood. Thromb. Haemost. 84, 492–498.

Gale, A.J., 2011. Current Understanding of Hemostasis. Toxicol. Pathol. 39, 273–280.

Gantenbein-Ritter, B., Sprecher, C.M., Chan, S., Illien-Jünger, S., Grad, S., 2011. Confocal imaging protocols for live/dead staining in three-dimensional carriers. Methods Mol. Biol. Clifton NJ 740, 127–140.

Geckil, H., Xu, F., Zhang, X., Moon, S., Demirci, U., 2010. Engineering hydrogels as extracellular matrix mimics. Nanomed. 5, 469–484.

Geelhoed, W.J., Moroni, L., Rotmans, J.I., 2017. Utilizing the Foreign Body Response to Grow Tissue Engineered Blood Vessels in Vivo. J Cardiovasc. Transl. Res. 10, 167–179.

Gibbins, J.M., Mahaut-Smith, M.P. (Eds.), 2004. Platelets and Megakaryocytes: Volume 1: Functional Assays, 2004 edition. ed. Humana Press, Totowa, N.J.

Gilio, K., Harper, M.T., Cosemans, J.M.E.M., Konopatskaya, O., Munnix, I.C.A., Prinzen, L., Leitges, M., Liu, Q., Molkentin, J.D., Heemskerk, J.W.M., Poole, A.W., 2010. Functional divergence of platelet protein kinase C (PKC) isoforms in thrombus formation on collagen. J. Biol. Chem. 285, 23410–23419.

Goonoo, N., Bhaw-Luximon, A., Bowlin, G.L., Jhurry, D., 2013. An assessment of biopolymer- and synthetic polymer-based scaffolds for bone and vascular tissue engineering. Polym. Int. 62, 523–533.

Gresele, P., Kleiman, N.S., Lopez, J.A., Page, C.P., 2017. Platelets in Thrombotic and Non-Thrombotic Disorders: Pathophysiology, Pharmacology and Therapeutics: an Update. Springer.

Gross, P.L., Aird, W.C., 2000. The Endothelium and Thrombosis. Semin. Thromb. Hemost. 26, 463–478.

Grynkiewicz, G., Poenie, M., Tsien, R.Y., 1985. A new generation of Ca2+ indicators with greatly improved fluorescence properties. J Biol Chem 260, 3440–50.

Guénet, J.L., 2005. The mouse genome. Genome Res. 15, 1729–1740.

Gundy, S., Manning, G., O'Connell, E., Ellä, V., Harwoko, M.S., Rochev, Y., Smith, T., Barron, V., 2008. Human coronary artery smooth muscle cell response to a novel PLA textile/fibrin gel composite scaffold. Acta Biomater. 4, 1734–1744.

Guthold, M., Liu, W., Sparks, E.A., Jawerth, L.M., Peng, L., Falvo, M., Superfine, R., Hantgan, R.R., Lord, S.T., 2007. A Comparison of the Mechanical and Structural Properties of Fibrin Fibers with Other Protein Fibers. Cell Biochem. Biophys. 49, 165–181.

Gutierrez-Pajares, J.L., Iturrieta, J., Dulam, V., Wang, Y., Pavlides, S., Malacari, G., Lisanti, M.P., Frank, P.G., 2015. Caveolin-3 Promotes a Vascular Smooth Muscle Contractile Phenotype. Front. Cardiovasc. Med. 2.

Harper, A.G., Mason, M.J., Sage, S.O., 2009. A key role for dense granule secretion in potentiation of the Ca2+ signal arising from store-operated calcium entry in human platelets. Cell Calcium 45, 413–20.

Hasan, A., Memic, A., Annabi, N., Hossain, M., Paul, A., Dokmeci, M.R., Dehghani, F., Khademhosseini, A., 2014. Electrospun scaffolds for tissue engineering of vascular grafts. Acta Biomater. 10, 11–25.

Heemskerk, J.W., Mattheij, N.J., Cosemans, J.M., 2013. Platelet-based coagulation: different populations, different functions. J Thromb Haemost 11, 2–16.

Heemskerk, J.W., Vuist, W.M., Feijge, M.A., Reutelingsperger, C.P., Lindhout, T., 1997. Collagen but not fibrinogen surfaces induce bleb formation, exposure of phosphatidylserine, and procoagulant activity of adherent platelets: evidence for regulation by protein tyrosine kinase-dependent Ca2+ responses. Blood 90, 2615–2625.

Heemskerk, J.W.M., Sakariassen, K.S., Zwaginga, J.J., Brass, L.F., Jackson, S.P., Farndale, R.W., Biorheology Subcommittee of the Ssc of the Isth, 2011. Collagen surfaces to measure thrombus formation under flow: possibilities for standardization. J. Thromb. Haemost. 9, 856–858.

Heit, J.A., Spencer, F.A., White, R.H., 2016. The epidemiology of venous thromboembolism. J. Thromb. Thrombolysis 41, 3–14.

Heizer, M.L., McKinney, J.S., Ellis, E.F., 1991. 14,15-Epoxyeicosatrienoic acid inhibits platelet aggregation in mouse cerebral arterioles. Stroke 22, 1389–1393.

Herring, M., Gardner, A., Glover, J., 1978. A single-staged technique for seeding vascular grafts with autogenous endothelium. Surgery 84, 498–504.

Hoenig, M.R., Campbell, G.R., Rolfe, B.E., Campbell, J.H., 2005. Tissue-Engineered Blood Vessels. Arterioscler. Thromb. Vasc. Biol. 25, 1128–1134.

Hoerstrup, S.P., Zünd, G., Sodian, R., Schnell, A.M., Grünenfelder, J., Turina, M.I., 2001. Tissue engineering of small caliber vascular grafts. Eur. J. Cardio-Thorac. Surg. Off. J. Eur. Assoc. Cardio-Thorac. Surg. 20, 164–169.

Hu, K.K., Shi, H., Zhu, J., Deng, D., Zhou, G.D., Zhang, W.J., Cao, Y.L., Liu, W., 2010. Compressed collagen gel as the scaffold for skin engineering. Biomed. Microdevices 12, 627–635.

Iafrati, M.D., Vitseva, O., Tanriverdi, K., Blair, P., Rex, S., Chakrabarti, S., Varghese, S., Freedman, J.E., 2005. Compensatory mechanisms influence hemostasis in setting of eNOS deficiency. Am. J. Physiol. Heart Circ. Physiol. 288, H1627-1632.

Isenberg, B.C., Williams, C., Tranquillo, R.T., 2006. Small-diameter artificial arteries engineered in vitro. Circ Res 98, 25–35.

Ishii, H., Uchiyama, H., Kazama, M., 1991. Soluble thrombomodulin antigen in conditioned medium is increased by damage of endothelial cells. Thromb. Haemost. 65, 618–623.

Jaffe, R., Deykin, D., 1974. Evidence for a Structural Requirement for the Aggregation of Platelets by Collagen. J. Clin. Invest. 53, 875.

Janssen, B.J., De Celle, T., Debets, J.J., Brouns, A.E., Callahan, M.F., Smith, T.L., 2004. Effects of anesthetics on systemic hemodynamics in mice. Am J Physiol Heart Circ Physiol 287, H1618-24.

Johnston-Cox, H.A., Yang, D., Ravid, K., 2011. Physiological implications of adenosine receptor-mediated platelet aggregation. J. Cell. Physiol. 226, 46–51.

Jung, Y., Ji, H., Chen, Z., Fai Chan, H., Atchison, L., Klitzman, B., Truskey, G., Leong, K.W., 2015. Scaffold-free, Human Mesenchymal Stem Cell-Based Tissue Engineered Blood Vessels. Sci. Rep. 5, 15116.

Kawamoto, Y., Kaibara, M., 1990. Procoagulant activity of collagen. Effect of difference in type and structure of collagen. Biochim. Biophys. Acta BBA - Gen. Subj. 1035, 361–368.

Kelm, J.M., Lorber, V., Snedeker, J.G., Schmidt, D., Broggini-Tenzer, A., Weisstanner, M., Odermatt, B., Mol, A., Zünd, G., Hoerstrup, S.P., 2010. A novel concept for scaffold-free vessel tissue engineering: self-assembly of microtissue building blocks. J. Biotechnol. 148, 46–55.

Kim, B.S., Putnam, A.J., Kulik, T.J., Mooney, D.J., 1998. Optimizing seeding and culture methods to engineer smooth muscle tissue on biodegradable polymer matrices. Biotechnol. Bioeng. 57, 46–54.

Kim, I., Moon, S.-O., Kim, S.H., Kim, H.J., Koh, Y.S., Koh, G.Y., 2001. Vascular Endothelial Growth Factor Expression of Intercellular Adhesion Molecule 1 (ICAM-1), Vascular Cell Adhesion Molecule 1 (VCAM-1), and E-selectin through Nuclear Factor-κB Activation in Endothelial Cells. J. Biol. Chem. 276, 7614–7620.

Kim, S., Cipolla, L., Guidetti, G., Okigaki, M., Jin, J., Torti, M., Kunapuli, S.P., 2013. Distinct role of Pyk2 in mediating thromboxane generation downstream of both G12/13 and integrin alphaIIbbeta3 in platelets. J Biol Chem 288, 18194–203.

Kjaergaard, A.G., Dige, A., Krog, J., Tønnesen, E., Wogensen, L., 2013. Soluble adhesion molecules correlate with surface expression in an in vitro model of endothelial activation. Basic Clin. Pharmacol. Toxicol. 113, 273–279.

Kleschyov, A.L., Muller, B., Schott, C., Stoclet, J.C., 1998. Role of adventitial nitric oxide in vascular hyporeactivity induced by lipopolysaccharide in rat aorta. Br. J. Pharmacol. 124, 623–626.

Kolev, K., Longstaff, C., 2016. Bleeding related to disturbed fibrinolysis. Br. J. Haematol. 175, 12–23.

Konstantinides, S., Ware, J., Marchese, P., Almus-Jacobs, F., Loskutoff, D.J., Ruggeri, Z.M., 2006. Distinct antithrombotic consequences of platelet glycoprotein Ibalpha and VI deficiency in a mouse model of arterial thrombosis. J. Thromb. Haemost. JTH 4, 2014–2021.

Krawiec, J.T., Vorp, D.A., 2012. Adult stem cell-based tissue engineered blood vessels: A review. Biomaterials 33, 3388–3400.

Kuijpers, M.J.E., Pozgajova, M., Cosemans, J.M.E.M., Munnix, I.C.A., Eckes, B., Nieswandt, B., Heemskerk, J.W.M., 2007. Role of murine integrin alpha2beta1 in thrombus stabilization and embolization: contribution of thromboxane A2. Thromb. Haemost. 98, 1072–1080.

Kulkarni, S., Jackson, S.P., 2004. Platelet factor XIII and calpain negatively regulate integrin alphaIIbbeta3 adhesive function and thrombus growth. J. Biol. Chem. 279, 30697–30706.

Kurz, K.D., Main, B.W., Sandusky, G.E., 1990. Rat model of arterial thrombosis induced by ferric chloride. Thromb Res 60, 269–80.

Laco, F., Grant, M.H., Black, R.A., 2013. Collagen-nanofiber hydrogel composites promote contact guidance of human lymphatic microvascular endothelial cells and directed capillary tube formation. J Biomed Mater Res A 101, 1787–99.

Lages, B., Weiss, H.J., 1988. Heterogeneous defects of platelet secretion and responses to weak agonists in patients with bleeding disorders. Br. J. Haematol. 68, 53–62.

Laine, P., Naukkarinen, A., Heikkilä, L., Penttilä, A., Kovanen, P.T., 2000. Adventitial mast cells connect with sensory nerve fibers in atherosclerotic coronary arteries. Circulation 101, 1665–1669.

Langer, R., Vacanti, J.P., 1993. Tissue engineering. Science 260, 920–926.

LaValley, D.J., Reinhart-King, C.A., 2014. Matrix stiffening in the formation of blood vessels. Adv. Regen. Biol. 1, 25247.

Lecut, C., Schoolmeester, A., Kuijpers, M.J.E., Broers, J.L.V., van Zandvoort, M.A.M.J., Vanhoorelbeke, K., Deckmyn, H., Jandrot-Perrus, M., Heemskerk, J.W.M., 2004. Principal role of glycoprotein VI in alpha2beta1 and alphaIIbbeta3 activation during collagen-induced thrombus formation. Arterioscler. Thromb. Vasc. Biol. 24, 1727–1733.

Ledford-Kraemer, M.R., 2010. Analysis of von Willebrand factor structure by multimer analysis. Am. J. Hematol. 85, 510–514.

Levick, S.P., Murray, D.B., Janicki, J.S., Brower, G.L., 2010. Sympathetic Nervous System Modulation of Inflammation and Remodeling in the Hypertensive Heart. Hypertension 55, 270–276.

Levis HJ, B.R., Daniels JT, 2010. Plastic compressed collagen as a biomimetic substrate for human limbal epithelial cell culture. Biomaterials 30, 7726–7737.

L'Heureux, N., Pâquet, S., Labbé, R., Germain, L., Auger, F.A., 1998. A completely biological tissue-engineered human blood vessel. FASEB J. Off. Publ. Fed. Am. Soc. Exp. Biol. 12, 47–56.

L'Heureux, N., Stoclet, J.C., Auger, F.A., Lagaud, G.J., Germain, L., Andriantsitohaina, R., 2001. A human tissue-engineered vascular media: a new model for pharmacological studies of contractile responses. FASEB J 15, 515–24.

Li, R., Fries, S., Li, X., Grosser, T., Diamond, S.L., 2013. Microfluidic assay of platelet deposition on collagen by perfusion of whole blood from healthy individuals taking aspirin. Clin. Chem. 59, 1195–1204.

Li, W., Febbraio, M., Reddy, S.P., Yu, D.-Y., Yamamoto, M., Silverstein, R.L., 2010. CD36 participates in a signaling pathway that regulates ROS formation in murine VSMCs. J. Clin. Invest. 120, 3996–4006.

Li, W., McIntyre, T.M., Silverstein, R.L., 2013. Ferric chloride-induced murine carotid arterial injury: A model of redox pathology. Redox Biol. 1, 50–55.

Li, Z., Delaney, M.K., O'Brien, K.A., Du, X., 2010. Signaling during platelet adhesion and activation. Arterioscler. Thromb. Vasc. Biol. 30, 2341–2349.

Liao, H., He, H., Chen, Y., Zeng, F., Huang, J., Wu, L., Chen, Y., 2014. Effects of long-term serial cell passaging on cell spreading, migration, and cell-surface ultrastructures of cultured vascular endothelial cells. Cytotechnology 66, 229–238.

Lin, L., Ding, W.-H., Jiang, W., Zhang, Y.-G., Qi, Y.-F., Yuan, W.-J., Tang, C.-S., 2004. Urotensin-II activates L-arginine/nitric oxide pathway in isolated rat aortic adventitia. Peptides 25, 1977–1984.

Liu, S.Q., Tay, R., Khan, M., Ee, P.L.R., Hedrick, J.L., Yang, Y.Y., 2009. Synthetic hydrogels for controlled stem cell differentiation. Soft Matter 6, 67–81.

Liu, X., Wu, H., Byrne, M., Krane, S., Jaenisch, R., 1997. Type III collagen is crucial for collagen I fibrillogenesis and for normal cardiovascular development. Proc Natl Acad Sci U A 94, 1852–6.

Lodish, H., Berk, A., Zipursky, S.L., Matsudaira, P., Baltimore, D., Darnell, J., 2000. Collagen: The Fibrous Proteins of the Matrix.

Lopez, &, Zheng, 2013. Synthetic microvessels. J Thromb Haemost 11 Suppl 1, 67–74.

Lordkipanidzé, M., Lowe, G.C., Kirkby, N.S., Chan, M.V., Lundberg, M.H., Morgan, N.V., Bem, D., Nisar, S.P., Leo, V.C., Jones, M.L., Mundell, S.J., Daly, M.E., Mumford, A.D., Warner, T.D., Watson, S.P., UK Genotyping and Phenotyping of Platelets Study Group, 2014. Characterization of multiple platelet activation pathways in patients with bleeding as a high-throughput screening option: use of 96-well Optimul assay. Blood 123, e11-22.

Ma, Z., He, W., Yong, T., Ramakrishna, S., 2005. Grafting of gelatin on electrospun poly(caprolactone) nanofibers to improve endothelial cell spreading and proliferation and to control cell Orientation. Tissue Eng. 11, 1149–1158.

Mainz, E.R., Gunasekara, D.B., Caruso, G., Jensen, D.T., Hulvey, M.K., Silva, J.A.F. da, Metto, E.C., Culbertson, A.H., Culbertson, C.T., Lunte, S.M., 2012. Monitoring intracellular nitric oxide production using microchip electrophoresis and laser-induced fluorescence detection. Anal. Methods 4, 414–420.

Manon-Jensen, T., Kjeld, N.G., Karsdal, M.A., 2016. Collagen-mediated hemostasis. J. Thromb. Haemost. 14, 438–448.

Marcus, A.J., Broekman, M.J., Drosopoulos, J.H.F., Olson, K.E., Islam, N., Pinsky, D.J., Levi, R., 2005. Role of CD39 (NTPDase-1) in thromboregulation, cerebroprotection, and cardioprotection. Semin. Thromb. Hemost. 31, 234–246.

Masedunskas, A., Milberg, O., Porat-Shliom, N., Sramkova, M., Wigand, T., Amornphimoltham, P., Weigert, R., 2012. Intravital microscopy. Bioarchitecture 2, 143–157.

Massberg, S., Gawaz, M., Grüner, S., Schulte, V., Konrad, I., Zohlnhöfer, D., Heinzmann, U., Nieswandt, B., 2003. A Crucial Role of Glycoprotein VI for Platelet Recruitment to the Injured Arterial Wall In Vivo. J. Exp. Med. 197, 41–49.

Mayer, B., Schmid, M., Klatt, P., Schmidt, K., 1993. Reversible inactivation of endothelial nitric oxide synthase by NG-nitro-L-arginine. FEBS Lett. 333, 203–206.

McCullen, S.D., Stevens, D.R., Roberts, W.A., Clarke, L.I., Bernacki, S.H., Gorga, R.E., Loboa, E.G., 2007. Characterization of electrospun nanocomposite scaffolds and biocompatibility with adipose-derived human mesenchymal stem cells. Int J Nanomedicine 2, 253–63.

Mehrbod, M., Trisno, S., Mofrad, M.R.K., 2013. On the Activation of Integrin αIIbβ3: Outside-in and Inside-out Pathways. Biophys. J. 105, 1304–1315.

Menitove, J.E., Frenzke, M., Aster, R.H., 1984. Use of prostacyclin to inhibit activation of platelets during preparation of platelet concentrates. Transfusion (Paris) 24, 528–31.

Merten, M., Chow, T., Hellums, J.D., Thiagarajan, P., 2000. A New Role for P-Selectin in Shear-Induced Platelet Aggregation. Circulation 102, 2045–2050.

Metcalfe, C., Ramasubramoni, A., Pula, G., Harper, M.T., Mundell, S.J., Coxon, C.H., 2016. Thioredoxin Inhibitors Attenuate Platelet Function and Thrombus Formation. PLOS ONE 11, e0163006.

Michelson, A.D., 2004. Platelet function testing in cardiovascular diseases. Circulation 110, e489-493.

Mitchell, J.A., Ali, F., Bailey, L., Moreno, L., Harrington, L.S., 2008. Role of nitric oxide and prostacyclin as vasoactive hormones released by the endothelium. Exp. Physiol. 93, 141–147.

Mitchell, S.L., Niklason, L.E., 2003. Requirements for growing tissue-engineered vascular grafts. Cardiovasc. Pathol. Off. J. Soc. Cardiovasc. Pathol. 12, 59–64.

Mizuno, M., Tomizawa, A., Ohno, K., Jakubowski, J.A., Sugidachi, A., 2016. A Novel Model of Intravital Platelet Imaging Using CD41-ZsGreen1 Transgenic Rats. PloS One 11, e0154661.

Mo, X.M., Xu, C.Y., Kotaki, M., Ramakrishna, S., 2004. Electrospun P(LLA-CL) nanofiber: a biomimetic extracellular matrix for smooth muscle cell and endothelial cell proliferation. Biomaterials 25, 1883–1890.

Mumford, A.D., Frelinger, A.L., Gachet, C., Gresele, P., Noris, P., Harrison, P., Mezzano, D., 2015. A review of platelet secretion assays for the diagnosis of inherited platelet secretion disorders. Thromb. Haemost. 114, 14–25.

Murata, T., Ushikubi, F., Matsuoka, T., Hirata, M., Yamasaki, A., Sugimoto, Y., Ichikawa, A., Aze, Y., Tanaka, T., Yoshida, N., Ueno, A., Oh-ishi, S., Narumiya, S., 1997. Altered pain perception and inflammatory response in mice lacking prostacyclin receptor. Nature 388, 678–682.

Na, S., Meininger, G.A., Humphrey, J.D., 2007. A Theoretical Model for F-actin Remodeling in Vascular Smooth Muscle Cells Subjected to Cyclic Stretch. J. Theor. Biol. 246, 87–99.

Nakagawa, T., Hirakata, H., Sato, M., Nakamura, K., Hatano, Y., Nakamura, T., Fukuda, K., 2002. Ketamine suppresses platelet aggregation possibly by suppressed inositol triphosphate formation and subsequent suppression of cytosolic calcium increase. Anesthesiology 96, 1147–52.

Navarro-Núñez, L., Pollitt, A.Y., Lowe, K., Latif, A., Nash, G.B., Watson, S.P., 2015. Platelet Adhesion to Podoplanin Under Flow is Mediated by the Receptor CLEC-2 and Stabilised by Src/Syk-Dependent Platelet Signalling. Thromb. Haemost. 113, 1109–1120.

Nerem, R.M., Ensley, A.E., 2004. The tissue engineering of blood vessels and the heart. Am. J. Transplant. 4, 36–42.

Nerem, R.M., Seliktar, D., 2001. Vascular tissue engineering. Annu. Rev. Biomed. Eng. 3, 225–243.

Nieman, M.T., 2016. Protease activated receptors in hemostasis. Blood blood-2015-11-636472.

Niklason, L.E., Gao, J., Abbott, W.M., Hirschi, K.K., Houser, S., Marini, R., Langer, R., 1999. Functional arteries grown in vitro. Science 284, 489–493.

Niklason, L.E., Ratcliffe, A., Brockbank, K., Bruley, D.F., Kang, K.A., 2002. Bioreactors and bioprocessing: breakout session summary. Ann. N. Y. Acad. Sci. 961, 220–222.

Nisbet, D.R., Forsythe, J.S., Shen, W., Finkelstein, D.I., Horne, M.K., 2009. Review paper: a review of the cellular response on electrospun nanofibers for tissue engineering. J Biomater Appl 24, 7–29.

Ogawa, K., Tanaka, S., Murray, P.A., 2001. Inhibitory effects of etomidate and ketamine on endothelium-dependent relaxation in canine pulmonary artery. Anesthesiology 94, 668–677.

Owens, A.P., Lu, Y., Whinna, H.C., Gachet, C., Fay, W.P., Mackman, N., 2011. Towards a standardization of the murine ferric chloride-induced carotid arterial thrombosis model. J. Thromb. Haemost. JTH 9, 1862–1863.

Ozüyaman, B., Gödecke, A., Küsters, S., Kirchhoff, E., Scharf, R.E., Schrader, J., 2005. Endothelial nitric oxide synthase plays a minor role in inhibition of arterial thrombus formation. Thromb. Haemost. 93, 1161–1167.

Palmer, R.M., Ashton, D.S., Moncada, S., 1988. Vascular endothelial cells synthesize nitric oxide from L-arginine. Nature 333, 664–666.

Palta, S., Saroa, R., Palta, A., 2014. Overview of the coagulation system. Indian J. Anaesth. 58, 515–523.

Pandit A, L.E., 2005. Design of Bioreactors for Cardiovascular Applications. Top. Tissue Eng. 2.

Pankajakshan, D., Agrawal, D.K., 2010. Scaffolds in tissue engineering of blood vessels. Can. J. Physiol. Pharmacol. 88, 855–873.

Patel, A., Fine, B., Sandig, M., Mequanint, K., 2006. Elastin biosynthesis: The missing link in tissue-engineered blood vessels. Cardiovasc Res 71, 40–9.

Paul, S., Feoktistov, I., Hollister, A.S., Robertson, D., Biaggioni, I., 1990. Adenosine inhibits the rise in intracellular calcium and platelet aggregation produced by thrombin: evidence that both effects are coupled to adenylate cyclase. Mol. Pharmacol. 37, 870–875.

Peck, M., Gebhart, D., Dusserre, N., McAllister, T.N., L'Heureux, N., 2012. The evolution of vascular tissue engineering and current state of the art. Cells Tissues Organs 195, 144–158.

Peyton, S.R., Kim, P.D., Ghajar, C.M., Seliktar, D., Putnam, A.J., 2008. The Effects of Matrix Stiffness and RhoA on the Phenotypic Plasticity of Smooth Muscle Cells in a 3-D Biosynthetic Hydrogel System. Biomaterials 29, 2597–2607.

Pfeiffer, S., Leopold, E., Schmidt, K., Brunner, F., Mayer, B., 1996. Inhibition of nitric oxide synthesis by NG-nitro-L-arginine methyl ester (L-NAME): requirement for bioactivation to the free acid, NG-nitro-L-arginine. Br. J. Pharmacol. 118, 1433–1440.

Plante, G.E., 2002. Vascular response to stress in health and disease. Metabolism. 51, 25–30.

Preissner, K.T., Nawroth, P.P., Kanse, S.M., 2000. Vascular protease receptors: integrating haemostasis and endothelial cell functions. J. Pathol. 190, 360–372.

Pugh, N., Simpson, A.M.C., Smethurst, P.A., de Groot, P.G., Raynal, N., Farndale, R.W., 2010. Synergism between platelet collagen receptors defined using receptor-specific collagen-mimetic peptide substrata in flowing blood. Blood 115, 5069–5079.

Reidinger, A.Z., Rolle, M.W., 2014. Culture medium effects on vascular smooth muscle cell contractile protein expression and morphology in 2D v. 3D, in: 2014 40th Annual Northeast Bioengineering Conference (NEBEC). Presented at the 2014 40th Annual Northeast Bioengineering Conference (NEBEC), pp. 1–2.

Ren, L., Ma, D., Liu, B., Li, J., Chen, J., Yang, D., Gao, P., 2014. Preparation of Three-Dimensional Vascularized MSC Cell Sheet Constructs for Tissue Regeneration [WWW Document]. BioMed Res. Int. URL https://www.hindawi.com/journals/bmri/2014/301279/ (accessed 8.31.17).

Rensen, S.S.M., Doevendans, P. a. F.M., van Eys, G.J.J.M., 2007. Regulation and characteristics of vascular smooth muscle cell phenotypic diversity. Neth. Heart J. Mon. J. Neth. Soc. Cardiol. Neth. Heart Found. 15, 100–108.

Roest, M., Reininger, A., Zwaginga, J.J., King, M.R., Heemskerk, J.W.M., the Biorheology Subcommittee of the SSC of the ISTH, 2011. Flow chamber-based assays to measure thrombus formation in vitro: requirements for standardization. J. Thromb. Haemost. 9, 2322–2324.

Roh, J.D., Sawh-Martinez, R., Brennan, M.P., Jay, S.M., Devine, L., Rao, D.A., Yi, T., Mirensky, T.L., Nalbandian, A., Udelsman, B., Hibino, N., Shinoka, T., Saltzman, W.M., Snyder, E., Kyriakides, T.R., Pober, J.S., Breuer, C.K., 2010. Tissue-engineered vascular grafts transform into mature blood vessels via an inflammation-mediated process of vascular remodeling. Proc. Natl. Acad. Sci. 107, 4669–4674.

Rosen, E.D., Raymond, S., Zollman, A., Noria, F., Sandoval-Cooper, M., Shulman, A., Merz, J.L., Castellino, F.J., 2001. Laser-Induced Noninvasive Vascular Injury Models in Mice Generate Platelet- and Coagulation-Dependent Thrombi. Am. J. Pathol. 158, 1613–1622.

Rowley, J.W., Oler, A.J., Tolley, N.D., Hunter, B.N., Low, E.N., Nix, D.A., Yost, C.C., Zimmerman, G.A., Weyrich, A.S., 2011. Genome-wide RNA-seq analysis of human and mouse platelet transcriptomes. Blood 118, e101-11.

Ruggeri, Z.M., 2007. The role of von Willebrand factor in thrombus formation. Thromb. Res. 120, S5–S9.

Ruggeri, Z.M., Dent, J.A., Saldívar, E., 1999. Contribution of Distinct Adhesive Interactions to Platelet Aggregation in Flowing Blood. Blood 94, 172–178.

Rumbaut, R.E., 2010. Platelet-Vessel Wall Interactions in Hemostasis and Thrombosis. Biota Publishing.

Saboor, M., Moinuddin, M., Ilyas, S., 2013. New Horizons in Platelets Flow Cytometry. Malays. J. Med. Sci. MJMS 20, 62–66.

Sachs, U.J.H., Nieswandt, B., 2007. In Vivo Thrombus Formation in Murine Models. Circ. Res. 100, 979–991.

Sakariassen, K.S., Hanson, S.R., Cadroy, Y., 2001. Methods and models to evaluate shear-dependent and surface reactivity-dependent antithrombotic efficacy. Thromb. Res. 104, 149–174.

Samuel, R., Duda, D.G., Fukumura, D., Jain, R.K., 2015. Vascular diseases await translation of blood vessels engineered from stem cells. Sci. Transl. Med. 7, 309rv6-309rv6.

Sandow, S.L., Gzik, D.J., Lee, R.M.K.W., 2009. Arterial internal elastic lamina holes: relationship to function? J. Anat. 214, 258–266.

Sankaran, K.K., Vasanthan, K.S., Krishnan, U.M., Sethuraman, S., 2014. Development and evaluation of axially aligned nanofibres for blood vessel tissue engineering. J Tissue Eng Regen Med 8, 640–651.

Sargeant, P., Sage, S.O., 1994. Calcium signalling in platelets and other nonexcitable cells. Pharmacol. Ther. 64, 395–443.

Sato, M., Hirakata, H., Nakagawa, T., Arai, K., Fukuda, K., 2003. Thiamylal and pentobarbital have opposite effects on human platelet aggregation in vitro. Anesth. Analg. 97, 1353–1359.

Savage, B., Ginsberg, M.H., Ruggeri, Z.M., 1999. Influence of fibrillar collagen structure on the mechanisms of platelet thrombus formation under flow. Blood 94, 2704–2715.

Sawa, Y., Sugimoto, Y., Ueki, T., Ishikawa, H., Sato, A., Nagato, T., Yoshida, S., 2007. Effects of TNF-alpha on leukocyte adhesion molecule expressions in cultured human lymphatic endothelium. J. Histochem. Cytochem. Off. J. Histochem. Soc. 55, 721–733.

Scotland, R.S., Vallance, P.J., Ahluwalia, A., 2000. Endogenous factors involved in regulation of tone of arterial vasa vasorum: implications for conduit vessel physiology. Cardiovasc. Res. 46, 403–411.

Seliktar, D., Black, R.A., Vito, R.P., Nerem, R.M., 2000. Dynamic mechanical conditioning of collagen-gel blood vessel constructs induces remodeling in vitro. Ann. Biomed. Eng. 28, 351–362.

Serbo, J.V., Gerecht, S., 2013. Vascular tissue engineering: biodegradable scaffold platforms to promote angiogenesis. Stem Cell Res. Ther. 4, 8.

Shao, J.-S., Cai, J., Towler, D.A., 2006. Molecular mechanisms of vascular calcification: lessons learned from the aorta. Arterioscler. Thromb. Vasc. Biol. 26, 1423–1430.

Shen, B., Delaney, M.K., Du, X., 2012. Inside-out, outside-in, and inside-outside-in: G protein signaling in integrin-mediated cell adhesion, spreading, and retraction. Curr. Opin. Cell Biol. 24, 600–606.

Shi, X., Yang, J., Huang, J., Long, Z., Ruan, Z., Xiao, B., Xi, X., 2016. Effects of different shear rates on the attachment and detachment of platelet thrombi. Mol. Med. Rep. 13, 2447–2456.

Shinohara, S., Kihara, T., Sakai, S., Matsusaki, M., Akashi, M., Taya, M., Miyake, J., 2013. Fabrication of in vitro three-dimensional multilayered blood vessel model using human endothelial and smooth muscle cells and high-strength PEG hydrogel. J Biosci Bioeng 116, 231–4.

Siljander, P.R.-M., Munnix, I.C.A., Smethurst, P.A., Deckmyn, H., Lindhout, T., Ouwehand, W.H., Farndale, R.W., Heemskerk, J.W.M., 2004. Platelet receptor interplay regulates collagen-induced thrombus formation in flowing human blood. Blood 103, 1333–1341.

Simon, D., Kunicki, T., Nugent, D., 2008. Platelet function defects. Haemophilia 14, 1240–1249.

Song, L., Zhou, Q., Duan, P., Guo, P., Li, D., Xu, Y., Li, S., Luo, F., Zhang, Z., 2012. Successful development of small diameter tissue-engineering vascular vessels by our novel integrally designed pulsatile perfusion-based bioreactor. PloS One 7, e42569.

Stalker, T.J., Newman, D.K., Ma, P., Wannemacher, K.M., Brass, L.F., 2012. Platelet Signaling. Handb. Exp. Pharmacol. 59–85.

Stefanini, L., Bergmeier, W., 2010. CalDAG-GEFI and platelet activation. Platelets 21, 239–243.

Stinson, R.H., Bartlett, M.W., Kurg, T., Sweeny, P.R., Hendricks, R.W., 1979. Experimental confirmation of calculated phases and electron density profile for wet native collagen. Biophys J 26, 209–21.

Stuart, K., Panitch, A., 2009. Characterization of gels composed of blends of collagen I, collagen III, and chondroitin sulfate. Biomacromolecules 10, 25–31.

Subramanian, A., Krishnan, U.M., Sethuraman, S., 2012. Fabrication, characterization and in vitro evaluation of aligned PLGA-PCL nanofibers for neural regeneration. Ann Biomed Eng 40, 2098–110.

Sundaram, S., Niklason, L.E., 2012. Smooth Muscle and Other Cell Sources for Human Blood Vessel Engineering. Cells Tissues Organs 195, 15–25.

Syedain, Z.H., Meier, L.A., Bjork, J.W., Lee, A., Tranquillo, R.T., 2011. Implantable arterial grafts from human fibroblasts and fibrin using a multi-graft pulsed flow-stretch bioreactor with noninvasive strength monitoring. Biomaterials 32, 714–722.

Tadokoro, S., Nakazawa, T., Kamae, T., Kiyomizu, K., Kashiwagi, H., Honda, S., Kanakura, Y., Tomiyama, Y., 2011. A potential role for α-actinin in inside-out αIIbβ3 signaling. Blood 117, 250–258.

Tang, C., Wang, Y., Lei, D., Huang, L., Wang, G., Chi, Q., Zheng, Y., Gachet, C., Mangin, P.H., Zhu, L., 2016. Standardization of a well-controlled in vivo mouse model of thrombus formation induced by mechanical injury. Thromb. Res. 141, 49–57.

Tao, J., Haynes, D.H., 1992. Actions of thapsigargin on the Ca(2+)-handling systems of the human platelet. Incomplete inhibition of the dense tubular Ca2+ uptake, partial inhibition of the Ca2+ extrusion pump, increase in plasma membrane Ca2+ permeability, and consequent elevation of resting cytoplasmic Ca2+. J. Biol. Chem. 267, 24972–24982.

Thomas, L.V., Nair, P.D., 2013. The effect of pulsatile loading and scaffold structure for the generation of a medial equivalent tissue engineered vascular graft. Biores Open Access 2, 227–39.

Torikai, K., Ichikawa, H., Hirakawa, K., Matsumiya, G., Kuratani, T., Iwai, S., Saito, A., Kawaguchi, N., Matsuura, N., Sawa, Y., 2008. A self-renewing, tissue-engineered vascular graft for arterial reconstruction. J Thorac Cardiovasc Surg 136, 37–45, 45 e1.

Townsend, N., Wilson, L., Bhatnagar, P., Wickramasinghe, K., Rayner, M., Nichols, M., 2016. Cardiovascular disease in Europe: epidemiological update 2016. Eur. Heart J. 37, 3232–3245.

Tschoepe, D., Spangenberg, P., Esser, J., Schwippert, B., Kehrel, B., Roesen, P., Gries, F.A., 1990. Flow-cytometric detection of surface membrane alterations and concomitant changes in the cytoskeletal actin status of activated platelets. Cytometry 11, 652–656.

Tseng, M.T., Dozier, A., Haribabu, B., Graham, U.M., 2006. Transendothelial migration of ferric ion in FeCl3 injured murine common carotid artery. Thromb. Res. 118, 275–280.

Undar, A., Eichstaedt, H.C., Clubb, F.J., Lu, M., Bigley, J.E., Deady, B.A., Porter, A., Vaughn, W.K., Fung, M., 2004. Anesthetic induction with ketamine inhibits platelet activation before, during, and after cardiopulmonary bypass in baboons. Artif. Organs 28, 959–962.

Unger, R.E., Krump-Konvalinkova, V., Peters, K., Kirkpatrick, C.J., 2002. In vitro expression of the endothelial phenotype: comparative study of primary isolated cells and cell lines, including the novel cell line HPMEC-ST1.6R. Microvasc Res 64, 384–97.

van Buul, J.D., van Rijssel, J., van Alphen, F.P.J., Hoogenboezem, M., Tol, S., Hoeben, K.A., van Marle, J., Mul, E.P.J., Hordijk, P.L., 2010. Inside-out regulation of ICAM-1 dynamics in TNF-alpha-activated endothelium. PloS One 5, e11336.

Van Kruchten, R., Cosemans, J.M., Heemskerk, J.W., 2012. Measurement of whole blood thrombus formation using parallel-plate flow chambers - a practical guide. Platelets 23, 229–42.

Varga-Szabo, D., Braun, A., Nieswandt, B., 2009. Calcium signaling in platelets. J. Thromb. Haemost. JTH 7, 1057–1066.

Vassalle, C., Domenici, C., Lubrano, V., L'Abbate, A., 2003. Interaction between Nitric Oxide and Cyclooxygenase Pathways in Endothelial Cells. J. Vasc. Res. 40, 491–499.

WAGENSEIL, J.E., MECHAM, R.P., 2009. Vascular Extracellular Matrix and Arterial Mechanics. Physiol. Rev. 89, 957–989.

Wagner, D.D., Frenette, P.S., 2008. The vessel wall and its interactions. Blood 111, 5271–5281.

Wallez, Y., Huber, P., 2008. Endothelial adherens and tight junctions in vascular homeostasis, inflammation and angiogenesis. Biochim. Biophys. Acta BBA - Biomembr., Apical Junctional Complexes Part I 1778, 794–809.

Watson, S.P., Herbert, J.M., Pollitt, A.Y., 2010. GPVI and CLEC-2 in hemostasis and vascular integrity. J Thromb Haemost 8, 1456–67.

Weibel, E.R., Palade, G.E., 1964. NEW CYTOPLASMIC COMPONENTS IN ARTERIAL ENDOTHELIA. J. Cell Biol. 23, 101–112.

Weinberg, C.B., Bell, E., 1986. A blood vessel model constructed from collagen and cultured vascular cells. Science 231, 397–400.

Weinberg, P.D., Ross Ethier, C., 2007. Twenty-fold difference in hemodynamic wall shear stress between murine and human aortas. J Biomech 40, 1594–8.

Wentworth, J.K.T., Pula, G., Poole, A.W., 2006. Vasodilator-stimulated phosphoprotein (VASP) is phosphorylated on Ser157 by protein kinase C-dependent and -independent mechanisms in thrombin-stimulated human platelets. Biochem. J. 393, 555–564.

Westrick, R.J., Winn, M.E., Eitzman, D.T., 2007. Murine Models of Vascular Thrombosis. Arterioscler. Thromb. Vasc. Biol. 27, 2079–2093.

Wilkens, C.A., Rivet, C.J., Akentjew, T.L., Alverio, J., Khoury, M., Acevedo, J.P., 2016. Layer-by-layer approach for a uniformed fabrication of a cell patterned vessel-like construct. Biofabrication 9, 15001.

Wu, Y.P., Vink, T., Schiphorst, M., van Zanten, G.H., IJsseldijk, M.J., de Groot, P.G., Sixma, J.J., 2000. Platelet thrombus formation on collagen at high shear rates is mediated by von Willebrand factor-glycoprotein Ib interaction and inhibited by von Willebrand factor-glycoprotein IIb/IIIa interaction. Arterioscler. Thromb. Vasc. Biol. 20, 1661–1667.

Xu, J., Shi, G.-P., 2014. Vascular wall extracellular matrix proteins and vascular diseases. Biochim. Biophys. Acta 1842, 2106–2119.

Yang, Y., Wimpenny, I., Ahearne, M., 2011. Portable nanofiber meshes dictate cell orientation throughout three-dimensional hydrogels. Nanomed. 7, 131–6.

Ye, Q., Zünd, G., Jockenhoevel, S., Hoerstrup, S.P., Schoeberlein, A., Grunenfelder, J., Turina, M., 2000. Tissue engineering in cardiovascular surgery: new approach to develop completely human autologous tissue. Eur. J. Cardiothorac. Surg. 17, 449–454.

Yoshida, K., Okamura, T., Kimura, H., Bredt, D.S., Snyder, S.H., Toda, N., 1993. Nitric oxide synthase-immunoreactive nerve fibers in dog cerebral and peripheral arteries. Brain Res. 629, 67–72.

Yu, X.X., Wan, C.X., Chen, H.Q., 2008. Preparation and endothelialization of decellularised vascular scaffold for tissue-engineered blood vessel. J Mater Sci Mater Med 19, 319–26.

Yuan, S.-M., 2015. α-Smooth Muscle Actin and ACTA2 Gene Expressions in Vasculopathies. Braz. J. Cardiovasc. Surg. 30, 644–649.

Yuan, S.Y., Rigor, R.R., 2010. The Endothelial Barrier. Morgan & Claypool Life Sciences.

Zanetta, L., Marcus, S.G., Vasile, J., Dobryansky, M., Cohen, H., Eng, K., Shamamian, P., Mignatti, P., 2000. Expression of Von Willebrand factor, an endothelial cell marker, is up-regulated by

angiogenesis factors: a potential method for objective assessment of tumor angiogenesis. Int. J. Cancer 85, 281–288.

Zhang, X., Wang, X., Keshav, V., Wang, X., Johanas, J.T., Leisk, G.G., Kaplan, D.L., 2009. Dynamic culture conditions to generate silk-based tissue-engineered vascular grafts. Biomaterials 30, 3213–3223.

Zheng, Y., Chen, J., López, J.A., 2014. Microvascular platforms for the study of platelet-vessel wall interactions. Thromb. Res. 133, 525–531.